Ontario

Ontario Geological Survey
Open File Report 6017

Regional Geology of the Sioux Lookout Orogenic Belt, Western Wabigoon Subprovince: Stages of Archean Volcanism, Sedimentation, Tectonism and Mineralization

2000

Ontario

ONTARIO GEOLOGICAL SURVEY

Open File Report 6017

Regional Geology of the Sioux Lookout Orogenic Belt, Western Wabigoon Subprovince: Stages of Archean Volcanism, Sedimentation, Tectonism and Mineralization

by

J.R. Devaney

2000

Open File Reports of the Ontario Geological Survey are available for viewing at the Mines Library in Sudbury, at the Mines and Minerals Information Centre in Toronto, and at the regional Mines and Minerals office whose district includes the area covered by the report (see below).

Copies can be purchased at Publication Sales and the office whose district includes the area covered by the report. Although a particular report may not be in stock at locations other than the Publication Sales office in Sudbury, they can generally be obtained within 3 working days. All telephone, fax, mail and e-mail orders should be directed to the Publication Sales office in Sudbury. Use of VISA or MasterCard ensures the fastest possible service. Cheques or money orders should be made payable to the *Minister of Finance.*

Mines and Minerals Information Centre (MMIC) Macdonald Block, Room M2-17 900 Bay St. Toronto, Ontario M7A 1C3	Tel:	(416) 314-3800 1-800-665-4480(toll free inside Ontario)
Mines Library 933 Ramsey Lake Road, Level A3 Sudbury, Ontario P3E 6B5	Tel:	(705) 670-5615
Publication Sales 933 Ramsey Lake Rd., Level A3 Sudbury, Ontario P3E 6B5	Tel: Fax: E-mail:	(705) 670-5691(local) 1-888-415-9845(toll-free) (705) 670-5770 pubsales@ndm.gov.on.ca

Regional Mines and Minerals Offices:

Kenora - Suite 104, 810 Robertson St., Kenora P9N 4J2

Kirkland Lake - 10 Government Rd. E., Kirkland Lake P2N 1A8

Red Lake - Box 324, Ontario Government Building, Red Lake P0V 2M0

Sault Ste. Marie - 70 Foster Dr., Ste. 200, Sault Ste. Marie P6A 6V8

Southern Ontario - P.O. Bag Service 43, Old Troy Rd., Tweed K0K 3J0

Sudbury - Level B3, 933 Ramsey Lake Rd., Sudbury P3E 6B5

Thunder Bay - Suite B002, 435 James St. S., Thunder Bay P7E 6S7

Timmins - Ontario Government Complex, P.O. Bag 3060, Hwy. 101 East, South Porcupine P0N 1H0

Toronto - MMIC, Macdonald Block, Room M2-17, 900 Bay St., Toronto M7A 1C3

Cette publication est disponible en anglais seulement.

Parts of this report may be quoted if credit is given. It is recommended that reference be made in the following form:

Devaney, J.R. 2000. Regional geology of the Sioux Lookout orogenic belt, western Wabigoon Subprovince: stages of Archean volcanism, sedimentation, tectonism and mineralization; Ontario Geological Survey, Open File Report 6017, 151p.

Contents

FIGURES

TABLES

MAP

Abstract

The Sioux Lookout orogenic ("greenstone") belt, a relatively small part of the western Wabigoon subprovince in northwest Ontario, is composed of the following tectonized stratigraphic units, from north to south: 1) the Northern Volcanic belt; 2) the Patara Formation; 3) the "Big Vermilion–Daredevil unit"; 4) the Ament Bay Formation; 5) the Daredevil Formation stratotype; 6) the Central Volcanic belt; 7) the Minnitaki Group; and 8) the Southern Volvanic belt. The Sioux Lookout belt is bounded to the north by the Winnipeg River subprovince and to the south by the Basket Lake batholith.

Tectono–stratigraphic analysis of the metamorphosed and variably deformed Archean supracrustal rocks of the Sioux Lookout belt suggests the accumulation of lower, older, subaqueous basaltic successions (Stage 1 magnesian tholeiites of MORB to arc character presumably were deposited in a narrow ocean; Stage 2 iron tholeiites of E–MORB character, ca. 2733 Ma old, represent a juvenile arc setting), followed by development of a local andesitic volcanic centre (Stage 3, ca. 2732 Ma: a partly rifted arc?), all of which were then capped by sequences of more felsic volcaniclastic and sedimentary rocks (Stage 4 calc–alkalic late arc dacites and rhyolites, including adakites, ca. 2714 Ma old). Associated sediments such as turbidite deposits (e.g., Minnitaki Group, Stage 4) were influenced by synchronous intermediate–felsic volcanism (interbedded tuffs, volcanic pebble–conglomerate, magnetite iron formation), and within one horizon, distal coarse clastic sedimentary facies and iron formation can be traced along strike to their probable proximal volcanic dome source.

A relatively small, 3 km thick, partly subaerial, andesitic stratovolcano succession (pyroclastic and sedimentary facies, lava flow facies, synvolcanic dikes) has a local (nonregional) distribution, suggestive of a fault–bounded volcanic basin such as a graben. This well preserved andesitic succession and its comagmatic dioritic subvolcanic intrusion (Stage 3) were coeval with similar rocks 60 km to the east at Sturgeon Lake (caldera complex pyroclastic rocks and the Beidelman Bay subvolcanic pluton). Such a correlation implies that the Sturgeon Lake caldera–hosted VMS deposits formed during Stage 3 tectonism (interpreted as a rifted arc phase). The sporadic presence of similar ca. 2733 Ma andesitic rocks at widespread sites in western Wabigoon subprovince suggests that a laterally discontinuous system of coeval rifts, graben and local andesitic volcanic centres formed at that time.

Geochronological relationships and sub–regional scale structural–stratigraphic map patterns suggest that approximately northwest–southeast compression segmented the original basin (arc units on early basalt, buried and flanked by younger volcanically sourced detritus) into an imbricate stack of numerous thrust slices that generally dip and young to the southeast (Stage 5: a foreland–vergent fold–and–thrust belt). Fluvial polymict conglomerates (Ament Bay Formation) accumulated in a narrow, linear (strike–parallel), intra–orogenic "molasse" piggyback basin and were overthrust by older volcanic rocks forming the bases of thrust slices (relative ages confirmed by published U/Pb zircon dates).

Many of the major faults in the Sioux Lookout orogenic belt appear to be sigmoidal sinistral strike–slip faults (Stage 6), some of which may be reactivated thrust faults (i.e., Stage 6 superimposed on Stage 5). Granitoid plutons appear to have intruded along some of these major faults; one small, undated plutonic complex has sanukitoid characteristics. Sub–regional map patterns suggest that late stage sinistral–sense strike–slip (to oblique–slip) motions produced features such as: 1) strike–slip duplexes (multi–scale clusters of 1–10 km long sigmoidal fault–bounded stratal lenses); 2) a pull–apart basin: the Patara Formation has a 20 km long, lazy S–shaped outline, and its basin fill sequence coarsens up to basalt–clast fluvial conglomerate (the basalt and accessory BIF clasts being derived from the adjacent "Northern Volcanic belt"); 3) releasing–bend (dilational jog) plutons (roughly sigmoidal in map view); and 4) a large "Riedel flake structure" (7 km diameter, rotated counter–clockwise). The regional–scale sinistral faulting is thought to be a record of movements near the west margin of the "Wabigoon Indenter", and the structural style of the northern half of the Sioux Lookout orogenic belt can be considered as the southwest continuation of the northeast–trending Miniss River Fault.

A large volume of basaltic strata (the “Northern Volcanic belt,” a formational unit which forms the northern part of the Sioux Lookout orogenic belt) was overturned adjacent to the microcontinental Winnipeg River subprovince foreland. The overturning was likely produced by large–scale faulting; specific hypotheses include: 1) the south margin of the Winnipeg River subprovince was a southeast–vergent Laramide–type uplift (i.e., a thick–skin thrust or the hangingwall block above a high–angle reverse fault, the major fault being the Miniss River Fault); and 2) listric–upward thrust wedging within transpressional positive flower (palm tree) structures rotated some thrust wedges into shallowly dipping orientations.

The nature of the mineralization in the belt is directly related to the different tectono–stratigraphic evolutionary stages. During Stages 1 and 2 deep water exhalites (magnetite iron formation, chert, pyrite) formed; pyrite was formerly mined in the area. Stage 3 volcanism produced ore deposits in an adjacent greenstone belt (the Cu–Zn VMS deposits at Sturgeon Lake), but in correlative rocks in the Sioux Lookout area no VMS deposits, no epithermal mineralization, and only insignificant amounts of porphyry copper–type mineralization, have been found. During Stage 4 basinal development a large magnetite iron formation unit accumulated in the southeast part of the belt, but in other areas only minor (uncommon) volcanogenic sulphide mineralization and sub–exhalite hydrothermal alteration are present, and the “FI” character of the Stage 4 dacitic–rhyolitic rocks does not suggest good VMS potential. Synorogenic (Stages 5 and/or 6) quartz veins appear to be thicker and more abundant, and contain more gold, near the major deformation zones (thrust and/or strike–slip faults), suggestive of formation as typical structurally–controlled Archean mesothermal lode gold deposits. At a regional (10 to 100 km) scale, gold occurrences appear to be located along lineaments which resemble a Riedel shear fracture system.

Recommendation for exploration: It is suggested that in order to explore for gold deposits in the Sioux Lookout belt (and in other similar areas), geologists should: 1) perform detailed mapping and sampling of quartz–veined areas in tectonic deformation zones (perhaps regardless of the type of rock hosting the veins); and 2) attempt to classify and interpret the history of the belt’s various, probably complex, late orogenic stage transtensional and transpressional structural domains.

Introduction

The Sioux Lookout orogenic belt (Figure 1) is a relatively small segment of the vast network of Late Archean (2.7 Ga) supracrustal rocks and associated intrusions that comprise the "western Wabigoon region" of the Wabigoon subprovince (Blackburn et al. 1991). The following preliminary reports of results from recent reconnaissance–scale bedrock mapping of the Sioux Lookout orogenic belt (an approximately 1000 km^2 study area; Devaney and Borowik 1994; Devaney et al. 1995a,b; Devaney and Babin 1996, Devaney 1997, 1998, 1999a), this report summarizes the descriptive and interpretative aspects of the various supracrustal units which constitute most of the Sioux Lookout orogenic belt (Figures 1, 2, and map in pocket), with an emphasis on the metasedimentary and fragmental metavolcanic units. This knowledge has been integrated with other geological data selected from previous studies in order to place the mineral occurrences of the Sioux Lookout orogenic belt in an improved tectono–stratigraphic context and thus aid mineral exploration.

ACCESS

The Sioux Lookout area is easily reached by road (Highway 72; Figure 1) and airplane. A network of subsidiary roads and highways and the larger lakes (Minnitaki, Little Vermilion, "Big" Vermilion, Abram, Pelican) provide excellent access throughout the area.

ACKNOWLEDGMENTS

Senior assistants A. Borowik, D. King and D. Babin mapped a significant part of the study area. Junior assistants M.McKenzie, M.Mitchell, B. MacFarlane, P. Smoter, M. Smethurst, D. Leng, J. Brownbill and W. Chisel provided fine field assistance, including some independent mapping by McKenzie, Smoter and Smethurst. D. Janes and G. Seim (Sioux Lookout Resident Geologist's Office) and the Ministry of Natural Resources provided much valuable support for the field operations. L.D. Ayres, P.C. Thurston, D.W. Davis and D.G.F. Long offered useful geological advice during their field visits. R.O. Page's gift of unpublished volcanological data, including a map of the Northeast Bay of Minnitaki Lake area, is greatly appreciated. Earlier versions of this manuscript were edited by P.C. Thurston, D.G.F. Long, and G.M. Stott.

PREVIOUS WORK

The distribution and apparent thickness (width of units perpendicular to strike) of the various lithological units in the Sioux Lookout orogenic belt study area (Figure 1) is shown in detail on the maps of Johnston (1969, 1972) and Devaney et al. (1995b; map in pocket). Figure 2 is a cross–section summarizing the general geology of the Sioux Lookout orogenic belt, and illustrates how previous studies contrast with this study.

Mapping of the Sioux Lookout orogenic belt appears to have followed a 20 year cycle, with the main periods of study in the 1930s, 1950s, 1970s and 1990s. Following the earliest geological exploration of the Sioux Lookout area, which include reports of gold mineralization dating back to 1898 (Johnston 1972), Hurst (1933) produced the first modern geological map of the Sioux Lookout orogenic belt and Horwood (1938) reported on mineralized areas east of Sioux Lookout (Zarn Lake area).

Pettijohn (1934, 1935, 1936, 1937, 1939) studied selected parts of the Sioux Lookout orogenic belt and was one of the first geologists to perform specialized sedimentological research on Archean metasediments, and his attempts at larger–scale stratigraphic correlation (Pettijohn 1937) are part of the foundation of similar contemporary efforts (Blackburn et al. 1985, 1991). New observations and interpretations of Pettijohn's "Patara Formation" (Figure 3) are an important part of the present study.

Many of the Sioux Lookout orogenic belt lithotectonic units extend to the Dryden area (Blackburn et al. 1991). East of Dryden, historically important tectono–stratigraphic relationships were investigated in the Thunder Lake area (Pettijohn 1939, Satterly 1943, Blackburn et al. 1985); gold mineralization near Thunder Lake is presently attracting strong economic interest (Blackburn et al. 1998). A few years of production at the Goldlund gold mine (*see:* Page 1984; Chorlton 1990, 1991), about halfway between Dryden and Sioux Lookout, likely spurred the mapping of the surrounding area by Armstrong (1951) and Harding (1951).

A compilation by Skinner (1969) offered little information about the Sioux Lookout orogenic belt. Detailed mapping of the Sioux Lookout orogenic belt by Johnston (1969, 1972) and reconnaissance mapping of the surrounding area by Breaks et al. (1976) and Sage et al. (1974) provided a foundation for the comprehensive work of Trowell and others, which included discussion of the volcanology, geochemistry, regional stratigraphy, and potentially economic mineralization of the Sioux Lookout orogenic belt and other western Wabigoon subprovince areas (Trowell et al. 1977, 1978, 1980, 1983; Blackburn et al. 1985, Trowell and Johns 1986). The plate tectonic scenario advanced by Blackburn (1980, Figure 4) was visionary for its time, and included a cross–section through the Sioux Lookout orogenic belt.

A series of 1:20 000 scale airborne electromagnetic maps (OGS 1982) can be used to outline major structures of the Sioux Lookout orogenic belt. This data was recently reprocessed and published in CD–ROM format (OGS 1997).

The publication of Johnston's (1969, 1972) preliminary and final maps likely spurred the following efforts. Walker and Pettijohn (1971) and Turner (1972; Turner and Walker 1973) performed detailed sedimentological studies of the Sioux Lookout orogenic belt metasedimentary units, drawing further attention to the well preserved strata of the Abram and Minnitaki groups (see above for earlier studies by Pettijohn). Gold mineralization in and marginal to felsic porphyry bodies was studied by Sutherland and Colvine (1979) and McMullan (1980). Page and Clifford (1977), Page et al (1978), and Page (unpublished data in OGS archives) studied the volcanology of the well preserved volcaniclastic deposits (pyroclastic to more sedimentary "reworked" facies) and lava flow facies in the Northeast Bay area of Minnitaki Lake. Page also mapped larger areas around Sioux Lookout (Page 1978, 1984; Page and Moller 1979a,b; Page and Christie 1980a,b), with an emphasis on volcanology and potentially economic mineralization. The writer has found Page's geological mapping of the Sioux Lookout orogenic belt to be particularly accurate.

Davis and Trowell (1982) and Davis et al. (1988) reported the first U/Pb dates of zircon grains extracted from Sioux Lookout orogenic belt rocks, data which is an extremely important part of the most recent geological syntheses of the Sioux Lookout orogenic belt (Blackburn et al. 1985, Davis et al. 1988, Davis 1990, Blackburn et al. 1991, Devaney 1997, 1999a, and this report). Having accurately dated rocks (e.g., plus or minus only a few million years) enabled geologists to offer more refined views of the tectonic evolution of the Sioux Lookout orogenic belt, including an emphasis on the likely role of thrusting (Davis et al. 1988, Beakhouse 1988, Davis 1990, Blackburn et al. 1991).

The geological mapping in the Sandybeach Lake area, southwest of the present study area, by Berger (1989, 1990) and Chorlton (1990, 1991) provides additional data for the along–strike extensions of most of the lithotectonic units described in this report. Aside from Pettijohn's (1934) brief note on the strike–slip nature of "shear faults" in the Sioux Lookout area, and Beakhouse's (1988) brief mention of "transcurrent faulting," Chorlton (1990, 1991) is the only previous worker to have recognized the probable importance of late tectonic strike–slip faulting, particularly sinistral sense motions, in the evolution of the Sioux Lookout orogenic belt. Chorlton's (1990, 1991) detailed structural analysis also suggested early thrusting, in agreement with the conclusions of Devaney (1997, 1999a) and this report.

Preliminary reports on parts of the present study are those by Devaney and Borowik (1994), Devaney et al. (1995a,b), Devaney and Babin (1996), Babin et al. (1996), and Devaney (1997, 1998, 1999a). Results from volcanological thesis work by McKenzie (1995) and D. Babin (in preparation) on Northeast Bay of Minnitaki Lake area stratovolcanic facies (Page and Clifford 1977, Devaney and Babin 1996, Devaney 1998) are incorporated in this report, and Figure 4 shows the transgression–regression cycle model (Devaney 1998) devised for the andesitic succession in this area.

A large number of assessment file reports concerning the geology and mineral deposits of small areas within the Sioux Lookout orogenic belt are available via either the Sioux Lookout Resident Geologist Office or the ERLIS system.

Areas surrounding the Sioux Lookout orogenic belt are: 1) to the NW and N, the eastern Winnipeg River subprovince (Breaks and Bond 1977, Breaks 1988, Sanborn–Barrie 1988, Beakhouse 1991, Corfu et al. 1995, Ciceri et al. 1996, Cruden et al. 1997); 2) to the NE and E, the Zarn Lake area (Page 1978, Page and Moller (1979a,b) and other areas which bridge the gaps between the Sioux Lookout orogenic belt and the Sturgeon Lake and Savant Lake belts (e.g., see Trowell references in Blackburn et al. 1991); 3) to the SE, the Basket Lake batholith (Sage et al. 1974, Szweczyk and West 1976), which is part of the western margin of the central Wabigoon region (Blackburn et al. 1991); and 4) to the S and SW, the Dinorwic and Dryden areas (Pettijohn 1939, Satterly 1943; Blackburn et al. 1985, 1991, 1998; Berger 1989, 1990; Chorlton 1990, 1991). At a regional scale, supracrustal rocks in the Sturgeon Lake and Savant Lake areas extend to the east and northeast of the Sioux Lookout orogenic belt (Blackburn et al. 1991, Figures 9.3, 9.40), and the recent interpretation of the evolution of the "Sturgeon–Savant belt" by Sanborn–Barrie and Skulski (1999) includes important similarities and differences with the proposed evolution of the Sioux Lookout orogenic belt (Devaney 1999a, and herein).

Geology of Stratigraphic Units

STRATIGRAPHIC OVERVIEW

The Sioux Lookout orogenic belt is composed of the following tectonized stratigraphic units, from north to south: 1) the Northern Volcanic belt (or Botham Bay Group); 2) the Patara Formation; 3) the "Big Vermilion–Daredevil unit"; 4) the Ament Bay Formation; 5) the Daredevil Formation stratotype; 6) the Central Volcanic belt (or Neepawa Group); 7) the Minnitaki Group; and 8) the Southern Volvanic belt (Figures 1, 2). The Sioux Lookout orogenic belt is bounded to the north by the Winnipeg River subprovince (Beakhouse 1991) and to the south by the poorly known Basket Lake batholith (Szewczyk and West 1976, Berger 1989, Blackburn et al. 1991). Previous stratigraphic and regional geological studies of the Sioux Lookout orogenic belt were summarized by Johnston (1969, 1972) and Blackburn et al. (1985, 1991). Most of the major stratigraphic units of the Sioux Lookout orogenic belt continue to the southwest, an area described in recent reports by Berger (1989, 1990), Chorlton (1990, 1991), and Page (1984), and some units continue to the east (Page and Moller 1979a,b; Trowell et al. 1982, 1983). Studies by Davis and Trowell (1982), Davis et al. (1988), Davis (1990) and Devaney (1999a) have provided a small number of radiometric ages for the rocks in and around the Sioux Lookout orogenic belt (Figure 2).

The distribution of the linear, belt–like lithological units which form the various stratigraphic units of the Sioux Lookout orogenic belt is shown in Figure 1, on the accompanying map (Devaney et al. 1995b), and on the older maps of Johnston (1969, 1972) and Blackburn et al. (1985; 1991, Figures 9.12, 9.40). The map width of the typically very steeply dipping units approximates their tectonized "stratigraphic" thickness. Geographic localities referred to below are shown on the accompanying map (Devaney et al. 1995b), the maps of Johnston (1969, 1972), and other maps cited herein.

Owing to: 1) a lack of detailed structural and geochronological studies; 2) the low amount of continuous exposure (including large covered intervals); and 3) the near total absence of exposed boundaries (contacts) between the major stratigraphic units, the degree of structural disturbance, both between and within the various stratigraphic units of the Sioux Lookout orogenic belt, is mostly unknown (or not reliably known), and in most cases lateral and vertical (upward) trends within the formation–like units cannot be reliably interpreted as true stratigraphic trends. As is common in the other Archean greenstone belts of northern Ontario, the nature of the exposure and potential structural complexity severely limit attempts at conventional stratigraphic descriptions and interpretations, and a more generalized, lithofacies–oriented approach must be taken. References regarding more general aspects of interpretation common to the supracrustal rocks of most Archean greenstone belts (e.g., the subaqueous origin of

pillowed basalt flows) are not given; if necessary, the reader should consult volcanological and sedimentological reviews and texts (e.g., Easton and Johns 1986, Cas and Wright 1987, Miall 1990, Walker and James 1992, McPhie et al. 1993).

The Northern Volcanic belt was not studied in detail. For the purposes of this study, its most important characteristics are its overturned nature (Trowell et al. 1977, 1978; Page 1984, Devaney 1999a) and its geochemical composition (see: below, and Trowell and Johns 1986).

Classification of the "Patara sediments" (Pettijohn 1935, Johnston 1972) or "Patara Group" (Blackburn et al. 1985, Davis et al. 1988) has varied over time, and the use of the term "Patara Formation" herein is based on a lithologically finer subdivision of units than in Johnston's (1972) maps (Devaney and Borowik 1994, Devaney et al. 1995b, Devaney 1999a) and a return to the original definition and mapping of Pettijohn (1934). Previously thought to be the oldest sedimentary unit in the Sioux Lookout orogenic belt, the Patara Formation is in fact one of the two youngest sedimentary formations in the Sioux Lookout orogenic belt; this interpretation (Devaney 1997, 1999a, and herein) was recently confirmed by geochronological data (Fralick and Davis 1999). Also, previous workers described the conglomeratic Patara Formation as unconformably (to conformably) overlying the Northern Volcanic belt, and did not recognize that the Patara Formation appears to form a moderately–dipping northwest–facing sequence that faces opposite to the adjacent overturned (southeast–younging and northwest–dipping) Northern Volcanic belt.

Volcanic and sedimentary facies of the "Big Vermilion–Daredevil unit," a recently proposed informal term (Devaney 1999a) described in detail for the first time herein, were previously considered part of the "Patara Sediments" of Johnston (1972), Turner and Walker (1973, Figure 1) and Trowell et al. (1977, 1978), the "Patara Group" of Blackburn et al. (1985, p. 104) and Davis et al. (1988), and the "Northern Sedimentary belt" of Beakhouse (1988). Based on similar lithofacies and dates obtained from zircon grains from both volcanic and detrital rocks, the Big Vermilion–Daredevil unit is interpreted to be correlative with the Daredevil Formation (see below) and related adjacent strata (Little Vermilion Formation of Turner and Walker 1973).

Previously, the term "Abram Group" was used (Pettijohn 1934, Turner and Walker 1973, Blackburn et al. 1985, 1991) for a triad of formations (from north to south: the Ament Bay, Daredevil and Little Vermilion formations) which presumably formed a continuous, south–younging, homoclinal ("homofacing") sequence. However, geochronological data of Davis et al. (1988) demonstrate, and interpretations by the author (Devaney 1999a, and herein) suggest, that the sequence is not continuous and homoclinal but is structurally disturbed, with an older formation (Daredevil) juxtaposed (faulted) over a younger formation (Ament Bay). This invalidates the "Abram Group" as a stratigraphic term, and its use must be discontinued.

The structural scenario above accounts for the apparent repetition of Daredevil–like stratigraphic units, with the Ament Bay Formation unconformably overlying the Big Vermilion–Daredevil unit (basal conglomerate of Turner 1972, Turner and Walker 1973) and structurally overlain by the Daredevil Formation type section.

Within the study area, the Daredevil Formation (*sensu stricto*: Pettijohn 1934, Turner and Walker 1973) appears to be a readily mappable unit only in its type area. The proposed Little Vermilion Formation was not found to be a readily mappable unit, so it is recommended that use of this stratigraphic term be discontinued.

The Central Volcanic belt (or Neepawa Group) is a large (thick), stratigraphically and structurally complex group of predominantly volcanic units. The various major units differ strongly in their lithofacies and geochemical composition, and likely represent volcanic centres and stratigraphic units of significantly different ages and tectonic settings. Owing to a lack of stratigraphic and structural resolution, the characteristics of the Central Volcanic belt are described separately for numerous distinct geographic areas. Some felsic volcanic units may be proximal equivalents of the adjacent, mostly sedimentary Minnitaki Group.

The term “Neepawa Group” is misleading because it gives the impression of a coherent stratigraphic group rather than the stratigraphically and structurally complex “package” of numerous, very different types of volcanic rocks which are present and represent approximately 30 Ma of volcanic episodes. Accordingly, use of the term “Neepawa Group” should be discontinued.

The Central Volcanic belt is notable for the extremely well preserved physical volcanological details of andesitic pyroclastic strata in the Northeast Bay, Minnitaki Lake area (Page and Clifford 1977, Devaney and Babin 1996, Devaney 1998). Interestingly, this distinctive sequence of north–trending, well preseved andesitic strata is oriented at a very high angle to the rest of the northeast– to east–trending Central Volcanic belt, and may represent a small (7 km diameter) rotated crustal flake (Devaney 1999a, and herein).

Descriptions and interpretations of the Minnitaki Group given below supplement the previous results of Walker and Pettijohn (1971). Proximal to distal stratigraphic trends appear to be present along strike, and structural repetition via folding and faulting within the Group is suspected.

The Southern Volcanic belt was not studied in detail. The present study relies partly on the previous work of Johnston (1969) and Trowell et al. (1982, 1983), and descriptions of the extensions of the Southern Volcanic belt to the west (Berger 1989, Chorlton 1991) and east (Trowell et al. 1983).

Because the western Wabigoon subprovince is a region known for its long–range stratigraphic (and other geological) correlations, implying broad similarities in geological evolution among the various individual greenstone “belt” segments comprising the region (Blackburn 1980, Trowell et al. 1980, Trowell and Johns 1986, Blackburn et al. 1985, 1991), the tectono–stratigraphic interpretations of the various units within the Sioux Lookout orogenic belt (Devaney 1999a, and herein) may also be applicable to other parts of western Wabigoon subprovince.

NORTHERN VOLCANIC BELT

The Northern Volcanic belt (or “Botham Bay Group”) is the northwestern–most supracrustal unit in the generally northeast–trending Sioux Lookout orogenic belt. As noted by Trowell and Johns (1986), it is correlative with the Jutten Group, located to the northeast in the Sturgeon–Savant belt, and other similar “older” tholeiitic mafic volcanic units of western Wabigoon subprovince (Blackburn et al. 1985, 1991). Note that much of the Northern Volcanic belt is outside of the present map area, and was well described by Page (1984), so its treatment herein is minimal.

Lithofacies

The Northern Volcanic belt is composed principally of mafic volcanic flow facies. The massive to pillowed (including pillow breccia) basalt flows are typically nonvesicular and nonporphyritic. Relatively large pillows are about 1 m in diameter (in horizontal outcrop plane views). Coarser gabbroic areas may represent sills or interiors of thick flows (in northern Ontario, this ambiguity and lack of resolution is a common problem owing to the typically small, discontinuous nature of the exposures).

Physical volcanological details of pillowed flows include: 1) quench–fractured pillow rims (brecciated, jigsaw–textured); 2) hyaloclastic chips; 3) breached pillow selvages that reveal sequential pillow budding; 4) small “bun” pillows in inter–pillow matrix areas; and 5) pipe vesicles. At a spectacular roadside outcrop (along Highway 664), overturned pillows have superbly defined shapes (keels at base, convex–up tops), gas cavities (lensoid; some are flat–floored, and thus serve as geopetal structures; typically in the upper half or third of a pillow), some concentric pillow structure, and superb fully to partly spalled–off hyaloclastic pillow rinds.

Pyroclastic rocks are rare; for example, one site with bedded and cross–bedded mafic lapilli–tuff was noted. Epiclastic sedimentary rocks were not observed, but Beakhouse (1988) noted interbeds of “quartz arenite” in one banded iron formation (BIF) unit.

Units of chert–magnetite (BIF), up to tens of metres thick, comprise a minor amount of the Northern Volcanic belt. The "bands" are tectonized laminae and beds; thicker bands are tens of centimetres thick.

Pyritic BIF is less common (e.g., thin massive to internally layered pyrite bands). A pyrite deposit in the Northern Volcanic belt, the former North Pines mine, was mined during the 1920s (Johnston 1972).

The BIF units form prominent stratigraphic (or lithotectonic) units, with the lateral continuity and strike length of these being best expressed on aeromagnetic maps (OGS 1982, 1997).

GEOCHEMISTRY

Trowell and Johns (1986) demonstrated the tholeiitic nature of the Northern Volcanic belt basalts and their strong similarity to the Jutten Group basalts. Data presented below (*see* "Geochemistry") and analyses by D. Wyman (written communication, 1998) show that the Northern Volcanic belt basalts have a MORB (mid–ocean ridge basalt) composition. Using Wyman's analyses, the Northern Volcanic belt can be subdivided into two geochemically defined units: a main northwestern unit, and a relatively thin unit along the southeast margin of the Northern Volcanic belt. (Importantly, the basaltic part of the northwestern Central Volcanic belt also displays the same two–part subdivision, suggesting correlation of the Northern Volcanic belt and Central Volcanic belt.)

Interpretation

The abundance of pillowed basalt flows, MORB–like composition, and the great extent of the Northern Volcanic belt appear to be diagnostic of oceanic crust, a deep marine mafic plain paleoenvironment. The chert–magnetite BIF units should represent exhalites precipitated from seawater to form interflow chemical sediments.

Although undated, such mafic sequences in western Wabigoon subprovince are thought to be older than the "diverse intermediate to felsic volcanic sequences" (Blackburn et al. 1991).

TOP INDICATIONS

Tops indications in the Northern Volcanic belt to the south or southeast, based mostly on pillow shapes, are very consistent. Also, reports of this top direction have been consistent from study to study: for example, Pettijohn (1934, 1935), Johnston (1972), and (Devaney et al. (1995b). However, despite brief mentions of the overturned nature of the Northern Volcanic belt sequence by Trowell et al. (1977, 1978) and Page (1984), it has not been previously stressed that these widespread tops to the southeast occur in moderately to steeply northwest–dipping strata. (Note that it is the orientation of schistosity, rather than bedding, which is more commonly recorded on most maps of the Northern Volcanic belt.)

Based on the maps of Johnston (1972) and Page (1984), and the results of the present study (Devaney et al. 1995b), overturned basaltic strata in the Northern Volcanic belt are widespread. This suggests the possibility that the entire Northern Volcanic belt has been overturned.

PATARA FORMATION

Introduction, Definition and Age

Use of the term "Patara Formation" herein is consistent with Pettijohn's (1934, 1935) original definition and mapping of the distinctive mafic–clast conglomerate unit present along the southeast margin of the

Northern Volcanic belt from central Vermilion Lake to south Pelican Lake. This 20 km long formation extends for a relatively short distance along strike compared with the other formations, lithological units or "belts" in the map area.

Other more felsic rocks lumped together as "Patara sediments" by Johnston (1972) and Blackburn et al. (1985) are herein considered to be stratigraphically equivalent to the Daredevil Formation, and are herein informally termed the "Big Vermilion–Daredevil unit" (see below, and Devaney 1999a). This an important point because Davis et al. (1988), using the geological framework of Johnston (1972), reported a ca. 2712 Ma age from a sample of supposed "Patara sediment." That sample is from the eastern part of the Big Vermilion–Daredevil unit, and is closely similar in age to other samples from the volcanic Daredevil Formation (type area) and the clastic Minnitaki Group dated by Davis et al. (1988). Fralick and Davis (1999) report an age of ca. 2700 Ma for detrital zircon grains from the sandy component of the mafic–clast conglomerate in the Patara Formation, which confirms the previous interpretation by the author (Devaney 1997, 1999a) of the synorogenic nature of the Patara Formation

Johnston (1972) reported trachytic dikes from the roadside section of the Patara Formation described below. Given the interpretations proposed herein for the Patara Formation, more study of the dikes is warranted.

Lithofacies

CONGLOMERATIC FACIES

Conglomerate–dominant outcrops or intra–outcrop horizons are typically crudely bedded, with vague coarser versus finer layers and rare well bedded lenses. Subtle compositional layering (e.g., clusters of clasts with recessively weathered rims) also defines bedding. Sandy interbeds are up to tens of centimetres thick, and commonly contain pebble bands. The conglomerate has a tightly clast–supported framework of pebbles and a coarse sandstone matrix.

Clast composition is mostly oligomict, consisting of mafic volcanic clasts (commonly dark brown to bluish coloured; some clasts weather very light brown or grey), plus a minor component of clasts of gabbro, magnetite BIF (with one 41 by 26 cm magnetite boulder clast), chert–magnetite BIF, and chert.

Rare clasts with recessively weathered rims could represent individual pillows transported as clasts, or intense weathering of some clast rims. Rare quartz pebbles are probably chert (recrytallized?). At some sites, gabbroic cobbles are the largest clasts; clast size may partly reflect the jointing and "toughness" of the source area lithologies.

The rounded form of many of the clasts appears to be a primary feature. Regarding the preservation of such primary features, it is notable that superbly preserved pillowed basalts are close by in the adjacent Northern Volcanic belt, and well preserved sedimentary structures are found to the south in the sandier facies of the Patara Formation, illustrating that well preserved primary fabrics are common.

Johnston (1972) considered the conglomerate along the line of inferred (unexposed) contact with the Northern Volcanic belt to be a "basal" horizon and described the Patara Formation as having a "basal breccia" unit. However, at several sites near the contact the clasts are round to sub–angular, and are thus do not constitute a breccia. Also, the view presented herein (see below) is that the conglomerates along the contact with the Northern Volcanic belt likely represent the top, not the base, of the Patara Formation

Small rare exposures of mafic–clast conglomerate may be present along strike east and west from the known disribution of the Patara Formation (along potential fault zones). One such exposure was identified just east of the town of Sioux Lookout (next to a bypass bridge built after publication of the map of Devaney et al. 1995b).

SANDIER FACIES

At central Vermilion Lake, some outcrops display a sandstone–dominated section, with lamination, cross–lamination, cross–bedding, fine–grained interbeds, and thin (10 cm) fine pebble conglomerate beds and pebble bands (all suggestive of a more distal facies suite than in the coarse conglomeratic areas; see below). At Pelican Lake, deformed laminated to thinly bedded mafic siltstone and sandstone may contain concretions.

Outcrops along Highway 664, southeast of the predominantly conglomeratic horizon, contain a moderately northwest–dipping cross–section of conglomerate and sandstone, with all top indications in this area to the northwest (Figure 3). The subequal amounts of conglomerate and sandstone present contrast greatly with the conglomeratic horizon adjacent to the north. A few sandy beds contain faint small crossbeds, cross–lamination (ripples, including rare bed plane views of straight ripple crests), and one bed with flat (paleo–horizontal) to low–angle laminae and regularly spaced small clusters of a few pebbles (interpreted as antidune laminae, with the pebble clusters as transverse ribs). One 4 m thick horizon contains two fining–upward sequences, defined by rhythmic repetition of the sequence conglomerate to sandstone to finer laminated sandstone.

MUDSTONE FACIES

Finer grained dark mudstone strata farther to the southeast along Highway 664 contain sharp–based laminae and very thin beds of fine to silty sandstone. Some of these coarser beds and laminae are graded, and others are cross–laminated and display small asymmetric ripple forms (e.g., “lenticular bedding” and “starved” ripples, including ripple forms less than 1 cm thick) and load structures, with all top indications to the northwest. Mud drapes are visible on some foreset micro–laminae, indicating alternating episodes of current and suspension deposition. The very dark colour of the fresh surfaces may indicate mafic silt content.

Interpretation

Coarse clastic strata of the Patara Formation are interpreted as fluvial (braided river) deposits. Evidence of marine deposits, such as turbidites, is absent, and the Patara fluvial facies are similar to many other conglomerate–sandstone units thought to be of braided river origin (e.g., Eriksson 1978, Boothroyd and Nummedal 1978, Miall 1978, Rust 1978, Devaney 1987). Based on the lithofacies and sedimentary structures present and their relative and local abundance within the section (this includes the local conglomerate to sandstone ratios), the best exposures, along the Highway 664 roadside section (Figure 3), consist of, from north (top) to south, fairly good examples of proximal, medial and distal facies.

The proximal facies is coarse conglomerate with very little interbedded sandstone, possibly of mixed alluvial fan and braided river origin (e.g., coarse horizons lacking sandstone interbeds may represent the mass flows of a higher paleoslope, alluvial fan sub–environment). The medial fluvial facies is a mixed conglomerate and sandstone horizon, with thin fining–upward sequences and crossbedded and cross–laminated sandstone. One laminated pebbly sandstone bed within the medial facies contains pebble lenses interpreted as transverse ribs, structures which are considered diagnostic of upper flow regime antidune deposits that develop in very shallow subaerial streamflow (e.g., Koster 1978). The distal facies are more thinly bedded, contain minor muddy laminae and thin beds, and are more deformed (e.g., metre–scale folds). They offer less information than the medial and proximal facies regarding their paleoenvironment, but are probably distal fluvial deposits based on the proximal to distal continuum of features present.

As recognized by previous workers (Pettijohn 1934, Trowell et al. 1978, Beakhouse 1988), the basaltic clast provenance directly reflects the erosion of the local (adjacent to the northwest) Northern Volcanic belt mafic volcanic rocks, with accessory magnetite and chert (BIF) clasts reflecting the relatively minor

amount of interbedded BIF units in the source area. Geochemical analyses (*see* "Geochemistry") confirm the compositional match between the basaltic Northern Volcanic belt and the Patara Formation basalt–clast conglomerate (three samples of each were analyzed).

Within the dark mudstone unit exposed along Highway 664, graded and rippled "event beds": 1) may be either tempestites (storm beds) or turbidites (density current, or gravity current, underflows); 2) may be either lacustrine or marine deposits; and 3) do not resemble the coarser and more thickly bedded monotonous successions of turbiditic graded beds so common in Archean greenstone belts (e.g., Ojakangas 1985).

The top indications and moderate dips to the northwest in this proximal to the northwest transect suggest a coarsening–upward (prograded) sequence. Because the top indications and other sedimentary details were not previously documented, this new prograded sequence interpretation may seem surprising. The presence of highly overturned pillows in the adjacent Northern Volcanic belt (in a long roadside outcrop along Highway 664: see above, and Figure 3) was not previously appreciated, and thus the potential importance of the highly overturned Northern Volcanic belt strata adjacent to oppositely facing Patara Formation strata was not previously recognized.

As noted previously (Devaney 1997, 1999a) and detailed below, the Patara Formation is herein interpreted as a synorogenic, 20 km long strike–slip basin (Sioux Lookout orogenic belt tectono–stratigraphic Stage 6), based partly on its lazy–S shape in map view. The prograded sequence of fine grained aquabasinal (lacustrine or marine) deposits coarsening upward to locally derived, partly bouldery proximal fluvial (and perhaps also alluvial fan) deposits is similar to the infill sequences of many strike–slip basins (e.g., Nilsen and McLaughlin 1985). Dates of ca. 2700 Ma detrital zircon grains from the Patara Formation roadside outcrops (Fralick and Davis 1999) confirm the synorogenic context (cf. Blackburn et al. 1991). Note that synorogenic, "Timiskaming–type" conglomerates in Superior Province usually have polymict clast compositions, but the Patara Formation is a synorogenic, nearly oligomict (basalt clasts) conglomerate.

Regarding the probable nature of the covered contact between the Northern Volcanic belt and the Patara Formation, interpretation of the Patara Formation as the infill of a strike–slip (to oblique–slip) basin would require that the contact was a subaerially exposed fault zone during deposition of the fluvial facies of the Patara Formation. As such, this basin margin fault zone would have been at least partly eroded, and the erosion surface would have been an angular unconformity. The present boundary between the Northern Volcanic belt and Patara Formation should represent a deep erosion–level view of the original Patara basin margin fault (plus the effects of any subsequent reactivation of the fault). Note that this scenario differs strongly from the view of previous workers (see above) that considered the Patara Formation to unconformably overlie the Northern Volcanic belt in a structurally continuous, southeast–younging sequence.

The south margin of the Patara Formation is hidden beneath a large covered interval, and thus the nature of its relationship with the adjacent Big Vermilion–Daredevil unit is uncertain. At central Vermilion Lake, outcrops display a variety of features (e.g., quartzose sandstone, finer pebbles, rare felsic pebbles, granulestone, rounded granules) that differ from Patara Formation facies. This site is located south of a tectonically folded horizon, and may represent a northern facies of the Big Vermilion–Daredevil unit near a potentially deformed contact (a fault?) with the Patara Formation.

The strike–slip basin interpretation for the Patara Formation implies that some sediment would have been supplied from highlands along the south margin of the basin, highlands presumably composed of the Big Vermilion–Daredevil unit. Evidence of such has not been recognized. More detailed study of the Patara Formation and Big Vermilion–Daredevil unit exposures would help, but the lack of exposure suggests that this piece of the regional geological puzzle is not likely to be solved.

Interestingly, "back–rotation" of the Sioux Lookout orogenic belt strata (about 60º to 80º to the northwest, about an axis along the general line of strike) would produce a mostly flat to moderately southeast–dipping Sioux Lookout orogenic belt (e.g., approximating the form of a thrust belt before

wrench–induced verticalization of strata, depicted as “Stage 5” in Devaney 1999a, Figure 23.1a), except for a highly overturned Patara Formation This suggests that the Patara Formation is significantly younger than the other Sioux Lookout orogenic belt stratigraphic units, including the polymict conglomeratic Ament Bay Formation

BIG VERMILION–DAREDEVIL UNIT

Introduction, Definition and Distribution

The informally named “Big Vermilion–Daredevil unit” is a tectonized volcaniclastic stratigraphic unit located north of the Ament Bay Formation and south of the Northern Volcanic belt and Patara Formation and extending continuously along strike across the map area. This newly defined unit groups together the similar lithologies on the maps of Johnston (1972), Turner and Walker (1973), Page (1984, and unpublished data), and Devaney et al. (1995b), and its distribution is shown on subsequent diagrams (Devaney 1999a, Figure 23.2, and figures herein). As described above, this unit appears to have been lumped in with the “Patara Group” sediments by Johnston (1972) and others. The name “Big Vermilion–Daredevil unit” is meant to imply a lithological similarity to, and probable correlation with, the “Daredevil Formation,” a geographically separate unit located south of and adjacent to the Ament Bay Formation at Little Vermilion Lake.

The eastern part of the Big Vermilion–Daredevil unit, at the northeast end of Abram Lake, was mapped as the Daredevil and Little Vermilion formations by Turner and Walker (1973, Figure 1) and was mapped as containing polymict conglomerate and “Patara sediments” by Johnston (1972). Johnston did not distinguish these supposed “conglomerate” exposures from the local polymict conglomerate of the Ament Bay Formation As noted by Devaney and Borowik (1994, p. 46), “some outcrops mapped by Johnston (1972) as “Abram metasedimentary conglomerate (5d)” and “Patara tuffaceous metasediments (3f)” are better considered as coarse, possibly pumiceous, intermediate to felsic pyroclastic rocks of the Daredevil Formation.” These rocks are now included in the Big Vermilion–Daredevil unit.

The central part of the Big Vermilion–Daredevil unit extends through an area with very little exposure (eastern Little Vermilion Lake to west Abram Lake). The western part of this unit in the study area appears to consist of two sub–units separated by a mafic volcanic unit. The separation is postulated to be structural (*see* discussion of sites 4 and 5 under “Analysis of a transect across the Sioux Lookout orogenic belt,” below), but detailed structural studies were not performed and much of this area is covered by Big Vermilion Lake.

West of the study area, the continuation of this unit was mapped by Page (1984), and contains an area of volcanic flows he termed the “Redhat volcanics.” These flows may have been a source area for the predominantly volcaniclastic facies that comprise most of the Big Vermilion–Daredevil unit.

Based on lithofacies descriptions, regional map patterns, and geochronological and geochemical data, the Daredevil Formation at its type locality, Little Vermilion Lake, is considered to be part of the larger “Big Vermilion–Daredevil unit.” However, because the Daredevil Formation is a unit with a long history (Pettijohn 1934, Turner and Walker 1973) and it does form a geographically separate unit, it is separately described below.

Lithofacies

The Big Vermilion–Daredevil unit is lithofacies suite comprised of a wide variety of intermediate to felsic volcanic rocks, especially volcaniclastic facies that likely vary from pyroclastic rocks (e.g., tuff to tuff–breccia, some crystal tuff) to presumably more distal facies variably reworked by sedimentary processes: for example, “volcanic pebble conglomerate”. Sedimentological and volcanological resolution is

limited by poor quality exposures, tectonic deformation, and a lack of detailed study of some portions of the unit.

Geochemical analyses of samples, including volcaniclactic facies, reveal adakite–like characteristics (*see* "Geochemistry").

WESTERN EXPOSURES

The far western exposures in the map area, in Echo and Lomond townships (Page and Christie 1980b, Page 1984) contain outcrops of felsic porphyry (flow or intrusion?), felsic "porkose" rock (tuff or porphyry? such ambiguity is a typical problem for Superior Province workers), and one example of a graphite band (5 cm thick) in tuff.

BIG VERMILION LAKE AREA

Facies that possibly indicate sedimentary reworking include examples of: 1) oligomict lapillistone (with amygdaloidal pumice clasts) as a pyroclastic or volcaniclastic bed, apparently overlain by a rippled layer (a reworked cap?); 2) conglomeratic rock with a slightly polymict clast composition (mixing of clasts from multiple oligomict flow deposits during sedimentary reworking?); 3) polymict conglomerate (intermediate–felsic volcanic clasts) with an interbedded sandy lens; and 4) one notably unusual, "sedimentary–looking" outcrop of polymict conglomerate (on an island at southwest Big Vermilion Lake: clast–supported, very coarse, with intermediate–felsic volcanic and porphyritic clasts; a potential precursor facies to the younger Ament Bay Formation conglomerates?).

The local porphyritic rocks are felsic, with visible quartz, and of "granitic" or quartzo–feldspathic composition. Davis et al. (1988, p. 182) gave an age of 2701.0–2705.4 Ma for a rock described by them as a "'subvolcanic quartz porphyry intruded into the Patara Group'" (as noted above, most of the former "Patara Group" and the lithological units at west Big Vermilion Lake are herein considered to be part of the Big Vermilion–Daredevil unit).

Unusual lithofacies exposed on island outcrops at Big Vermilion Lake include a distinctive white felsite (brittle, highly fractured and veined; the fractures do not equal clast boundaries) and a black–clast breccia (tightly clast–supported, sandy matrix, very angular clasts). The well developed black–clast breccia fabric appears to be volcanic or sedimentary, not tectonic, and may represent highly proximal, formerly glassy brittle clasts.

The colour of volcanic rocks is not always a reliable indicator of their composition. For example, light "felsic–looking" clasts (low colour index) may be altered fragments of a more mafic protolith, and dark "mafic–looking" clasts are problematic: are they mafic, intermediate, felsic (e.g., black rhyolite), or altered? Similarly, dark matrix sandstone or tuff in the matrix areas of conglomerate, lapillistone or tuff–breccia may represent originally felsic glassy fragments (vitric grains) which were altered and/or metamorphosed to darker chloritic grains.

Mafic volcanic rocks, some of which may be gabbroic, are problematic in that they may be structurally interleaved slices of another lithostratigraphic unit rather than a true component of the Big Vermilion–Daredevil unit.

BIG VERMILION LAKE AREA ALTERATION AND MINERALIZATION

Calcium carbonate is common as veins and a few prominent bands (metre–wide to small outcrop–scale). Geochemical analyses (*see* "Geochemistry") suggest minor additions of CaO and CO_2.

Samples from the Big Vermilion Lake area (unpublished data: G. Seim, written communication, 1995) are notable for their intermediate silica content (andesite–dacite?) and carbonate content (carbonate

alteration). Low–intensity mafic alteration appears to have been developed, based on the presence of relatively high amounts of iron and magnesium oxides in some samples.

Some exposures of lapillistone (or volcanic pebble conglomerate) are rusty weathering (pyritic gossan). Only low–grade disseminated sulphide minerals appear to be present in the outcrops. The weak alteration suggested by geochemical analyses and the calc–alkalic nature of the rocks (see Geochemistry section) do not suggest good potential for VMS (volcanogenic massive sulphide) deposits.

The “Eimiller occurrence” is a gold showing on the south shore of Big Vermilion Lake (Johnston 1972, Trowell et al. 1978). Tuffs or sandy sedimentary rocks are in sharp, tectonized contact with quartz porphyry, with quartz–carbonate alteration and veins near the contact (especially within 1 m of it). This seems to be an example of veining at a site of competency contrast.

HIGHWAY 664 AREA

Along Highway 664 (the road to Hudson, which crosses the stratigraphy), the contact between the Patara Formation and the Big Vermilion–Daredevil unit lies beneath a large covered interval. Near this contact, tectonized sandstone and siltstone exposures that presumably are part of the Big Vermilion–Daredevil unit are coarser and more thickly bedded than an exposure of dark, fine grained, laminated, cross–laminated, and graded beds that is located to the northwest and is thought to be a southern portion of the Patara Formation

Small folds may be soft–sediment (penecontemporaneous) features rather than tectonic, based on apparent partial erosion and truncation of some of the folds.

A very rusty–weathered series of roadside outcrops contain clast–supported fine pebble conglomerate which is poorly sorted and crudely bedded, with sandy matrix and thin laminated sandstone interbeds (e.g., 5 cm thick). The distinctive white siliceous (felsic volcanic) clasts are small (few centimetres) and round to angular. The rounding of such a hard, physically and chemically resistant clast lithology indicates a significant degree of sedimentary reworking, hence the intense rusty weathering at this outcrop is probably not reflective of any volcanogenic sulphide mineralization.

FROG RAPIDS AREA

Near Frog Rapids (between the western parts of Pelican and Abram lakes), roadside outcrops consist mostly of highly sheared tuff or very fine–grained wacke to siltstone. Some beds are graded, with rare cross–laminae. More siliceous bands could represent felsic ash layers or alteration related to the local quartz veins. Other features noted in the vicinity include: graded clast–supported fine pebble conglomerate or lapillistone (fining to the south), pebbly sandstone or lapilli–tuff with light (“felsic”) clasts, and odd small (about 1 m long) dark alteration(?) lenses.

Highly deformed bedded rocks, suggesting the presence of a fault zone, are prominent in one roadside outcrop. Distinguishing the fabrics of tectonic deformation from soft–sediment deformation can be difficult and uncertain, but in this case the following observed features are likely tectonic: thin lensoid layers (tectonic truncation via transposition of layering, rather than sedimentary erosion or slumping), veining, pinching and swelling of bed width/thickness (boudinage), cleavage, brecciation (with interlocking jigsaw–clast shapes and highly local (0.5 m scale) variation in breccia development), a “pebbly” layer of pseudo–clasts, a fault plane (obvious offset), kinks, Z–folds, rusty (pyritic) layers (probably the result of fault permeability along fractures rather than pyritic exhalite laminae), and sigmoidal fabrics (shear zones).

PELICAN LAKE AREA

Shoreline outcrops at Pelican Lake contain tectonized, laminated to thinly bedded tuff or wacke–siltstone, thinly layered magnetite (not mapped by Johnston 1972), and crudely bedded conglomerate (or lapillistone)

with small intermediate–felsic volcanic clasts and rare intraclasts. Rare very siliceous layers may be fine felsic tuff, similar to those at Frog Rapids (see above). Rare dikes may be the “trachyte” mapped by Johnston (1972).

Conglomerates and coarse sandy beds interbedded with magnetite (lean BIF) and fine grained clastic facies suggest deposition of “resedimented” subaqueous conglomerates.

In one outcrop area, polymict conglomerate contrasts with oligomict conglomerate located to the north; this may be the contact between the north margin of the Big Vermilion–Daredevil unit and the south margin of the Patara Formation.

A western exposure of polymict volcanic pebble conglomerate is clast–supported, with small felsic pebbles common (e.g., felsic volcanic clasts; notable porphyry clasts; one quartz (chert?) cobble). This conglomerate is not as polymict as the Ament Bay Formation but is more polymict than the nearly oligomict Patara Formation. The contrasts in composition with other conglomeratic facies in the Big Vermilion–Daredevil unit, such as the white felsic clast conglomerate (along Highway 664; described above) and other conglomerate exposures nearby on Pelican Lake, indicate that a variety of different source areas provided clasts.

CENTRAL ABRAM LAKE AREA

Sample 7 (fraction 26) of Davis et al. (1988) is from this area, in which the rocks were classed as as “Patara sediments” by Johnston (1972). Davis et al. (1988) used Johnston’s terminology, so, in order to avoid confusion, the reader should note that the ca. 2712 Ma age of this “tuff” sample, herein considered to be representative of the Big Vermilion–Daredevil unit, should not be confused with a younger (ca. <2700 Ma) detrital zircon age obtained from a different unit, the Patara Formation (mafic clast conglomerate unit; see above).

The local strata contain polymict fine volcanic pebble conglomerate (e.g., intermediate–felsic volcanic clasts, variable clast size of mostly small pebbles, variable texture), and coarse to fine sandstone interbeds, some of which are laminated.

NORTHEAST ABRAM LAKE AREA

Coarse pyroclastic strata were previously mapped by Johnston (1972) as polymict conglomerate with the same map code as nearby exposures of the Ament Bay Formation.

Thinly bedded felsic lapilli–tuffs which are coarse and poorly sorted (felsic fragments in “pebbly beds”) are locally common, with some graded beds (tops to south).

One outcrop is notable for its slightly polymict, clast–supported (lapillistone) to matrix–supported (lapilli–tuff) rock, with large dark pumice clasts (of felsic composition, with visible quartz) in a coarse tuff matrix. In this outcrop, the pumice clasts are more flattened than the lithic fragments nearby. The layers richer in pumice clasts may reflect a density grading of clast types.

A minor amount of BIF is present as a thin (intra–outcrop) unit of thinly layered magnetite and wacke (varies from coarse–grained to very fine–grained to siltstone; laminated to thinly bedded, with graded beds). The paleoenvironmental interpretation is similar to that of other sandstone–hosted BIF units: a low–energy deep water setting where fine sediments and precipitated magnetite settled from suspension, with episodic deposition of turbidites via coarser sandy density currents.

Stratigraphic Conclusion

Much of the Big Vermilion–Daredevil unit appears to be composed of subaqueously deposited “volcaniclastic” facies, varying from pyroclastic to sedimentary in character, but the unit appears to offer

few clues regarding the specific sedimentary and volcanic processes and paleoenvironments of the original Late Archean (ca. 2712 Ma) basin. This may be because in a volcanically active basin, factors such as eruptions of pyroclastic material, earthquakes, and steep depositional slopes will result in a high sedimentation rate and an abundance of thick (to very thick) sediment gravity flows ("resedimented" facies; refer to Cas and Wright 1987, McPhie et al. 1993). Such a volcaniclastic succession is likely to differ strongly from classical sedimentary successions which typically consist mostly of thinly layered, well structured lithofacies assemblages that conform to various well known sedimentary facies models.

More detailed study would be required to resolve the potential structural and stratigraphic complexities of this unit. As suggested by Davis et al. (1988) using older stratigraphic terminology and Devaney (1997, 1999a) using newer terms, the Big Vermilion–Daredevil unit may be correlative with the Minnitaki Group. If so, the Big Vermilion–Daredevil unit and the Daredevil Formation might represent a more proximal and varied assemblage of lithofacies than in the Minnitaki Group. (As expanded upon below, all of these stratigraphic units are interpreted to have formed the sedimentary to pyroclastic infill of "Stage 4" basinal areas.)

Stratigraphic Patterns, Potential Correlations, and Faulting

It is notable that a few kilometeres to the south in the Central Volcanic belt there is a stratigraphic pattern similar to that at Big Vermilion Lake: in each area, porphyritic and pyroclastic rocks are situated southeast of a monotonous pillowed mafic volcanic succession. This repeated pattern in generally southeast–younging strata suggests that faulting (e.g., large thrust slices) may repeat the gross stratigraphic succession of lower mafic volcanic units transitional upward to compositionally and texturally more diverse intermediate–felsic volcanic units with associated subvolcanic porphyries.

AMENT BAY FORMATION

Lithofacies

The Ament Bay Formation is a conglomerate–dominant lithofacies assemblage with thin sandstone interbeds (Pettijohn 1934, Turner 1972, Turner and Walker 1973). Sandstone–rich units within the formation are found at Ament Bay (Turner and Walker 1973) and in the southwest part of the map area (east of Kathlyn Lake Road: Page and Christie 1980).

Clast–supported polymict conglomerate, up to cobble or boulder grade in places, is crudely to well bedded (e.g., beds tens of centimetres thick, sharp contacts, some scour pockets).

As previously described by Turner (1972, Turner and Walker 1973), a wide variety of volcanic and plutonic rocks are present as clasts in the conglomerate and pebbly sandstone. Rare and notable clast lithologies include: granitic gneiss (one 1 m clast observed), chert–magnetite BIF, recessive weathered mafic volcanic clasts, clasts with preerosion veining, a clast with a xenolith in it (see also Turner and Walker 1973), a pyritic pebble, and some muddy intraclasts in sandstone. The largest clasts are mostly granitoid, plus some large felsic volcanic clasts. Davis et al. (1988, p. 183) provided dates for two clasts: a 2887–2919 Ma "foliated tonalite clast" and a 2694–2702 Ma "massive granodiorite clast."

Beds of coarse–grained sandstone are usually pebbly and up to tens of centimetres thick. These sandy lenses and wedges contain plane laminae, crossbedding (e.g., finer versus coarser foresets, rare large trough cross–sets), cross–laminae (trough ripples), scour–based lenses, pebble bands, and small–scale lateral facies changes.

In the western part of the map area (the Kathlyn Lake Road area), coarse sandstone with pebble bands and thin (10–20 cm) pebbly conglomerate beds displys trough crossbedding, scours, and cross–lamination (ripples) and plane laminae in notably finer grained sandstone beds.

Interpretation

The conglomeratic assemblage displays features typical of deposition in a proximal braided river environment (e.g., Eriksson 1978, Boothroyd and Nummedal 1978, Miall 1978, Rust 1978, Devaney 1987). The thick sandy horizons (Turner and Walker 1973) should represent a more medial to distal braided fluvial facies. (Note: older references on the sedimentology of braided river deposits have been used intentionally; the generally poor quality of the small exposures does not provide the level of resolution necessary for the more sophisticated and contemporary "fluvial architecture" approach.) Some conglomerates deposited in deep marine settings can resemble some coarse fluvial facies (Hein 1984), but the features of a resedimented or turbiditic facies assemblage (Hein 1984, Ojakangas 1985) are not present in the Ament Bay Formation

Turner and Walker (1973) considered the Ament Bay Formation to consist of alluvial fan rather than fluvial deposits, but their interpretation was based on criteria which now, as a result of subsequent research on fluvial facies models (see references above), would be considered antiquated and incorrect. Alluvial fan sequences usually contain sediment gravity flow and hyperconcentrated flow deposits (Blair and McPherson 1994), and such facies do not appear to be present in the Ament Bay Formation. However, it should be remembered that, based on observations of modern fan settings, alluvial fans can be constructed partly or wholly by braided streams (Schumm 1977).

Sedimentological details, mostly from the best exposures, at Ament Bay, include: 1) cobble bands, with no small pebbles present, along scour surfaces (suggestive of high–energy winnowed lag surfaces); 2) a fining– and thinning– upward sequence 2.8 m thick (typical of thin braided river channel fill sequences); 3) an unusual example of clast imbrication; in this case, disc–shaped clasts lie flat along foreset surfaces and thus dip toward the paleoflow direction, or downflow, opposite to the typical upflow–dipping clast imbrication fabric produced via traction of clasts in gravelly braided rivers; 4) subtle top indicators; 5) wedging of beds (produced by thinning near channel margins and/or erosional truncation by overlying beds); 6) an intra–outcrop horizon of thin conglomerate beds shingled obliquely to the main strike of bedding (low–angle cross–stratification or lateral accretion surfaces); 7) beds in which the larger clasts are well rounded (in both two– and three–dimensional views) versus smaller, more angular clasts (suggesting that smaller clasts were less abraded during transport and primary clast shapes are well preserved); and 8) the largest clast observed, a 1.40 by 1.05 m granitoid boulder (on an island at central Abram Lake).

Sedimentological details in the western sandstone–dominant unit include: 1) rare sigmoidal foresets; 2) overturned foresets (tractional drag–induced soft– sediment deformation); 3) downclimbing foresets (deposition on downstream accretion surfaces); 4) argillite–clast breccia (intraclastic channel floor lag); 5) load structures and convoluted laminae (balls, loads and flames); 6) mudstone laminae (slack water or waning stage mud drapes); 7) a tiny dewatering pipe; 8) "ripple trains" (i.e., beds composed of a regularly spaced series of asymmetric ripples); 9) odd nodules (concretions?); 10) desiccation cracks; 11) a 1 m thick bed composed mostly of mafic clasts (sourced from a highly local ("short–headed") stream or weathered mafic boulder?); and 12) possible fining–upward sequences. The various well preserved sedimentary structures top to the south.

In this western area, ripple paleocurrents are to the west, versus crossbed foresets indicating paleoflow to the east. The small number of observations makes any paleocurrent analysis difficult and unreliable. Two speculative scenarios are that the ripples could be: 1) the result of eolian reworking on the subaerially exposed tops of sandbars; or 2) tidal deposits (e.g., tidal flood stage–oriented ripples versus fluvial crossbeds?). No evidence diagnostic of eolian or tidal environments was noted.

There may be a proximal (conglomeratic) to the east, distal (sandy) to the west pattern in the Ament Bay Formation in the study area, but stratigraphic resolution is severely limited by the paucity of exposure and potential stratigraphic and structural complexities.

The highly polymict suite of clast lithologies implies a fairly complete or diverse erosional sampling of greenstone belt–type lithologies, such as would result from synorogenic erosion of a greenstone belt (which

seems to be the case here; see discussions of Stage 5, below), plus a minor input of gneissic clasts (one of 2.9 Ga age) presumably supplied from the Winnipeg River subprovince. The 2694–2702 Ma age of the youngest clast known from the Ament Bay Formation is not precisely a "maximum age for deposition" (term of Davis et al. 1988, p. 183) because a period of time (probably at least a few million years) must be allowed for the erosional unroofing of the source granodiorite intrusion (a pluton?). Thus the Ament Bay is highly unlikely to be older than 2700 Ma and could easily be younger than 2690 Ma, but is likely to be older than the ca. 2680 Ma regional strike–slip faulting interpreted by Devaney (1999a) to have affected the Ament Bay Formation Such strike–slip faulting in the region was subsequently documented and dated by Bethune et al. (1999) at ca. 2680–2690 Ma.

The geochemical composition of the one sample of Ament Bay Formation sandstone analyzed is similar to that of samples from the Big Vermilion–Daredevil unit and Daredevil Formation (*see* "Geochemistry"), suggesting that the sand in the Ament Bay Formation sample was derived from older Big Vermilion–Daredevil exposures in the provenance area.

BASAL CONGLOMERATE OUTCROP

Turner and Walker (1973) described and interpreted a basal conglomerate outcrop (not observed during the present study) at the north margin of the Ament Bay Formation Interpretations presented in this report (below) allow for a section of volcanic rocks at Big Vermilion Lake (the Big Vermilion–Daredevil unit) to be unconformably overlain by the Ament Bay Formation.

Stratigraphic Revision: Invalidation of the Term "Abram Group"

Based on the original stratigraphic work by Pettijohn (1934) and Turner and Walker (1973), Blackburn et al. (1985, 1991) and others considered the Ament Bay Formation to be the oldest unit in the "Abram Group" (i.e., a supposedly south–younging sequence of the Ament Bay Formation, overlain in turn by the Daredevil Formation and the Little Vermilion Formation). However, the geochronological results of Davis et al. (1988) require that: 1) most or all of the Ament Bay Formation be younger than one of its granitoid clasts dated at 2694–2702 Ma; and 2) the Ament Bay Formation is thus younger than the ca. 2715 Ma volcanic rocks of the Daredevil Formation Therefore the term "Abram Group" is no longer valid and usage of the term must be discontinued.

The abrupt contact between the Ament Bay and Daredevil formations was thought by Turner and Walker (1973) to be the result of a subaerial ash fall blanketing an area of alluvial fans, followed by continued volcaniclastic deposition to form a continuous stratigraphic section. However, as outlined below, the sharp linear contact between the Ament Bay and Daredevil formations at their type locality, Little Vermilion Lake, is likely a thrust fault juxtaposing older, south–younging Daredvil Formation on top of the younger, south–younging Ament Bay Formation Interestingly, Pettijohn's (1934) original work in this area noted the many likely faults along the long straight shorelines of the lakes, but he and subsequent workers interpreted that a continuous and homoclinal section of formations was present.

Northeast Conglomerate Unit

A smaller separate unit of polymict conglomerate and sandstone crops out east of Sioux Lookout (Johnston 1972, Devaney et al. 1995b). The rocks are more deformed in this northeast part of area than in the main, larger part of the Ament Bay Formation This is a tectono–stratigraphically problematic unit; possible scenarios for its origin include: 1) it is a structural repetition of the main polymict conglomerate unit in the Sioux Lookout orogenic belt; 2) it represents a separate synthrust (piggyback) basin; or 3) it represents a strike–slip basin infilled by polymict gravel, and thus differs from the Ament Bay Formation (For tectono–stratigraphic interpretations and discussion, see below.)

DAREDEVIL FORMATION

As described above, the Daredevil Formation is likely correlative with the "Big Vermilion–Daredevil unit"; that is, it is interpreted that they were originally deposited in the same basinal succession, and later

separated by faulting into the two geographically separate units exposed today. The name “Daredevil Formation” is retained only for the strata in the type area (of Pettijohn 1934; see also Turner 1972, Turner and Walker 1973) at Little Vermilion Lake, which appear to be volcaniclastic deposits varying from pyroclastic to more reworked sedimentary facies.

Lithofacies

The northernmost (basal) facies is very coarse–grained, poorly sorted crystal lapilli–tuff with broken grains, quartz grains, poor bedding, and rare accessory/accidental clasts (very dark, mafic). Turner and Walker (1973, Figure 10) also described this “felsic crystal tuff.” The directly volcanic nature of this basal facies is important because the ca. 2713–2719 Ma age of sample 8 dated by Davis et al. (1988, p. 179, 183) is from this distinctive facies/unit. This age should represent the time of direct volcanic deposition, unlike the case of reworked tuffs, for which the age of deposition may be considerably younger than the contained detrital zirons.

The remainder of the Daredevil Formation, as observed in shoreline exposures mostly along the north shore of Little Vermilion Lake, consists of “volcaniclastic” rocks; pyroclastic or sedimentary classification terms may be equally valid. Thickly bedded, coarse–grained strata (lapillistone, lapilli–tuff) contrast with thinly bedded finer strata (e.g., very fine–grained tuff or siltstone). Graded beds, some with AB, ABD, and BCD “Bouma sequences,” are likely turbidites rather than tempestites because no shallow water wave–formed structures were recognized.

Sedimentary structures present in the sandstone beds are vague scours and ripples, starved ripples (ripple forms surrounded by muddy sediment), and penecontemporaneous (soft–sediment) deformation structures (loads, injections, potential slump horizons). Contorted bedding may form a slump horizon correlatable for kilometres along strike. Top directions are predominantly to the south to southeast.

The coarsest facies is fine volcanic pebble conglomerate (or clast–supported lapillistone and tuff–breccia) with sandy matrix, and coarse sandstone–tuff interbeds. The clast composition is “slightly polymict,” with variety of types of intermediate to felsic clasts, no granitoid clasts, and rare dark (mafic?) clasts.

LITTLE VERMILION FORMATION

Rejection of the Term “Little Vermilion Formation”

During field work, the author could not reliably identify the previously proposed “Little Vermilion Formation.” According to Turner and Walker (1973, Figure 1), exposures of the turbiditic Little Vermilion Formation occur at western Little Vermilion Lake and eastern Abram Lake. Because the “Little Vermilion Formation” is not a distinctive, regional–scale lithological unit mappable in the field, it fails the test for being a formation, and the supposed “Little Vermilion Formation” deposits are herein lumped with other stratigraphically contiguous and similar lithofacies units to form the Big Vermilion–Daredevil unit (described above).

At the type area of Little Vermilion Lake, significant differences between the “Little Vermilion” and Daredevil formations were not recognized in the exposures visited. The general similarity of the lithofacies within all three of the Daredevil Formation, “Little Vermilion Formation” and Big Vermilion–Daredevil unit suggests that they originally formed together in one volcaniclastic basin (see above).

CENTRAL VOLCANIC BELT: NORTHWEST (LOWER) BASALTIC PART

The northwest part of the Central Volcanic belt consists predominantly of massive to pillowed mafic volcanic rocks, with relatively minor felsic volcanic rocks, intrusive gabbro and felsic porphyry (Johnston

1969, 1972; Trowell et al. 1977, 1978; Reid 1978). Some mafic flow facies are vesicular or porphyritic. Top directions from pillow shapes are to the southeast; given the predominance of tops to the southeast throughout the Central Volcanic belt, this northwest part is probably the lower part. In deformation zones, shear lenses may resemble the form of pillows.

Geochemical analyses (*see* "Geochemistry") show that within this band of tholeiitic basaltic rocks along the northwestern–most part of the Central Volcanic belt, two different "sub–units" are present, a northwest sub–unit and a southeast sub–unit. This subdivision was not apparent from field studies. This is similar to the case for the Northern Volcanic belt, and illustrates the importance of geochemistry in outlining cryptic stratigraphy and suggesting correlations. The southeast sub–unit has the compositional characteristics of E–MORB (enriched–MORB) basalts (*see* "Geochemistry").

The portions of the Central Volcanic belt dominated by mafic volcanic flow facies were not examined in detail; brief highlights of some areas are listed below (in east to west order).

Superior Junction

Rhyolitic rocks crop out in the Superior Junction area in the northeast part of the map area, and are more abundantly exposed to the east in the adjacent Zarn Lake map area (Page and Moller 1979a,b). These felsic volcanic rocks are highly siliceous (whitish colour, low colour index, visible quartz, waxy lustre). Some outcrops contain lapilli–tuff (e.g., poorly sorted fabric, subangular to subround clasts, flow–banded clasts), minor amounts of recognizable bedding, and porphyritic (quartz–phyric) areas.

These Superior Junction area rhyolitic rocks differ greatly from the rest of the Central Volcanic belt and are thus difficult to relate to the other volcanic stratigraphic units. The restricted distribution of these rhyolitic rocks may record a local felsic volcanic centre. Geochemical analyses (*see* "Geochemistry") suggest that these undated calc–alkalic rhyolitic rocks are "Stage 4" volcanic rocks (see below). Based on data provided by D. Wyman (written communication, 1998), these rhyolites differ geochemically from other white rhyolitic rocks in the Central Volcanic belt, such as those near Miles Lake (see below).

Abram Lake

Along the south shore of western Abram Lake, pillowed mafic flow rock is interlayered with rare interflow chemical sedimentary facies (e.g., brecciated chert with accessory sulphide minerals).

An age of 2731.6–2733.9 Ma was obtained by Davis and Trowell (1982) from a felsic lapilli–tuff sample taken from a Highway 72 roadside outcrop near the west end of Abram Lake.

Little Vermilion Lake

The local mafic rocks are partly fine– to medium–grained, massive to sheared, and notably metagabbroic in places (green, metamorphosed). Chorlton (1991) described metagabbroic rocks in outcrops along strike to the southwest.

Highway 72 Roadside Outcrops

Felsic porphyritic intrusions are locally notable; highlights include: 1) thick felsic porphyry dikes which are schistose (and therefore predate regional deformation), and are cross–cut by syntectonic quartz veins; 2) a contact outcrop, with pillowed mafic flow facies north of felsic lapilli–tuff, both intruded by feldspar porphyry sills and dikes, plus later (cross–cutting) quartz veins; and 3) some rounded–margin phenocrysts, which could be mistaken for lapilli.

Miles Lake

At the west end of Miles Lake, highly siliceous, white felsic volcanic rock, with visible quartz grains and a waxy lustre, is intensely deformed (e.g., lensoid fabric areas, shear bands, folded veinlets, fractures).

A very similar white felsic rock crops out at eastern Big Vermilion Lake, suggesting a possible correlation between two separate predominantly mafic units (i.e., correlation of the southern marginal horizons of the Northern Volcanic belt and Central Volcanic belt, each with minor felsic bodies). White felsic volcanic rock is also notable in the Central Volcanic belt in the northeast part of the map area (at Superior Junction; see above), but the geochemistry of the Miles Lake area rhyolitic rock differs substantially from that of the Superior Junction area calk–alkalic rhyolites. Based on data from D.Wyman (written communication, 1998), the Miles Lake area rhyolite is significantly more evolved and less fractionated (suggesting a tholeiitic affinity) than the Superior Junction rhyolites.

A gold occurrence near Miles Lake (Johnston 1969) appears to have been based on analysis of a quartz vein in mafic volcanic rock (no *in situ* outcrop at this site, only blasted rubble).

Lateral Lake

Highly schistose amphibolite contains pink granitic veins (sourced from the local granitic pluton?). The boudinaged form of some of the veins demonstrates that they are not posttectonic granitic rocks.

Southwest Echo Township

The region near the former Goldlund gold mine, notable for its auriferous quartz veins in an area of mafic volcanic and felsic porphyritic rocks, was only briefly examined. The reader is referred to reports by Page (1984) and Chorlton (1991) for detailed descriptions and interpretations of the local geology and mineralization.

CENTRAL VOLCANIC BELT: NORTHEAST BAY OF MINNITAKI LAKE AREA

The volcanology of the rocks in the Northeast Bay, Minnitaki Lake area was studied by Page and Clifford (1977), Page et al. (1978), and Page (unpublished map and other data). Owing to the near absence of penetrative deformation in much of the strata in this particular area, physical volcanological features are extremely well preserved. These features have more recently been described and interpreted by the author and his former field assistants (McKenzie 1995, Devaney et al. 1995a,b; Devaney and Babin 1996, Babin et al. 1996, Devaney 1998).

The well preserved strata at Northeast Bay occur mostly within an ovoid area, the margin of which is vaguely outlined by faults or deformation zones (Johnston 1972, Page and Clifford 1977, OGS 1982, 1997; Devaney et al. 1995b, Devaney 1999a). Covered intervals, including Minnitaki Lake, limit resolution of this margin. Within this ovoid area, various facies of volcanic flows, pyroclastic to “volcaniclastic” strata, and minor sedimentary interbeds form a 4–6 km thick, somewhat “homoclinal” and apparently continuous (structurally undisturbed) succession. The lower part of this succession is dominated by subaqueous mafic flows and the upper part is a varied and complex suite interpreted herein as subaerial to subaqueous, andesitic pyroclastic facies with coeval lava flows and dikes. The succession has been subdivided into various scales of stratigraphic units (Page and Clifford 1977, Figure 89.1 and Table 89.1; Page, unpublished map; Devaney and Babin 1996, Figure 9.1). For the present study, equivalent strata to the southwest of the ovoid area (Page and Clifford 1977, Figure 89.1) received less detailed examination.

Page and Clifford (1977) interpreted the predominantly pyroclastic succession in the upper part of the the Northeast Bay succession as proximal facies of a “composite cone” (stratovolcano) or “vent complex,” and inferred that the adjacent Northeast Bay pluton or dioritic complex (see below) was the coeval subvolcanic magma chamber source of the proximal volcanic facies. Subsequent work (cited above) and the present study confirm this interpretation. However, Page and Clifford (1977) did not explicitly describe subaerial facies.

Pending the completion of a M.Sc. thesis by D. Babin. The following description is summarized from discussions with D. Babin and the author’s field observations.

Eastern Predominantly Basaltic Units

The eastern (lower) part of the volcanic succession in the Northeast Bay area is composed predominantly of mafic flows with well defined pillows. Flows (or flow units) with an internal east–to–west stratigraphy of massive to pillowed to pillow breccia facies (tops to the west) are common. Some units are porphyritic, with large (centimetre–scale) and abundant plagioclase phenocrysts.

The pillowed flows indicate a subaqueous depositional environment (e.g., a mafic plain or shield volcano). Physical volcanological details include examples of: 1) top indications via vesicles concentrated near the arcuate, convex–to–west rims (upper parts) of pillows; 2) pillow breccia fragments near the inferred top of one flow unit that appear to have sagged down, as load structures, into the formerly soft flow below; 3) a metre–scale “infolded cusp” shape at one flow contact, suggestive of localized loading of part of an upper flow downward into a partly cooled lower flow; 4) westward (upward) increases in the abundance of vesicles/amygdules within flows; 5) scoria, highly vesicular fragments in lapilli tuff or pillow breccia; and 6), at northern Alcona Bay, pillow breccia with a matrix containing superb examples of small clasts with the form of vitric shards (e.g., triangular and cuspate shapes, and some internally jigsaw–fractured clasts).

Minor amounts of interbedded felsic tuff or wacke–siltstone exhibit grading, lamination, cross–lamination (ripples), load structures, and rare scours. These units are interpreted as interflow sediments deposited in deep water (below wave base).

Western Predominantly Andesitic Pyroclastic Units

The mixed volcanic and sedimentary succession in the western (upper) part of the Northeast Bay area is notable for its basaltic andesite composition and the excellent preservation of a wide variety of pyroclastic and sedimentary features. Pyroclastic to variably reworked “volcaniclastic” facies are predominant, with less common flows and dikes.

STRATIFICATION

Bedding is crude to well defined, with crude bedding defined by subtle variations in clast size and sorting that form layers parallel to local well defined bedding. Massive horizons are more poorly sorted and lack obvious fabrics. Coarse massive to poorly internally stratified beds suggest deposition by gravity flows, either hot pyroclastic flows or cold sediment gravity flows.

It is common for the coarser beds to be relatively thick and finer beds to be relatively thin. The typical proportionality of grain size to bed thickness is a primary sedimentological relationship (and is widely useful for recognizing primary layering in deformed metasedimentary rocks).

PRIMARY FRAGMENTAL FABRICS

Most of the tuffs and the local clasts, flows and dikes contain coarse plagioclase grains or crystals. Because the clasts and matrix may be very similar in appearance, it can be difficult to distinguish porphyritic clasts

(plagioclase–phyric clasts are very common) from crystal tuff matrix (similar size and appearance of plagioclase grains) in this area. Geochemical analysis shows that the local tuffs, clasts, flows, and dikes are of strongly similar andesitic composition (see Geochemistry section), reflecting their co–magmatic origin.

In the coarser beds, both the clast frameworks and matrix tuff are typically poorly sorted. Clasts may be tightly packed, particularly in more well sorted lapillistone beds, or beds may appear loosely clast–supported, transitional to a more matrix–supported lapilli tuff

CLAST COMPOSITION

Although most or all clasts are of intermediate (andesitic) volcanic composition, and thus should be classed as oligomict in composition, some beds contain multiple types of intermediate clast lithologies and thus appear polymict. Beds described in the field as “variably polymict” or “slightly polymict” include “texturally polymict” facies (e.g., clasts are andesitic but are of different grain sizes, and some clasts may be porphyritic). Local contrasts in the composition of clasts in different beds or units (e.g., oligomict versus more polymict compositions, amygdaloidal versus porphyritic clasts) reflect compositional stratification. Leucocratic, apparently “felsic” clasts may be light–weathering intermediate composition clasts.

Clusters of similar to identical clasts define compositional bedding, which may reflect individual pyroclastic flows, (e.g., a block and ash flow sourced from a lava flow during dome collapse), or local sedimentary reworking of a volcanic flow. One outcrop contains a rare example of beds of matrix–supported tuff–breccia with porphyritic clasts that have angular, fractured–looking outlines and some jigsaw (interlocking) shapes (Devaney and Babin 1996, Photo 9.2), suggesting emplacement as a pyroclastic breccia: e.g., a block and ash flow or avalanche deposit, with cooling–cracked clasts.

Other notable aspects of clast composition include: 1) an unusual oligomict mega–clast band (representing some type of sediment gravity flow?); 2) very rare coated bombs, with features interpreted to be an asymmetric coating and a coating coarser than the bomb clasts; 3) clasts in one bed with discontinuous rims in the matrix surrounding the clasts, interpreted as “heat–welded” rims that developed in a hot pyroclastic flow; 4) rare clasts with spherules, suggesting a devitrification texture developed in vitric clasts; 5) clasts with highly vesicular (“bubble–supported”) texture, interpreted as pumice clasts; and 6) rare large flow–banded clasts (suggesting erosion of local proximal lava flows).

CLAST SHAPE

Clast outlines vary from angular to round, with increased rounding presumably reflecting an increased degree of sedimentary reworking. Angular shapes are triangular, diamond, hexagonal, and polygonal (polyhedral); the latter were likely sourced from jointed flows or blocks, with little or no sedimentary reworking. Unusual and rare clast shapes include: 1) a jigsaw micro–fractured clast rim, interpreted as a quench fabric of subaqueously erupted or peperitic lava; and 2) an outcrop horizon with large straight–edged clasts, interpreted as products of steam–fracturing (phreatic or phreato–magmatic activity) and disaggregation of solidified lava flows.

CLAST SIZE

Coarser lithofacies such as tuff–breccia and lapillistone are abundant; this western succession is not dominated by tuff. In the Northeast Bay area, relatively large clasts have long dimensions of 30 cm or more. The largest clast identified was a 1.8 m by 1.8 m mega–block, and one large, carefully studied outcrop contains a partly exposed rock body thought to be a >10 m mega–clast (Devaney and Babin 1996, Photo 9.1). The typically small size of outcrops and fairly continuous exposed surfaces (metres to tens of metres) limits resolution of very large clasts and very thick beds.

GRADING

Grading in pyroclastic rocks is problematic for field geologists in deformed successions because, particularly in coarser beds, pyroclastic flows and similar sediment gravity flows may either fine or coarsen

upward. Examples of both westward–fining (normal graded, fining–upward) tuff–breccia and westward–coarsening (inversely graded, coarsening–upward) tuff–breccia and lapilli–tuff were identified in the Northeast Bay area. Reliable top indications from such types of grading require corroborating top indications from within the same outcrop of a structurally undisturbed sequence of beds. The best examples of inverse grading are from an outcrop in which other types of top indications to the west are present (e.g., faintly defined cross–laminae, open matrix–filling laminae texture), and also because in the entire Northeast Bay succession tops to the west are ubiquitous, the coarsening–west beds are considered to be inversely graded.

Graded tuffs are not common, suggesting that neither turbiditic subaqueous flows nor direct deposition of air fall or waterlain graded tuffs were important processes in the deposition of the finer units of the succession.

SEDIMENTARY STRUCTURES

One outcrop contains thick beds of well laminated tuff/sandstone (well defined planar and parallel laminae; parallel to the strike of other local beds and thus probably orginally horizontal laminae) which may be interpreted as either airfall tuff or fluvial sheetflood deposits. A laterally discontinuous band of clasts between laminated horizons represents either volcanic bombs or a sedimentary erosional lag horizon. Only one bed containing well defined volcanic bomb–sag laminae was identified.

Crossbedding is rare. Cross–lamination (ripple foresets) is uncommon, with cross–sectional views of locally very well preserved ripple features. Apparent paleocurrent directions of the cross–laminae, defined by steep foreset slopes and the preserved stoss and lee shapes of some asymmetric ripple shapes, are nearly always to north (to northwest). The ripples appear to be asymmetric current ripples; no symmetric ripples or wave ripple structures were identified. Most of the ripples are in units or stratigraphic horizons interpreted to have been deposited in a subaerial setting, and the consistent paleocurrent direction is thought to reflect fluvial transport in an environment with a high–angle paleoslope (e.g., flank of a stratovolcano reworked by braided streams).

Rare examples of slump facies include contorted layering in tuff beds, and very rare soft–sediment injection fabrics which may be related to slumping.

A spectacular >10 m block (the size is approximate because the block or mega–clast is larger than the outcrop) with flanking conglomerate beds, pebble bands and sandstone beds is interpreted as a slump block buried by fluvial deposits. The block is internally stratified, an erosion surface cross–cuts the intra–block layering, and the onlapping clastic beds, which are parallel to the generally north–striking beds in the area, are angularly discordant to the intra–block layering. In one relatively small area adjacent to the block, angular clasts form a small wedge of breccio–conglomerate, with some clasts identical to thinly bedded strata inside the block. The wedge is interpreted as a local colluvium deposit of block–derived talus.

At one lapillistone outcrop, a minor amount of quartz is sporadically present in matrix (inter–clast) areas, suggesting the precipitation of quartz via subaerial vapour phase crystallization (McPhie et al. 1993) in inter–clast pore spaces. (Nearby outcrops contain other features suggestive of subaerial deposition.)

At one of the outcrops studied by McKenzie (1995), a wide variety of pyroclastic features have been identified by the author, McKenzie, and others. Highlights of this well bedded outcrop include: 1) normal and inversely graded lapilli–tuff beds, some of which are low–angle strata (i.e., having depositional dip angles several degrees from the paleo–horizontal), interpreted as pyroclastic surge deposits, with the low–angle strata similar to that of the large–scale antidune deposits of Rowley et al. (1985); 2) unusual small clasts with round to ovoid outlines, some of which appear indented or deformed, and some of which display fine concentric laminae, interpreted as accretionary lapilli; some of these soft clasts were dented during deposition; 3) very angular and broken–looking clasts (including odd “ridgy” textured clasts), suggestive of the explosive fragmentation of solidified (preconsolidated) lava; and 4) one bed with discontinuous rims in the matrix surrounding large clasts (as noted above, interpreted as heat welding of the matrix by hot bomb clasts).

Part of this outcrop (about 1 m of section) contains laterally discontinuous bands of accretionary lapilli (described above) which are capped by cross–laminated (rippled) beds, and are interpreted as a genetically linked sequence of beds. In this scenario: a) within an ash cloud, some ash grains formed accretionary lapilli and other grains acted as condensation nuclei for raindrops; b) accretionary lapilli landed on the earth surface; c) during or after the rain event, ephemeral runoff deposited tuffaceous sandy laminae and cross–laminae that buried the accretionary lapilli bands; and d) following a runoff event, mud in slack water pools settled from suspension to form ripple drapes (flaser bedding). Alternative interpretations are available in McKenzie (1995), who recognized neither accretionary lapilli nor ripples, and interpreted this deposit as a "hyper–concentrated flow" (by definition, hyperconcentrated flows do not contain lower flow regime structures such as ripples: e.g., Smith and Lowe 1991).

An adjacent outcrop (to the west) displays facies of a more sedimentary upper part of the local cross–section, with crossbedding, a small scour or channel, cross–laminae (ripples), and load structures.

LAVA FLOW BRECCIA FACIES: SUBAERIAL DEPOSITS

Lava flow facies are a minor component of the predominantly volcaniclastic western andesitic succession. Parallelism of plagioclase phenocrysts locally defines flow banding (regarding this fabric, note that no schistosity is readily observable in these rocks).

Autoclastic flow breccias are composed of plagioclase–phyric porphyritic andesite, with ovoid shapes representing vaguely defined breccia clasts and curvilinear "wisps" of darker matrix outlining large "pseudo–clasts." These subtly defined clast fabrics suggest incipient brecciation. At one unusual site, laminated sandstone is present in one triangular matrix area between clasts. This is interpreted as an open framework–filling "sieve" deposit; sand from the upper surface of the flow, and/or sand produced by the mutual abrasion of blocks within a moving flow, was funneled down into a large open matrix space between clasts to form infilling laminae.

Breccias with sharply defined fragments consist of angular, blocky oligomict clasts, some of which fit together in interlocking fabric (jigsaw clasts, or crackle breccia). The degree of brecciation, clast interlocking, and packing density of clasts all vary locally (e.g., over 0.1–1.0 m scale). Such breccias are interpreted as aa flows (rubbly flows or flow tops) or flow–marginal talus deposits. Some clasts are flow banded, suggesting that in some lava flows, laminar flow formed rheomorphic flow banding, followed by cooling, brecciation, and continued flow as an aa–type aggregate of blocks.

Because of the high viscosity of these types of flows, indicated by the flow banded and variably developed rubbly flow breccia fabrics, such flows are typically interpreted to have been short and thick (versus the long thin form of low viscosity flows: Cas and Wright 1987) and thus should indicate a vent–proximal setting. The lack of quench fabrics suggest deposition in a subaerial setting.

DIKES

Dikes are less common than flows in this area. Based on both field observations and geochemical analyses, the dikes are of the same composition as the surrounding clasts, tuffs and flows, demonstrating their comagmatic origin (*see* "Geochemistry"). A few gabbroic dikes are also present.

Most notable are the rare examples of dikes with margins that are "squiggly" (tortuous and embayed, at a 10 cm scale), chilled and vesicular. This squiggly form shows that such dikes intruded into unconsolidated volcaniclastic sediments, with some sagging and loading of the dike margin by the surrounding sediments. Kokelaar (1982) has suggested that the presence of a vapour film at a dike margin would provide the cohesiveness necessary to prevent the peperitic mixing of dike magmas with host sediments.

Other examples of unusual dike structures include an outcrop of crystal tuff showing the lateral termination of a dike and irregularly shaped dike margins (boudinaged and swirly to wispy to embayed

shapes, suggesting intrusion into soft sediments and subsequent deformation before cooling), with a dark band in the country rock possibly the result of minor hydrothermal alteration (dikes would have heated the local pore water).

ALTERATION FABRIC

Rare examples of irregular dark (chloritic?) fracture patterns (e.g., at northwest Neepawa Island), previously identified as autoclastic flow breccia by Johnston (1972), are thought to represent small–scale hydrothermal conduits that produced a pseudo–breccia fabric in lapilli–tuff. (Breccia fabrics are commonly problematic for field geologists; e.g., Allen (1988) and McPhie et al. (1993) have described the difficulties of describing and interpreting breccia fabrics.) Geochemical analysis of rock from this site does not suggest any strong degree of alteration.

SEDIMENTARY FACIES: SUBAERIAL (FLUVIAL) REWORKING

An unusual outcrop contains sedimentary rather than pyroclastic facies. Polymict, tightly clast–supported conglomerate and sandstone with plane laminae, pebble bands, and rare crossbedding are well exposed. The notably well rounded clasts in the conglomerate contrast strongly with the angular to subround clasts in the local pyroclastic rocks. Other evidence of sedimentary reworking at this site includes the polymict clast composition (more polymict than much of the local, more oligomict coarse pyroclastic rocks), the tightly packed clast framework (produced by the clast–by–clast accretion of tractionally rolled clasts), and stratified sandy matrix, indicative of stages of open–framework infilling in a subaerial setting. This suite of features is typical of braided fluvial deposits. Adjacent outcrops contain pyroclastic breccia fabrics (aa or talus flows, and potentially phreatic “steam–fractured” clasts, as described and interpreted above), so the stratigraphic section records fluvial reworking of a predominantly volcanic environment.

Another example of potential sedimentary reworking is a wedge–shaped bed of well layered sandstone capping (to the west of) a breccia bed displaying tightly packed clasts and minor jigsaw–clast fabric, interpreted as an autoclastic or aa flow breccia (not a fluvial conglomerate) capped by a thin fluvial channel fill of thinly bedded sandstone.

The rarity of fluvial deposits in the Northeast Bay area (these two examples above, plus the example of fluvial deposits onlapping a mega–clast described above) suggests that subaerial sedimentary reworking of the preserved parts of the succession was minor.

SEDIMENTARY FACIES: SUBAQUEOUS DEPOSITS

Exposures in the northwest part of Northeast Bay contain well stratified (thinly to thickly bedded) sandy facies, climbing ripples, and scours, features which indicate, respectively, a prevalence of currents, rapid sedimentation (perhaps from suspension to traction), and turbulent flows, in a subaqueous (lacustrine or marine) setting.

Another outcrop in this northwest area, consisting of thinly layered fine sedimentary facies with thick interbeds containing laterally discontinuous clusters and bands of large clasts, is interpreted as a low–energy aquabasinal setting periodically invaded by coarse gravity flows.

MAFIC TO INTERMEDIATE FLOW FACIES: SUBAQUEOUS DEPOSITS

These flows are massive or pillowed, and up to metres thick where measured in the typically small outcrops. Some flows appear to be mafic in composition (dark green, high colour index), but the few geochemical analyses performed indicate a basaltic andesite composition.

Pillows are locally abundant and form laterally continuous units. Physical volcanological details include: 1) concentric layering within pillows (or pillow tubes?); 2) pillow budding (lateral sequential development of pillows via breached margins); 3) downward pointing keels; 4) thin selvages; 5) vesicles (recording exsolution of gas in a shallow water environment); 6) large (1 m) pillows; 7) pillow breccia (flow top breccia, plus some flow margin or flow snout rubble facies); 8) one example of a flow with pillow imbrication (pillows were rolled forward, flow to the south); 9) spalled–off hyaloclastic pillow rims; 10) rare concentric zonation of varioles within pillows; and 11) rare gabbroic areas (co–magmatic dikes?).

Pillow structures are characteristic of subaqueous flows, and are usually assumed to be marine deposits. For parts of this western andesitic succession, the possibility of a lacustrine paleoenvironment for the pillowed flows merits consideration. It is well known that volcanic eruptions often disturb fluvial drainage and create lakes (e.g., Cas and Wright 1987). This situation would allow for a minor amount of subaqueous units within a predominantly subaerial succession. Alternatively, this predominantly volcaniclastic succession may have been submerged by marine transgressions during some periods of mafic–intermediate (basaltic andesite) flow deposition.

OTHER LITHOLOGIES

Quartz porphyry dikes with coarse (0.5–1 cm) phenocrysts, and some finer–grained felsic to granitic dikes, are rare.

The absolute age of these felsic dikes is unknown, but the quartz porphyry dikes appear to cross–cut the youngest pyroclastic unit in the Northeast Bay area. It would be of interest to see whether these dikes correspond to a younger stage of more felsic volcanism (e.g., Stage 4), or are related to postvolcanic granitic intrusions (e.g., Stage 6; for stages, se below). In the latter case, the dikes might record the "stitching together" of components of the orogenic belt by granitic intrusions.

Rocks identified during the present study as coarse–grained mafic–intermedite volcanic rocks and a very different looking coarse intrusive trondjhemite–diorite were all classed as "diorite" by Johnston (1972). A brief description of the dioritic intrusive body in the Northeast Bay area is given below.

Johnston (1972) grouped mafic pillow breccia with intermediate tuff–breccia as "mafic–intermediate agglomerate". Distinction of these lithologies by Devaney et al. (1995b) improves stratigraphic resolution of this portion of the map area.

Interpretation of Paleoenvironments and Stratigraphic Trends

As also noted in previous preliminary reports (Devaney and Babin 1996, Devaney 1998, 1999a), the present study interprets the upper andesitic, predominantly pyroclastic succession as proximal to medial, subaqueous to subaerial deposits with minor sedimentary reworking. Evidence of hot deposition is rare, but the unreworked nature (e.g., angular clasts, poor sorting, poor stratification) of much of the strata suggests that they are indeed pyroclastic (or slightly reworked, more equivocal "volcaniclastic" facies), rather than more fully reworked sedimentary facies. Thin pillowed units are thought to be subaqueous deposits, versus the thicker units of coarse fragmental facies, most of which are interpreted to be subaerial deposits. The latter coarse, supposedly subaerial units do not contain features such as mudstone beds or units, exhalite layers, and common quenched lava fabrics which might indicate a subaqueous paleoenvironment, and do not contain deposits indicative of shallow water (above wave base) conditions (e.g., wave–formed structures such as wave ripples, hummocky cross–stratification, and crossbedded shoreface sequences). Primary structures potentially diagnostic of deposition in a subaerial environment (interpreted above) include: antidune laminae in pyroclastic surge beds, heat welded rims on blocks, airfall bomb clasts, subaerial vapour phase crystallization in lapillistone, aa flows lacking quench fabrics, a colluvial talus wedge adjacent to a mega–block, asymmetric current ripples with paleocurrents approximately to the north (suggestive of fluvial paleoflow away from the inferred proximal volcanic vent area), and well stratified fluvial beds with laminated conglomerate (open framework–filling laminae) and notably rounded clasts.

The abundance of very coarse and angular clasts of volcanic composition, including mega–blocks, suggests a proximal to medial setting. The proportion of lava flow facies present is minor, suggesting that the depositional sites were more commonly in medial, rather than proximal, zones. Most of the section does not appear to be distal in nature; a greater proprtion of finer, more thinly bedded facies with more abundant evidence of sedimentary reworking would be expected in a distal setting. The variety of facies and sedimentological and volcanological features described above suggest deposition in a stratovolcanic cone setting subdivisible into proximal and distal zones (e.g., models of: Easton and Johns 1986, Cas and Wright 1987, Hackett and Houghton 1989). Page and Clifford (1977) suggested that the source vent for the pyroclastic deposits was only a few kilometres away, with the Northeast Bay pluton representing the subvolcanic feeder pluton to the pyroclastic succession. However, for the present study, it has not been assumed that only one vent area was present, and the potential presence of multiple satellite vents would complicate the generalizations about proximal–distal trends.

Although the physical volcanological and sedimentological features present seem to indicate a stratovolcano succession, the geochemical compositional variability typical of stratovolcanoes (Cas and Wright 1987) is not present. Page and Clifford (1977) described this upper pyroclastic part of the succession as a mix of basaltic, andesitic, dacitic and felsic rocks. The variable colour of the rocks in field exposures does suggest such a range in composition, but the geochemical analyses of the present study (*see* "Geochemistry") show that these rocks are mostly of basaltic andesite composition.

It is postulated that transgression–regression cycles (Figure 4) may be preserved in the upper pyroclastic part of the succession, an apparently homoclinal, continuous and orderly section of well preserved subaerial to subaqueous facies. In this scenario, major episodes of volcanic aggradation and progradation would have caused subaerial emergence and a regressional shift of paleoenvironmental facies, versus major episodes of submergence, and possibly also subsidence (e.g., caused by the loading effect of the volcanic pile, and/or evacuation of magma chambers?), which would account for transgressive shifts to subaqueous facies (Devaney 1998). Three large–scale stratovolcanic transgression–regression cycles (or sequences), about 1 km thick each, may be present, and would represent the cyclic alternation and accumulation of subaerial and subaqueous facies belts (stratigraphic units), somewhat similar to the cyclic transgression–regression cycles of clastic marine successions (e.g., Galloway 1989). The transgressive units need not be marine; volcanic deposits can dam fluvial drainage to form lakes.

At the scale of the Sioux Lookout orogenic belt, the volcanic succession at Northeast Bay represents a distinctive, relatively small, local volcanic centre within the Central Volcanic belt. Similar volcanic strata are thought to be present over extents of about 10 km along strike to the west and northeast (Page and Clifford 1977; Page, unpublished map; Page and Moller 1979a,b), but the local nature contrasts strongly with other much more extensive volcanic units in the Central Volcanic belt. The fault–bounded nature of the volcanic succession at Northeast Bay (an ovoid area suggested to be a crustal flake rotated during late tectonism; see the introduction to this Northeast Bay section, above, and discussion of site 15 in Figure 23 under "Analysis of a transect across the Sioux Lookout orogenic belt," below) suggests structural reactivation of an originally fault–bounded basin such as a volcanic graben (see below and Devaney 1999a). In western Wabigoon subprovince, the sporadic distribution of andesitic and dioritic units of ca. 2732 Ma age (Blackburn et al. 1991), the geochemical composition of older, coeval and younger arc–like units, and the presence of the ca. 2734 Ma VMS deposits at Sturgeon Lake (Davis et al. 1985, Morton et al. 1991) collectively suggest the interpretation of partially rifted arc settings for the various ca. 2732–2734 Ma rocks, including the Northeast Bay succession of the Sioux Lookout orogenic belt (see below and Devaney 1999a).

CENTRAL VOLCANIC BELT: NORTHEAST BAY PLUTON (DIORITIC COMPLEX), NORTHEAST BAY OF MINNITAKI LAKE AREA

The Northeast Bay pluton was previously described by Johnston (1972), Page and Clifford (1977) and Trowell et al. (1983). As noted above, Page and Clifford (1977) considered this pluton to represent a volcanic neck or core (feeder pluton) below a vent area located at or near the west end of the pluton, and

geochemical data (*see* "Geochemistry") confirm the co–magmatic link between this pluton and the nearby andesitic volcanic rocks. In one relatively small part of this western area, multiple dikes and lithological variability suggest the presence of a marginal dike swarm (Devaney and Babin 1996; see below).

Based on lithological and geochemical similarities, the author correlated the Northeast Bay volcanic centre and subvolcanic pluton with the Sturgeon Lake volcanic centre (caldera succession of Morton et al. 1991) and subvolcanic Biedelman Bay pluton (Poulsen and Franklin 1981), located about 60 km to the east along strike. (Devaney 1997). D.W. Davis (Royal Ontario Museum) dated a rock from this dioritic plutonic complex at 2730–2734 Ma (Davis, written communication 1998; Devaney 1999a). Therefore the Northeast Bay pluton is the same age (within experimental error) as the Biedelman Bay subvolcanic pluton and the South Sturgeon volcanics (dates of Davis et al. 1985, Blackburn et al. 1991), and the ages confirm the previous lithological correlation.

Lithologies

Rocks of intermediate composition, identified in the field as diorite, tonalite, and trondjhemite (leuco–tonalite), are fine– to medium–grained (minor coarse–grained areas too), with a good crystalline igneous texture of interlocking crystals. (One northeastern exposure appears to be more granitic.)

Dike features include chill margins, porphyritic textures, and late quartz veins. Both felsic dikes and small fractures have the same "X" pattern (conjugate fractures?), suggesting that various types of fluids (felsic magmas, sulphidic and siliceous fluids) followed the same fracture pathways. Some marginal areas of the pluton contain small mafic bands or brecciated blocks with sharp contacts which may represent inclusions, xenoliths or dikes; poor exposure limits resolution.

Sulphide minerals are concentrated along rusty fracture planes and 1 m wide pyritic gossans along vertical fractures in the diorite; malachite stain is rare. It is not known to what degree the sulphides may have been "remobilized" during recent weathering of the outcrops.

Note that Cu–Mo showing on Johnston's (1972) map is actually in the mafic volcanic country rock at the border area and not in the dioritic intrusion.

The presence of very minor amounts of Cu and Mo in a dioritic pluton suggest a possible porphyry copper type of mineralization. Note the similarities with mineralization identified farther east in the coeval and lithologically similar Beidelman Bay intrusion (Poulsen and Franklin 1981).

Heavily Diked Zone (Potential Pluton–margin Dike Swarm)

The shoreline exposures along the islands exposing the southwestern end of dioritic complex display complex and unusual features.

Numerous thin (<1 m wide) plagioclase–phyric dikes, some trending east–southeast, are commonly spaced several metres apart. There is a general alternation of pyroclastic rocks and porphyry bodies along the island shore outcrops, but outcrop resolution of contacts is poor. The better exposures reveal dikes at perpendicular angles to each other, and other examples of multiple generations of cross–cutting dikes (eg. younger porphyry in older coarser porphyry). The high density and variability of dikes appears to define a dike swarm, which may have functioned as feeder dikes to stratigraphically higher pyroclastic and lava flow facies.

One outcrop contains an odd brecciated zone with large (<0.5 m) dioritic breccia blocks. Highly variable dioritic lithologies display polygonal to irregular patterns and interlocking (jigsaw–clast) shapes, suggesting multiple stages of dioritic "auto–injection," and perhaps marking a border zone of the dioritic intrusion.

One small island outcrop contains the only example seen in the study area of concentrically zoned and rimmed clasts (alteration "shells," similar to those illustrated by McPhie et al. (1993, Plate 43–5)). These are located near potential examples of dark alteration conduits and an intrusion (equivocal field data). It is suggested that the numerous dikes in the vicinity caused local episodes of hydrothermal flow and alteration around the rims of clasts, producing the unusual zoned and multiply altered clasts.

A complex area of flows and tuff without dikes appears to mark the west margin of the dioritic area (the covered interval of Minnitaki Lake limits resolution).

CENTRAL VOLCANIC BELT: CENTRAL MINNITAKI LAKE AREA

The stratigraphy at Troutfish and Lyons bays, with abundant pyroclastic rocks, resembles that of Northeast Bay (Page and Clifford 1977), versus the lithological units at south Burnthut and south Neepawa islands which are more similar to the rocks in the southwest Minnitaki Lake area. Page and Clifford (1977) and Page (unpublished data) thought there was an orderly stratigraphy in the Troutfish–Lyons area, outlining anticline–syncline pairs, but this was not confirmed by the present study. However, because the present study was not as detailed as Page's careful volcanological mapping, Page's stratigraphy and folds are considered to be reasonable interpretations.

Lithofacies

A wide variety of intermediate–felsic pyroclastic to volcaniclastic facies are present (Devaney et al. 1995b). Highlights include rare examples of: 1) well–bedded graded tuff–wacke; 2) tightly clast–supported beds with a high percentage of fairly well sorted, rounded, very small clasts (local evidence of a significant sedimentary reworking history); and 3) two outcrops with superbly preserved flow banding and rubbly aa flow fabrics.

Mafic volcanic rocks are commonly porphyritic, with large plagioclase phenocrysts and typical pillow and pillow breccia fabrics. Some problematic outcrops contain light "clasts" in a dark matrix. (The continuum of fabrics in various outcrops suggests that the "clasts" are variably deformed pillows rather than the clasts of a sheared–up pyroclastic breccia with dark (altered?) matrix). At Burnthut and Neepawa islands, carbonate zones (orange–brown, cross–cut by quartz veinlets) are developed in fine– to medium–grained flow facies with vesicular pillows. Sedimentary interbeds of chert and laminated to rippled sandstone are rare.

BURNTHUT ISLAND

This small area is notable for its variety of lithologies and its history of exploration for gold (Johnston 1972).

At Burnthut Island, the following four lithological units (described below) crop out from south to north: felsic porphyry, basalt, wacke, and tuff. The quartz–feldspar porphyry is mesoscopically similar to the nearby Pickerel Arm porphyry bodies (see below, and Johnston 1969) along strike to the west. Distinguishing intrusive porphyritic rock fabrics from potential pyroclastic fabrics is locally problematic and uncertain (as is common for some Archean felsic rocks). Mafic volcanic rocks reveal few volcanological details, probably as a result of tectonism (the rock is highly veined in places, with quartz and epidote veins). Beds in a minor unit of sandstone (wacke) are laminated, cross–laminated, and graded (some top reversals), and are variably sheared, particularly in the finer–grained (slaty) and more schistose layers. Pyroclastic facies along the north shore of the island vary from tuff–breccia (oligomict, with large porphyry clasts) to tuff.

CENTRAL VOLCANIC BELT: PICKEREL ARM OF MINNITAKI LAKE AREA

Rocks in the following four areas form a predominantly felsic and volcanic unit of the Central Volcanic belt that crops out between the basaltic part of the Northern Volcanic belt to the north and the Minnitaki Group to the south.

Highway 72 Roadside Outcrop: Alteration and Exhalite Sequence

In the southwest corner of the map area, a geologically complex outcrop with sulphide mineralization and rusty weathering displays the following characteristics. From inferred base to top, the following sequence of units 1 to 3 is interpreted as a footwall alteration zone sequence beneath an exhalite deposit (unit 4); the sequence of units 1 to 4 is 150 m wide, with unit 1 forming the lower half: 1) layers of "FIM" (felsic–in–mafic) breccia (garnetiferous mafic alteration bands) in coarse felsic tuff–breccia; 2) felsic pyroclastic rocks (including lapillistone, clast–supported tuff–breccia, porphyritic clasts, rusty matrix); clast resolution is lost upward as alteration intensity increases; 3) a silicified "underlayer" (uppermost footwall), with pseudo–breccia texture and vague jigsaw fractures; and 4) a chert–magnetite–pyrite BIF unit (lower chert, upper pyrite; laminated; weak magnetism may reflect pyrrhotite content; centimetres thin massive pyrite layers).

This sequence illustrates that "VMS–type" footwall alteration also occurs below BIF units, and implies that the alteration is hydrothermal and sub–*exhalite* rather than VMS–related. Evidence of similar alteration is present along strike nearby to the southwest outside the map area (Chorlton 1991).

Franciscan Creek Area BIF Unit

Chorlton (1991) mapped the BIF unit in the Franciscan Creek area. Some exposures of thinly layered chert–magnetite contain structures interpreted herein as brittle deformation features. An equivocal example of this fragmental fabric ("intraformational breccia" of Chorlton 1991, Plate 2) could be of either sedimentary (intraclastic breccia) or tectonic origin.

Exposures of FIM breccia (e.g., "felsic" tuff–breccia to lapillistone, with mafic matrix, sulphides and magnetite) in the vicinity are interpreted to represent weak mafic hydrothermal alteration of footwall strata beneath the BIF unit.

Pickerel Arm Area Pyroclastic Rocks

Along the north shore of western Pickerel Arm of Minnitaki Lake, a variety of pyroclastic rocks are found: lapilli–tuff, clast–supported lapillistone, and crudely bedded (beds tens of centimetres to metres thick) polymict tuff–breccia. The coarse pyroclastic rocks contain intermediate–felsic volcanic clasts (including quartzose felsic volcanic clasts, porphyry clasts, and dark clasts which are not mafic) and a few horizons with very coarse clasts (up to 2.5 by 0.5 m) and some relatively large dark vesicular (pumice) clasts. (Small black accessory clasts are similar in appearance to those in outcrops of Daredevil Formation crystal tuff at Little Vermilion Lake, but contrasting geochemical compositions do not support a potential correlation.

Field identification of the local feldspar porphyry (with subhedral phenocrysts) is problematic (i.e., distiguishing lapilli crystal tuff with rare accidental clasts from intrusive porphyry with rare xenoliths). Distinguishing sigmoidal shear lenses from subtly defined clasts can also be an uncertain exercise.

A feldspar porphyry dike in tuff may be similar to dikes present in the nearby central and southwest Minnitaki Lake area wacke exposures.

AGE AND UNCERTAIN STRATIGRAPHIC CONTEXT

A sample of "quartz–phyric felsic tuff" (Davis 1990, p.3) exposed along the north shore of Pickerel Arm (Davis 1990, Figure 2) was considered to be from the Minnitaki Group by Davis (1990) but these rocks are described herein as part of the Central Volcanic belt. The problem is that these rocks are located along a zone that may be *between* the Central Volcanic belt and the Minnitaki Group, and their stratigraphic affinity is thus uncertain: they may be part of the Central Volcanic belt, the Minnitaki Group, or they may be part of a small, thin younger volcanic unit. The sampled tuff's age of 2701–2707 Ma is based on a single zircon grain, and this unpublished but repeatedly cited age was quoted with certainty by Blackburn et al. (1991, Figure 9.40). This age might be flawed (Devaney 1999a, p.161; i.e., about 10 Ma too young for Minnitaki Group deposition?), but other volcanic rocks (which may include reworked tuffs?) of this ca. 2704 Ma age have recently been found elsewhere in the western Wabigoon subprovince (e.g., Sanborn–Barrie and Skulski 1999) and other parts of Superior Province, so the 2704 Ma age may be valid for the Pickerel Arm area pyroclastic rocks. (Because postarc orogenic activity in western Wabigoon subprovince has previously been thought to begin at ca. 2710 Ma (Davis et al. 1988, Davis 1990, Blackburn et al. 1991), it is not clear whether these apparently ca. 2704 Ma volcanic rocks represent late arc volcanism or synorogenic volcanism. Perhaps late arc volcanism overlapped with early orogenesis during the 2700–2710 Ma period?)

Pickerel Arm Area Porphyry Bodies

Slightly mineralized (gold–copper) felsic porphyry bodies, which may represent subvolcanic intrusions, were previously described by Johnston (1969), Sutherland and Colvine (1979) and McMullan (1980). These porphyry bodies occur at or near the contact between the basaltic part of the Central Volcanic belt (to the north; thought to be the lower part of the Central Volcanic belt) and the Minnitaki Group (Johnston 1969, 1972; Devaney et al. 1995a,b), but the nature and amount of any structural repetition or disturbance of the original stratigraphic section is unknown.

At the largest porphyry body (east end of Pickerel Arm), compositional variability within the porphyry and the presence of dikes suggests either border phase variability within the intrusion, or a composite intrusion. The adjacent mafic volcanic rocks contain felsic porphyry dikes (some quartz porphyry, with notably round quartz "eyes" up to 1 cm, and some feldspar porphyry). Minor pyrite, malachite stain, and rusty weathering were observed at the surface exposures. (Most of the old trenches and pits shown on the map of Johnston (1969) could not be located.)

INTERPRETED STRATIGRAPHIC CONTEXT

The age of the porphyry bodies is unknown. The geochemical composition of the similar porphyry at Burnthut Island (see above) suggests that the calc–alkalic porphyry (see Geochemistry section) is related to "Stage 4" volcanism (the youngest stage of volcanism in the Sioux Lookout orogenic belt, and broadly correlative with the Minnitaki Group; see below). If the felsic porphyry bodies are indeed Stage 4 subvolcanic intrusions, they may represent parts of the volcanic centres which were sources of clastic detritus (e.g., felsic volcanic and porphyry clasts, volcanic sand–size rock fragments) and minor tuffaceous interbeds during Minnitaki Group deposition. Trowell et al. (1983, p. 68) made a similar suggestion regarding the provenance of the Minnitaki Group. (Stratigraphic evidence of this type of proximal volcanic source area appears to be preserved in the southeastern–most part of the Minnitaki Group; see below).

Stratigraphic Interpretation

The stratigraphic context of the rocks exposed in the above four areas is not reliably known, and potential structural complexity precludes simple stratigraphic correlations. However, the rocks in these areas have characteristics of facies and rock bodies commonly considered to be proximal to "felsic" (rhyolitic to dacitic) volcanic centres (e.g., coarse pyroclastic facies, potentially subvolcanic porphyry bodies, exhalative

BIF units, sub–exhalite alteration), and may collectively form a suite/assemblage of proximal units compared with more distal volcanic and sedimentary deposits of the Big Vermilion–Daredevil unit and Minnitaki Group (i.e., it can be interpreted that they are all “Stage 4” deposits of a mixed volcanic–sedimentary basin; see Devaney 1999a, and below). The presence of “felsic” volcanic or porphyritic clastic detritus, “felsic” pyroclastic units or interbeds, and exhalative BIF units in both the Big Vermilion–Daredevil unit and the Minnitaki Group supports this interpretation.

Previous workers considered the predominantly volcanic and felsic rocks in the above Pickerel Arm area sites to be part of the Central Volcanic belt, but these Pickerel Arm area rocks could alternatively be assigned to the Minnitaki Group, or could be considered to represent the stratigraphic interfingering of the Central Volcanic belt and the Minnitaki Group. If the Central Volcanic belt and Minnitaki Group in this area (Pickerel Arm–central Minnitaki Lake) are lumped together there is, in a very broad sense, an overall north to south transition from felsic pyroclastic facies to clastic sedimentary facies (wacke–dominated) with detritus likely sourced from the felsic pyroclastic facies. The mafic flow facies in the northwesternmost part of the Central Volcanic belt could also be considered as part of the generalized north to south transition. This is why the gross sequence in this area was previously described as “transitional,” and it was suggested that the Minnitaki Group could be considered as the uppermost part of the Central Volcanic belt (Devaney et al. 1995a, p. 27). Geochronological data suggest that there is likely a major time gap between the basaltic part of the Central Volcanic belt (Stage 2) and the younger rocks to the south (e.g., Stage 4 Minnitaki Group, presumed Stage 4 Pickerel Arm area felsic and volcanic rocks, and the Pickerel Arm area pyroclastic rocks dated at ca. 2704 Ma and discussed above), and more geochronological work would be required to refine these interpreted stratigraphic scenarios (for interpretations, including Stages 2 and 4, see below).

MINNITAKI GROUP

Following very early work by Pettijohn (1936), the deep–water sedimentary deposits of the Minnitaki Group, including turbidites, were described in detail and interpreted by Walker and Pettijohn (1971), and are further discussed below. Two main types of facies assemblages are present: thinly bedded facies (e.g., typical sandy turbidites) and thickly bedded facies (coarser; includes “resedimented” conglomerate, possible channel facies). The preservation of sedimentary structures and sedimentological relationships (e.g., bed thickness trends) is commonly excellent in this area. Important proximal–to–distal stratigraphic trends appear to be resolvable too.

Lithofacies

THINLY BEDDED FACIES

The thinly bedded facies assemblage consists of laminated to thinly bedded sandstone (wacke) and siltstone. The typical greenish grey colour of the wacke indicates that it is a muddier sandstone than the “clean” whitish arenities seen elsewhere in the Minnitaki Group.

Graded bedding is very common (e.g., BC turbidites). Cross–lamination, which may form the C layer in Bouma sequences, outlines well defined asymmetric ripples, micro–ripples, ripple trains, starved ripples, and climbing ripples. Convolute lamination (including slightly folded to loaded ripples), load structures and small scours are locally present. Interestingly, the approximate direction down paleoslope suggested by flame structure asymmetry (“flames” being upward pointing cusps between downwardly convex lobate load structures; flames point downslope where soft sediment–shearing during gravity–induced flowage has rotated the flames toward the downslope direction) agrees with that indicated by local ripple paleocurrents.

Anomalous green (chloritic?), coarse–grained interbeds in one outcrop are interpreted to be tuff, and thus constitute a rare small–scale example of interfingering of volcanic facies (synchroneity of volcanism

and sedimentation). Other good examples of rare tuff interbeds seen at southwest Minnitaki Lake (Pickerel Arm wackes).

At one site, mudstone appears to contain small (centimetre–scale) concretions.

THICKLY BEDDED FACIES

Sandy strata in the thickly bedded facies assemblage, characterized by an abundance of very coarse to coarse sandstone in beds tens of centimetres thick (up to about 1 m thick), are more thickly bedded and generally coarser than in the thinly bedded facies (above). Many very thick "beds" are actually vertically amalgamated sets of beds; recognition of such usually requires careful examination for subtle bed contacts (e.g., shown via grain size changes, rippled bed tops, muddy intraclast bands).

Beds which are pebbly only near the base exhibit "coarse–tail grading." Load structures (including flame structures) are present where some beds were loaded down into muddier layers.

Conglomerate beds are typically clast–supported. Clast size varies widely, from poorly sorted frameworks with rare boulders, to better sorted fine pebble conglomerate. Stratification within conglomerate horizons is defined by clast size variations, sharp bed contacts, and scour surfaces.

Regarding graded conglomerates, because grading can be normal (fining–upward) or inverse (coasening–upward) in conglomeratic sediment gravity flows, other evidence for the local top direction is usually necessary. For example, for one normal graded conglomerate bed a load structure indicated the way up, and inverse grading in another conglomerate bed was shown by the upward concavity of a nearby scour pocket.

The clast framework composition is typically oligomict to slightly polymict (e.g., only two clast types), with quartz porphyry clasts and some "felsic" (light–coloured intermediate–felsic) volcanic fragments too. Black intraclasts (rip–up clasts), some of which are large blocks, are distinctive versus the whitish porphyry clasts. Some associated pebbly sandstone is notably feldspathic (arkosic), further illustrating the probable strong influence of porphyritic, volcanic source rocks on the composition.

The presence of both a round quartz "eye" inside a clast (presumably resorbed quartz) and a round quartz sand grain in nearby sandstone suggests that, in contrast with more normal sedimentary processes, sand grain rounding was not necessarily erosional in this area, and provides a general lesson that sandstone proximal to source areas with porphyry may contain little–eroded but well rounded quartz grains.

Deformed strata with features suggestive of penecontemporaneous deformation, including small–scale soft–sediment injection fabrics, are locally present. Widely separated outcrops of red–weathering deformed strata appear to be correlative over about 1 km along strike (interpreted as a slump horizon; loading/injection/slumping produced dismembered or contorted layering). In some exposures it can be difficult to distinguish the clast–like appearance of highly contorted fine thin beds from true rip–up clasts.

FINER (DISTAL) CONGLOMERATIC FACIES

In the Redpine Bay area, thin clast–supported beds of fine pebble conglomerate with rip–up clasts and some felsic volcanic fragments (but still a predominantly quartz–feldspar porphyry clast composition) are interbedded with graded beds and "clean" whitish arenite. The thin beds of small clasts indicate a more distal setting than that represented by the coarser and more thickly bedded conglomeratic exposures common to the east. Although distal, these pebbly and arenitic distal facies are still fairly coarse–grained, high–energy facies, with little mud present except as intraclasts.

PICKEREL ARM AREA WACKES AND LAPILLI–TUFF

Notable local details are the presence of argillite or slate beds, sandy sections with wacke beds tens of centimetres thick, dark mudstone intraclasts at the bases and tops of some beds, and small felsic volcanic pebbles which define coarse–tail grading in some beds.

One outcrop contains important examples of probable tuffs (the best examples found in the Minnitaki Group in the study area). These anomalous, generally thin interbeds are coarse–grained, dark, green to brown weathering, relatively recessive weathered, and centimetres to tens of centimetres thick. One compound unit of three vertically amalgamated beds has a cross–laminated (rippled) bed cap on top of one of the beds, suggesting inter–event reworking of the bed top. The beds contain only a few white, pebble–size, felsic volcanic lapilli, including flow–banded clasts. The clasts in these lapilli–tuff beds are significantly larger than the tiny pebbles present in the wackes, which suggests that these tuffs are indeed more proximal and more volcanic than the potentially "volcanogenic" wackes.

CENTRAL MINNITAKI LAKE AREA

Local sedimentological details include: 1) graded beds up to 0.5 m thick; 2) a soft–sediment fold; 3) a rare small channel fill; 4) some very felsic graded beds (tuffs?); 5) felsic volcanic pebbles in wacke (generally rare; e.g., a wacke outcrop may contain only one felsic volcanic pebble); and 6) felsic fragments in coarser "arkosic" sandstone. In one lapilli–tuff interbed, clasts thought to be pumiceous have a pitted, highly vesicular, "bubbly" appearance and are far more flattened (less structurally competent) than the lithic clasts present.

Clast–supported fine pebble conglomerate is texturally polymict (two types of porphyry clasts present), with prominent white quartz porphyry clasts, rare pumice, and some angular (proximal?) clasts. Thick conglomerate beds are coarser than the local thinner ones, illustrating a common sedimentary relationship (proportionality of bed thickness to grain size) and thus showing that at least some of the bedding does not consist of random tectonic strips and panels.

Felsic porphyry sills are 1–2 m thick, with chill margins and structurally sheared margins.

Mafic volcanic flow facies with pillows and pillow breccia, may represent structurally interleaved units rather than stratigraphically intercalated units (Devaney 1999a).

Southeast Area Lithofacies: Southeast and Twin Bays of Minnitaki Lake

Strata in the Southeast Bay and Twin Bay areas are similar to the local Minnitaki Group suite of facies but are not part of the main contiguous map unit of Minnitaki Group strata. The two areas are separated from the main unit by a west–tapering volcanic unit (Trowell et al. 1982, Devaney et al. 1995b) and are probably part of a separate thrust slice (see interpretations outlined below).

A facies suite of conglomerate, sandstone, and magnetite BIF is present. Some of the coarse sandstone is whitish (mud–free, "clean"; a high–energy facies). Grading is common (turbidite beds), including one example of a scour pocket which preserved coarser sand than in the rest of the bed (representing an early phase of turbidity current flow that bypassed most of this depositional site).

Clasts are of felsic porphyry and felsic volcanic composition. The coarse sandstone, with its 2–3 mm quartz grains, further suggests derivation from a source area of quartz–feldspar porphyry (such as the "felsic" rocks present nearby to the east along strike; see below).

Magnetite BIF units are about 1 m thick each, and are internally laminated to micro–laminated, including accessory chert layers. Within some units, thinner magnetite bands have regular thicknesses (1–2 cm) and spacing (centimetre–scale), possibly suggesting cyclic sedimentation (e.g., waxing and waning of chemical sedimentation). The source area for the presumably exhalative BIF may be the same volcanic area nearby to the east along strike that appears to have supplied clasts and sand (see below).

The presence of some sedimentary stratification patterns, such as outcrop cross–sections in which sandstone bed thicknesses increase upward (tops from grading) as the abundance of magnetite decreases

(illustrating how an increased clastic sedimentation rate drowned out the effects of chemical sedimentation), show that portions of the bedded strata represent structurally undisturbed sequences of layers.

Horizons of fine–grained, greenish (metamorphosed muddy matrix), laminated sandstone and magnetite BIF indicate deposition in a low–energy setting with background chemical sedimentation. In contrast, coarse, white (arenitic), more thickly bedded sandstone, with deeper scours than in the local thinly bedded sandstone, represents a higher–energy sub–environment, with conglomeratic beds representing flows of the greatest power and competency.

One odd interbed identified as lapilli–tuff/crystal tuff might represent the stratigraphic interfingering of unreworked pyroclastic facies and the proximal volcanic equivalent of more reworked coarse white sandstone. Some beds of “siltstone” to very fine–grained “sandstone” may be distal felsic ash layers.

Based on coarseness, bed thicknesses, and map patterns, these strata in the Southeast Bay–Twin Bay area are interpreted to be some of the most proximal facies of the Minnitaki Group.

Interpretation

The Minnitaki Group is a predominantly sandy, turbiditic succession that records significant transport and reworking of material from a volcanic source area by sedimentary processes. The immature nature of the clastic sedimentary facies, the interbedded exhalite facies (BIF presumably sourced from a local volcanic centre during inter–eruptive periods), and a very minor amount of directly volcanic products (tuffs) interpreted to be to be present, show that sedimentation was synchronous with volcanism. Because of this synchroneity, the ca. 2713 Ma age obtained from Minnitaki Group detrital zircon grains by Davis et al. (1988) should closely approximate the age of both the volcanism and the probable rapid redeposition of volcaniclastic material via sedimentary processes.

Predominantly turbiditic successions such as the Minnitaki Group are usually interpreted as having been deposited in a deep marine setting such a submarine fan or ramp. Submarine fan interpretations were often based on faith in what was, for many years, the sole available paleoenvironmental model. It is notable that even in younger and better exposed turbiditic successions, it is very rare to find evidence for actual fan shapes, such as a radial paleocurrent pattern (in plan view) or wedge– to lens–shaped rock bodies (in cross–section). An alternative paleoenvironmental setting for a turbiditic succession is that of a submarine ramp, an “unstructured” ramp, apron or slope with a “line source” area from which sediment flows were supplied, as opposed to the “point source” of a submarine fan (Heller and Dickinson 1985). Other alternative paleoenvironmental settings are structural troughs in which most of the turbitic flows are funnelled longitudinally, and the submarine slopes of conical volcanic edifices.

Sites with quartz porphyry clast conglomerate, rip–up clasts, and “clean” (nonmuddy) white sandstone represent a high–energy facies, confirmed by the local presence of bouldery conglomerate, scours and small (intra–outcrop) channels (e.g., coarse conglomerate and rapid facies changes in the compound infill of a small channel unit). The conglomeratic facies likely represent sub–environments such as channel fills on a suprafan lobe or channels crossing a ramp surface. The abundance of turbidites and the presence of climbing ripples and slump facies suggest a high rate of sedimentation during episodic sedimentation events (e.g., slumps high on a ramp triggered sediment gravity flows down a sloping ramp).

Stratigraphic Aspects

At the best continuous exposure (and the best stratigraphic section), smaller–scale (5–15 m thick) fining–upward sequences are part of a larger (approximately 100 m thick) sandier–upward sequence (i.e., an overall coarsening upward, with upward increases in the “sand:shale” ratio and mean bed thickness suggesting a progradational trend).

Most of the apparent paleocurrents from ripples are approximately to the west (data from flat two–dimensional outcrops allow only approximations of paleocurrents; only a few paleocurrents are to the east).

Within the main conglomeratic "horizon" of the Minnitaki Group (approximately along the south shore of Minnitaki Lake, from East Bay islands to Redpine Bay), conglomerate beds generally become finer, thinner, and less abundant (i.e., inter–related features typical of a decrease in the conglomerate:sandstone ratio) to the southwest along strike, indicating a proximal to the east, distal to the west polarity. The same distal to the west pattern is present in what appears to be a separate and approximately parallel unit of the Minnitaki Group at Southeast and Twin bays (see above), with the likely volcanic source area preserved along strike to the east (suggesting a volcanic to sedimentary facies change; see Devaney 1998, 1999a, and interpretations below). There may also be a facies change to more distal strata, from south to north or from southeast to northwest, that links the two presumably related stratigraphic units of the Minnitaki Group (different thrust slices?).

It is notable that within the Minnitaki Group, along strike stratigraphic trends are reasonably well preserved, but vertical (cross–sectional) trends are commonly not well defined. This is likely the result of structural disturbance of the section; for example, structural repetition obscures the original cross–section of the entire Minnitaki Group, but leaves the stratigraphy well preserved within thrust slices and the limbs of upright folds (see Devaney 1999a, and below).

THE "MUD PROBLEM"

Regarding the paucity of slate/argillite exposures, mud seems to be "under–represented" in many Archean greenstone belts (see reviews of Archean metasediments by Ojakangas (1985) and Eriksson et al. (1994)), including the Sioux Lookout orogenic belt. (Admittedly, a significant amount of mud forms the tops of turbiditic graded beds, but there is still a general uncommonness of thick mudstone or slate units in the Archean sedimentary record, particularly in deep water facies in which mud would have been very likely to accumulate.) This under–representation is likely a result of exposure bias; recessive weathering of muddy lithologies has produced a biased lithological record, with the coarser, more resistant lithologies tending to form outcrops and the less resistant slates or mudstones more commonly lying beneath covered intervals. Structural overprinting can further enhance this exposure bias; faults and more deformed zones might tend to follow the less competent finer grained lithologies in a heterogeneously layered sequence, with deformed fine–grained zones more susceptible to weathering than undeformed ones.

However, a volcanological/sedimentological explanation might be even more relevant. If a basin's source of clastic detritus was pyroclastic edifices which experienced little or no chemical weathering (as would be expected in a submarine setting, or a rapidly eroded subaerial setting), very little fine mud (clay) would be transported to the more distal parts of the basin. (Obviously, Precambrian basins lack the biogenic mud component common in Phanerozoic basins.) The sandy, volcaniclastic composition of many Archean clastic sediments suggests that this was a common scenario during the Archean (Ojakangas 1985).

Both exposure bias and the likely influence of coarse pyroclastic source areas that supplied little clay may be significant factors in accounting for the rarity of the fine mud fraction in the Minnitaki Group and other similar units (e.g., the Big Vermilion–Daredevil unit, and stratigraphic units in other greenstone belts).

SOUTHERN VOLCANIC BELT

The predominantly mafic volcanic rocks of the Southern Volcanic belt were previously mapped by Pettijohn (1936), Johnston (1969, 1972) and Trowell et al. (1982, 1983), and were only briefly examined as part of the present study. Top directions from pillowed mafic flows are predominantly to the south (Trowell et al. 1982, Devaney et al. 1995b). These Southern Volcanic belt mafic volcanic rocks extend along strike to the southwest (Berger 1989) and to the east toward the Sturgeon Lake area (Trowell et al. 1982, 1983).

For the present study, attention was focused on a relatively small intermediate–felsic pyroclastic unit exposed on the east side of Southeast Bay.

Volcanic Fragmental Lithofacies

Fragmental intermediate to felsic facies vary from tuff to tuff–breccia (although a directly volcanic origin is not certain for most exposures and some facies may be slightly reworked "volcaniclastic" deposits). These facies are the "Southeast Bay Pyroclastics" of Trowell et al. (1983).

In contrast with the Minnitaki Group sedimentary rocks to west at Twin Bay and Southeast Bay, only 3–4 km away along strike, the eastern pyroclastic facies are: 1) partly composed of tuff (including crystal tuff), much of which is as coarse as the western sandstone; 2) more poorly sorted than the western sandstone; 3) not as well bedded as the western sedimentary facies; and 4) not as diverse a facies suite as that in the western sedimentary facies suite.

The lesser development of sorting, bedding and facies diversity present to the east likely reflects the predominance of volcanic, rather than sedimentary, processes there. Johnston (1972) mapped the tuff–breccia as sedimentary conglomerate, but the oligomict clast composition, poor sorting, and poor stratification present, plus the presence of some other features suggestive of volcanic processes (see below, and Trowell et al. 1983), support classification as volcanic rocks.

Distinguishing some feldspar–phyric porphyritic rocks from arkosic rocks can be problematic for the field geologist dealing with less than ideal exposures. Locally, rare clasts in lapilli–tuff and the presence of bedding demonstrate a pyroclastic or volcaniclastic origin.

Local volcanological details include: 1) one area with white, nonporphyritic clasts, defining compositional bedding at both large and small scales; 2) a few interlocking clasts (jigsaw fractures) in tuff–breccia (possibly the products of high–energy collisions, such as in an avalanche deposit, or cooling cracks in a once–hot pyroclastic flow); and 3) straight–edged clasts in tuff–breccia (possibly the products of phreatic steam–fracturing of a jointed flow?).

One good example of autoclastic flow breccia displays variably defined, mostly vague ("ghost–like") clast outlines. Subangular pseudo–clasts are of similar composition and appearance to the matrix, with some vague jigsaw shapes. Darker areas may be slightly altered, or are a matrix of finer–grained porphyry (e.g., later, fracture–filling phases that cooled more quickly).

Interpretation

Results of the present study agree with the interpretation of Trowell et al. (1983, p. 67): "The coarse clast size and the general lack of rounding of the clasts suggest that this major pyroclastic sequence was likely a proximal, near–vent deposit." The coarse facies could represent pyroclastic avalanche or sedimentary talus deposits proximal to an exogenous subaqueous volcanic dome, with rare lava flow facies (e.g., autoclastic flow breccia) deposited on or very near the dome. Exhalative venting of hydrothermal fluids from seafloor sites in the vicinity of these proximal facies and subsequent local precipitation of magnetite to form chemical sediments likely accounts for the major BIF unit present along strike nearby to the west.

These pyroclastic facies appear to be a source area contiguously linked along strike to the west to the Minnitaki Group sediments (Devaney et al. 1995a,b; Devaney 1998, 1999a). In contrast, the map of Trowell et al. (1982) placed a large northerly trending fault beneath the middle of Southeast Bay, based on a geophysical signature. Visual depictions of the amount of apparent offset along this supposed fault have varied over the years, but the facies documented herein (*see* both "Volcanic fragmental lithofacies" of the Southern Volcanic belt and "Southeast area lithofacies: Southeast and Twin bays of Minnitaki Lake" of the Minnitaki Group, above) and the map pattern present suggest that at Southeast Bay a transition (or facies

change) from eastern pyroclastic facies to coeval, stratigraphically equivalent, western sedimentary facies of the Minnitaki Group is preserved in a single stratigraphic unit. A fault may indeed be present beneath Southeast Bay, but it does not appear to have disturbed the above well preserved stratigraphic pattern, and such a fault may have been synvolcanic (which could have allowed magma to reach the paleo–seafloor and form the interpreted felsic dome).

As a proximal volcanic centre, these eastern pyroclastic facies are a probable source for the quartz porphyry clasts in the Minnitaki Group conglomerates. Note that clast lithologies need not match exactly the rocks of their proposed source areas, because some lithologies may have been completely eroded and transported away from the ancient source area (or may lie hidden beneath today's surface as subcropping units) and would therefore not be preserved there (or are hidden from view).

The geology of the Southeast Bay area is similar to the pattern interpreted for the Central Volcanic belt and Minnitaki Group at Pickerel Arm (volcanic centres as sediment sources; see above), but with a different porphyry, a greater amount of conglomerate, and more magnetite BIF in the southeastern area.

OTHER LITHOLOGICAL UNITS

Granitoid Intrusions

The few granitoid intrusions in and near the area of supracrustal rocks mapped for this study are located mostly in the northern part of the Sioux Lookout orogenic belt, particularly in the Northern Volcanic belt (Johnston 1972). These granitic plutons are not part of the present study and were only briefly examined. Their teardrop to sigmoidal outlines in map view may be an important aspect of the late orogenic development of the Sioux Lookout orogenic belt (speculated upon below). The Lateral Lake stock, dated by Davis (1990) at ca. 2708 Ma, was described by Colvine and McCarter (1977) and Page (1984), and is notable for its molybdenite mineralization.

Granitic plutons are more abundant in the extensions of the Sioux Lookout orogenic belt to the east (Page and Moller 1979a,b) and to the southwestwest of the mapped study area. Two granitic intrusions in the southwest continuation of the Sioux Lookout orogenic belt (Berger 1989, 1990; Chorlton 1990, 1991) have been dated at 2693–2699 Ma (Crossecho Lake stock) and 2693–2697 Ma (Sandybeach Lake stock) by Davis (1990).

Northeast Intrusive Complex

Geochemical analyses of intrusive rocks from the "Northeast Intrusive Complex," an area between Northeast Bay and Superior Junction (Johnston 1972, Devaney et al. 1995b), have compositions similar to sanukitoid rocks (*see* "Geochemistry"). By analogy with other sanukitoid plutons in Superior Province, the undated Northeast Intrusive Complex may be a relatively young synorogenic to postorogenic intrusion (e.g., <2690 Ma, very late tectono–magmatic context). Major faults are prominent in the area around the Northeast Intrusive Complex (Johnston 1972, Page and Moller 1979a, Devaney 1999a), and may have been the conduits along which late sanukitoid magmas were intruded.

Winnipeg River Subprovince Gneiss

The Sioux Lookout orogenic belt is bounded to the north by the Winnipeg River subprovince (Beakhouse 1991). The granitic gneisses of the Winnipeg River subprovince are not part of the present study and were only briefly examined. In a roadside outcrop at the east edge of the Sioux Lookout airport (Devaney et al. 1995b), "hybrid" gneiss (multiple lithologies, including tonalite) contains steeply plunging lineations. Such lineations are consistent with potential southeast–directed faulting of the Winnipeg River subprovince over the Sioux Lookout belt, which is the regional sense of faulting suggested by Williams et al. (1992).

Structural Geology

Because the focus of the present study is on the sedimentology, volcanology and stratigraphy of the sedimentary and volcaniclastic units that comprise large parts of the Sioux Lookout orogenic belt, the structural geology of the Sioux Lookout orogenic belt was not studied systematically or in detail. However, small–scale (intra–outcrop scale) structural features are briefly described, interpreted and discussed below for two reasons. Firstly, some documentation of observations of small–scale structures is a basic (and thus expected) part of the descriptive mapping process when dealing with rocks which have been tectonically deformed to varying degrees. Secondly, there is the need on the part of the author to demonstrate that, during the present study, sedimentary and volcanic structures have been reliably distinguished from tectonic structures.

A discussion of the various previously interpreted major faults (or deformation zones) in the Sioux Lookout orogenic belt, features which are rarely exposed but are very likely (and, in some cases, undoubtedly) present, is also given below. Interpretations of the roles of these and other large–scale structures in the multi–stage tectonic evolution of the Sioux Lookout orogenic belt are listed below under "Analysis of a transect across the Sioux Lookout orogenic belt."

SMALL–SCALE STRUCTURES

Deformation zones are defined by the presence of one or more of the following features in outcrops:

1) a highly schistose fabric, versus much less schistose rocks away

   from such zones;

2) transposed layering ("shear lenses" or "bed shreds"), with lenses of laterally discontinuous strata (commonly observed at the 0.1 m scale) rather than the presumably originally laterally continuous strata;

3) laterally discontinuous schistosity–parallel veins;

4) sigmoidal fabrics;

5) small tight to isoclinal folds (e.g., 0.01–0.1 m amplitudes and wavelengths), with rarely observed axial planar cleavage in some sequences of folded bedding; and

6) variable (reversing) top indications (with observations biased toward thinly bedded sedimentary units, which normally contain more top indications than do most other lithological suites).

Aspects of the structural geology which overlap with stratigraphic description, such as top indications and the nature of some of the contacts between units, are discussed above under "Geology of stratigraphic units."

Brittle features include kinks, tension gashes, fractures (some X–shaped conjugate patterns), and small fault offsets. Kinks tend to be developed preferentially in thinly layered strata. Ductile features include various folds (e.g., tight, asymmetric), shear zone and boudinage fabrics, and deformed clasts (oblate or flattened clasts most common; only rare examples of prolate stretched clasts observed).

Bedding–cleavage/schistosity relationships, some of which are documented on the accompanying map (Devaney et al. 1995b), were not studied in detail. Both bedding and cleavage/schistosity are normally steeply dipping.

Quartz veins, locally folded and boudinaged, are very common in all of the Sioux Lookout orogenic belt supracrustal units. Some quartz–carbonate veins are present, particularly in or near basaltic units. Accessory sulphide minerals are generally rare. Epidote veins are also found in the more mafic units.

Quartz veins with low to flat dips are uncommon to rare. The potential importance of low–dipping quartz veins to a specific structural scenario favourable for gold mineralization is discussed below, under "Mineralization in the Sioux Lookout orogenic belt."

Interpretations of the above features 1–4 are:

1) highly schistose fabric presumably reflects more intense recrystallization focused along faults and other deformation zones (e.g., along surfaces of relative displacement between lithological units, with the "units" varying from beds to kilometre–thick units);

2) transposed layering formed via layer–parallel shearing, particularly in the more thinly layered and heterogeneously layered sequences (e.g., in thinly bedded wacke–mudstone, shear was preferentially along the less competent mudstone laminae and beds);

3) laterally discontinuous veins parallel to the main fabric, normally schistosity, presumably represent originally more continuous veins disrupted by transposition along schistosity planes (alternatively, in some cases, such discontinuous veins may represent filling of extensional fractures); evidence such as tectonically disrupted bedding may corroborate a transposition origin; and

4) sigmoidal features likely formed via the: a) folding of older fabrics, such as bedding, at restraining bends (a transpressional sigmoid) and releasing bends (a transtensional sigmoid); and b) creation of new cleavage or fractures/veins (e.g., a shear zone fabric defined by shear sigmoids between schistosity planes; a transtensional "tension gash").

Regarding the orientation of folds, as is commonly the case for the generally flat and smooth outcrops of northern Ontario, good three dimensional exposure of fold axes is rare, and thus the ratio of upright folds to sideways closing folds is not reliably known. (Simplistically, upright folds are often interpreted to form during an early compressional stage, versus sideways closing folds produced during a later wrenching phase.)

Regarding the scale of folds, large folds (e.g., wavelengths and amplitudes of >5 m) are probably present in the Sioux Lookout orogenic belt, but resolution of large folds is strongly limited by the fact that the areas of covered intervals typically greatly exceed the size of the small scattered outcrops. A general absence of marker beds also limits reslotion of large folds. Such scale and resolution problems are common to northern Ontario field studies.

The scale and lateral continuity of deformation zones are problematic because of the nature of northern Ontario Shield exposures. Although maps of the Sioux Lookout orogenic belt (and many other "greenstone belts") commonly depict long (e.g., 0.5–20 km) curvilinear deformation zones, the normally discontinuous nature of the small exposures does not allow reliable distinction of the "medium–scale" (e.g., 0.01–0.1 km) form of the deformation zones (e.g., identification of planar versus braided fault zones, presence or absence of fault splays).

The effects of relative lithological competency in heterogeneously layered sequences are also important in defining deformation zones. Although deformation zones might be most ideally defined by contrasts or gradients within structural units of one uniform lithology (e.g., a highly schistose massive basalt zone flanked by weakly schistose massive basalt), deformation along the contacts between major units composed of different lithologies is very common in the Sioux Lookout orogenic belt, and most other deformed belts. At such sites of lithological contrast, allowance must be made for the easier development of schistosity in originally more micaceous lithologies (e.g., weakly schistose metawacke versus slaty mudstone).

Regarding the form of veins, although folded and boudinaged veins obviously reflect postvein deformation, deformed veins do not necessarily imply a major "early" tectonic stage of vein development versus "late" tectonic stage vein deformation: multiple late increments of deformation may deform tectonically late veins. Also, in cases of complex strain partitioning within orogens, some lithotectonic units may be less deformed internally (e.g., early veins unaffected by "late" tectonism) while other units become very deformed (e.g., "early" and/or "late" veins affected by late tectonism). Detailed structural study would be required to resolve various episodes of veining and deformation and their spatial variability.

LARGE–SCALE STRUCTURES

Description and structural analysis of the large–scale structures of the Sioux Lookout orogenic belt is beyond the scope of the present stratigraphic study. However, large–scale structures and map patterns evident from past and present mapping obviously need to be incorporated into any regional geological interpretations. Aside from the extensive faults and deformation zones discussed below, large–scale structural features of the Sioux Lookout orogenic belt are summarily listed and briefly interpreted under "Analysis of a transect across the Sioux Lookout orogenic belt" (see below) and by Devaney (1999a).

DISCUSSION OF PREVIOUSLY MAPPED FAULTS

As a result of previous mapping of the Sioux Lookout orogenic belt by Johnston (1969, 1972), numerous linear and curvilinear "faults" were depicted on Johnston's three maps (Maps 2155, 2242, 2243). Most of these faults are parallel to the strike of the major lithostratigraphic units in the Sioux Lookout orogenic belt, plus a few faults at high angles to strike (splays, "cross–faults") and some faults of limited extent in small areas of relatively deformed rocks. Using some terms defined during earlier work by Pettijohn (1934–1937), the longer and presumably more important faults were named and described in some detail by Johnston (1969, 1972). In more contemporary terms, these "faults" might be better described as more broadly defined "deformation zones" (see above). (Faults are brittle features by definition, and in some cases, more ductile features such as shear zone fabrics are present along these Sioux Lookout orogenic belt "fault zones.")

Importantly, it is noted in the legend for Johnston's (1969, 1972) maps that the presence of these faults in the Sioux Lookout orogenic belt is "assumed" (i.e., interpreted) rather than observed. This is because, as is commonly the case in the glaciated Shield terrain of northern Ontario, faults and other deformation zones tend to have been recessively weathered and lie beneath covered intervals such as lakes. Thus, as is also the case for many other geological maps of northern Ontario greenstone belts, on Johnston's (1969, 1972) Sioux Lookout orogenic belt maps *interpreted* features such as the faults inferred to be present have been mixed with *descriptive* data.

Even though the interpretations of the presence of faults by Johnston (1969, 1972) may be very reasonable, the general lack of exposure of the major deformation zones presents a huge problem for geologists who would like to actually observe, map and interpret the structural features in the area. Many of the faults depicted on Johnston's (1969, 1972) maps were incorporated directly into the map of Devaney et al. (1995b; see accompanying map).

The faults on Johnston's (1969, 1972) maps were suggested by the presence of both large–scale map patterns (e.g., long straight shorelines near the contacts between major lithostratigraphic units: Pettijohn 1934) and small–scale deformation fabrics in the outcrops near the inferred faults. As direct evidence of deformation within or adjacent to the mapped faults, Johnston (1969, 1972) emphasized the presence of one or more of the following: relatively intensely developed schistosity; "shearing"; alteration (especially carbonitization); quartz veins (or, more rarely, epidote veins); and occurrences of certain minerals (e.g., gold, sulphide minerals).

Although the present study is focused on regional stratigraphic descriptions and interpretations rather than documentation of structural fabrics, field observations confirmed the importance of the five features listed above in defining Sioux Lookout orogenic belt deformation zones. Intense schistosity along deformation zones contrasts markedly with the weakly schistose rocks which make up most of the Sioux Lookout orogenic belt. (Rocks with well preserved primary volcanological and sedimentological fabrics and little or no readily observable mesoscopic schistosity are locally common in the Sioux Lookout orogenic belt). Indeed, basaltic and conglomeratic rocks along the shoreline of eastern Abram Lake (near where the "Little Vermilion Fault" and "Abram Lake Fault" converge, according to Johnston 1972) are so schistose, with "slaty" cleavage in places, that modern erosion has formed "shingle beaches" of platy clasts.

Observations made during the present study confirm the probable presence of major deformation zones at the following localities mapped as faults by Johnston (1969, 1972): Big Vermilion Lake ("Whitefish Bay Fault"); Little Vermilion and Abram lakes ("Little Vermilion Fault" and "Abram Lake Fault"); northwest shore of Northeast Bay of Minnitaki Lake; southeast shore of Northeast Bay of Minnitaki Lake (part of the "Ruby Island Fault"); Neepawa Island; Burnthut Island; and Pickerel Arm (particularly along the north shore). In the western half of the study area, within the predominantly basaltic part of the northern Central Volcanic belt, the extent (along–strike continuity) of deformation zones near Miles and Misfit lakes is unknown.

The presence of most of the larger scale faults proposed and depicted by Johnston (1969, 1972) can be inferred from contrasts and discordances in patterns of total field magnetism (e.g., data in OGS 1982, 1997).

Of all of the major faults proposed by Johnston (1972), only one, a supposedly west–northwest–trending fault located immediately east of the town of Sioux Lookout, is rejected as unlikely. The stratigraphy presented herein (*see* "Big Vermilion–Daredevil unit," above; see also accompanying map) suggests that the major lithostratigraphic units present east of the Sioux Lookout town area are laterally continuous rather than truncated or offset by a fault (e.g., an apparent sinistral offset of "Patara metasediments" shown on Johnston's (1972) Map 2243). The supposed fault is in a linear area with almost no bedrock exposures. Geophysical maps (e.g., total field magnetism: OGS 1982, 1997) suggest that, at the 5 km scale, strata (probably part of the Northern Volcanic belt) may have been warped into a west–northwest–striking orientation by the intrusion of a granitic pluton in the Pelican Lake area. One of these west–northwest lineaments, which are discordant to surrounding east–trending and east–northeast–trending lithostratigraphic units, may have been mistaken as a fault.

Many of the faults interpreted by Johnston (1972) are very relevant to the structural scenarios outlined in the present report (see below). The "Little Vermilion Fault" along the north margin of the Central Volcanic belt should be a north– to northwest–vergent thrust which placed the Central Volcanic belt above younger sedimentary and volcaniclastic units to the north (Davis et al. 1988), and the "Daredevil Fault" should be a northwest–vergent thrust which juxtaposed the older Daredevil Formation above the younger Ament Bay Formation (Devaney 1999a). Johnston (1972) agreed with Pettijohn's (1934) suggestion that strike–slip faulting was important in the Sioux Lookout orogenic belt, and mapped some strike–slip faults ("Ruby Island Fault, Twinflower Fault, East Bay Fault") as being sinstral–oblique (Johnston 1972, Figure 2). The "bending" and "horsetailing" of some of Johnston's (1972) faults define map patterns suggestive of sinistral strike–slip duplexes (see Devaney 1999a, and below). Indeed, Johnston (1972, p. 30) recognized that the faults in the northern Sioux Lookout orogenic belt are likely a southwest extension of the Miniss River Fault, which is considered herein (see Devaney 1999a, and below) to be a key aspect of the large–scale regional geology.

Although detailed mapping of the faults and deformation zones of the Sioux Lookout orogenic belt by a structural geology specialist would obviously be a good complement to the stratigraphic work presented herein, and would be very relevant to improved understanding of gold mineralization in the region (probable late tectonic, mesothermal lode gold deposits), a structural specialist should expect to be frustrated by the general absence of exposure of the deformation zones and the poor quality of most exposures (e.g., small, discontinuous exposures; unclean outcrop surfaces; rarity of good three–dimensional exposure). (Note: exposure quality considered "poor" by global standards would be considered as "typical" or even "good" by many workers with experience biased towards northern Ontario terrain. The more global standard has been used herein.)

Geochemistry

Lithogeochemical analyses of 85 samples from the Sioux Lookout orogenic belt study area (Figure 5: sample location map) are given in Table 1. The analyses were performed by the Geoscience Laboratories, Ontario Ministry of Northern Development and Mines, using: X–ray fluorescence (major oxides, Ba, Cr,

As, Pb, Zr, Y); inductively coupled plasma–optical emission spectroscopy (Cu, Zn, Ni, Sc, Au, Co, Mo, V), inductively coupled plasma–mass spectroscopy (REE, Th, U, Hf, Ta, Rb, Sr, Nb, Cs), anion analysis (Cl, F), and atomic absorption spectroscopy (Ag, Cd, Li, Hg).

The samples are listed according to their stratigraphic unit, lithology and type of alteration in Table 2. (The rock types listed in Table 1 are field terms, and differ slightly from those in Table 2.) Averages of the major oxide composition of the principal units are shown in Table 3. For Figures herein which use major oxide values, recalculated volatile–free values have been used. Total iron oxides are listed as Fe_20_3.

In most cases, geochemical analysis confirmed the correctness of the field identification of the various rock types. Despite some alteration, the SiO_2 content of the different stratigraphic or lithologic units is appropriate for the assigned rock type names (e.g., averages in Table 3). Identification of the altered nature of some of the samples (Tables 2, 4) is based on relatively high or low abundances of oxides or volatiles; for example, abundances above or below arbitrarily chosen threshold levels. Following this approach, and in agreement with threshold levels derived from other studies (e.g., Devaney 1996), rocks with >4% LOI and/or >1% CO_2 and/or <1% Na_2O are considered to be altered. Regarding the sample codes used in Tables 2, 4 and 5, samples prefixed with a: a) "B," or having no prefix, are "94JRD–" samples in Table 1; and b) "DB" are "95JRD–" samples in Table 1.

GEOCHEMICAL SUBDIVISION OF STRATIGRAPHIC UNITS

Previous studies of the major element geochemistry of the Sioux Lookout orogenic belt and surrounding areas (Trowell et al. 1983, Blackburn et al. 1985, Trowell and Johns 1986, Blackburn et al. 1991) established a general stratigraphic framework of older magnesian tholeiitic basalts versus younger high–iron, high–titanium tholeiitic basalts and a diverse suite of calc–alkalic volcanic rocks.

Selected basaltic discrimination diagrams (Figure 6a–e) and plots of the contents of selected high field strength elements (HFSEs; e.g., TiO_2, P_2O_5, Zr) and Zr/Y versus SiO_2 provide subdivisions of both the volcanic rock samples (Figure 7a–c) and the entire Sioux Lookout orogenic belt sample set (Figure 8a–f). These subdivisions (unlabelled) are defined by discrete data point clusters according to sample lithology and/or stratigraphic unit; many such clusters are mutually exclusive with other clusters.

Based on selected trace element ratios and plots of selected high field strength elements (Ti and P oxides, and La, Nb, Th, Zr) and Zn versus SiO_2 (Figure 9a–g), the sampled basaltic subunits of the Sioux Lookout orogenic belt form 2 discrete groups (Tables 5, 6). Very similar compositions allow the correlation of the Northern Volcanic belt and the northern Central Volcanic belt basalts (as one group), versus the distinctly different, more southern Central Volcanic belt basalts.

The Central Volcanic belt "mostly dacitic pyroclastic rocks" sample group in Table 2 (intermediate–to–felsic volcanic ("ifv") in Tables 3, 6, and 7) can be subdivided into 3 subgroups via plots such as Th/Ta or $(La/Yb)_{CN}$ versus TiO_2 (Figure 10a,b).

As expanded upon below, the discrete and coherent lithological subdivisions (data point clusters) apparent in Figures 6 to 10 directly reflect the orderly contrasts in composition of the various Sioux Lookout orogenic belt stratigraphic units.

RARE EARTH ELEMENT DATA

The rare earth element (REE) data (Table 1) for each sample group are presented in chondrite–normalized plots (Figure 11; note some subgroups) and in N–MORB–normalized extended trace element plots (Figure 12; data are normalized to chondrite and N–MORB reference standards of Sun and McDonough 1989).

Basalts of the Northern Volcanic belt (Figure 11a) and northern Central Volcanic belt (Figure 11c) have fairly flat REE plot slopes (low $[La/Yb]_{CN}$ ratios) and REE abundances at about 10x chondrite level.

REE characteristics of the Patara Formation mafic sediments (Figure 11b) mimic those of the Northern Volcanic belt basalts (Figure 11a), consistent with the probable derivation of the Patara sediments from the Northern Volcanic belt. Slightly higher REE concentrations (up to 20x chondrite level) in some Patara samples may be due to sedimentary enrichment (e.g., via winnowing) of REE–bearing heavy mineral sand grains.

Contrasting with the above basalts, more southern basalts of the Central Volcanic belt (Figure 11c) have low REE plot slopes ($[La/Yb]_{CN}$ ratio of about 6) and LREE abundances of about 40–70x chondrite level. These basalts are more evolved (E–MORB; criteria of Pearce and Peate 1995) and fractionated (steeper REE plot slope) than the more primitive (N–MORB–like) basalts of the Northern Volcanic belt and north Central Volcanic belt (Figure 11a,c; see also Figure 12a,c).

Most of the remainder of the plots (Figure 11d–n), of intermediate to felsic rocks, display high slopes with chondritic abundances of about 100x (La) decreasing to 10x (Yb). Elevated LREE content is notable in some dacitic to rhyolitic rocks (Figure 11j,k) and Northeast Intrusive Complex samples (Figure 11m). Superior Junction rhyolite samples display slightly elevated HREE content in 4 of 5 samples (Figure 11j). The atypical composition (low HREE abundance) of sample J–92 (Figure 11i), a tuffaceous sandstone, could reflect carbonate alteration (HREE lost to carbonate–bearing fluids: Kerrich and Fryer 1979) or some volcanic or sedimentary mixing of grains from multiple source areas (e.g., mafic and felsic sediments deposited together at bed scale).

The basaltic andesites of the Northeast Bay of Minnitaki Lake area are of similar REE composition in the lower, middle and upper parts of the stratigraphic section (east to west; Figure 11d,e,f, respectively). The various distinct lithofacies (flows, dikes, coarse and fine pyroclastics) also have uniform REE characteristics, suggesting little or no disturbance of “pyroclastic” facies by sedimentary reworking (much sedimentary transport would segregate heavy minerals) and thus fairly proximal conditions. The strong similarity between the plots of the dioritic Northeast Bay pluton and the upper (and other) basaltic andesite samples (Figure 11d–h) is further evidence of their co–magmatic relationship.

Within the entire Sioux Lookout orogenic belt sample set (Figure 11), negative Eu anomalies are more common than a positive anomaly or no anomaly. Negative Eu anomalies are the results of plagioclase fractionation or alteration, with the latter case involving loss of Eu during the chemical breakdown of feldspar grains (Rollinson 1993). Because the Superior Junction rhyolites are likely altered (shown by abundances of some major and minor elements: Table 4), the large negative Eu anomalies in these rocks (Figure 11j) may also be an alteration signature. Plagioclase–phyric dikes in the Northeast Bay of Minnitaki Lake andesites (Figure 11e) have a greater negative Eu anomaly than in tuffaceous samples from nearby sites, suggesting the greater influence of plagioclase fractionation for the dike samples.

Extended trace element plots (“spidergrams”) normalized to N–MORB composition are shown in Figure 12. Most notable are the slight/minor negative Nb anomalies in the basaltic rocks, a larger (moderate) negative Nb–Ta anomaly in the basaltic andesites, and the large (more prominent) negative Nb–Ta anomalies in the dacitic–rhyolitic rocks (Figure 12i,j,k), granitoids (Figure 12n) and 2 of 3 Northeast Intrusive Complex samples (Figure 12m).

The Hf data for the more mafic rock samples appears to be experimentally flawed (Tomlinson et al. 1999) and thus the apparent negative Hf anomalies are considered to be false ones.

GOLD ASSAY DATA

Lithogeochemical analyses and assays resulted in only one important new gold occurrence, sited on the mainland west of Burnthut Island, at the “Number 3 zone” reported by Johnston (1972, p. 43). A sample from a pyritic quartz vein yielded assays of 2.12 and 2.34 ounces Au per ton (Devaney et al. 1995a); a previous assay reported by Johnston (1972) yielded only 0.04 ounces Au per ton, illustrating the erratic or variable nature of the gold mineralization.

DISCRIMINATION PLOTS

Data from the Sioux Lookout orogenic belt basaltic samples are shown on 5 different discrimination diagrams (Figure 6a–e). Such diagrams were designed for elucidating the tectonic setting of basaltic rocks, but some workers (e.g., Wood 1980) also include more felsic rocks for purposes of comparison. Table 7 summarizes the fields that the various Sioux Lookout orogenic belt volcanic stratigraphic units plot in, which allow the interpretations summarized in Table 8.

Using a Rb versus Y+Nb plot (Pearce et al. 1984a, Christiansen and Keith 1996), all of the plutonic samples plot in the "I–type" or "volcanic arc granite" field (Figure 13a), and nearly all of the intermediate to felsic volcanic rock samples plot in the same field (Figure 13b).

SUBDIVISION VIA Mg#

The Sioux Lookout orogenic belt sample groups define fairly discrete fields on a Mg# versus SiO_2 plot (Figure 14a; Mg# = MgO/[MgO+Fe_2O_3*]: Rollinson 1993, p. 74; recalculated volatile–free oxide values used herein). A plot of Mg# versus K_2O for samples with less than 3% K_2O (Figure 14b) shows the low–K nature of the magnesian basalts (Northern Volcanic belt, north Central Volcanic belt; Mg# >0.3; Stage 1 magnesian tholeiites), ferro–basalts (south Central Volcanic belt; Mg# <0.3; Stage 2 iron tholeiites), and many of the basaltic andesites (Northeast Bay of Minnitaki Lake; average Mg# is 0.30; Stage 3). A plot of Mg# versus La/Sm (Figure 14c; the latter ratio defines LREE fractionation or enrichment) provides a particularly good subdivision of the various rock types and genetic (evolutionary) stages.

Rocks from the Sioux Lookout orogenic belt with a Mg# of greater than 0.3 (Northern Volcanic belt and north Central Volcanic belt Stage 1 basalts; many of the Northeast Bay of Minnitaki Lake Stage 3 andesites; 2 of 3 Northeast Intrusive Complex sanukitoid samples) can be considered to be more "primitive" ("quasi–primitive"?) than those with a lower Mg#. Concentrations of Ni and Cr are high (>90 ppm Ni, >130 ppm Cr), relative to other Sioux Lookout orogenic belt rocks, in these "quasi–primitive" rocks. Note that the change from Stage 2 to more primitive Stage 3 volcanic rocks coincides with an interpreted "rifted arc" extensional phase (see below, under "Evolutionary stages of the Sioux Lookout orogenic belt"). The primitive nature of the possibly late–stage Northeast Intrusive Complex sanukitoid rocks (see below) reflects their probable mantle derivation (e.g., Stern and Hanson 1991, Evans and Hanson 1997).

FEATURES OF E–MORB CLASSIFICATION

For basalts, a plot of Zr/Yb versus Nb/Yb shows the enriched versus depleted continuum within a MORB array of values (Pearce and Peate 1995). In Figure 15, southern Central Volcanic belt basalts (relatively more E–MORB–like; Stage 2) are more enriched than the Northern Volcanic belt and northern Central Volcanic belt basalts (which are closer to average N–MORB values; Stage 1), a distinction which is in agreement with other discrimination plots.

A plot of Th/Nb versus Nb/Y (Syme et al. 1996, Figure 16) shows southern Central Volcanic belt basalts in or near the E–MORB field (Figure 16), versus the Northern Volcanic belt and northern Central Volcanic belt basalts which plot in the "N–types with arc signature" field (the "arc signature" being the negative Nb anomaly, or Th/Nb of >0.1).

FEATURES OF BACK–ARC BASIN BASALT CLASSIFICATION

Basalt samples which have negative Nb anomalies and slight LREE enrichment (relative to N–MORB) and which plot in a transitional N–MORB to island arc tholeiite field on discrimination diagrams (see Figures

6a–c and Figures 12a,c) are commonly interpreted as back arc basin basalts (e.g., Saunders and Tarney 1984, 1991; Day 1990, Donato 1991). Both the Northern Volcanic belt and Central Volcanic belt basalts (Stages 1, 2) could be interpreted as back arc basin basalts. However, in the case of the Sioux Lookout orogenic belt, there is no known arc sequence of appropriate age (Stages 1, 2) and location (probably southeast of the Sioux Lookout orogenic belt) that would have been required in order for a linked arc and back–arc pair to have existed, so the term "pre–arc" (Pearce et al. 1984b), rather than back–arc, may be more appropriate for Stage 1 basalts. Stage 2 basalts may represent a change to a juvenile arc setting (Table 8). (Note: although coeval and older arc sequences are present to the east of the Sioux Lookout orogenic belt at Sturgeon Lake (Blackburn et al. 1991, Sanborn–Barrie and Skulski 1999), the Sioux Lookout orogenic belt is not considered to be a back–arc area relative to the similar arc sequences at Sturgeon Lake. At an appropriately large scale of view (200 km), the Sioux Lookout orogenic belt, relative to the Sturgeon Lake area, is considered to be in an "along–arc," rather than "back–arc," position.)

Based on the geochemical diagrams and discussion of Saunders and Tarney (1991), the ratio plots in Figures 17a–c show that the Sioux Lookout orogenic belt basalts (Northern Volcanic belt, Central Volcanic belt) have back arc basin basalt to island arc characteristics, with the southern Central Volcanic belt basalts in the E–MORB field (in agreement with other discrimination plots) in Figure 17b (Ce/Zr vs. Ba/Zr).

ADAKITES

Adakites are high–Al trondhjemite–tonalite–dacite/granodiorite rocks) with geochemical signatures thought to have been produced via partial melting of subducted slabs of MORB–type basalt (oceanic lithosphere; Sajona et al. 1993, Drummond et al. 1996). The adakitic signatures apparently were not obscured by the ascent of slab melts through mantle wedge regions.

Based on the geochemical diagrams and discussion of Drummond et al. (1996), the ratio plots in Figure 18a–e show that the Big Vermillion–Daredevil unit and some Central Volcanic belt dacitic rocks (both Stage 4) have adakite characteristics, and the Northeast Bay of Minnitaki Lake basaltic andesites (Stage 3) have "island arc andesite–dacite–rhyolite" to transitional adakite characteristics. Potential mobility of Sr and Cs has not been a problem because the same trends are seen in both the unaltered and altered samples. Nb–enriched basalts tend to be associated with adakites (Drummond et al. 1996); note that the Northeast Bay of Minnitaki Lake basaltic andesites contain approximately 10–20 ppm Nb, a relatively high concentration for the Sioux Lookout orogenic belt samples and a further indication of their near–adakitic nature.

FI–FII FELSIC VOLCANIC ROCKS

Plots (not shown) of Zr/Y versus Y and chondrite–normalized La/Yb versus Yb (e.g., Lentz 1998) for Sioux Lookout orogenic belt felsic volcanic rocks (Stage 4) have FI (Lesher et al. 1986) to unclassified characteristics. These highly fractionated, calc–alkalic rocks can thus be considered to have poor VMS potential. Unanalyzed and undated rhyolites spatially associated with Stage 1 or 2 basalts (e.g., in western Sioux Lookout orogenic belt, at Miles and Franciscan lakes; see site 12 in Figure 23 and maps of Johnston (1969) and Page and Christie (1980b)) may be of a more tholeiitic nature (e.g., an earlier stage bimodal basalt–rhyolite succession?) and might have better VMS potential.

SANUKITOID CHARACTERISTICS OF THE NORTHEAST INTRUSIVE COMPLEX SAMPLES

Three samples from the northeast intrusive complex are highly fractionated (steep REE plot slopes) with high LREE content and little or no Eu anomaly (Figure 11m). These REE characteristics, the mean Mg# (0.33; see also Fig. 14a), and the mean contents of LILEs (e.g., Ba: 1266 ppm; Sr: 1187 ppm) and transition elements (e.g., Cr: 128 ppm; Ni: 43 ppm; Co: 15 ppm) meet most of the criteria of Stern and Hanson (1991) for intermediate intrusive sanukitoid rocks.

It is notable that the Northeast Intrusive Complex, a small plutonic unit, is located where interpreted strike–slip faults are clustered and converge in the northeast part of the Sioux Lookout orogenic belt; late orogenic faults are commonly thought to have provided conduits for sanukitoid magmas (Kerrich 1989).

VOLCANIC ARC GEOCHEMICAL EVOLUTIONARY STAGES

By synthesizing stratigraphic relationships, geochronological data (Davis et al. 1988, Davis 1990), and the geochemical descriptions and interpretations presented above, the Sioux Lookout orogenic belt samples can be interpreted to represent 4 main volcanic stages plus other postvolcanic sedimentary and plutonic stages (Tables 5, 6, 7, 8).

Sioux Lookout orogenic belt volcanism developed from early tholeiitic mafic stages to late calc–alkalic intermediate to felsic stages (Tables 3, 6) during the ca. 2740–2710 Ma period. A REE plot combining a representative sample from each interpreted volcanic stage (Figure 19) shows that the Sioux Lookout orogenic belt volcanic rocks became more evolved and fractionated over time. An extended trace element plot of the same 4 samples (Figure 20) illustrates the progressively increased magnitude of the arc (subduction) signature (negative Nb or Nb–Ta anomaly: Hofmann 1988; Pearce 1996) developed over time.

A plot of the measures of arc signature ([Th/Nb] normalized to N–MORB) versus fractionation (chondrite–normalized [La/Yb]) for all the Sioux Lookout orogenic belt samples (Figure 21) shows that both the volcanic stages (1 to 4) and the individual sample groups (stratigraphic or plutonic units) occupy discrete fields on the diagram, thus providing a useful descriptive and interpretative tool. Stage 1 volcanic rocks appear to have a greater “arc” signature than the Stage 2 volcanic rocks, but this need not necessarily indicate an arc setting. The higher Th/Nb ratio in the Stage 1 rocks may reflect crustal contamination (i.e., contamination by mixing with, or assimilation of, nonprimitive material of more felsic or sedimentary heritage) rather than a true or pure subduction signature. (Isotope data would be required for sophisticated testing for the potential effects of crustal contamination.) Such crustal contamination, as evidenced by negative Nb anomalies, elevated LILE and LREE content, and low HFSE abundances, is well known from studies of continental tholeiitic flood basalts (e.g., Dupuy and Dostal 1984, Arndt and Jenner 1986, Jolly 1987, Hawkesworth et al. 1992, Saunders et al. 1992, Pearce 1996). Also, some geochemical signatures of subduction are interpreted to have been inherited from much older (unrelated) subduction events and rocks (e.g., Fitton et al. 1991, Hawkesworth et al. 1992, Bacon et al. 1997); increasing documentation of such complicating factors can likely be expected in the future.

Evolutionary Stages of the Sioux Lookout Belt

Figure 22 outlines the proposed main stages of development of the Sioux Lookout orogenic belt in cross–section. The earlier the stage, the more speculative its interpretation. The series of stages are “time slices” spaced about 10 to 15 Ma apart. Note that the cartoons are not to scale and represent different scales. For simplicity, basinal water levels are not shown (deposits during Stages 1, 2 and 4 were subaqueous, Stage 3 deposits were partly subaerial, and Stage 5 and 6 deposits were mostly subaerial fluvial). Qualifying statements and explanatory comments regarding each of the cartoon views of the stages are listed below. Because of both the flat, peneplained type of Shield exposure and the stratigraphic reconnaissance nature of this project, data on three–dimensional fault kinematic indicators are presently not available; interpretations such as Stage 6 sinistral faulting are based on large–scale map patterns and, to a far lesser degree, small–scale structures. Use of the term “orogenic belt” rather than “greenstone belt” is intended to draw attention to the similarities the tectonized Sioux Lookout orogenic belt has with many post–Archean orogenic belts. (This section is taken, with modifications and additions, from Devaney 1999a).

Aspects of the interpreted evolutionary stages which rely on geological patterns seen in map view are summarized below under “Analysis of a transect across the Sioux Lookout orogenic belt.”

STAGES 0, 1

The hypothesis that the Winnipeg River subprovince (Beakhouse 1991) and central Wabigoon region (Blackburn et al. 1991) were formerly joined as a (micro–)cratonic block and were subsequently rifted apart (Figure 22; see also Blackburn 1980) is admittedly highly speculative; presently there is no match of specific geological features between the two areas, and there are no known rift sediments or faults. (Could any rifting have been subaqueous, with no subaerial erosion and no alluvial fan–fluvial sedimentation?) The vertical "wall" between the cratonic areas and the basinal basaltic pile is a diagrammatic simplification.

Massive to pillowed tholeiitic basalt flows and associated facies of the Northern Volcanic belt (or "Botham Bay Group": Trowell and Johns 1986) and Southern Volcanic belt (Berger 1989) are predominantly deep water deposits ("mafic plain"–type assemblage of Williams et al. 1992, Table 25.2; "lower mafic sequences" of Blackburn et al. 1991). Trace element patterns indicate transitional MORB–VAB (mid–ocean ridge basalt–volcanic arc basalt) compositions (Pearce 1996; *see* "Volcanic geochemistry highlights," below). It has been suggested by Ayer (1991) that the basalts may have floored a back–arc basin, but there is no known arc succession of appropriate age (>2735 Ma) for the basalts to have been behind (in "back" of), so the term "pre–arc" basin basalts (Pearce et al. 1984b) may be more accurate.

Exhalite deposition likely produced the interlayered magnetite and pyrite iron formation units, which include the site of the North Pines pyrite mine of the 1920s (Johnston 1972).

STAGE 2

There are distinct geochemical differences between the Central Volcanic belt (or "Neepawa Group") E–MORB basalts and the Northern Volcanic belt MORB basalts; e.g., TiO_2 content (*see* "Volcanic geochemistry highlights," below). In rocks to the southwest, Berger (1989) noted similar differences between the basalts of the Southern Volcanic belt and Central Volcanic belt.

The 2734–2732 Ma age reported for the Central Volcanic belt (Davis and Trowell 1982, Davis et al. 1988, Blackburn et al. 1991, Figure 9.40) is from a "felsic tuff" interlayered with basalt; unless the dated tuff is a thrusted basal layer of the Central Volcanic belt, some of the underlying Central Volcanic belt basalts must be older than this (and thus also older than the 2734–2730 Ma age of Stage 3).

STAGE 3

A partly subaerial basaltic andesite stratovolcano succession about 3 km thick appears to lie on a Stage 2–type basaltic platform (Devaney and Babin 1996; see Figure 22 and Figure 23, sites 15, 16). The comagmatic dioritic subvolcanic pluton (see Figure 23, site 16) has a preliminary age of 2734–2730 Ma (D. Davis, written communication, 1998).

The areally restricted (nonregional) distribution of andesitic rocks (Figure 23) offers admittedly weak support for the interpretation of a fault–bounded local volcanic centre (e.g., a graben in Figure 22), but the presumed presence of a concentration of synvolcanic faults prone to later (Stage 5, 6) tectonic reactivation would help account for the abnormal orientation of a large (7 km) ovoid part of the andesites (see comments on site 15 in Figure 23, below).

RELATIONSHIP OF SIOUX LOOKOUT OROGENIC BELT STAGE 3 DEPOSITS TO CORRELATIVE VOLCANOGENIC MASSIVE SULPHIDE DEPOSITS AT STURGEON LAKE

Given that the Sioux Lookout orogenic belt andesitic stratovolcano succession and its feeder pluton (2730–2734 Ma) can now be correlated with the caldera–hosted VMS deposits and subvolcanic intrusion

(ca. 2734 Ma) 60 km to the east at Sturgeon Lake (same ages, similar subvolcanic pluton geochemistry, but significantly different volcanic facies: Davis et al. 1985, Morton et al. 1991, Blackburn et al. 1991), it is suggested that extensional volcanic regimes developed at both sites (Figure 22). Indeed, a "rifted arc" scenario such as this is commonly thought to be favourable for the generation of VMS deposits (e.g., Cathles et al. 1983, Syme et al. 1996).

The partially intermediate/andesitic volcanic units/centres of similar age (about 2733 Ma) and character (lithology, paleoenvironment, geochemistry) that are sporadically distributed throughout western Wabigoon subprovince (Atikwa–Lawrence area of Edwards and Davis 1984; southwest continuation of Sioux Lookout orogenic belt, area of Berger 1990; Manitou lakes area of Berger 1991; Blackburn et al. 1991) may have a common origin, perhaps reflecting a regional extensional event that developed only local areas of extension, transtension or partial rifting. Within this group of supposedly tectono–stratigraphically related areas that might have elevated potential for VMS deposits, the south Sturgeon Lake belt is presently the only known area in western Wabigoon subprovince where conditions were suitable for the formation and preservation of economic VMS deposits (e.g., a subaqueous caldera as a restricted basin; the Biedelman Bay intrusion as an adequately large and deep subvolcanic "heat engine" for the hydrothermal system). It is suggested that the ca. 2733 Ma volcanic–subvolcanic systems in the Sioux Lookout orogenic belt and south Sturgeon Lake belt formed during the same rifted arc episode (Sioux Lookout orogenic belt Stage 3 in Figure 22). (For a Proterozoic example of andesites in intra–arc graben, see Thompson 1993.)

STAGE 4

Stage 4 basinal deposits (Fig. 22) record a continuum of volcanic to sedimentary processes, with the latter being more common. In both the northern and southern areas (Figures 22, 23): proximal lava flow/dome facies (Trowell et al. 1983, Page 1984) are rare; unequivocal primary (unreworked) pyroclastic tuffs (Devaney and Borowik 1994, Devaney et al. 1995a) are extremely rare (felsic tuff dated at ca. 2719–2713 Ma: Davis et al. 1988, Table I); magnetite iron formation signifies volcanogenic exhalative chemical sedimentation during eruptive quiescence; thin bedded turbiditic wackes (Walker and Pettijohn 1971) are very common (they are ubiquitous to the south, in the Minnitaki Group, versus more variable degrees of sedimentary reworking in the Big Vermilion–Daredevil unit and Daredevil Formation to the north); and resedimented conglomerates are interbedded with the turbiditic wackes and iron formation. The conglomerates are composed of intrabasinally–sourced felsic volcanic and/or felsic porphyry clasts ("quartz porphyry" clast dated at 2714–2711 Ma: Davis et al. 1988).

The names used for these Stage 4 units have been a source of stratigraphic terminological confusion. The revised, simpler and more linear stratigraphy presented herein is supported by mapping (Devaney et al. 1995b). To the north, the correlative Big Vermilion–Daredevil unit and Daredevil Formation are exposed in different fault slices (see Figure 23, sites 7, 10). The "Little Vermilion Formation" of Turner and Walker (1973) is not a readily mappable unit and has been grouped herein with these northern units. A rock containing zircons ranging from 2720 to 2702 Ma ("best analysis" is 2712 Ma: Davis et al. 1988, p.183) was considered by Davis et al. (1988) to be from the "Patara Formation" of Johnston (1972), but is here considered part of the eastern Big Vermilion–Daredevil unit. (The Patara Formation is described herein as a unit of very different character, consistent with Pettijohn's (1934) original definition.) A felsic pyroclastic rock supposedly from the western Minnitaki Group has been dated at 2707–2701 Ma (Davis 1990, Blackburn et al. 1991, Figure 9.40), based on a single zircon grain. However, this dated sample is from either the southern Central Volcanic belt or northern Minnitaki Group, and has lithological and geochemical similarities with Stage 4 rocks, which suggests the following two interpretations. The felsic pyroclastic rock may be a Stage 4 deposit more than 2710 Ma old, implying that the ca. 2704 Ma age is incorrect, or alternatively, a minor volcanic unit of ca. 2704 age is present in a stratigraphically and structurally complex small area, implying that Stage 4 late arc volcanism continued until ca. 2704 Ma and may have overlapped with early Stage 5 tectonism (the ca. 2710–2695 Ma period).

With regard to the interpreted volcanic arc context (Stages 2 to 4; compare with the stages of evolution of the Okinawa Trough back–arc basin: Letouzey and Kimura 1986), any accretionary prism and

subduction zone was likely to have been located beyond the south margin of the Wabigoon subprovince (e.g., Blackburn et al. 1985, Figure 17; Devaney and Williams 1989). Despite interpretative suggestions of accretionary prism lithotectonic assemblages within the western Wabigoon region (Blackburn 1980, Sanborn–Barrie and Skulski 1999), there is no evidence for such prism assemblages in this region. Note that the commonly turbiditic Stage 4 sequences (Minnitaki Group, and correlative Warclub "sediments") also contain units which record coeval arc volcanism, which likely negates any prism interpretation for these turbiditic sequences.

VOLCANIC GEOCHEMISTRY HIGHLIGHTS

Contents of SiO_2 versus TiO_2, P_2O_5, Zr and Zr/Y provide useful stratigraphic subdivisions of the metavolcanic rock samples. Based on plots of SiO_2 versus TiO_2, P_2O_5, La, Nb, Th, Zr and Zn, the basaltic subunits of the Sioux Lookout orogenic belt form two discrete groups; strongly similar compositions allow the correlation of most of the Northern Volcanic belt with the northern Central Volcanic belt basalts (as one group), versus the distinctly different (higher Ti, P, La, Nb, Th, Zr and Zn content), more southern (probably younger) Central Volcanic belt basalts and similar basalts along the south margin of the Northern Volcanic belt.

Basalts of the Northern Volcanic belt (excepting the south margin sub–unit noted above) and northern Central Volcanic belt have flat REE plot slopes and REE abundances at about 10x chondrite level. More southern Central Volcanic belt basalts have low REE plot slopes (chondrite–normalized La/Yb ratios of about 6) and abundances of about 40–70x chondrite level; these basalts are more evolved (E–MORB) and fractionated than the more primitive (transitional MORB–VAB) basalts of the Northern Volcanic belt and north Central Volcanic belt. Most of the intermediate to felsic volcanic rocks display high REE plot slopes with chondrite–normalized abundances of about 100x La to 10x Yb.

Use of tectonic discrimination diagrams (Wood 1980, Pearce 1996) suggests the following progression: Stage 1 tholeiitic MORB–VAB seafloor basalt (pre–arc spreading); Stage 2 tholeiitic to more variable (E–MORB) basalt, of transitional oceanic to juvenile island arc character; Stage 3 calc–alkalic (transitional to tholeiitic) basaltic andesite, of variable within–plate to island arc character, and with relatively high Nb content (for rifted arc interpretation, see above); and Stage 4 calk–alkalic dacite–rhyolite of mature island arc character (see Table 7), including adakitic rocks. Similar histories based on geochemical interpretations have been suggested for the extreme western end of Wabigoon subprovince by Day (1990) and Ayer and Davis (1997).

On extended trace element plots normalized to N–MORB composition, Stage 1 and 2 basalts display minor negative Nb anomalies, versus larger negative Nb anomalies (arc signature) in Stage 4 dacitic–rhyolitic rocks.

Thus the geochemical signatures corroborate the inferred tectono–stratigraphic scenarios in Figure 22 and the thrust repetition of the two–stage basaltic lower part of the basin (Figure 23).

STAGE 5

The predominantly layered architecture of the Stage 4 basin was compressed and segmented into a north–to northwest–vergent fold–and–thrust belt (Figures 22, 24), with the Winnipeg River subprovince as a microcontinental foreland and the Central Wabigoon region of Wabigoon subprovince as a hinterland block or thick–skin thrust. This interpretation is based on geochronology (in parallel units with the same prevalent younging direction, two cases of older units juxtaposed over younger ones), map patterns (Figure 23), and field geology (e.g., faults in the Sioux Lookout orogenic belt are narrow, highly deformed zones in a belt typified by supracrustal rocks with well preserved primary features). Beakhouse (1988) and Davis et al. (1988) previously offered generalized interpretations of the thrusted nature of the Sioux Lookout orogenic belt.

The Stage 5 cartoon (Figure 22) is schematic; it is not a balanced cross–section. The nature of the sub–basaltic basement is unknown. Presumed mountainous topography is not shown, for ease of comparison with the Stage 6 cartoon. The beginning of postarc orogenesis in western Wabigoon subprovince was during the ca. 2710–2700 period (Davis et al. 1988, Davis 1990, Blackburn et al. 1991).

The conglomeratic Ament Bay Formation (Pettijohn 1934, Turner and Walker 1973, Devaney and Borowik 1994) contains a granitic clast dated at 2702–2694 Ma (Davis et al. 1988), establishing a maximum age for deposition of at least some of the formation. The erosion of a presumably high–relief thrust belt exposed numerous layers of different lithologies, resulting in the highly polymict composition of clasts in the Ament Bay Formation. Braided rivers transported sand and gravel to an intermontane basin, probably a piggyback basin atop a thrust slice (Figures 22, 25; e.g., Steidtmann and Schmitt 1988). The molassoid conglomerates were then overridden during continued thrusting (confirmed by geochronology: see Figure 23, sites 10, 11; compare with the Alpine molasse (Butler 1992) and Slave Province thrust–tip conglomerates (Kusky 1991)).

The north/northwest limits of sedimentation in the Stage 4 and 5 cartoons (Figure 22) have been drawn conservatively, according to what has been preserved; extensions onto the Winnipeg River subprovince (e.g., Cruden et al. 1997) are speculative. Detrital zircons in metawacke indicate sedimentation at a site in the Winnipeg River subprovince during the ca. 2717–2700 Ma period (Cruden et al. 1997). It is uncertain whether this age signifies the northwest continuation of the Sioux Lookout orogenic belt Stage 4 volcaniclastic basin or a Stage 5 foreland basin, or some other type of basin coeval but unrelated to the Sioux Lookout orogenic belt.

STAGE 6

Interpretation of late orogenic, Stage 6 sinistral strike–slip faulting is based on the geometric forms of sub–regional map patterns (mostly “lazy S”–shaped sigmoidal forms; see Figure 26 and Figure 23, sites 2, 3, 6, 15) which appear to postdate the Stage 5 thrust belt structures. Northward movement of the “Wabigoon Indenter” (Stott and Corfu 1991, Corfu et al. 1995), a large crustal block now exposed as the Central Wabigoon region of Wabigoon subprovince, resulted in sinistral faulting along the indenter’s western flank, where the Miniss River Fault (Bethune et al. 1999) and the Sioux Lookout orogenic belt are located (i.e., the Miniss River Fault forms a diffuse sinistral fault zone throughout the northern half of the Sioux Lookout orogenic belt).

Note: in the Stage 6 cartoon (Figure 22a), the hook–shaped forms with north–younging black arrows show mapped younging reversals interpreted to have been produced by hangingwall anticlines (Figure 27; Stage 5 features?), and the sill–like form of the granitoid intrusions (compare with the interpretive cross–section of the Barberton belt by de Wit et al. (1987, Figure 8)) is wholly conjectural. The Basket Lake batholith is poorly known; Szewczyk and West (1976) proposed that it is an 8 km deep intrusion.

In order to account for the widespread overturning of the Northern Volcanic belt, two main hypotheses are suggested (Figure 28). The southeast margin of the Winnipeg River subprovince (not studied in this project) may be a southeast–vergent, Laramide–type thrusted uplift (probably an oblique–slip fault, given the regional sinistral faulting; e.g., faulting within a “broken foreland”: Jordan 1995), which could have rotated the north marginal strata of the Sioux Lookout orogenic belt away from the foreland, similar to the rotation and overturning seen adjacent to Laramide–type uplifts (e.g., Erslev 1986, Spang and Evans 1988, Allmendinger 1992). Similar overturning in correlative boundary units far to the southwest was described by Ciceri et al. (1996) and Cruden et al. (1997). Along the boundary to the northeast, the “northwestern hanging–wall of the northeast–trending, sinistral, oblique–slip Miniss River Fault... brings to the surface granulite facies supracrustal gneisses” (Williams et al. 1992, p. 1289; see also Beakhouse 1991, p. 297, and Bethune et al. 1999). South– to southeast–directed reverse faulting of the north margin of the Sioux Lookout orogenic belt, between the above two areas, seems reasonable given this regional context.

Alternatively, a second hypothesis suggests that steeply oriented strata near the belt boundary may have been transpressed into large flower structures (for explanation and examples of flower or palm tree

structures, see: Christie–Blick and Biddle 1985, Harding 1985, Nance 1987, Ramsay and Huber 1987; Sylvester 1988, Schreurs and Colletta 1998), in which slices of the basaltic Northern Volcanic belt were thrust upward and outward (Figures 28, 29; south–vergent slices would be overturned). Regardless of the tectonic mechanism, uplifted basaltic areas supplied basalt clasts and a few iron formation clasts (a nearly oligomict composition) to the adjacent Patara strike–slip basin (Figure 23, site 6). The relatively shallowly dipping, predominantly north–dipping and north–younging Patara succession contrasts sharply with the other sedimentary units in the Sioux Lookout orogenic belt.

RESOLUTION AND TIMING OF STAGE 5 AND 6 OROGENIC EVENTS

The sequence of various orogenic events is not yet precisely subdivided or tightly constrained. The orogenic scenario of Stage 5 thrusting followed by Stage 6 sinistral strike–slip ("wrench") faulting, summarized in the highly idealized cartoons in Figure 22, largely agrees with the results of the detailed structural study by Chorlton (1990, 1991) of the area adjacent to the southwest of the present Sioux Lookout orogenic belt study area.

In the Sioux Lookout orogenic belt and other parts of western Wabigoon subprovince, postarc orogenesis began during the ca. 2710–2700 period (Davis et al. 1988, Davis 1990, Blackburn et al. 1991). As noted above (see "Stage 4"), any ca. 2704 Ma late arc volcanism may have overlapped with early orogenic events. Deposition of some, but not necessarily all, of the synthrust Ament Bay Formation must postdate its youngest dated clast (2702–2694 Ma); if the date represents the upper part of this apparently thick formation, the lower part could be significantly (5–10 Ma) older. Also, a few million years should probably be allowed for the erosional unroofing of the granitic plutonic source of the clast. The subsequent sinistral motions along the Miniss River Fault, and presumably also within the northern Sioux Lookout orogenic belt as the southwest continuation of the fault, occurred at ca. 2690 Ma (Bethune et al. 1999). Thus, deposition of the dated part of the Stage 5 synthrust molasse deposition of the Ament Bay Formation was most likely during the 2700–2690 Ma period, presumably followed by the increased compression (or transpression) and steepening of strata to vertical in the Ament Bay and other Sioux Lookout orogenic belt formations and units. If Stage 6 strike–slip faulting occurred when the Sioux Lookout orogenic belt stratal units had finally become predominantly steeply dipping (i.e., oriented in the "proper mechanical alignment" for "wrenching" during regional horizontal compression/transpression), at about 2690 Ma, this implies that much of the presently observed stratigraphy of the Sioux Lookout orogenic belt was rotated from flat or low dips to steep dips during about 10 Ma (ca. 2700–2690 Ma) of tectonism.

During Stage 6 deposition of the Patara Formation strike–slip basin (see site 6 in Figure 23, and its discussion below), zircon–bearing sand was supplied from source areas containing rocks as young as 2700 Ma. The ca. 2700 Ma detrital age should not be treated as a potential depositional age; it is important to note that the "structurally anomalous" Patara Formation was not orogenically steepened in the manner that the other Sioux Lookout orogenic belt stratigraphic units were, reflecting the postthrusting, Stage 6 timing of its deposition and deformation. Based on the geological arguments presented herein, the age of the Patara Formation should be considered to be about 2690 Ma or younger.

The syntectonic basinal setting of the Ament Bay Formation, including its northeast conglomerate unit, could have been more complex than the generalized interpretation offered herein. For example, as the Ament Bay Formation was tectonized, could it have been uplifted and partly eroded, with polymict clasts redeposited in Stage 6 strike–slip basins on top of or alongside the original Ament Bay Formation units? Such "auto–cannibalization" of an older unit to form a younger one could be very difficult to recognize without good data on unconformities and other structural relationships.

Because the schistosity in the Ament Bay Formation conglomerate and sandstone: a) must postdate the accumulation of these sedimentary facies during Stage 5 thrusting; and b) resembles the main schistosity fabric seen in the other pre–Patara Sioux Lookout orogenic belt units (very steeply dipping; parallel to the strike of the large–scale stratigraphic units), much of the schistosity in all of the pre–Patara units is likely a late orogenic feature; that is, it likely formed principally during Stage 6 strike–slip faulting (and perhaps

also during later phases of Stage 5 thrusting). If so, features such as veins with very low dips that crosscut the very steep schistosity indicate increments of vertical extension during the later phases of Stage 6 tectonism. Such vertical extension would be expected at any transpressional sites within the Sioux Lookout orogenic belt, and larger–scale transpressional structures such as positive flower structures may also have developed (*see* above under "Stage 6"; *see* below under "Mineralization in the Sioux Lookout orogenic belt").

The specific role(s) of synorogenic granitic intrusions is poorly known. With the exception of the Lateral Lake stock (2711–2705 Ma: Davis 1990) at the west margin of the present study area, granitic plutons within the study area are undated. Chorlton (1990, 1991) thought that pluton intrusion (at ca. 2695 Ma: Davis 1990; see below) followed thrusting and preceded sinistral strike–slip faulting in the part of the Sioux Lookout orogenic belt immediately west of the study area. However, two lines of evidence require or suggest a longer history of granitic plutonism. Firstly, an abundance of coarse granitic clasts in the Ament Bay Formation suggests granitoid intrusion within or near the Sioux Lookout orogenic belt before or during Stage 5 thrusting. Secondly, the somewhat sigmoidal form in map view that some of the granitic plutons display suggests that they may have formed during Stage 6 strike–slip faulting (see site 3 in Figure 23, and its discussion below).

Immediately southwest of the study area there is a kink–like bend in the regional layering of the supracrustal belt, so the possibility that 2699–2693 Ma and 2697–2693 Ma granitic plutons (Crossecho, Sandybeach: Davis 1990, Larbi et al. 1996) may have formed in large releasing bends or a northwest–trending kink–band mega–structure (Figure 30; cf. Fernandez and Castro 1997) should be investigated.

Postorogenic granitic and pegmatitic intrusions in areas near the Sioux Lookout orogenic belt are as young as ca. 2650 Ma (Larbi et al. 1996, 1999), and represent a potential seventh stage in the region's development.

Analysis of a Transect Across the Sioux Lookout Belt

Figure 23 is a semi–schematic map (some north–south exaggeration of scale for graphical purposes; compare with maps of Johnston 1972 and Devaney et al. 1995b) of a north–south transect across the Sioux Lookout orogenic belt. Most of the major contacts between units of different lithologies are not exposed or are poorly exposed, but are thought to be faulted. The presence of the faults is largely inferred in that they are recognized mostly via map–scale patterns (discussed below) and the relatively few observations of outcrop–scale features indicative of high strain. The latter suggests the rare exposure of deformation zones (e.g., more easily eroded zones covered by lakes and overburden) versus the abundant exposure of less deformed "panels" of supracrustal rocks bounded by the faults or deformation zones.

As outlined in Figure 22 and below, the map pattern (Figure 23) is interpreted to represent a pre–arc to arc succession compressed into a predominantly south–younging, steeply south–dipping fold–and–thrust belt which was subsequently significantly modified by strike–slip faulting. The evolutionary Stages 1 to 6 referred to below are those of Figure 22.

The most geologically important features of the area are labelled as sites 1 to 27 in Figure 23 and are discussed in sequence in the correspondingly numbered paragraphs below. (This section is taken, with modifications, from Devaney 1999a.)

1) There is no evidence that the Winnipeg River subprovince–Sioux Lookout orogenic belt boundary was also the depositional margin of a volcanic or sedimentary basin (Stages 1 to 4); that is, the Sioux Lookout orogenic belt supracrustal units may or may not have extended past this present north margin of the Sioux Lookout orogenic belt (e.g., Figure 22 versus scenario of Cruden et al. 1997). This boundary is interpreted as a zone affected by early orogenic thrusting (Stage 5, approximately north–vergent toward a foreland Winnipeg River subprovince), late orogenic (Stage 5 and/or 6) high–angle reverse faulting (e.g., a

Laramide–type uplift, south–vergent toward the hinterland), and sinistral strike–slip faulting (Stage 6; Figures 22, 26, 28).

2) BIF horizons (Stage 1 exhalite deposits) within the Northern Volcanic belt (Johnston 1972, OGS 1982) may have acted as weak detachment (decollement) surfaces during later deformation events, such as Stage 5 thrusting and Stage 6 sinistral faulting (Figures 22, 26).

Notably, this presumed intra–Northern Volcanic belt thrust stacking occurs where the Northern Volcanic belt is widest and/or thickest (Figures 1, 23).

The sigmoidal distribution ("lazy–S" shape) of the faulted BIF horizons appears to help define sinistral–sense fault–bound "lozenges" (horses) within the Northern Volcanic belt (Figure 23). Sets of laterally continuous lozenges may be grouped into strike–slip duplexes (Figures 23, 26).

In Figure 23, one sigmoidal BIF horizon is collinear with the east part of the Winnipeg River subprovince–Sioux Lookout orogenic belt boundary, suggesting that both may be faulted, or are present along one fault.

Schistosity within the Northern Volcanic belt dips moderately (e.g., 60º) to steeply to the NW or N, but the top directions from well preserved lava pillow structures are to the SE (Pettijohn 1935, Johnston 1972, Devaney et al. 1995b) and strata are thought to be overturned. Severe overturning is widespread within the Northern Volcanic belt, and may be the result of south–vergent Laramide–type faulting and/or motion along flower stuctures produced by strike–slip faulting (Figures 28, 29).

3) Based on the maps of Johnston (1972) and OGS (1997), the four northern granitoid plutons within the Northern Volcanic belt (one cross–cuts the Patara Formation too) have tapered or partly sigmoidal outlines and appear to be preferentially located in releasing bend areas (dilational jogs or transtensional sub–zones; loosely analogous to large–scale tension gashes) marginal to sigmoidal, sinistral strike–slip faults (Figures 23, 26, 31). Intrusion into transtensional sites such as fault releasing bends has been proposed as a generally common mode of dike and pluton intrusion by granite specialists (e.g., Guineberteau et al. 1987; Hutton 1988, 1992; Glazner 1991; D'Lemos et al. 1992), which suggests the interpretation that these four undated plutons were intruded during Stage 6 strike–slip faulting of the Sioux Lookout orogenic belt. This interpretation relies on map–scale (15–20 km) patterns; note that the fault–bound panels (discussed above) which contain the plutons are sigmoidal (lazy–S shaped) fault lozenges.

4) The nature of the contact between the Northern Volcanic belt and the Big Vermilion–Daredevil unit adjacent to the south (except where the Patara Formation is present) is poorly known because it is generally not exposed and at western (Big) Vermilion Lake it is likely structurally complex and possibly repeated. The contact may have been a Stage 4 stratigraphic contact, modified by subsequent Stages 5 (Figure 22) and 6 faulting. Map patterns suggest modification by Stage 6 sinsitral strike–slip faulting (Figures 23, 26).

5) The structural nature of the east–tapering mafic volcanic unit exposed at the west half of (Big) Vermilion Lake (Johnston 1972, Page 1984) is poorly known owing to poor exposure and probable structural complexity (see #4, above) and lack of study. Potential explanations for the presence of this unit include a thrust–faulted repetition of part of the Northern Volcanic belt (Figure 22) or a position as the basaltic core of an anticline. (Presently there are no kinematic data with which to constrain these suggestions.)

6) The 20 km–long Patara Formation (Figures 23, 26; Pettijohn 1934) consists mostly of coarse clastic detritus, the coarsest material being conglomerate composed predominantly of basalt pebbles to boulders. The clast litholgies present (basalt, chert–magnetite iron formation) and the geochemical composition (Tables 1, 3, 6) of coarse clastic samples of the Patara Formation match well with the lithofacies and chemical composition of the Northern Volcanic belt, showing that the Patara Formation was derived from the Northern Volcanic belt adjacent to the north (This implies that the Northern Volcanic belt was adjacent to the north *both* at the time of sedimentation *and* in present exposures.) The best cross–sectional transect shows a north–dipping, north younging, coarsening–upward sequence (good top indications present) from

aquabasinal (lacustrine?) mudstones and graded beds to fluvial sandstone to bouldery conglomerate. Pillowed metabasaltic rocks of the Northern Volcanic belt immediately adjacent to the north are south–younging and highly overturned (moderately north–dipping). The coarsening–upward sequence of the Patara Formation (Figures 3, 28) is interpreted as the result of infilling of a late (Stage 6, syntectonic) pull–apart basin bounded to the north by a sigmoidal sinistral strike–slip fault (Figures 3, 23, 26, 31) which may have been part of a positive flower (palm tree) or pop–up structure.

The present–day sigmoidal outline of the Patara Formation should also represent roughly the syndepositional shape of the original basin and not the folding of a formerly straight (linear) dipping unit; that is, the along–strike distribution of the Patara Formation is restricted to the extent of the formerly and presently sigmoidal fault margin of the basin, suggesting that strike–slip (or oblique–slip) faulting was active during deposition. If correct, the viewpoint that the original shape of the basin appears to be fairly well preserved indicates that it was a very late feature in the development of the Sioux Lookout orogenic belt, as is required by its interpretation as a Stage 6 (late orogenic) feature in Figure 22. Note that this contrasts sharply with previous views that the Patara metasediments were the oldest sedimentary unit in the Sioux Lookout orogenic belt and were a south–younging unit lying unconformably on top of the Northern Volcanic belt.

Note that the Patara Formation lacks granitic clasts (Pettijohn 1935), and the granitic pluton which cross–cuts the Patara Formation is younger and was not a source area for clasts. (If both the Patara Formation and the granitic pluton formed in a transtensional strike–slip setting (Stage 6), the pluton must be at least slightly younger.)

Following interpretations of the Patara Formation as a Stage 6 unit (Devaney 1997, 1999a, and herein), Fralick and Davis (1999) reported that detrital zircon grains from the Patara Formation are as young as 2700 Ma, confirming the synorogenic (postvolcanic) age of this clastic formation (<2700 Ma). Note that this date is in effect a minimum age of the source terrain and a maximum age of sedimentation, and is not the exact age of Patara sedimentation (i.e., the presence of a 2700 Ma detrital zircon grain in the Patara Formation does not mean that the Patara Formation is older than the Ament Bay Formation).

7) In contrast with previous mapping (Johnston 1972), the “Big Vermilion–Daredevil” unit on Figure 23; likely equal to the “Redhat volcanics” of Page 1984) has been mapped as a much more laterally continuous, tectonized, formation–scale unit of intermediate–felsic, predominantly fragmental metavolcanic rocks (Devaney et al. 1995b). Two small magnetite iron formation units (at the two 7s in Figure 23) signify at least partly subaqueous deposition for the unit. The west one, at Pelican Lake, is interbedded with conglomerate and sandstone (Devaney et al. 1995b) and was not recognized by previous workers. Near the east one, pumiceous lapilli–tuff similar to exposures of the Daredevil Formation at Little Vermilion Lake (Turner and Walker 1973, Figure 1) was previously mapped as “polymict conglomerate” of the Ament Bay Formation by Johnston (1972). Dates from zircon grains (Davis et al. 1988) demonstrate correlation with both the type area of the Daredevil Formation (Pettijohn 1934, Turner and Walker 1973) to the southwest (see #10, below) and the Minnitaki Group (Figure 22).

According to Turner (1972, Turner and Walker 1973), the two BIF units are part of the “Little Vermilion Formation”, but because the present writer does not consider the Little Vermilion Formation to be a readily mappable unit, the two BIF units have been grouped in with the predominantly volcaniclastic Big Vermilion–Daredevil unit.

8) Coarse sandstone and highly polymict conglomerate of the Ament Bay Formation (Pettijohn 1934, Turner 1972, Turner and Walker 1973, Devaney and Borowik 1994) are braided river deposits interpreted to have formed in a linear, strike–parallel, intra–orogenic, synthrust piggyback “molasse” basin (Figures 22, 23, 25; *see* “Stage 5,” above). Based partly on U/Pb dating by Davis et al. (1988), the Ament Bay Formation is interpreted as a postarc, ca. <2694 Ma deposit that was overthrust by the older Central Volcanic belt (ca. 2733 Ma) to the east and the older Daredevil Formation (ca. 2711–2719 Ma) to the west.

Structural features of the Ament Bay Formation, such as south–younging beds, steep dips, and schistosity (oblate clasts), are typical of most of the supracrustal units in the Sioux Lookout orogenic belt,

and contrast sharply with structural features in the Patara Formation (see #6, above). As the Ament Bay Formation thins eastward at eastern Abram Lake, along the north margin of the Central Volcanic belt, it becomes extremely deformed.

9) A geographically separate northeastern unit of polymict conglomerate (Ament Bay Formation, or an equivalent unit) may have been separated from the more extensive exposure of the Ament Bay Formation by faulting or folding, or rather than the deposition of one continuous sheet or wedge of sediment, the Ament Bay Formation may have been deposited in two separate orogen–parallel valleys (Stage 5 longitudinal partitioning, with multiple thrust slices and multiple molassoid valley fill sequences).

Alternatively, the northeastern polymict conglomerate unit could represent a small Stage 6 pull–apart basin, its polymict composition reflecting the variety of lithologies in the immediately surrounding source area (and the present northeast map area) versus the oligomict composition of the Patara Formation pull–apart basin conglomerates derived from the Northern Volcanic belt.

10) At Little Vermilion Lake, the type locality of the Daredevil Formation (Pettijohn 1934, Turner 1972), and presumably also in areas along strike to the southwest (e.g., Page 1984), south–topping, older (ca. 2713 Ma) Daredevil Formation strata are structurally juxtaposed (thrust) over the south–topping, younger Ament Bay Formation (at least part of which must be younger than the ca. <2694 Ma clast that it contains; dates from Davis et al. 1988).

Even though Pettijohn (1934) noted the linear and most likely faulted nature of the Ament Bay Formation–Daredevil contact, an *apparently* conformable, south–dipping succession of Ament Bay Formation overlain by the Daredevil Formation, comprising the lower part of the "Abram Group," was described by previous workers (e.g., Pettijohn 1934, Turner and Walker 1973, Blackburn et al. 1985, 1991). Because of the highly probable presence of a thrust fault at the Ament Bay Formation–Daredevil contact (i.e., along the south margin of the Ament Bay Formation and the north margin of the Daredevil Formation; Figure 23), interpretation of a continuous and conformable succession is now considered erroneous, and thus use of the term "Abram Group" must now be considered nonvalid and should be discontinued.

Similar lithofacies (Johnston 1972, Devaney et al. 1995b) and radiometric dates (Davis et al. 1988) suggest that the Daredevil Formation is correlative with the Big Vermilion–Daredevil unit (hence the name), and the Daredevil Formation and Big Vermilion–Daredevil unit may have formed a laterally continuous, Stage 4 volcaniclastic sequence (Figure 22) that was later broken into separate fault slices by Stage 5 thrusting (Figures 22, 23).

11) Metagabbroic intrusive bodies are present near the north margin of the Central Volcanic belt (Johnston 1972), which should be the base of the (lowest?) Central Volcanic belt thrust slice. It is thought that within the Central Volcanic belt section there was probably a structural competency contrast between a deep–level basaltic section, one heavily intruded by gabbroic bodies and thus "welded" together, and a shallow–level, well stratified, less welded–together section of basaltic flows with few gabbroic intrusions. During regional compression (Stage 5), a (sub–)horizontal thrust fault might be expected to have formed along the irregular contact between the lower gabbro–rich section and the upper gabbro–poor section, with a few of the uppermost gabbro bodies transported away in the lower part of the resultant thrust slice and exposed today near the north margin of the Central Volcanic belt (Figure 23).

Geochronology by Davis et al. (1988; Blackburn et al. 1991, Figure 9.40) demonstrate out–of–sequence stratigraphy, and the map patterns present thus require north–vergent thrusting of the Central Volcanic belt over the younger Daredevil and Ament Bay formations (see 10 and 8, above).

12) Various undated felsic volcanic bodies (lavas, porphyries, and associated tuff–breccia) exposed at or near the southern margin of the main basaltic part of the Central Volcanic belt (Figure 23; Johnston 1969, 1972; Devaney et al. 1995b) have been interpreted as proximal volcanic dome facies (Trowell et al. 1978, 1983; McMullan 1980, Page 1984, Chorlton 1991) and signify either: 1) an apparent stratigraphic change from basaltic volcanism (Stage 2) to more felsic volcanism (Stage 4; Stage 3 is restricted to areas discussed below under #14, 15 and 16), or 2) Stage 2 bimodal basalt–rhyolite volcanism (these rhyolites are undated).

Note that similar felsic volcanic rocks are seen at the south margin of the Northern Volcanic belt at (Big) Vermilion Lake (Johnston 1972, Devaney et al. 1995b), suggesting that this stratigraphic, mafic–to–felsic transition has been repeated by thrusting at widely separated localities within the Sioux Lookout orogenic belt.

A felsic "pyroclastic" rock from the southeast part of the study area (western Pickerel Arm of Minnitaki Lake) has been dated at ca. 2704 Ma, based only on a single zircon grain (Davis 1990; Blackburn et al. 1991, Figure 9.40), and is herein considered to represent an erroneous age, an intrusive porphyry, or a relatively very young volcanic unit. Examination of pyroclastic rocks near the probable sample site (north shore of Pickerel Arm) suggests that the rocks resemble Stage 4 (>2710 Ma) dacitic pyroclastic deposits, therefore the reported ca. 2704 Ma age might be erroneous, perhaps about 10 Ma too young. If the age and assessment as pyroclastic are both correct, an episode of volcanism localized in a small intra–orogenic basin (e.g., a pull–apart basin, with a transtensional fault zone conduit for the magma) might account for the presence of ca. 2704 ma felsic pyroclastic rocks.

13) Some felsic volcanic bodies, interpreted as subvolcanic to volcanic dome deposits (Sutherland and Colvine 1979, McMullan 1980), likely assisted in "welding" basaltic sections of flows together into more structurally competent units that later formed thrust slices (similar to the gabbroic case described for #11, above).

The faulting in this area (Pickerel Arm: Johnston 1969) is poorly known and is likely very complex (the map patterns here are not as easily interpreted as elsewhere in the map area), thus the display of faults on Figure 23 is highly conjectural (e.g., interpretation of basalt–based north–vergent thrusts). Felsic porphyry bodies are near notable quartz vein–hosted gold occurrences (Johnston 1969; Devaney et al. 1995a: two assays of 2.1 and 2.3 oz./ton from a pyrite–bearing quartz vein west of Burnthut Island, at the "Number 3 zone" of Johnston (1972, p.43)).

14) From the area of Butterfly Lake, Lyons Bay and Troutfish Bay (Johnston 1969, 1972; Devaney et al. 1995b; Page, unpublished data), there is an eastward structural, and possibly also stratigraphic, thickening of intermediate (andesitic) pyroclastic to volcaniclastic rocks, with probable complex folding and faulting (e.g., anticline–syncline pairs: Page and Clifford 1977). These andestic rocks have been studied in more detail farther to the east where they are less deformed and likely form a less disturbed, more continuous stratigraphic sequence (see #16, below).

15) The 4–6 km thick supracrustal pile at the Northeast Bay of Minnitaki Lake area (Johnston 1972, Page and Clifford 1977, Devaney et al. 1995a,b; Devaney and Babin 1996) is interpreted to consist of a volcanic succession having lower (eastern) basaltic shield volcano facies (Stage 2 or 3) and upper (western) basaltic andesite, partly subaerial, proximal to medial stratovolcano facies (Stage 3 deposits). The subaerial facies are comparable to facies on modern volcanoes such as Ruapehu (Hackett and Houghton 1989), Mt. St. Helens (e.g., large pyroclastic surge antidunes of Rowley et al. 1985), and Mt. Pelee (e.g., fractured block–and–ash flow pyroclasts described by Perret 1937; for facies model, see Easton and Johns 1986), and may form the upper parts of three transgression–regression cycles (Figure 4; Devaney 1998). Subvolcanic intrusions (see #16, below) likely helped to "weld" the section together to form a rigid block or flake that was structurally competent and internally resistant to deformation during subsequent tectonic episodes.

It is thought that before strike–slip faulting (Stage 6) affected much of the Sioux Lookout orogenic belt, strata of the Northeast Bay area were tilted, perhaps by synvolcanic graben formation (Stage 3 in Figure 22a) and/or synthrust (Stage 5) rotation or folding, to form a north–younging succession. It is interpreted that during Stage 6 sinistral strike–slip faulting, the Northeast Bay area acted as a 7 km diameter "Riedel flake" structure (Figure 32; term of Gallo et al. 1980 and Sengor et al. 1985) which was *rotated* counter–clockwise, presumably above a fault (a detachment surface; e.g., reactivation of a Stage 3 synvolcanic graben sole fault or the bowl–shaped base of a caldera fill succession?) at a shallow crustal depth, to form the north–striking, west–younging succession preserved inside the Riedel flake structure. The southwest margin of this Riedel flake is under the waters of Northeast Bay and its presence there is thus inferred, but the other margins of the structure are expressed as deformation zones (faults along the northwest and southeast margins of the flake structure) and schistosity orientations (e.g., east– to

southeast–striking schistosity along the proposed north to northeast margin of the flake structure) on previous maps (Johnston 1972, Page and Clifford 1977; Page, unpubl., OGS 1982; see also OGS 1997).

16) Much of the thick section of lower basaltic and upper andesitic facies described above (#15) is cross–cut by a subvolcanic (synvolcanic, comagmatic) diorite–trondhjemite intrusion (Page and Clifford 1977, Devaney and Babin 1996; "Northeast Bay pluton" of Trowell et al. 1983) with a preliminary age (based on U–Pb content in two zircon grains) of 2734–2730 Ma (D.W. Davis, written communication, 1998). An aureole of contact metamorphism is *not* present, supporting the synvolcanic interpretation (intrusion into a wet supracrustal pile, heat convected away). Geochemical analyses of the dioritic rocks are very similar to those of the andesitic rocks (flows, related dikes, pyroclastic facies) in the upper part of the adjacent stratovolcanic succession (Figure 11d–h).

In the vicinity of the western margin of the intrusion, the following suite of features suggests the presence of a dike swarm near the inferred apex of the pluton: great lithologic variability of intermediate rocks over small (10–100 m) areas, dikes of variable grain size and fabric, dikes within dikes, sulphide mineralization (pyrite, chalcopyrite) along fractures, and an unusual breccia (probably a marginal intrusion breccia).

This subvolcanic intrusion and its mineralization (trace Cu and Mo) are similar to the subvolcanic, ca. 2734 Ma Beidelman Bay pluton (Poulsen and Franklin 1981, Morton et al. 1991) situated about 60 km to the east, in the Sturgeon Lake belt (Blackburn et al. 1991). This suggested a correlation of the two areas *before* the 2734–2730 Ma age from the Sioux Lookout orogenic belt was obtained (Devaney 1997), and is perhaps also suggestive of an extensional setting for both areas (Stage 3 in Figure 22): a subaqueous caldera at Sturgeon Lake (Morton et al. 1991) and partly subaerial graben at Northeast Bay (Sioux Lookout orogenic belt).

17) Highly deformed rocks along or near the contact between the Central Volcanic belt and the Minnitaki Group (Johnston 1972; Page, unpubl.) are continuous along strike to the northeast with the "Alcona Deformation Zone" (Zarn Lake area: Page 1978, Page and Moller 1979b). Distinctive andesitic pyroclastic strata in the Zarn Lake and Northeast Bay (see #15, above) areas appear to be sinistrally offset by about 7 km (Figure 32).

18) Multiple basaltic units within the folded and faulted Minnitaki Group may be interpreted as volcanic–cored anticlines (Pettijohn 1937) or basalt–based thrusts which repeat sections of the Minnitaki Group and an underlying layer of basalt (Stage 5 imbricate thrusts; Figures 22, 23, 24). If the view of thrust–repeated basalt–wacke "couplets" is correct, this calls into question the concept of "upper mafic sequences" (Blackburn et al. 1991) in the western Wabigoon region.

19) Laterally persistent (2 km scale), strike–parallel zones of uniform top indications (from graded bedding) suggest alternating anticline–syncline pairs (perhaps as originally "upright" folds, with quasi–horizontal hinges later tilted or folded?), interpreted as the result of synthrust (Stage 5) compressional folding of a thinly bedded sandy turbidite succession (Minnitaki Group). In such a thrust–faulted succession, drag–folded hangingwall anticlines and footwall synclines might be expected (Figure 27).

20) The conglomeratic horizon (deep–water turbidites) in the southern exposures of the Minnitaki Group fines and appears to become thinner along strike to the southwest (individual conglomerate beds also are thinner and less abundant southwestward; the actual (total) horizon thickness is not readily measurable), indicating a general proximal to the east, distal to the west polarity. The felsic porphyry clasts that make up much of the conglomerate are thought to have been sourced from a volcanic dome now exposed in a separate thrust slice to the southeast (see #22, below).

21) Major faults may be present along: a) a horizon with four small, widely separated outcrops of mafic rock (present over a 10 km distance along strike; Johnston 1969), possibly representing faulted "slivers" of an "exotic" lithology within the Minnitaki Group; or b) an hypothesized detachement (decollement) surface along a structurally weak BIF horizon.

22) At Southeast Bay of Minnitaki Lake (Trowell et al. 1982, 1983) there is lithological contrast between eastern exposures of coarse intermediate–felsic pyroclastic facies (tuff–breccia, autobreccia) and western exposures of Minnitaki Group sediments (conglomerate, coarse and fine sandstone with graded beds, magnetite BIF) with clasts of volcanic porphyry. Based on a geophysical signature (OGS 1982) and mapping of apparently "offset" stratigraphy, previous workers interpreted a north–south fault underneath the 3 km wide covered interval of Southeast Bay (Trowell et al. 1982, 1983). The present study has found no significant offset of stratigraphy (map of Devaney et al. 1995b) and interprets the along–strike lithological contrast as a *lateral facies change* from an eastern proximal volcanic dome to western, more distal, subaqueous clastic detritus and BIF exhalite layers (both sourced from the dome area; Devaney 1998). (There is no direct evidence for the dome being subaqueous, but the BIF layers were likely sourced from a subaqueous volcanic site, such as a smoker vent, with the eastern dome area being the most likely candidate for the source area).

Regarding the presence of the supposed north–south fault near the site of the interpreted abrupt facies change, volcanic dome development may have been localized above a synvolcanic fault, one subject to later tectonic reactivation (Devaney 1998).

23) To the east, at Southeast Bay, top directions within the moderately south–dipping pillowed metabasalts of the Southern Volcanic belt are predominantly to the south (Trowell et al. 1982, 1983), toward the belt–marginal "batholith", with more variable top directions near the faulted north margin of the Southern Volcanic belt (*versus* the case in #24, below). This does not support older views (e.g., Trowell and Johns 1986, p. 51) that "lower" mafic volcanic sequences/units "invariably" face away from the large belt–marginal granitic batholiths in western Wabigoon subprovince.

24) To the west, "anomalous" north–younging top directions in pillowed flows near the north margin of the Southern Volcanic belt (Pettijohn 1937, Figure 4; Johnston 1969) may represent a hangingwall anticline, a drag fold (e.g, north–younging north limb, south–younging south limb) that formed near the base of a thrust in a generally north–vergent thrust belt (i.e., thrusting of the Southern Volcanic belt over the Minnitaki Group; Figures 22, 23, 24, 27).

25) Berger (1989) provided evidence of intrusion of the Basket Lake Batholith (BLB) into the Southern Volcanic belt, but the composite BLB is poorly known to the east and elsewhere (see Szewczyk and West 1976, Blackburn et al. 1991). Gneissic rocks of the BLB to the east may be older and part of a "Central Wabigoon Region" cratonic block (Blackburn et al. 1991) or "Wabigoon Indenter" (Stott and Corfu 1991). The presence of such a "thick–skinned" cratonic block pushing north to northwestward might account for the "thin–skinned," north–vergent thrust belt style that appears to have been preserved (despite subsequent sinistral strike–slip faulting) in the Sioux Lookout orogenic belt. (Compare with larger scale, thin–skinned Phanerozoic orogens having thick–skinned hinterlands: e.g., Appalachians: Hatcher and Hooper 1992; British Columbia Cordillera: Brown and Journeay 1987.)

26) Farther to the southwest along strike, the Sandybeach Lake granitic pluton crops out (Berger 1989; Chorlton 1990, 1991; 2697–2693 Ma old: Davis 1990). Note that the supracrustal successions in the Sioux Lookout area have a paucity of granitic plutons, versus the more intruded areas adjacent to the east and west (see Blackburn et al. 1991).

27) Farther to the southwest along strike, the deformed, granitic Lateral Lake stock crops out (Colvine and McCarter 1977; Page 1984; 2711–2705 Ma titanite minimum age: Davis 1990). The Lateral Lake stock appears to form the intrusive core of a local anticlinal structure.

TESTING OF INTERPRETATIONS AND HYPOTHESES

Further testing of the interpretative ideas proposed herein will require much detailed mapping of the faults, deformation zones, and pluton margins in the Sioux Lookout orogenic belt, including their form and orientation at depth. Small–scale kinematic indicators and other structures that formed during Stage 5

thrusting may be difficult or impossible to distinguish from those that formed during Stage 6 strike–slip/transpressional/transtensional faulting (e.g., were early orogenic, synthrust horizontal lineations later rotated to vertical, or were vertical lineations formed by late orogenic transpressive dip–slip movements?) For relevant discussions of transpressional "lineation switching" and variability, see: Tikoff and Greene (1997), Dewey et al. (1998) and Ebert and Hasui (1998).

Suggested geochronological priorities for the Sioux Lookout orogenic belt are dating of the: 1) Northern Volcanic belt (basalt or any clastic interbeds; compare with older ages in western Wabigoon subprovince); 2) rhyolitic bodies in the Central Volcanic belt (test for the possibity of ca. 2735 Ma bimodal basalt–rhyolite volcanism); 3) small, roughly sigmoidal granitic plutons within the Northern Volcanic belt (this may date the Stage 6 strike–slip faulting); 4) Northeast Intrusive Complex (did these sanukitoid rocks intrude very late in the tectonic history?); and 5) Patara Formation sandstone beds (how young is the sand in this pull–apart basin?). Although the Patara Formation is now known to contain detrital zircon grains as young as ca. 2700 Ma (Fralick and Davis 1999), more dates could potentially characterize any variability within the formation.

Mineralization in the Sioux Lookout Belt

STAGES 1–4 VOLCANOGENIC MINERALIZATION IN THE SIOUX LOOKOUT OROGENIC BELT

As shown in Figure 22, the different types of mineralization found in the Sioux Lookout orogenic belt appear to have been generated during specific tectono–stratigraphic stages. The interpreted mineralization processes conform with standard contemporary ore deposit models and are appropriate to the lithologies and structures present at mineralized sites.

Within a basalt–floored oceanic basin (Stages 1 and 2), some hydrothermal flow of metalliferous fluid upward along sub–seafloor features such as extensional faults, fractures and permeable horizons likely would have occurred during periods of local eruptive quiescence. Layered exhalite units (e.g., BIF) would have formed via either seafloor venting of the fluid ("smokers") and gravity settling of precipitates, or fluid diffusion within the upper volcano–sedimentary pile.

The subvolcanic Northeast Bay pluton (Stage 3) contains only minor amounts of sulphide mineralization and rare accessory Cu and Mo, suggesting very weakly developed porphyry copper–type mineralization. In the comagmatic and most likely coeval basaltic andesite stratovolcanic succession, the paleoenvironment is interpreted as having been partly subaerial (subaerial regressive periods alternated with subaqueous transgressive periods: Devaney 1998), which would not have been conducive to the preservation of any vented hydrothermal fluid. During subaqueous periods, the subvolcanic pluton(s) was too small to create a hydrothermal system large or hot enough to generate exhalite deposits.

In contrast, elsewhere in the western Wabigoon region, at Sturgeon Lake (approx. 60 km east of the Sioux Lookout orogenic belt), conditions during synchronous volcanism (ca. 2734 Ma) were far more favourable for the generation and preservation of VMS deposits: the Beidelman Bay pluton acted as a large subvolcanic "heat engine," able to drive an adequately large hydrothermal system, and a subaqueous caldera setting allowed local (sub–basinal) concentration and preservation of VMS deposits (Morton et al. 1991).

The highly local distribution of andesitic pyroclastic units in the Sioux Lookout orogenic belt (forming a Stage 3 volcanic centre: sites 14 and 15 in Figure 23) and similarities with some examples of intra–arc andesitic (sub–)basins suggests the accumulation of the andesitic succession in a small fault–controlled basin, such as a local graben. (Later fault reactivation appears to have obscured any direct evidence of synvolcanic faulting.)

Given that the adjacent Sturgeon Lake belt also records similar synchronous (Stage 3, ca. 2733 Ma) plutonism, volcanism and a local extensional sub–basin (caldera), there were likely similar tectonic conditions (an extensional or rifted arc stage) in both the Sioux Lookout orogenic belt and the Sturgeon Lake belt (Figure 22). Indeed, the conditions in the two areas are probably merely regional variations (within the western Wabigoon region) of the *same* volcano–plutonic event, but the "components" (subvolcanic pluton, subaqueous volcanic centre, extensional sub–basin) were all *larger* at Sturgeon Lake, an essential factor in forming the economic–grade VMS deposits there.

Note that this is the first interpretation of the Sturgeon Lake VMS deposits as having formed in a rifted arc setting (Devaney 1997). However, the conclusion should not be surprising given that the rifted arc setting, including some back–arc basins, is now thought to be one of the most favourable toward generation of economic VMS deposits (e.g., Syme et al. 1996, Lentz 1998).

At ca. 2733 Ma, the proposed rifted arc phase (Sioux Lookout orogenic belt Stage 3) produced relatively small, localized volcanic centres within the western Wabigoon region (Edwards and Davis 1984, Berger 1991), versus the much more widespread volcanic units of earlier and later volcanic stages. The various ca. 2733 Ma volcanic centres could be explored in more detail regarding their potential volcanogenic mineralization.

Stage 4 deposits are typically dactic pyroclastic to volcaniclastic rocks with highly fractionated FI type geochemical characteristics (*see* "Geochemistry") and only minor amounts of rusty weathering (gossan) of pyrite in outcrop. These features signify poor VMS potential. Iron formation units (magnetite, chert, pyrite) with probable "footwall alteration," including "felsic–in–mafic" breccias with hyrothermally altered matrixes (e.g., Devaney 1996), are present (Chorlton 1991) rather than VMS layers.

A REGIONAL RIEDEL SHEAR LINEAMENT PATTERN OF GOLD OCCURRENCES?

Figure 33 shows gold occurrences in the area of the Sioux Lookout orogenic belt and equivalent rock units to the southwest, plus a proposed lineament pattern connecting the occurrences. Major stratigraphic and fault surfaces trend at approximately 64º (Johnston 1969, 1972; Devaney et al. 1995b). Given the importance of late (Stage 6) sinistral strike–slip faulting outlined above, structural theory (see Figures 33, 34) allows that a conjugate Riedel shear fracture set (R and R' surfaces) could have formed. Based on this pattern, it is hypothesized that a regional–scale network of such R and R' fractures (Figure 33) formed a permeability system for the flow of gold–bearing fluids (i.e., the present auriferous quartz veins; for Teck–Corona gold prospect and Goldlund Mine, see: Page 1984, Chorlton 1991, Blackburn et al. 1998).

Although other lineament patterns are also possible (e.g., transpressional P shears), it is suggested that an orderly sinistral set of R and R' surfaces (faults, fractures, shears) might be expected as late transtensional tectonic features in such a region of sinistral strike–slip faulting. The lineaments of the proposed R and R' system are *not* mapped continuous faults, but may be preferred sites and orientations for discontinuously developed fracture, fault or shear systems. Note that planar features need not be in their "ideal" orientations; late faulting and progressive deformation may have rotated R, R' and other surfaces from their ideal theoretical orientations (e.g., Tchalenko 1970, Hempton and Neher 1986), and local anisotropies are likely to have influenced or deflected stresses.

This R–R' hypothesis (Figure 33) is consistent with much of the detailed structural analysis of Chorlton (1990, 1991), whose study of the area immediately southwest of the present study area noted the importance of northeast– and east–northeast–trending veins and shear zones (some auriferous) and sinistral movements, amidst various structural complexities, in the southwest area's late stage tectonism and related gold mineralization.

If the concept of a regional–scale Riedel shear/fracture set pattern (Figure 33) is correct, the pattern would have to be a very late, cross–cutting overprint on the previously complexly tectonized Sioux

Lookout orogenic belt. This would conform with the common view that gold was typically deposited very late in the tectonic history of Superior Province greenstone belts (e.g., Colvine et al. 1988, Groves and Foster 1991). Any similarly late granitic plutons intruded into transtensional sites (e.g., releasing bends) could have provided heat for hydrothermal vein systems.

Given that regional–scale Riedel and P–shear/fracture patterns in other orogenic belts have been interpreted as controlling factors in pluton emplacement (Petford and Atherton 1992, Tikoff and Teyssier 1992) and Archean gold mineralization (Mueller et al. 1988, Peterson 1997), the similar interpretation in Figure 33 might be mechanically reasonable. Although requiring much future testing, this new hypothesis could serve as an exploration model for the Sioux Lookout orogenic belt and other similar areas.

DISCUSSION OF THE POTENTIAL IMPORTANCE OF TRANSPRESSION, VERTICAL EXTENSION, AND HORIZONTAL VEINS

As demonstrated by a number of recent studies concerning variable strain partitioning in orogens, particularly in wrenched belts (e.g., Holdsworth et al. 1998), at intra–orogen sites where transpressional (obliquely compressional) forces are near to orthogonal to strata (i.e., at a greater than 70º angle to the main, steeply dipping, planar orogenic fabric) rather than closer to parallel, vertical motions are to be expected. Because of natural geometric irregularities in the orientation of faults, such vertical extension as the result of transpressional forces may be localized at appropriately oriented fault restraining bends (e.g., in a sinistral setting, lazy–Z sigmoidal forms of opposite sense to the lazy–S sigmoidal forms of transtensional fault releasing bends), in contrast with zones where transpressional forces are closer to parallel with faults and strike–slip faulting will occur. Vertical extensional forces may result in: vertical (or steep) displacements along faults, vertical or steep lineation or stretching fabrics (Tikoff and Greene 1997, Dewey et al. 1998), and horizontal (or nearly so) planar fractures and veins. Structures that form via the vertical displacement of blocks or slices at transpressional sites such as fault releasing bends are known as “pop–up” structures (and various synonymous terms: “push–up” structures, “positive flower” structures, or “palm tree” structures: Harding 1985, Sylvester 1988), and occur at scales of centimetres to entire orogens.

Planar veins with very low dip angles are uncommon in the Sioux Lookout orogenic belt, but are worthy of future detailed study owing to their potential similarities with documented gold–bearing vein systems. Sibson et al. (1988) noted a common association of high–angle reverse faults with “vein flats” (i.e., vein systems with flat or low dips) in selected areas of gold mineralization. In such cases, it is suggested that a steeply oriented reverse fault might represent part of a positive flower or pop–up structure, and vertical extension associated with the localized transpressional strain within and around the pop–up structure would have created the vein flats (Devaney 1999b).

Thus, zones with (quasi–)vertical extension features may be expected within wrenched belts or transpressional orogens (e.g., much of Superior Province) and are potential hosts for auriferous veins.

SUMMARY

The nature of the mineralization in the belt is directly related to the different tectono–stratigraphic evolutionary stages (Figure 22). During Stages 1 and 2 deep water exhalites (magnetite iron formation, chert, pyrite) formed; pyrite was formerly mined in the area. Stage 3 volcanism produced ore deposits in an adjacent greenstone belt (the Cu–Zn VMS deposits at Sturgeon Lake), but in correlative rocks in the Sioux Lookout area no VMS deposits, no epithermal mineralization, and only insignificant amounts of porphyry copper–type mineralization, have been found. During Stage 4 basinal development a large magnetite iron formation unit accumulated in the southeast part of the belt, but in other areas only minor (uncommon) volcanogenic sulphide mineralization and sub–exhalite hydrothermal alteration are present, and the “FI” character of the Stage 4 dacitic–rhyolitic rocks does not suggest good VMS potential. Synorogenic (Stages 5 and/or 6) quartz veins appear to be thicker and more abundant, and contain more gold, near the major deformation zones (thrust and/or strike–slip faults), suggestive of formation as typical

structurally–controlled Archean mesothermal lode gold deposits. At a regional (10 to 100 km) scale, gold occurrences appear to be located along lineaments which resemble a Riedel shear fracture system.

RECOMMENDATION FOR MINERAL EXPLORATION

It is suggested that in order to explore for gold deposits in the Sioux Lookout orogenic belt (and in other similar areas), geologists should: 1) perform detailed mapping and sampling of quartz–veined areas in tectonic deformation zones (perhaps regardless of the type of rock hosting the veins); and 2) attempt to classify and interpret the history of the belt's various, probably complex, late orogenic stage transtensional and transpressional structural domains. Given: 1) the affinity of mesothermal and epithermal gold deposits for late tectonic strike–slip faults in both Archean and younger orogens (Colvine et al. 1988, Mueller et al. 1988, Wyman and Kerrich 1988, Kerrich 1989, Eisenlohr et al. 1989, Vearncombe et al. 1989, Nesbitt 1991, Groves and Foster 1991, Henley and Adams 1992, Hagemann et al. 1992, Hodgson 1993, DeRonde and De Wit 1994, Robert and Poulsen 1997); 2) the numerous examples of gold mineralization hosted by quartz veins in late tectonic structures in the Sioux Lookout belt (Johnston 1969, 1972; Page 1984; Brown 1985; Chorlton 1990, 1991; Devaney et al. 1995a; see also Sutherland and Colvine 1979, McMullan 1980); and 3) the importance of late orogenic strike–slip faulting in the Sioux Lookout orogenic belt (documented by Chorlton (1990, 1991) and interpreted herein), the strong relevance of structural geological concepts in the search for mesothermal lode gold deposits in areas such as the Sioux Lookout orogenic belt should be apparent.

Discussion: Relevance of Results of This Study to the Western Wabigoon Subprovince and Other Areas

This report provides a new synthesis of the Sioux Lookout orogenic belt, a synthesis emphasizing sedimentary geology but also integrating a variety of other geological subdisciplines (e.g., volcanology, geochemistry, regional tectonics). The main conclusion of this study is that the Sioux Lookout orogenic belt was produced during multiple, very different stages of evolution; this "greenstone belt" represents not one, but *several*, types of successively developed Late Archean volcanic–sedimentary basins (Figure 22). The different types of mineralization present correspond directly with different stages of basinal evolution and, at the largest scale, plate tectonic evolution. The final form of the Sioux Lookout orogenic belt is that of an orogenic belt similar in style to other belts of both Precambrian and Phanerozoic age.

The Sioux Lookout orogenic belt may serve as a model or "template" to interpret other similar parts (belts) of the western Wabigoon subprovince and perhaps also similar orogenic belts of any age. Geologists have long noted broad stratigraphic similarities within the entire western Wabigoon subprovince (Pettijohn 1937, Trowell et al. 1980, Blackburn et al. 1985, 1991), so it may prove useful to extrapolate and test ideas generated as parts of this study throughout the rest of the subprovince. (Models are idealistic, so local minor variance from the Sioux Lookout orogenic belt model should be expected. If there is major variance between the Sioux Lookout orogenic belt model and a belt undergoing comparison, the model would not apply to the compared belt.) As the following discussion builds on content previously presented and referenced herein, see the previous sections of this report for supporting data and interpretations.

In the case of multiple available models, this requires critical evaluation by the reader in order to choose the best model to apply. Because Sanborn–Barrie and Skulski (1999) offered a significantly different model of the part of the western Wabigoon subprovince adjacent to the east and northeast of the Sioux Lookout orogenic belt, discussion of the strengths and weaknesses of their model (see below) is relevant to its potential application to the Sioux Lookout orogenic belt and other parts of the subprovince.

STAGE 1: INITIAL RIFTING AND THE FORMATION OF A WESTERN WABIGOON OCEAN BASIN

Evidence of an initial rifting stage may have been only rarely and locally preserved in the large "basin" represented by the western Wabigoon subprovince. Sanborn–Barrie and Skulski (1999; see also Cortis et al.

1988) interpreted the basal unit of the Sturgeon–Savant belt, quartzose coarse clastic facies of the Jutten Group, as a rift margin deposit overlain by magnesian tholeiitic submarine basalts. These Jutten Group basalts are equivalent to the Stage 1 basalts of the Sioux Lookout orogenic belt (e.g., the Northern Volcanic belt) and are very similar or equivalent to the lower mafic sequences present throughout the western Wabigoon subprovince (Trowell and Johns 1986, Blackburn et al. 1991, Ayer and Davis 1997). This suggests that the Stage 1 scenario in Figure 22a, a basalt–floored narrow oceanic basin, is broadly applicable to the entire western Wabigoon region. Owing to rarity of isotopic data, the potential influences of (felsic) crustal contamination on Stage 1 basalt compositions are not yet well constrained or understood, but are suspected (*see* "Geochemistry," and Sanborn–Barrie and Skulski 1999).

If this rift to ocean extensional basin scenario is correct, it need not be assumed that a simple single basin formed. Large rifted areas may be compartmentalized into a number of stratigraphically discrete sub–basins (e.g., the "multi–rift model" of Tamaki 1985, 1988), a concept which could help to account for variability (including geochemical composition) among the individual belts (sub–basins?) which together comprise the western Wabigoon subprovince. Although early stage structures such as rift–related fault systems would have been present, subsequent episodes of tectonism appear to have completely obscured the record of any such mega–structures. Any speculations about whether the present distribution of early basaltic units might directly reflect former Late Archean extensional sub–basins are unconstrained.

STAGES 1 TO 3: OLDER BASALTIC UNITS, WITH COMMENTS ON SUPPOSED "BACK–ARC BASALTS"

Based on the geochemical characteristics of the older basaltic units in the western Wabigoon subprovince, some workers have suggested that these units represent the infill of back–arc basins (e.g., Day 1990, Ayer 1991, Ayer and Davis 1997). However, no arc to back–arc linkage (stratigraphic polarity) or paleogeographic relationships have been documented. Ideally, ancient back–arc basins should be interpreted via their stratigraphic and tectonic context, and not merely via the relative abundances of certain trace elements as plotted on the currently popular "tectonic discrimination diagrams."

Stage 2 basalts, interpreted as juvenile arc deposits, presumably developed in what was formerly a nonarc rift basin (Figure 22), implying that the ascent of magmas from a subduction zone took advantage of the available rift basin site to form an arc. Alternatively, both the Stage 1 and 2 basalts may have been products of subduction, similar to the early stages in some continental back–arc basin models (e.g., Okinawa Trough: Letouzey and Kimura 1986).

Sequences of predominantly volcanic rocks which are interpreted as ca. 2745–2704 Ma arc sequences are exposed to the east and northeast of the Sioux Lookout orogenic belt, in the Sturgeon Lake and Savant Lake areas of western Wabigoon subprovince (Blackburn et al. 1991, Sanborn–Barrie and Skulski 1999). In a broad regional sense (i.e., at a 200 km scale of view), these areas are along regional strike from the Sioux Lookout orogenic belt, and thus coeval volcanic rocks of the Sioux Lookout orogenic belt would have been in an "along–arc" rather than "back–arc" position. The nature of any segmentation of a western Wabigoon arc into intra–arc basins or sub–basins, perhaps influenced by the locations of any earlier rift sub–basins (see above), is poorly known. Note too that because of tectonic deformation, the present configuration of the individual orogenic belt segments in the tectonized western Wabigoon region need not clearly reflect their relative positions 2.7 Ga ago (e.g., the potentially displacive role of the Lewis Lake batholith (Blackburn et al. 1991, Figure 9.3) is unknown).

STAGE 3: PARTIAL OR INCIPIENT RIFTING OF AN ARC?

Following the work of Page and Clifford (1977), results presented herein provide more detailed descriptions and interpretations of the sequence of andesitic volcaniclastic rocks (and related flows and dikes) exposed in the Northeast Bay of Minnitaki Lake area. Documented occurrences of subaerial volcanic facies and andesites are generally rare in Superior Province, so their presence in the Sioux Lookout orogenic belt should be of general interest to Superior Province workers.

This andesitic sequence and its comagmatic subvolcanic pluton, newly dated at ca. 2732 Ma, are correlative with the VMS–bearing caldera succession and subvolcanic Beidleman Bay pluton at Sturgeon Lake (Devaney 1997, 1999a). These and other widely scattered ca. 2735–2732 Ma dioritic and andesitic rocks within western Wabigoon subprovince (e.g., Edwards and Davis 1984) may represent intermediate–felsic volcanic centres and related subvolcanic plutons that developed at local sites of incipient or partial rifting of a western Wabigoon arc basin. Scenarios involving such types of extensional volcanic sub–basins within arcs, including VMS–mineralized intra–arc basins, are increasingly being documented from both Archean and younger arc successions (Cathles et al. 1983, Smellie 1995, Syme et al. 1996, Lentz 1998). Some "extensional" volcanic sub–basins may actually be transtensional pull–apart volcanic basins (e.g., Sasso and Clark 1998, van Wyk de Vries and Merle 1998); such resolution would depend on preservation of good quality regional structural data and might not be available for many Archean belts and subprovinces.

POTENTIAL RESOLUTION PROBLEMS INVOLVING GEOCHRONOLOGICAL DATA AND THE EQUIVOCAL IDENTIFICATION OF "TUFFS"

Some of the geochronological database for the western Wabigoon subprovince and other areas is based on rocks which have in the past been identified as "tuffs" or other pyroclastic rocks. However, Superior Province workers have long appreciated the difficulties involved in dinstinguishing tuffs from wackes (e.g., Pettijohn 1935, p. 1902), and some recent volcanological research (Cas and Wright 1987, 1991) asserts that many volcanic fragmental (tephra) deposits are/were generally highly prone to sedimentary reworking, suggesting the need for a more critical assessment of rocks identified as "tuffs" and coarser pyroclastic facies.

Because sedimentary mass flow (or gravity flow) deposits have depositional fabrics similar or identical to those of many unwelded hot pyroclastic (or other directly volcanic) mass flow deposits, and field evidence of hot emplacement tends to be very rare in Superior Province rocks, an unknown number of Archean "tephra" beds may be resedimented "volcaniclastic" facies rather than beds of truly pyroclastic origin (Devaney 1999c).

There may be a mapping bias against thick beds and mass flow deposits, versus more easily recognizable thin beds of current deposits (e.g., turbiditic wackes). Massive or poorly bedded fragmental facies with accessory oligomict volcanic clasts (e.g., a "felsic lapilli tuff") have commonly been identified as pyroclastic rocks, but in some (or perhaps many?) cases they may be thickly bedded proximal sedimentary facies rather than pyroclastic facies. Particularly problematic would be any very thick (>5–10 m) mass flow beds, beds thicker than the width of the typically small outcrops in northern Ontario. Along a volcanic to sedimentary facies gradient, thickly bedded proximal sedimentary facies composed of originally volcanic grains and clasts would represent an intermediate zone between a highly proximal volcanic centre and a more distal, probably finer grained and deeper water facies (Devaney 1999c).

Zircon grains in any such resedimented "tuffs" are detrital, suggesting the need for re–examination of some Superior Province data and interpretations. For example, it has been assumed by Sanborn–Barrie and Skulski (1999) that the ca. 2775 Ma age of the "Fourbay sequence" of the Sturgeon–Savant belt (see also Davis et al. 1988) reflects the volcanic deposition of true tuffs, and hence dates the early stage development of "oceanic basement" in the belt (equal to Sioux Lookout orogenic belt Stage 1 Northern Volcanic belt). However, neither Davis et al. (1988) nor Sanborn–Barrie and Skulski (1999) have provided descriptions or arguments that might allow for discrimination of these supposed "tuffs" as either true tuffs or resedimented facies. In the latter case, the dated grains would be detrital, and thus the depositional age could be considerably younger than 2775 Ma.

Similarly, the 2734–2732 Ma age (Davis and Trowell 1982) of a felsic tuff interbedded in the Sioux Lookout orogenic belt Stage 2 basaltic section of the Central Volcanic belt may be less reliable than previously thought. Brief observations of this outcrop did not suggest that the distinction between a pyroclastic or sedimentary origin could be made reliably.

In contrast, the ca. 2719–2713 Ma age of a distinctive felsic crystal tuff from the Sioux Lookout orogenic belt Stage 4 Daredevil Formation (lithology: Turner and Walker 1973; date: Davis et al. 1988) is considered to record the directly pyroclastic deposition of this apparently non–resedimented rock.

If sedimentary reworking rapidly followed volcanic deposition, the gap between the time of volcanic deposition (e.g., as recorded in zircon grains) and the time of sedimentary deposition would be minor or trivial. In volcanically active basins, steep depositional slopes and earthquakes would be expected, and resedimentation in proximal zones would be characteristic. This is thought to have been the case for the deposition of the Minnitaki Group, for which the ca. 2714 Ma age of detrital zircon grains should approximate the age of the synchronous volcanism, BIF deposition and clastic sedimentation in the Sioux Lookout orogenic belt Stage 4 deep marine arc basin.

Consideration of the above factors may improve future resolution of other volcanic and sedimentary events elsewhere in the western Wabigoon subprovince.

STAGES 4 TO 6: NEW DESCRIPTIVE AND INTERPRETATIVE STRATIGRAPHY OF VOLCANICLASTIC ARC DEPOSITS AND SYNOROGENIC CONGLOMERATIC FORMATIONS

The new descriptive stratigraphy presented for the Big Vermilion–Daredevil unit (informal term) and surrounding formations is a simpler framework of more linear map units than that of previous mapping, and is consistent with geochronological data. The old term “Abram Group” has been invalidated by this geochronological data, which require that the “Abram Group” cannot be a continuous and conformable sequence of three formations, as was previously thought. Thus the reviews of the Sioux Lookout orogenic belt in the summaries of the western Wabigoon subprovince by Blackburn et al. (1985, 1991) require updating:

1) the Patara Formation, formerly thought to be the oldest sedimentary unit in the Sioux Lookout orogenic belt, is now known to be one of the youngest sedimentary units (probably the youngest unit in the Sioux Lookout orogenic belt), a synorogenic conglomerate;

2) the Ament Bay Formation, formerly thought to form the basal unit of the “Abram Group” and to conformably underlie the Daredevil Formation, is now known to be younger than the Daredevil Formation, and is one of the youngest sedimentary units in the Sioux Lookout orogenic belt, a synorogenic conglomerate.

Recognition of conglomeratic units which underlie other units structurally (e.g., because of thrust faulting) rather than stratigraphically (as in older views of “homoclinal” sequences), as exemplified by the context of the Ament Bay Formation, may prove equally useful in other parts of the western Wabigoon subprovince. Thrust faults responsible for the stacking of “homoclinal–looking” sequences may be narrow, cryptic or unexposed, and may be revealed by geochronology rather than field mapping.

APPLICATION OF SIOUX LOOKOUT OROGENIC BELT STAGE 4, 5 AND 6 STRATIGRAPHIC AND STRUCTURAL CONCEPTS TO INTERPRETATION OF THE STURGEON–SAVANT BELT: REJECTION OF A “FOREDEEP BASIN” INTERPRETATION

The scenario described above, concerning older turbiditic and volcaniclastic facies in fault contact with younger conglomerates, is worthy of consideration for part of the Sturgeon–Savant belt, for which Sanborn–Barrie and Skulski (1999) placed a polymict conglomerate unit (which contains a 2705–2703 Ma granitoid clast) below “turbiditic wacke,” tuff and iron formation (with detrital zircon grains as young as 2704 Ma), supposedly together forming the “conformable” (“same–facing”) infill of a “foredeep” basin as

young as 2701 Ma. However, a few million years should probably be allowed for the erosional unroofing of the 2705–2703 Ma granitoid clast, which would require deposition of that part of the conglomerate unit to be of about 2700 Ma age or younger

The "turbiditic sediments" of the proposed foredeep basin (i.e., Savant Lake and Quest Lake sediments: Sanborn–Barrie and Skulski 1999, p. 216, 219) and associated tuff and iron formation resemble the suite of facies in the Stage 4 rocks of the Sioux Lookout orogenic belt (ca. <2714 Ma to 2704 Ma: Minnitaki Group, Big Vermilion–Daredevil unit). Thus, based on the points listed above, it is proposed that:

1) the conglomerate unit in the Sturgeon–Savant belt (probably <2701 Ma) may be younger, rather than older, than the ca. 2704–2701 Ma turbiditic Savant–Quest sediments;

2) the conglomerate unit in the Sturgeon–Savant belt may be cryptically in fault contact with the turbiditic Savant–Quest sediments; according to M. Sanborn–Barrie (personal communication, 1999), field relationships do not suggest a faulted contact, but in the Sioux Lookout orogenic belt similar contacts (e.g., Ament Bay Formation–Daredevil Formation contact, Patara Formation–Northern Volcanic belt contact) were for many decades considered to be in conformable rather than faulted contact, which may be a useful lesson concerning the difficulty of recognizing subtly faulted contacts;

3) because the polymict conglomerate in the Sturgeon–Savant belt is distributed along late ("D2") deformation zones (M. Sanborn Barrie and T. Skulski, personal communications, 1999), this suggests that it may be a synorogenic conglomerate broadly correlative with the <2700 Ma synorogenic conglomerate units in the adjacent Sioux Lookout orogenic belt; and

4) the turbiditic wackes, tuffs and iron formation (Savant–Quest sediments) of the Sturgeon–Savant belt were deposited in the same mature arc basin, or a similar and coeval arc basin, as the Stage 4 units of the Sioux Lookout orogenic belt (Figure 22a) rather than in the "Savant sedimentary foredeep basin" of Sanborn–Barrie and Skulski (1999, p. 219).

Furthermore, the deposits of a foreland or foredeep basin, by definition (e.g., Miall 1995), would be positioned adjacent to an orogenic belt (not *within* it, as is the case for the Sturgeon–Savant belt) and would be supplied with clastic sediments from the tectonized (usually thrusted) rocks of an adjacent orogenic belt (no such adjacent orogenic belt has been recognized by Sanborn–Barrie and Skulski (1999) or any other workers). Because the proposed foredeep basin interpretation satisfies neither of these basic criteria, it is rejected in favour of the arc subaqueous basin (Sioux Lookout orogenic belt Stage 4 depositional style) interpretation. The record of volcanism as active during sedimentation of turbiditic sequences (e.g., interbedded felsic tuffs and exhalative iron formation) further supports an arc rather than foreland context (In contrast with the conventional foreland/foredeep basin definition (e.g., Miall 1995) used above, DeCelles and Giles (1996) have proposed a different, expanded, four–fold subdivision of foreland basins. In their scheme, piggyback basins would be part of an orogenic "wedge–top depozone" adjacent to a "foredeep depozone." Recognition of syndepositional thrusting is essential in order to apply these terms.)

It is suggested that attempts to apply models directly based on interpretations of the Sioux Lookout orogenic belt (e.g., Figures 22a, 25, 31) may be useful in elucidating the history of the Sturgeon–Savant belt, allowing for some local (belt–to–belt) variance.

REJECTION OF INTERPRETATIONS OF ACCRETIONARY PRISM DEVELOPMENT WITHIN THE WESTERN WABIGOON SUBPROVINCE

There is no unequivocal evidence in Sioux Lookout orogenic belt, or elsewhere in western Wabigoon subprovince, for the development of the type of subduction zones and accretionary prism assemblages proposed by Blackburn (1980) and Sanborn–Barrie and Skulski (1999). It is suggested that any proposed subduction zone *within* the western Wabigoon subprovince (Blackburn 1980, Figure 4; Sanborn–Barrie and Skulski 1999, Figure 13) would have been unrealistically small, even in a microplate context, versus

interpretations of an appropriately larger scale, north–dipping subduction zone with a trench located south of the Wabigoon subprovince (Blackburn et al. 1985, Figure 17; Devaney and Williams 1989).

It has been suggested that an accretionary prism succession might lie buried beneath "foreland" deposits in the Sturgeon–Savant belt (T. Skulski, personal communication, 1999). However, this hypothesis is problematic because the interpretation of "foreland" deposits has been rejected (see above) and the hypothesis cannot be tested by field mapping. Given the scale considerations noted above, the accretionary prism presumably generated by the subduction which produced the ca. 2745–2704 Ma volcanic arc successions in the western Wabigoon subprovince is likely represented by the metasedimentary–plutonic Quetico subprovince (Blackburn et al. 1985, Figure 17; Devaney and Williams 1989).

Similar problems of scale and lack of evidence of any prism succession apply to the interpretation by Sanborn–Barrie and Skulski (1999, Figure 13) of a small subduction zone presumed to have sourced older (ca. 2745–2718 Ma) "Handy arc" volcanic rocks. Note that a sediment–starved trench would not likely develop during such a major period of arc growth and generation of huge volumes of pyroclastic to volcaniclastic detritus, so any subduction zone–related trench present should have accumulated and accreted much sediment in an accretionary prism. The absence of such a prism succession favours instead the far–distant Quetico prism scenario noted above.

The tectono–stratigraphic style of the Minnitaki Group of the Sioux Lookout orogenic belt, a predominantly turbiditic wacke succession with intercalated basaltic units speculatively interpreted as an internally folded thrust stack (Figure 23), might suggest to some workers an origin as an accretionary prism. However, no "melange" or "broken formation" fabrics (Cowan 1985, Rast and Horton 1989, Maltman 1998), or other evidence of accretionary prism rather than arc basin development, have been recognized in the Minnitaki Group. (In contrast, sedimentological and structural evidence supporting an accretionary prism interpretation for the Quetico subprovince has been presented by Williams (1989, 1991) and Fralick et al. (1992).)

ADAKITIC MATURE ARC (STAGE 4) ROCKS, AND THEIR RELEVANCE TO POTENTIAL PLATE TECTONIC SCENARIOS

Volcaniclastic rocks (i.e., pyroclastic rocks, or products of minor sedimentary reworking of pyroclasts; not as "fully reworked" as true sedimentary facies) of the Big Vermilion–Daredevil unit have adakitic characteristics. Documentation of adakites has only recently begun for Superior Province and other Archean cratons. The preservation of an orderly geochemical pattern, such as an adakitic signature, in volcaniclastic rocks implies that there has been little or no problematic sedimentary reworking of the original primary pyroclastic composition, and subsequent alteration and metamorphism also have not obscured orderly signatures.

The potential plate tectonic context of adakites (late arc, preorogenic compression?) is relevant to regional interpretations of the Sioux Lookout orogenic belt and the rest of western Wabigoon subprovince. Adakitic magmas are thought to be products of the subduction of young (e.g., <25 Ma) oceanic lithosphere (Drummond et al. 1996). In such convergent plate margin settings, the subduction of younger, hotter and less dense oceanic crust is expected to have been at lower dip angles and to have caused regional compressional stresses, versus the case for older, colder and denser crustal slabs subducting under conditions of regional extension (e.g., Morris and Witt 1997, Figure 9; see also Busby et al. 1998). As the slab subduction angle decreases, the mantle wedge region (Pearce and Peate 1995) would become smaller and thus slab melts would increasingly be less likely to be diluted in the mantle wedge region, therefore increasing the likelihood of adakitic metasomatism of the mantle wedge and the "survival" of the adakitic signature in magmas eventually erupted as volcanic rocks.

Following this model view, adakitic rocks of the Sioux Lookout orogenic belt (some Stage 4 volcanic rocks), which ideally would reflect the Late Archean low–angled subduction of then–young oceanic crust and thus the presence of regional compressional stresses, would have been deposited between Stage 3

volcanism (interpreted extensional stresses: e.g., intra–arc rifting above a steeply subducting slab) and Stage 5 early orogenic collision and compression (thrusting of older Sioux Lookout orogenic belt arc sequences). Perhaps, as appears to be the case for the Sioux Lookout orogenic belt, the generation of adakitic magmas can signal the forthcoming end of subduction and onset of collisional orogenesis. Such geochemically–based scenarios may be relevant to models of arc evolution (e.g., the extensional to compressional model of Busby et al. 1998).

TECTONO–STRATIGRAPHIC CONTEXT OF CA. 2704 Ma VOLCANIC ROCKS

Sites in the western Wabigoon subprovince of volcanic rocks dated at ca. 2704 Ma (Davis 1990, Sanborn–Barrie and Skulski 1999) are becoming more numerous and widespread. These volcanic rocks may be interpreted as: a) late arc deposits, which would require that postarc orogenic events occurred after ca. 2700 Ma; or b) synorogenic deposits, with orogenesis beginning at ca. 2710–2705 Ma and volcanic centres perhaps localized at sites of intra–orogenic wrenching (e.g., magma conduits in transtensional zones) or other types of large structures; or c) representative of a transitional phase during which terminal arc development overlapped with early collisional orogenesis (e.g., transition from a Stage 4 compressional arc to a Stage 5 fold–and–thrust belt).

GEOCHEMICAL PATTERNS AND TRENDS

This study has provided new Sioux Lookout orogenic belt geochemical data, especially for the (meta)volcanic rocks. The upward transition from tholeiitic mafic to calk–alkalic intermediate–felsic volcanic rocks, typical of Archean greenstone belts, is present. The change in basalt composition from Stage 1 (N–MORB/“arc”) to Stage 2 (E–MORB) rocks should indicate a shift from a depleted to a more enriched mantle source (e.g., Figure 15) and may reflect the onset of subduction. Rocks of Stages 2 to 4 record progressive (orderly?) evolution of an arc: for example, increased fractionation of magmas over time, and an increasingly negative Nb anomaly over time (Figures 19, 20, 21). Along with this Nb anomaly trend, the change in composition from Stage 3 “transitional adakites” to Stage 4 adakites (Figure 18) indicates an increasingly strong subduction signature over time. The increase in fractionation presumably reflects a thickening of the arc crust over time, the thicker crust being able to contain more vertically stacked magma chambers, which would have allowed more opportunities for multiple fractionation of magmas.

The geochemical (“geodynamic”) signatures present in the Sioux Lookout orogenic belt (*see* “Geochemistry”) have been identified: a) from both unaltered and altered rocks, suggesting that the supposedly “immobile” trace elements which define most of these signatures were indeed immobile, and any obfuscating effects of alteration have been averaged out in the sample groups; and b) from both volcanic flows and volcaniclastic facies in Stage 3 and 4 units, suggesting that any resedimentation, which could have formed disorderly (“disequilibrium”) assemblages of clastic grains, was not a problematic factor. These results indicating multi–stage tectono–magmatic evolution are comparable with those of the more geochemically sophisticated studies of other western Wabigoon subprovince volcanic successions by Ayer and Davis (1997) and Sanborn–Barrie and Skulski (1999).

SEDIMENTARY PATTERNS AND TRENDS

Small–scale sedimentological and physical volcanological features recognized in the Sioux Lookout orogenic belt help define a larger–scale stratigraphy which is supported by geochemistry and geochronology (Figures 2, 21, 22) and reflects stages of evolution typical of arcs (Stages 2 to 4) and orogenic belts (Stages 5 and 6). Clastic and chemical sedimentary facies faithfully record the differences among these stages, and such facies analysis may be similarly useful elsewhere in the western Wabigoon subprovince.

The predominantly basaltic Stages 1 and 2 record only a very low amount of clastic sedimentation (e.g., deepwater "starved" basinal facies) versus far more significant exhalative chemical sedimentation. The Stage 3 andesitic succession, a local volcanic centre, records abundant pyroclastic deposition and minor clastic reworking in both subaerial and subaqueous, proximal to medial settings. Stage 4 pyroclastic facies and slightly to highly reworked ("resedimented") sedimentary deposits, including the classic graded turbiditic wackes so common in the arc portions of Archean greenstone belts, form large stratigraphic units and contain interbedded BIF units. Stage 5 and 6 formations are coarse clastic units containing neither chemical sedimentary facies nor volcanic facies

The composition of the Stage 1, 2 and 4 chemical sedimentary facies (e.g., magnetite, pyrite and chert in BIF units) directly reflects broadly synchronous volcanism, which provided the heat to drive the circulation of hydrothermal fluids in the volcanic basement beneath the seafloor, followed by venting of those fluids on the seafloor, presumably during inter–eruptive hiatal periods.

(Any exhalative facies in the VMS deposits at Sturgeon Lake represent Stage 3 chemical sedimentation.)

There are sharp contrasts between the coarse clastic, synorogenic, predominantly fluvial, Stage 5 and 6 formations. The Stage 5 Ament Bay Formation is a large unit with a highly diverse (polymict) composition of clasts, versus the significantly smaller Stage 6 Patara Formation and its near oligomict suite of very locally derived (from the Northern Volcanic belt) basalt clasts. The composition of the clasts in these two synorogenic conglomeratic units contrasts sharply with the exclusively intermediate–felsic volcanic clasts (including porphyritic clasts) of the relatively minor conglomeratic units in the Stage 3 and 4 successions.

OROGENIC STAGES 5 AND 6: GENERALIZATIONS

The term "orogenic" has been considered herein to apply to the postvolcanic, postarc stages of the Sioux Lookout orogenic belt when most of the supracrustal rocks presumably acquired their penetrative deformation fabrics. (Technically, some workers would consider arc development to be one type of orogenesis, and because arcs can be variably deformed as they develop, the "late orogenic" events of some workers may equal the "late arc" events of others.)

Postarc orogenesis in the western Wabigoon subprovince began at about 2710–2700 Ma (Blackburn et al. 1991). The escape of magma and heat, which was presumably formerly confined to the western Wabigoon volcanic arc, became more diffused, as recorded by widespread 2710–2690 Ma synorogenic plutonism in both the western Wabigoon subprovince and the adjacent Winnipeg River subprovince (Beakhouse 1991, Corfu et al. 1995).

The results presented for the Sioux Lookout orogenic belt are in general agreement with Chorlton's (1990, 1991) structural study of the area adjacent to the southwest, and are consistent with Davis' geochronological framework (Davis and Trowell 1982, Davis et al. 1988, Davis 1990, Blackburn et al. 1991, Devaney 1999a). Prior to the present study, only Pettijohn (1934) and Chorlton (1990, 1991) recognized the importance of strike–slip faulting in the development of the Sioux Lookout orogenic belt.

The pattern of thrust faulting followed by strike–slip faulting ("wrenching") inferred for the Sioux Lookout orogenic belt Stages 5 and 6 has been commonly recognized in orogenic belts of all ages, and presumably reflects the concepts that: a) an adequately long period of orogenic compression or transpression of any belt is likely to steepen its strata considerably; and b) as strata steepen to near vertical orientation, with regionally oblique compression (i.e., transpression) more likely than perfectly orthogonal compression, strike–slip (to oblique–slip) motions will likely result. During later orogenic wrenching stages, predominantly steep permeable horizons such as faults and shear zones would have been suitably oriented to tap deeper crustal fluids, which may account for the commonly late orogenic timing of plutons and quartz vein–hosted gold deposits. (Regarding the form and continuity of the steep faults and shear zones at depth, whether they would flatten listrically at some depth(s) or continue steeply to great depths is

beyond the resolution of surface bedrock mapping, but ongoing LITHOPROBE seismic reflection studies in northwest Superior Province (Cruden and Hynes 1999) should help answer such questions.)

It would be of interest to see how widely a simple scenario of thrusting (e.g., northwest–vergent, plus other vergences influenced by the orientation of any underlying older crustal blocks?) followed by strike–slip faulting ("wrenching," likely with many local geometrical complexities) could be applied to the rest of the western Wabigoon subprovince. "Strike–slip faulting" would probably have to be treated as an over–simplification, given: a) the curvilinear rather than linear nature of most belts; b) the high potential for oblique–slip and dip–slip motions in transtensional and transpressional zones (Holdsworth et al. 1998); and c) the likely presence of some zones of more distributed, rather than discretely partitioned, shear. The Patara Formation of the Sioux Lookout orogenic belt and the Stormy Lake Group of the Manitou Lakes area (Blackburn et al. 1991, Mueller and Corcoran 1998) are the only strike–slip basin successions described so far from the western Wabigoon subprovince.

SYNOROGENIC CONGLOMERATIC UNITS

As the example of the Sioux Lookout orogenic belt illustrates, more than one type of synorogenic conglomeratic unit can be present in a belt. The presence of multiple conglomeratic units with different clast compositions, areal extent (sizes of formations), and prevalent top indication trends, representative of different types of basins within a belt, would likely require a more detailed tectono–stratigraphic subdivision than the application of one simple "Timiskaming–type" scenario.

Regarding the terminology for synorogenic strike–slip basins, use of the provincial and antiquated term "Timiskaming–type" basin should be discontinued in favour of more detailed and sophisticated contemporary classifications of strike–slip basins and other synorogenic basins (e.g. Nilsen and Sylvester 1995, Miall 1995). However, detailed resolution of the precise type of strike–slip basin (e.g., a transrotational basin) may not be possible for many Archean belts, so a more general assessment as a "strike–slip basin" or "pull–apart basin" may be more realistic. Also, pull–apart basins may occur as intra–arc basins (e.g., Hathway 1993, Sasso and Clark 1998). Although this is a potentially problematic point, most Archean polymict conglomeratic units are easily interpreted as postarc deposits because they: a) contain clasts of synorogenic granitoid rocks; b) have been radiometrically (U–Pb) dated as synorogenic; and c), particularly in some late orogenic strike–slip basins, may be less deformed (e.g., lower dips, less intense penetrative deformation) than the older stratigraphic units. Associated shoshonitic to alkalic volcanic units (Williams et al. 1992, Mueller and Corcoran 1998) are not diagnostic of arc versus postarc settings; they may be either late arc deposits (Hathway 1993, Ayer and Davis 1997) or postarc synorogenic deposits.

In contemporary usage, "successor basins" are postorogenic, not synorogenic (Ingersoll and Busby 1995, p. 50), so use of this term for Archean synorogenic clastic units should be discontinued (e.g., as has been done by Mueller and Corcoran 1998).

The Stage 5 Ament Bay Formation (piggyback basin) is a smaller stratigraphic unit than the Stage 4 units (late arc sequences: Big Vermilion–Daredevil unit, Minnitaki Group and the correlative Warclub Group), and the Stage 6 Patara Formation (strike–slip or pull–apart basin) is a smaller formation than the Ament Bay Formation, implying structural partitioning into smaller, tectonically controlled basins over time, as is typical in orogenic belts.

EARLY STAGE OROGENIC BELT DEVELOPMENT: A FOLD–AND–THRUST BELT (SIOUX LOOKOUT OROGENIC BELT STAGE 5) ADJACENT TO A BROKEN FORELAND

Despite a rarity of good small–scale structural evidence, Late Archean thrust stacking of supracrustal successions in the Sioux Lookout orogenic belt (Beakhouse 1988, Davis et al. 1988, Chorlton 1990, 1991;

Devaney 1997, 1999a) and other parts of western Wabigoon subprovince (Blackburn et al. 1991), based partly on recognition of "out–of–sequence" stratigraphy via radiometric dating, is widely accepted.

Most of the *interpreted* thrusts in the Sioux Lookout orogenic belt (Figures 22 to 25), some of which are very speculative, are based on map patterns suggestive of apparent repetition of orderly stratigraphy in an imbricate thrust stack. In areas lacking both radiometric dates and adequate exposure of deformation zones, such speculative interpretations may be the only interpretations possible. If the inference of thrusting of the Northern Volcanic belt over a Winnipeg River subprovince foreland (Figure 22) is correct, the Northern Volcanic belt would constitute obducted oceanic crust and would thus be *ophiolitic.*

Regarding the question of what was pushing the northwest–vergent, "thin–skinned," Sioux Lookout orogenic belt Stage 5 fold–and–thrust belt, there is a severe lack of resolution of the presumed southeastern hinterland area (a thick–skinned block?). Presumably, the western flank of the central Wabigoon subprovince region ("CWR" of Blackburn et al. 1991) acted as an older stable block which pushed against the Sioux Lookout orogenic belt; if there was a major horizontal detachment surface within this central Wabigoon block, it would have been a "thick–skinned" block or crustal sheet. At a larger scale, this central Wabigoon region functioned as the "Wabigoon Indentor," the motion of which accounts for the late orogenic sinistral faulting along the Miniss River Fault (Stott and Corfu 1991, Corfu et al. 1995) and within the Sioux Lookout orogenic belt (Stage 6 events).

Regarding the nature of the western Wabigoon–Winnipeg River subprovincial boundary, interpretation of the south margin of the Winnipeg River subprovince as a Laramide–type uplift (Figures 22, 28) is one of the few ways to account for the overturned Northern Volcanic belt along the north margin of the Sioux Lookout orogenic belt and similar structural relationships farther to the (south)west. The large folds depicted in the Figure 22 Stage 6 cartoon need not be considered an overly speculative or radical interpretation, because similar large folds in strata adjacent to Laramide uplifts have been documented (eg. Erslev 1986, Spang and Evans 1988).

In a scenario involving thrusting onto a foreland block (e.g., Sioux Lookout orogenic belt Stage 5 in Figure 22a), it need not be assumed that the foreland was perfectly tectonically stable or inactive. An important alternative is the broken foreland model (Jordan 1995), in which: a) the cratonic foreland is partitioned into fault blocks by major reverse faults; b) movement along these faults produces Laramide–type uplifts; c) the reverse fault(s) may verge opposite to thrusts in the synchronous fold–and–thrust belt; and d) "broken–foreland basins" form adjacent to uplifted blocks. Broken forelands tend to be associated with episodes of low angle subduction (Jordan 1995), which potentially allows a broad correlation of ca. 2715–2690 Ma compressional events in the Sioux Lookout orogenic belt:

1) Stage 4 compressional arc conditions may have resulted in eruption of adakitic volcanic rocks (see above), consistent with late arc stages involving low–angle subduction in the arc models of Morris and Witt (1997) and Busby et al. (1998), followed by

2) the collisional orogenesis (increased compression?) recorded by the Stage 5 fold–and–thrust belt and adjacent broken foreland (with the oblique–slip Miniss River Fault and other parts of the present Wabigoon–Winnipeg River subprovince contact (Figures 22, 23) as the steep reverse fault bounding a Laramide–type uplift "breaking" the Winnipeg River subprovince foreland) as potential indications of continued low–angle subduction and regional compression.

Such broken foreland scenarios have not been widely considered in the past by Archean geologists, and may be worthy of increased attention or emphasis in the future. The "differential uplifts" produced by "sinistral wrench faulting and thrusting along the Miniss River Fault and subsidiary structures in the interior of the" English River subprovince (Corfu et al. 1995, p.1232, 1230) are likely examples of a broken foreland regional setting.

Based on arguments presented herein, the Ament Bay Formation and potentially similar and correlative sedimentary units elsewhere in the western Wabigoon subprovince (e.g., in the Sturgeon and Savant lakes area: Sanborn–Barrie and Skulski 1999) should not be interpreted as foreland basin deposits. A foreland

basin would be adjacent to an orogenic belt, not inside it. Piggyback basins would be inside a thrust belt (as has been proposed for the Stage 5 Ament Bay Formation of the Sioux Lookout orogenic belt: Figure 25), versus a foreland basin which would be on top of a stable foreland block, which would in this case be the Winnipeg River subprovince. Given the probable post–Archean erosion of any tectonically unburied supracrustal rocks deposited late in the evolution of the area, Late Archean foreland basins would have had a low preservation potential, versus piggyback basins which would have been partly buried, and thus preserved, by the advance of thrust slices. (For an Archean example of a deformed foreland basin sequence in the Barberton belt, see: Jackson et al. 1987, Eriksson et al. 1994, and Heubeck and Lowe 1994.)

Regarding the chronostratigraphic resolution of orogenic events, a thick clastic unit can *span an age range* and thus one radiometric date is not necessarily representative of an entire formation. Using the Ament Bay Formation of the Sioux Lookout orogenic belt as an example, if the 2702–2694 Ma age of the youngest dated clast (i.e., the "maximum age" of sedimentation) is from the upper part of the formation, the lower part and the timing of related thrusting could be significantly (several Ma) older.

LATE STAGE OROGENIC BELT DEVELOPMENT (SIOUX LOOKOUT OROGENIC BELT STAGE 6): EMPHASIS ON STRIKE–SLIP FAULTING

Because the quartz–vein hosted gold deposits in the Sioux Lookout orogenic belt (and elsewhere) have the characteristics of mesothermal lode gold deposits generally thought to have formed during late orogenesis, all of the "Stage 6" aspects discussed below are potentially directly relevant to understanding the regional structural context of gold mineralization.

The interpretation of major, late orogenic sinistral faults in the Sioux Lookout orogenic belt has been based on recognition of (sub–) belt–scale map patterns (1–50 km features), not small–scale (1 cm to 1 m) structural fabrics. One potential advantage of this approach is that while small–scale fabrics are subject to tectonic overprinting and thus may preserve a poor record, or no record at all, of earlier deformation events, many larger scale structures or patterns are too large to be destroyed by subsequent tectonism. Also, efforts to document the small–scale fabrics of faults and other deformation zones are likely to be frustrated by the common lack of exposure or poor exposure; in northern Ontario, the actual locations of many mapped deformation zones are inferred rather than based on direct observations.

For these two reasons (greater preservation of large–scale structures, rarity of exposure of the actual deformation zones), increased investigations of potential large–scale strike–slip tectonic structures in the western Wabigoon subprovince (and elsewhere) are recommended. Such investigations could focus on large–scale sigmoidally shaped structures: for example, potential late orogenic pull–apart basins and plutons selectively located in or near transtensional zones, such as releasing bend areas of faults, versus potential transpressional zones in restraining bend areas as sites for steeply dipping reverse faults and fault–bounded pop–up structures (Devaney 1999b). For example, the lazy–Z shape of the conglomeratic Crowduck Lake Group in the Lake of the Woods belt (Blackburn et al. 1991, Figures 9.9 and 9.36b) suggests an origin as a dextral–sense pull–apart basin, but the presence of supposed early fabrics argues against this. Any interpretation of synchronous synorogenic dextral strike–slip faulting and Crowduck pull–apart basin deposition, presumably followed by increments of deformation of the basin, would require that early, preorogenic deformation fabrics are not present within Crowduck strata; rather, multiple late orogenic fabrics would be present

The Sioux Lookout orogenic belt is along strike from the Miniss River Fault, a fault with documented late orogenic sinistral strike–slip to oblique–slip motions (Williams et al. 1992, Bethune et al. 1999). The interpreted late orogenic sinistral strike–slip faults in the northern half of the Sioux Lookout orogenic belt can be considered as the diffused southwest extension of the Miniss River Fault through the area. Such sinistral faulting is consistent with the regional (northwest Superior Province) tectonic pattern of a conjugate set of major east–trending dextral faults and northeast–trending sinistral faults (Williams et al. 1992) and the interpreted effects of the "Wabigoon Indentor" (Stott and Corfu 1991, Corfu et al. 1995).

It is notable that a simplistic back–rotation of Sioux Lookout orogenic belt strata (down to the northwest, about an axis along the strike–line) of about 60º would produce a belt with mostly low–dipping

strata (flat to 30º dip southeast), except in two areas: the Northeast Bay of Minnitaki Lake area, and the site of the Patara Formation These are the two most important large structures (7–20 km scale) that are interpreted to have formed during Stage 6 strike–slip faulting, the Northeast Bay area as a rotated crustal flake ("Riedel flake" in Fig. 32), and the Patara as a strike–slip (pull–apart) basin (Figures 26, 31) potentially adjacent to a flower structure (Figures 28, 29).

The Riedel flake interpretation (Figure 32) is only the second cited example from Superior Province of a large–scale rock body interpreted to have been rotated about a steeply plunging axis. (The other example is that of Hale and Lloyd, cited in Stott and Corfu 1991, p.200 and 221.) Although an uncommon type of tectonic structure, Riedel flakes and potentially rotated blocks might be worthy of the increased attention by Superior Province workers.

Regarding verticalization of strata in the Sioux Lookout orogenic belt, because synthrust strata of Stage 5 were deposited as flat unlithified beds, and Stage 5 deposits form a unit (Ament Bay Formation) with very steeply dipping schistose strata similar to the fabric in the older units of the belt, this could imply that the rotation to vertical and acquisition of schistosity in all of the Sioux Lookout orogenic belt Stage 1 to 5 units occurred during late Stage 5 and Stage 6. (Is this scenario of late orogenic wrenching and development of subvertical schistosity also broadly applicable to other Archean belts?)

Testing of the speculative R–R' lineament pattern hypothesis illustrated in Figure 33 would require years of detailed structural mapping.

Study of the Sioux Lookout orogenic belt Stage 6 Patara Formation has generated results and ideas broadly relevant to views regarding Archean synorogenic deformation. The importance of the newly documented top indications and other descriptive data presented herein illustrates that there are still basic contributions to be made to the mapping of geological features in the field in northwest Ontario; oft–visted roadside outcrops are still yielding new data (Figure 3). The new strike–slip basin interpretation for the Patara Formation emphasizes that more than one type and age of synorogenic clastic unit may be present in a "greenstone" belt. The lazy–S shaped, sigmoidal map view outline of the deformed Patara Formation is consistent with an origin via sinistral strike–slip faulting; note that late orogenic events would be the ones least likely to be tectonically overprinted, implying good preservation potential for at least the gross outlines of the primary shapes of large–scale late orogenic features. Recently published detrital zircon data (Fralick and Davis 1999) confirms that the Patara Formation is synorogenic (<2700 Ma) and thus is *not* the oldest sedimentary unit in the belt (versus earlier views: e.g., Blackburn et al. 1985). The newly identified structural contact between the oppositely facing Northern Volcanic belt and Patara Formation (Figure 3), which contrasts with the older interpretation of an unconformable contact in a homoclinal sequence (Blackburn et al. 1985), is an unusual relationship and may indicate vertical "upthrusting" and overturning of a fault slice at the margin of a positive flower structure (Figures 28, 29). How many flower structures might be present in Superior Province?

Note that the maximum age of the Patara Formation (<2700 Ma) does not require that it be older than the Ament Bay Formation, which has a maximum age of <2702–2694 Ma, because the ages of the detrital grains date rocks eroded from the provenance area(s), not the time of sedimentary deposition in a basin. (Obviously, dating of a cross–cutting intrusion would bracket the age range of deposition.) Furthermore, much of the Patara Formation is lower dipping and less deformed than the Ament Bay Formation, potentially reflecting a longer deformation history for the latter.

It is important that the Sioux Lookout orogenic belt Stage 6 Patara Formation, like other units interpreted as Archean late orogenic strike–slip basins, has been tectonized and does not consist of flat or low–dipping beds. This implies that increments of very late stage synorogenic deformation (compression and/or transpression) postdated the late orogenic creation and infilling of the Patara basin and other similar Archean strike–slip basins. (In strike–slip belts, many of the numerous deformation "increments" would have been discrete earthquakes.) Such deformation increments can be geometrically complex; as a response to variations in local and/or regional stress regimes, strike–slip basins and intra–orogenic blocks may be transtensionally downdropped and transpressionally uplifted (such up and down displacement has been termed "porpoising" by Nilsen and Sylvester 1995, p.426), producing a "strike–slip" belt with significant oblique–slip and dip–slip displacements also.

The moderately to steeply dipping, variably penetratively deformed nature of the Patara Formation and other similar units also implies that they were *not* produced during orogenic collapse. Extensional basins associated with orogenic collapse (Hossack 1984, Dewey 1988, Windley 1995, Devaney 1999b) would likely consist of low–dipping rift basin stratigraphic sequences having little or no penetrative deformation within them (unless modified by subsequent major orogeny).

SYNOROGENIC GRANITIC INTRUSIONS

As discussed above (under "Resolution and timing of Stage 5 and 6 orogenic events"), the temporal linkages between granitic intrusion and tectonic events in the Sioux Lookout orogenic belt is not finely resolved. Some granitic plutonism preceded the Stage 5 thrusting. The ages of a granitic clast in the Ament Bay Formation (2702–2694 Ma: Davis et al. 1988) and two granitic plutons immediately to the southwest of the study area (2699–2693 and 2697–2693 Ma: Davis 1990) show that, during the ca. 2700–2690 Ma period, granitic plutonism was followed by the deposition and subsequent thrusting of the dated part of the Ament Bay Formation

The geology of the few granitic intrusions in the Sioux Lookout orogenic belt study area was not investigated in the present study, and the interpretation that some of these undated granitic plutons may have intruded into transtensional sites such as Stage 6 fault releasing bends (Figure 31) is speculative but incorporates recent modelling of granitic intrusion processes. Many synorogenic granitoid intrusions are increasingly viewed as having been intruded into extensional or transtensional sub–zones within orogenic belts (e.g., Guineberteau et al. 1987, Hutton 1988, 1992; Glazner 1991, D'Lemos et al. 1992, Tikoff and and Tikoff and Teyssier 1992), including the intrusion of some plutons in Archean "greenstone" belts (Devaney 1997, 1999a; Lacroix et al. 1998), and such scenarios are now popular as a way of accounting for the "room problem" regarding plutonic intrusion in general. Regarding resolution of the timing of any granitoid deformation, particularly near pluton margins, potential complexities include the need to distinguish deformation structures formed during pluton cooling from those of later solid–state deformation (e.g., Paterson et al. 1988, 1989; Fernandez et al. 1997). Such models of granitoid intrusion, including potential direct links between pull–apart basin development at the paleo–surface and pluton intrusion at depth (D'Lemos et al. 1992, Devaney 1999b), could probably also be applied elsewhere in the western Wabigoon subprovince.

CRATONIZATION AND POSTOROGENIC EVENTS

Late orogenic events, such as those of Sioux Lookout orogenic belt Stage 6, are key parts of the cratonization process. Stable cratonic areas do not suddenly appear after orogenic belt development; rather, orogenesis gradually cratonizes an orogenic belt and may firmly attach such a belt to adjacent crustal blocks. Based on accounts of orogens of various ages (e.g., Windley 1995), it is expected that as the components of an orogenic belt become increasingly "welded together" by synorogenic intrusions, motions along geometrically complex networks of interconnected fault–bounded blocks should become increasingly difficult (e.g., the "final lateral locking" stage of Chorlton 1990, 1991) and the orogenic belt should be transformed into a relatively stable, less structurally partitioned crustal block. If the belt is firmly attached to adjacent crustal blocks, it will be part of a larger craton.

Following such progressive cratonization, postorogenic events in the western Wabigoon subprovince and surrounding regions include intrusion of pegmatite dikes and granitic plutons at ca. 2680 to 2650 Ma (Corfu et al. 1995, Larbi et al. 1999) and Early Proterozoic faulting (Kamineni et al. 1990).

"TERRANE" TERMINOLOGY

Regarding use the terms "terrane" and "Sioux Lookout terrane" by some workers (e.g., Beakhouse 1988, Larbi et al. 1996, 1999, Sanborn–Barrie and Skulski 1999), in these cases the use of "terrane" may be

misleading because it normally suggests an exotic or allochthonous relationship to adjacent areas (Schermer et al. 1984), including the docking or accretion of one “exotic” terrane with another terrane having a very different history as a result of the two terranes having developed at sites far apart. As shown in Figure 22a, the Sioux Lookout orogenic belt (and also, by extrapolation of this model, the rest of the western Wabigoon subprovince) is thought to have been adjacent to the older crustal blocks of the Winnipeg River subprovince and central Wabigoon subprovince throughout its history, with orogenic faulting along the Sioux Lookout orogenic belt margin modifying only to a minor degree the largely autochthonous (“parautochthonous”) relationship of the Sioux Lookout orogenic belt with its foreland (Winnipeg River subprovince) and hinterland (central Wabigoon subprovince) bounding regions. Within the western Wabigoon subprovince, there is no known unequivocal evidence for either the subduction zone(s) proposed by Blackburn (1980) and Sanborn–Barrie and Skulski (1999) or the long–distance horizontal translation required for the identification of a discrete “exotic” terrane.

An exception to the comments above would be the case of the “transpressional terranes” of Ave Lallemant and Oldow (1988), in which one terrane is very different from the terrane on the opposite side a major strike–slip fault and the terranes need not be exotic with respect to each other (e.g., there was no accretion of an outboard exotic terrane; instead, there may have been long–distance displacement of a block within a single terrane, making the block appear “exotic” at its new location).

References

Allen, R.L. 1988. False pyroclastic textures in altered silicic lavas, with implications for volcanic–associated mineralization; Economic Geology, v.83, p.1424–1446.

Allmendinger, R.W. 1992. Fold and thrust tectonics of the western United States exclusive of the accreted terranes; *in* Burchfiel, B.C., Lipman, P.W. and Zoback, M.L., eds., The Geology of North America, Vol. G–3, The Cordilleran Orogen: Conterminous U.S., Geological Society of America, p.583–607.

Armstrong, H.S. 1951. Geology of Echo Township; *in* Ontario Department of Mines Annual Report, vol. LIX, part V, 1950, p.1–40.

Arndt, N.T. and Jenner, G.A. 1986. Crustally contaminated komatiites and basalts from Kambalda, Western Australia; Chemical Geology, v.56, p.229–255.

Ave Lallemant, H.G. and Oldow, J.S. 1988. Early Mesozoic southward migration of Cordilleran transpressional terranes; Tectonics, v.7, p.1057–1075.

Ayer, J.A. 1991. The northwestern Wabigoon Subprovince: an accreted Late Archean back–arc segment in the southern Superior Province?; abstract *in* Geological Association of Canada Annual Meeting, Program with Abstracts, v.16, p.A5.

Ayer, J.A. and Davis, D.W. 1997. Neoarchean evolution of differing convergent margin assemblages in the Wabigoon Subprovince: geochemical and geochronological evidence from the Lake of the Woods greenstone belt, Superior Province, Northwestern Ontario; Precambrian Research, v.81, p.155–178.

Babin, D., Devaney, J.R. and Long, D.G.F. 1996. Evidence for an Archean subaerial volcanic edifice, Minnitaki Lake, Sioux Lookout; abstract *in* Program with Abstracts, Geological Association of Canada–Mineralogical Association of Canada Annual Meeting, v.21, p.A5.

Bacon, C.R., Bruggman, P.E., Christiansen, R.L., Clynne, M.A., Donnelly–Nolan, J.M. and Hildreth, W. 1997. Primitive magmas at five Cascade volcanic fields: melts from hot, heterogeneous sub–arc mantle; The Canadian Mineralogist, v.35, p.397–423.

Beakhouse, G.P. 1988. The Wabigoon–Winnipeg River Subprovince boundary problem; *in* Summary of Field Work and Other Activities 1988, Ontario Geological Survey Miscellaneous Paper 141, p.108–115.

Beakhouse, G.P. 1991. Winnipeg River Subprovince; *in* Thurston, P.C., Williams, H.R., Sutcliffe, R.H. and Stott, G.M., eds., Geology of Ontario, Ontario Geological Survey Special Volume 4, Part 1, p.279–301.

Berger, B.R. 1989. Precambrian geology, Melgund Lake area; Ontario Geological Survey, Report 268, 68p.

Berger, B.R. 1990. Precambrian geology, Laval and Hartman townships; Ontario Geological Survey, Report 272, 74p.

Berger, B.R. 1991. Precambrian geology, Manitou Stretch area; Ontario Geological Survey, Report 284, 45p.

Bethune, K.M., Helmstaedt, H. and Hrabi, B.R. 1999. Structural analysis of faults in the apical region of the Wabigoon Subprovince; *in* Harrap, R.M. and Helmstaedt, H.H., eds., 1999 Western Superior Transect Fifth Annual Workshop, Lithoprobe Report 70, Lithoprobe Secretariat, University of British Columbia,Lithoprobe Report 70, p.5–14.

Blackburn, C.E. 1980. Towards a mobilist tectonic model for part of the Archean of northwestern Ontario; Geoscience Canada, v.7(2), p.64–72.

Blackburn, C.E., Bond, W.D., Breaks, F.W., Davis, D.W., Edwards, G.R., Poulsen, K.H., Trowell, N.F. and Wood, J. 1985. Evolution of Archean volcanic–sedimentary sequences of the western Wabigoon Subprovince and its margins: A review; *in* Ayres, L.D., Thurston, P.C., Card, K.D. and Weber, W., eds., Evolution of Archean Supracrustal Sequences, Geological Association of Canada, Special Paper 28, p.89–116.

Blackburn, C.E., Hinz, P., Storey, C.C., Kosloski, L. and Ravnaas, C.B. 1998. Report of Activities 1997, Resident Geologist Program, Red Lake Regional Resident Geologist's Report: Red Lake–Kenora Districts; Ontario Geological Survey, Open File Report 5969, 68p.

Blackburn, C.E., Johns, G.W., J. Ayer and Davis, D.W. 1991. Wabigoon Subprovince; *in* Thurston, P.C., Williams, H.R., Sutcliffe, R.H. and Stott, G.M., eds., Geology of Ontario, Ontario Geological Survey, Special Volume 4, Part 1, p.303–381.

Blair, T.C. and McPherson, J.G. 1994. Alluvial fans and their natural distinction from rivers based on morphology, hydraulic processes, sedimentary processes, and facies assemblages; Journal of Sedimentary Research, v.A64, p.450–489.

Boothroyd, J.C. and Nummedal, D. 1978. Proglacial braided outwash: a model for humid alluvial fan deposits; *in* Miall, A.D., ed., Fluvial Sedimentology, Canadian Society of Petroleum Geologists, Memoir 5, p.641–668.

Breaks, F.W. 1988. Geology of the eastern Lac Seul granulite–amphibolite facies transition zone; *in* Summary of Field Work and Other Activities, Ontario Geological Survey, Miscellaneous Paper 141, p.81–88.

Breaks, F.W. and Bond, W.D. 1977. English River Subprovince (Marchington Lake Area), District of Kenora; *in* Summary of Field Work, 1977, Ontario Geological Survey, Miscellaneous Paper 75, p.18–28.

Breaks, F.W., Bond, W.D., Harris, N., Westerman, C.J. and Desnoyers, D.W. 1976. Operation Kenora–Ear Falls, Sandybeach–Route Lakes Sheet, District of Kenora; Ontario Division of Mines, Preliminary Map P.1204, Geological Series, scale 1:63 360.

Brown, P.E. 1985. Au–only and Au–Ag–base metal ores of the Sioux Lookout–Sturgeon Lake area, NW Ontario – A comparison; abstract *in* Abstracts with Programs 1985, Geological Society of America 98th Annual Meeting, p.533.

Brown, R.L. and Journeay, J.M. 1987. Tectonic denudation of the Shuswap metamorphic terrane of southeastern British Columbia; Geology, v.15, p.142–146.

Busby, C., Smith, D., Morris, W. and Fackler–Adams, B. 1998. Evolutionary model for convergent margins facing large ocean basins: Mesozoic Baja California, Mexico; Geology, v.26, p.227–230.

Butler, R.W.H. 1992. Structural evolution of the western Chartreuse fold and thrust system, NW French Subalpine chains; *in* McClay, K.R., ed., Thrust Tectonics, Chapman & Hall, p.287–298.

Cas, R.A.F. and Wright, J.V. 1987. Volcanic Succession – Modern and Ancient; Chapman and hall, 528 p.

Cas, R.A.F. and Wright, J.V. 1991. Subaqueous pyroclastic flows and ignimbrites: an assessment; Bulletin of Volcanology, v.53, p.357–380.

Cathles, L.M., Guber, A.L., Lenagh, T.C. and Dudas, F.O. 1983. Kuroko–type massive sulfide deposits of Japan: products of an aborted island–arc rift; *in* Ohmoto, H. and Skinner, B.J., eds., The Kuroko and Related Volcanogenic Massive Sulfide Deposits, Economic Geology Monograph 5, p.96–114.

Chorlton, L. 1990. Regional setting of vein–style gold mineralization around the Goldlund mine, Sandybeach Lake area, northwestern Ontario; Canadian Journal of Earth Sciences, v.27, p.1590–1608.

Chorlton, L. 1991. Geological history of the Sandybeach Lake area, Sioux Lookout–Dinorwic Belt, Wabigoon Subprovince, and its implications for gold exploration; Ontario Geological Survey, Open File Report 5752, 198p.

Christiansen, E.H. andf Keith, J.D. 1996. Trace element systematics in silicic magmas: a metallogenic perspective; *in* Wyman, D.A., ed., Trace Element Geochemistry of Volcanic Rocks: Applications for Massive Sulphide Exploration, Geological Association of Canada, Short Course Notes Vol. 12, p.115–151.

Christie–Blick, N. and Biddle, K.T. 1985. Deformation and basin formation along strike–slip faults; *in* Biddle, K.T. and Christie–Blick, N., eds., Strike–Slip Deformation, Basin Formation, and Sedimentation, Society of Economic Paleontologists and Mineralogists, Special Publication 37, p.1–34.

Ciceri, D.L., Cruden, A.R. and Robin, P.Y.–F. 1996. Structural and metamorphic gradients across the Winnipeg River/Western Wabigoon Subprovince boundary, Superior Province, NW Ontario; *in* Harrap, R.M. and Helmstaedt, H., eds., Western Superior Transect Second Annual Workshop (Oct. 20–21, 1995), Lithoprobe Report #53. Lithoprobe Secretariat, University of British Columbia, p.9–13.

Colvine, A.C., Fyon, J.A., Heather, K.B., Marmont, S., Smith, P.M. and Troop, D.G. 1988. Archean Gold Deposits in Ontario; Ontario Geological Survey, Miscellaneous Paper 139, 136p.

Colvine, A.C. and McCarter, P. 1977. Geology and mineralization of the Lateral Lake Stock, District of Kenora; *in* Summary of Field Work, 1977, Ontario Geological Survey, Miscellaneous Paper 75, p.205–208.

Corfu, F., Stott, G.M. and Breaks, F.W. 1995. U–Pb geochronology and evolution of the English River Subprovince, an Archean low P–high T metasedimentary belt in the Superior Province; Tectonics, v.14, p.1220–1233.

Cortis, A.L., Stott, G.M., Osmani, I.A., Atkinson, B. and Thurston, P.C. 1988. A geological re–evaluation of northwestern greenstone belts; *in* Summary of Field Work and Other Activities 1988, Onario Geological Survey, Miscellaneous Paper 141, p.28–52.

Cowan, D.S. 1985. Structural styles in Mesozoic and Cenozoic melanges in the western Cordillera of North America; Geological Society of America Bulletin, v.96, p. 451–462.

Cruden, A.R., Davis, D.W., Menard, T. and Robin, P.–Y.F. 1997.Structural and geochronological relationships between theWinnipeg River and Wabigoon Subprovinces: implications forthe terrane accretion model; *in* Harrap, R.M. and Helmstaedt, H., eds., 1997 Western Superior Transect Third Annual Workshop, Lithoprobe Report #63, Lithoprobe Secretariat, University of British Columbia, p.18–26.

Cruden, A.R. and Hynes, A. 1999. Western Superior LITHOPROBE seismic reflection lines 2a and 2c: comparison with surface geology and preliminary interpretation; *in* Harrap, R.M. and Helmstaedt, H.H., eds., 1999 Western Superior Transect Fifth Annual Workshop, Lithoprobe Report 70, Lithoprobe Secretariat, University of British Columbia, p.48–54.

Davis, D.W. 1990. Geological study of Winnipeg River – Wabigoon Subprovince boundary; EMR Research Agreement No. 45 Final Report – 1990 (unpublished manuscript).

Davis, D.W., Krogh, T.E., Hinzer, J. and Nakamura, E. 1985. Zircon dating of polycyclic volcanism at Sturgeon Lake and implications for base metal mineralization; Economic Geology, v.80, p.1942–1952.

Davis, D.W., Sutcliffe, R.H. and Trowell, N.F. 1988. Geochronological constraints on the tectonic evolution of a Late Archaean greenstone belt, Wabigoon Subprovince, northwest Ontario; Precambrian Research, v.39, p.171–191.

Davis, D.W. and Trowell, N.F. 1982. U–Pb zircon ages from the eastern Savant Lake – Crow Lake metavolcanic–metasedimentary belt, northwest Ontario; Canadian Journal of Earth Sciences, v.19, p.868–877.

Day, W.C. 1990. Petrology of the Rainy Lake area, Minnesota, USA –implications for petrotectonic setting of the Archean southern Wabigoon subprovince of the Canadian Shield; Contributions to Mineralogy and Petrology, v.105, p.303–321.

DeCelles, P.G. and Giles, K.A. 1996. Foreland basin systems; Basin Research, v.8, p.105–123.

DeRonde, C.E.J. and De Wit, M.J. 1994. Tectonic history of the Barberton greenstone belt, South Africa: 490 million years of Archean crustal evolution; Tectonics, v.13, p.983–1005.

Devaney, J.R. 1987. Sedimentology and stratigraphy of the northern and central metasedimentary belts in the Beardmore–Geraldton area of northern Ontario; M.Sc. thesis, Lakehead University, Thunder Bay, Ontario, 227 p.

Devaney, J.R. 1996. Altered metavolcanic rocks of the Melchett Lake Belt, eastern English River Subprovince; *in* Summary of Field Work and Other Activities 1996, Ontario Geological Survey, Miscellaneous Paper 166, p.16–18.

Devaney, J.R. 1997. Stratigraphy and tectonics of the Sioux Lookout orogenic belt, western Wabigoon Subprovince; abstract *in* Harrap, R.M. and Helmstaedt, H., eds., 1997 Western Superior Transect Third Annual Workshop (April 11–12, 1997), Lithoprobe Report #63, Lithoprobe Secretariat, University of British Columbia, p.96.

Devaney, J.R. 1998. Stratigraphy of Archean subaerial stratovolcano and deep water volcaniclastic deposits, Sioux Lookout greenstone belt, NW Ontario; abstract *in* Geological Association of Canada Annual Meeting, Abstract Volume 23, p.A44.

Devaney, J.R. 1999a. Stages of volcanism, sedimentation, tectonism, and mineralization in the evolution of the Sioux Lookout orogenic belt, western Wabigoon Subprovince; *in* Summary of Field Work and Other Activities 1988, Ontario Geological Survey, Miscellaneous Paper 169, p.156–167.

Devaney, J.R. 1999b. Late orogenic stage wrench tectonics: strike–slip faulting, transpressional pop–up structures, transtensional pluton sites and pull–apart basins, block movements, and application to greenstone belts and lode gold deposits of Superior Province; *in* Harrap, R.M. and Helmstaedt, H.H., eds., 1999 Western Superior Transect Fifth Annual Workshop, Lithoprobe Report 70, Lithoprobe Secretariat, University of British Columbia, p.154–155.

Devaney, J.R. 1999c. Some major problems in Archean sedimentary basin analysis; abstract *in* Geological Association of Canada Annual Meeting, Abstract Volume 24, p.30.

Devaney, J.R. and Babin, D. 1996. Physical volcanology of the Neepawa Group, northern Minnitaki Lake area, Sioux Lookout greenstone belt; *in* Summary of Field Work and Other Activities 1996, Ontario Geological Survey, Miscellaneous Paper 166, p.25–27.

Devaney, J.R. and Borowik, A. 1994. Straigraphic reconnaissance of Archean supracrustal rocks, Sioux Lookout area, western Wabigoon Subprovince; *in* Summary of Field Work and Other Activities 1994, Ontario Geological Survey, Miscellaneous Paper 163, p.44–47.

Devaney, J.R., Borowik, A., King, D. and Babin, D. 1995b. Precambrian geology, Sioux Lookout area; Ontario Geological Survey, Preliminary Map P.3342, scale 1:50 000.

Devaney, J.R., King, D. and Babin, D. 1995a. Reconnaissance stratigraphy of Archean supracrustal rocks, Sioux lookout area, western Wabigoon Subprovince; *in* Summary of Field Work and Other Activities 1995, Ontario Geological Survey Miscellaneous Paper 164, p.26–28.

Devaney, J.R. and Williams, H.R. 1989. Evolution of an Archean subprovince boundary: a sedimentological and structural study of part of the Wabigoon–Quetico boundary in northern Ontario; Canadian Journal of Earth Sciences, v.26, p.1013–1026.

Dewey, J.F. 1988. Extensional collapse of orogens; Tectonics, v.7, p.1123–1139.

Dewey, J.F., Holdsworth, R.E. and Strachan, R.A. 1998. Transpression and transtension zones; *in* Holdsworth, R.E., Strachan, R.A. and Dewey, J.F., eds., Continental Transpressional and Transtensional Tectonics, Geological Society, London, Special Publication 135, p.1–14.

De Wit, M.J., Armstrong, R., Hart, R.J. and Wilson, A.H. 1987. Felsic igneous rocks within the 3.3–3.5 Ga Barberton greenstone belt: high crustal level equivalents of the surrounding tonalite–trondhjemite terrain, emplaced during thrusting; Tectonics, v.6, p.529–549.

D'Lemos, R.S., Brown, M. and Strachan, R.A. 1992. Granite magma generation, ascent and emplacement within a transpressional orogen; Journal of the Geological Society, London, v.149, p.487–490.

Donato, M.M. 1991. Geochemical recognition of a captured back–arc basin metabasaltic complex, southwestern Oregon; Journal of Geology, v.99, p.711–728.

Drummond, M.S., Defant, M.J. and Kepezhinskas, P.K. 1996. Petrogenesis of slab–derived trondhjemite–tonalite–dacite/adakite magmas; Transactions of the Royal Society of Edinburgh: Earth Sciences, v.87, p.205–215.

Dupuy, C. and Dostal, J. 1984. Trace element geochemistry of some continetal tholeiites; Earth and Planetary Science Letters, v.67, p.61–69.

Easton, R.M. and Johns, G.W. 1986. Volcanology and mineral exploration: The application of physical volcanology and facies studies; *in* Wood, J. and Wallace, H., eds., Volcanology and Mineral Deposits, Ontario Geological Survey, Miscellaneous Paper 129, p.2–40.

Ebert, H.D. and Hasui, Y. 1998. Transpressional tectonics and strain partitioning during oblique collision between three plates in the Precambrian of southeast Brazil; *in* Holdsworth, R.E., Strachan, R.A. and Dewey, J.F., eds., Continental Transpressional and Transtensional Tectonics, Geological Society, London, Special Publication 135, p.231–252.

Edwards, G.R. and Davis, D.W. 1984. Petrogenesis and metallogenesis of the Atikwa–Lawrence volcanic–plutonic terrane; *in* Geoscience Research Grant Program, Summary of Research 1983–1984, Ontario Geological Survey, Miscellaneous Paper 121, p.222–239.

Eisenlohr, B.N., Groves, D. and Partington, G.A. 1989. Crustal–scale shear zones and their significance to Archaean gold mineralization in Western Australia; Mineralium Deposita, v.24, p.1–8.

Eriksson, K.A. 1978. Alluvial and destructive beach facies from the Archaean Moodies Group, Barberton Mountain Land, South Africa and Swaziland; *in* Miall, A.D., ed., Fluvial Sedimentology, Canadian Society of Petroleum Geologists, Memoir 5, p.287–311.

Eriksson, K.A., Krapez, B. and Fralick, P.W. 1994. Sedimentology of Archean greenstone belts: signatures of tectonic evolution; Earth–Science Reviews, v.37, p.1–88.

Erslev, E.A. 1986. Basement balancing of Rocky Mountain foreland uplifts; Geology, v.14, p.259–262.

Evans, O.C. and Hanson, G.N. 1997. Late– to post–kinematic Archaean granitoids of the S.W. Superior Province: derivation through direct mantle melting; *in* De Wit, M.J. and Ashwal, L.D., eds., Greenstone Belts, Oxford University Press, p.280–295.

Fernandez, C. and Castro, A. 1997. Further evidences of permisive intrusion related to strike–slip releasing structures in the Central Extremadura batholith, Spain; abstract *in* Geological Association of Canada–Mineralogical Association of Canada Annual Meeting, Abstract Volume 22, p.A49.

Fernandez, C., Castro, A., de la Rosa, J.D. and Moreno–Ventas, I. 1997. Rheological aspects of magma transport inferred from rock structures; *in* Bouchez, J.L., Hutton, D.H.W. and Stephens, W.E., eds., Granite: From Segregation of Melt to Emplacement Fabrics, Kluwer Academic Publishers, p.75–91.

Fitton, J.G., James, D. and Leeman, W.P. 1991. Basic magmatism associated with late Cenozoic extension in the western United States: compositional variations in space and time; Journal of Geophysical Research, v.96, p.13 693–13 711.

Fralick, P. and Davis, D. 1999. The Seine–Coutchiching problem revisited: sedimentology, geochronology and geochemistry of sedimentary units in the Rainy Lake and Sioux Lookout areas; *in* Harrap, R.M. and Helmstaedt, H.H., eds., 1999 Western Superior Transect Fifth Annual Workshop, Lithoprobe Report 70, Lithoprobe Secretariat, University of British Columbia, p.5–14.

Fralick, P., Wu, J. and Williams, H.R. 1992. Trench and slope basin deposits in an Archean metasedimentary belt, Superior Province, Canadian Shield; Canadian Journal of Earth Sciences, v.29, p.2551–2557.

Gallo, D.G., Sengor, A.M.C., Sloan, H.S. and Kidd, W.S.F. 1980. Large angular rotations of blocks along strike–slip zones as shallow decollement features; abstract *in* EOS, v.61(46), p.1120.

Galloway, W.E. 1989. Genetic stratigraphic sequences in basin analysis I: architecture and genesis of flooding–surface bounded depositional units; American Association of Petroleum Geologists Bulletin, v.73, p.125–142.

Glazner, A.F. 1991. Plutonism, oblique subduction, and continental growth: an example from the Mesozoic of California; Geology, v.19, p.784–786.

Groves, D.I. and Foster, R.P. 1991. Archaean lode gold deposits; *in* Foster, R.P., ed., Gold Metallogeny and Exploration, Blackie and Son Ltd., p.63–103.

Guineberteau, B., Bouchez, J.L. and Vigneresse, J.L. 1987. The Mortagne granite pluton (France) emplaced by pull–apart along a shear zone: Structural and gravimetric arguments and regional implication; Geological Society of America Bulletin, v.99, p.763–770.

Hackett, W.R. and Houghton, B.F. 1989. A facies model for a Quaternary andesitic composite volcano: Ruapehu, New Zealand; Bulletin of Volcanology, v.51, p.51–68.

Hagemann, S.G., Groves, D.I., Ridley, J.R. and Vearncombe, J.R. 1992. The Archean lode gold deposits at Wiluna, Western Australia: high–level brittle–style mineralization in a strike–slip regime; Economic Geology, v.87, p.1022–1053.

Harding, T.P. 1985. Seismic characteristics and identification of negative flower structures, positive flower structures, and positive structural inversion; American Association of Petroleum Geologists Bulletin, v. 69, p. 582–600.

Harding, W.D. 1951. Geology of the Gullwing Lake–Sunstrum Area; *in* Ontario Department of Mines Annual Report, vol. LIX, Part IV, 1950, p.1–29. Acc. by Map 1950–2, scale 1:63 360.

Hatcher, R.D., Jr. and Hooper, R.J. 1992. Evolution of crystalline thrust sheets in the internal parts of mountain chains; *in* McClay, K.R., ed., Thrust Tectonics, Chapman & Hall, p.217–233.

Hathway, B. 1993. The Nadi Basin: Neogene strike–slip faulting and sedimentation in a fragmented arc, western Viti Levu, Fiji; Journal of the Geological Society, London, v.150, p.563–581.

Hawkesworth, C.J., Gallagher, K., Hergt, J.M. and McDermott, F. 1993. Mantle and slab contributions in arc magmas; Annual Review of Earth and Planetary Sciences, v.21, p.175–204.

Hawkesworth, C.J., Gallagher, K., Kelley, S., Mantovani, M., Peate, D.W., Regelous, M. and Rogers, N.W. 1992. Parana magmatism and the opening of the South Atlantic; *in* Storey, B.C., Alabaster, T. and Pankhurst, R.J., eds., Magmatism and the Causes of Continental Break–up, Geological Society, London, Special Publication 68, p.221–240.

Hein, F.J. 1984. Deep–sea and fluvial braided channel conglomerates: a comparison of two case studies; *in* Koster, E.H. and Steel, R.J., eds., Sedimentology of Gravels and Conglomerates, Canadian Society of Petroleum Geologists, Memoir 10, p.33–49.

Heller, P.L. and Dickinson, W.R. 1985. Submarine ramp facies model for delta–fed, sand–rich turbidite systems; American Association of Petroleum Geologists Bulletin, v.69, p.960–976.

Hempton, M.R. and Neher, K. 1986. Experimental fracture, strain and subsidence patterns over en echelon strike–slip faults: implications for the structural evolution of pull–apart basins; Journal of Structural Geology, v.8, p.597–605.

Henley, R.W. and Adams, D.P.M. 1992. Strike–slip fault reactivation as a control on epithermal vein–style gold mineralization; Geology, v.20, p.443–446.

Heubeck, C. and Lowe, D.R. 1994. Late syndepositional deformation and detachment tectonics in the Barberton Greenstone Belt, South Africa; Tectonics, v.13, p.1514–1536.

Hodgson, C.J. 1993. Mesothermal lode–gold deposits; *in* Kirkham, R.V., Sinclair, W.D., Thorpe, R.I. and Duke, J.M., eds., Mineral Deposit Modeling, Geological Association of Canada, Special Paper 40, p.635–678.

Hofmann, A.W. 1988. Chemical differentiation of the Earth: the relationship between mantle, continental crust, and oceanic crust; Earth and Planetary Science Letters, v.90, p.297–314.

Holdsworth, R.E., Strachan, R.A. and Dewey, J.F. 1998. Continental Transpressional and Transtensional Tectonics, Geological Society of London, Special Publication 135, 360 p.

Horwood, H.C. 1938. Geology of the Superior Junction–Sturgeon Lake Area; *in* Ontario Department of Mines, Annual Report, vol. XLVI, part VI, 1937, p.1–25. Acc. by Map 46d, scale 1:126 720 and Map 46e, scale 1:47 520.

Hossack, J.R. 1984. The geometry of listric growth faults in the Devonian basins of Sunnfjord, W Norway; Journal of the Geological Society, London, v.141, p.629–637.

Hurst, M.E. 1933. Geology of the Sioux Lookout Area; *in* Ontario Department of Mines, Annual Report, vol. XLI, part VI, 1932, p.1–33. Acc. by Map 41h, scale 1:95 040.

Hutton, D.W.H. 1988. Granite emplacement mechanisms and tectonic controls: inferences from deformation studies; Transactions of the Royal Society of Edinburgh: Earth Sciences, v.79, p.245–255.

Hutton, D.W.H. 1992. Granite sheeted complexes: evidence for the dyking ascent mechanism; Transactions of the Royal Society of Edinburgh: Earth Sciences, v.83, p.377–382. (Co–published as Geological Society of America Special Paper 272.)

Ingersoll, R.V. and Busby, C.J. 1995. Tectonics of sedimentary basins; *in* Busby, C.J. and Ingersoll, R.V., eds., Tectonics of Sedimentary Basins, Blackwell Science, p.1–51.

Jackson, M.P.A., Eriksson, K.A. and Harris, C.W. 1987. Early Archean foredeep sedimentation related to crustal shortening: a reinterpretation of the Barberton sequence, Southern Africa; Tectonophysics, v.136, p.197–221.

Johnston, F.J. 1969. Geology of the western Minnitaki Lake area, District of Kenora; Ontario Department of Mines, Geological Report 75, 28p. Acc. by Map 2155, scale 1:31 680.

Johnston, F.J. 1972. Geology of the Vermilion–Abram lakes area, District of Kenora; Ontario Division of Mines, Geological Report 101, 51p. Acc. by Maps 2242 and 2243, scale 1:31 680.

Jolly, W.T. 1987. Lithophile elements in Huronian low–Ti continental tholeiites from Canada, and evolution of the Precambrian mantle; Earth and Planetary Science Letters, v.85, p.401–415.

Jordan, T.E. 1995. Retroarc foreland and related basins; *in* Busby, C.J. and Ingersoll, R.V., eds., Tectonics of Sedimentary Basins, Blackwell Science, p.331–362.

Kamineni, D.C., Stone, D. and Peterman, Z.E. 1990. Early Proterozoic deformation in the western Superior province, Canadian Shield; Geological Society of America Bulletin, v.102, p.1623–1634.

Kerrich, R. 1989. Geodynamic setting and hydraulic regimes: shear zone hosted mesothermal gold deposits; *in* Bursnall, J.T., ed., Mineralization and Shear Zones, Geological Association of Canada, Short Course Notes, v.6, p.89–128.

Kerrich, R. and Fryer, B.J. 1979. Archaean precious–metal hydrothermal systems, Dome Mine, Abitibi Greenstone Belt. II. REE and oxygen isotope relations; Canadian Journal of Earth Sciences, v.16, p.440–458.

Kokelaar, B.P. 1982. Fluidization of wet sediments during the emplacement and cooling of various igneous bodies; Journal of the Geological Society of London, v.139, p.21–33.

Koster, E.H. 1978. Transverse ribs: their characteristics, origin and paleohydraulic significance; *in* Miall, A.D., ed., Fluvial Sedimentology, Canadian Society of Petroleum Geologists, Memoir 5, p. 161–186.

Kusky, T.M. 1991. Structural development of an Archean orogen, western Point Lake, Northwest Territories; Tectonics, v.10, p.820–841.

Lacroix, S., Sawyer, E.W. and Chown, E.H. 1998. Pluton emplacement within an extensional transfer zone during dextral strike–slip faulting: an example from the late Archaean Abitibi Greenstone Belt; Journal of Structural Geology, v.20, p.43–59.

Larbi, Y., Stevenson, R., Machado, N., Breaks, F. and Gariepy, C. 1996. The generation of Late Archean leucogranites and continental collision in the western Superior Province; *in* Harrap, R.M. and Helmstaedt, H., eds., Western Superior Transect Second Annual Workshop (Oct. 20–21, 1995), Lithoprobe Report #53, Lithoprobe Secretariat, University of British Columbia, p.47–53.

Larbi, Y., Stevenson, R., Breaks, F., Machado, N. and Gariepy, C. 1999. Age and isotopic composition of late Archean leucogranites: implications for continental collision in the western Superior Province; Canadian Journal of Earth Sciences, v.36, p.495–510.

Lentz, D.R. 1998. Petrogenetic evolution of felsic volcanic sequences associated with Phanerozoic volcanic–hosted massive sulphide systems: the role of extensional geodynamics; Ore Geology Reviews, v.12, p.289–327.

Lesher, C.M., Goodwin, A.M., Campbell, I.H. and Gorton, M.P. 1986. Trace–element geochemistry of ore–associated and barren, felsic metavolcanic rocks in the Superior Province, Canada; Canadian Journal of Earth Sciences, v.23, p.222–237.

Letouzey, J. and Kimura, M. 1986. The Okinawa Trough: genesis of a back–arc basin developing along a continental margin; Tectonophysics, v.125, p.209–230.

Maltman, A.J. 1998. Deformation structures from the toes of active accretionary prisms; Journal of the Geological Society, London, v.155, p.639–650.

McKenzie, M.C. 1995. Volcaniclastic rocks of the Archean Neepawa Group, Sioux Lookout, Ontario: Modes of fragmentation, transport, and deposition; unpublished B. Sc. thesis, University of Manitoba, Winnipeg, Manitoba, 119 p.

McMullan, S.R. 1980. Geology and petrography of the Pickerel Arm body, Minnitaki Lake, northwestern Ontario; unpublished B. Sc. thesis, University of Waterloo, Waterloo, Ontario, 49 p.

McPhie, J. 1993. The Tennant Creek porphyry revisited: A synsedimentary sill with peperite margins, Early Proerozoic, Northern Territory; Australian Journal of Earth Sciences, v.40, p.545–558.

McPhie, J., Doyle, M. and Allen, R. 1993. Volcanic textures: a guide to the interpretation of textures in volcanic rocks. Centre for Ore Deposit and Exploration Studies, University of Tasmania, 196 p.

Meschede, M. 1986. A method of discriminating between different types of mid–ocean ridge basalts and continental tholeiites with the Nb–Zr–Y diagram; Chemical Geology, v.56, p.207–218.

Miall, A.D. 1978. Lithofacies types and vertical profile models in braided river deposits: a summary; *in* Miall, A.D., ed., Fluvial Sedimentology, Canadian Society of Petroleum Geologists, Memoir 5, p. 597–604.

Miall, A.D. 1990. Principles of Sedimentary Basin Analysis, 2nd ed.; Springer–Verlag, 668p.

Miall, A.D. 1995. Collision–related foreland basins; *in* Busby, C.J. and Ingersoll, R.V., eds., Tectonics of Sedimentary Basins, Blackwell Science, p.393–424.

Morris, P.A. and Witt, W.K. 1997. Geochemistry and tectonic setting of two contrasting Archaean felsic volcanic associations in the Eastern Goldfileds, Western Australia; Precambrian Research, v.83, p.83–107.

Morton, R.L., Walker, J.S., Hudak, G.J. and Franklin, J.M. 1991. The early development of an Archean submarine caldera complex with emphasis on the Mattabi ash–flow tuff and its relationship to the Mattabi massive sulphide deposit; Economic Geology, v.86, p.1002–1011.

Mueller, A.G., Harris, L.B. and Lungan, A. 1988. Structural control of greenstone–hosted gold mineralization by transcurrent shearing: a new interpretation of the Kalgoorlie mining district, Western Australia; Ore Geology Reviews, v.3, p.359–387.

Mueller, W.U. and Corcoran, P.L. 1998. Late–orogenic basins in the Archaean Superior Province, Canada; Sedimentary Geology, v.120, p.177–203.

Nance, R.D. 1987. Dextral transpression and Late Carboniferous sedimentation in the Fundy coastal zone of southern New Brunswick; *in* Beaumont, C. and Tankard, A.J., eds., Sedimentary Basins and Basin–Forming Mechanisms, Canadian Society of Petroleum Geologists, Memoir 12, p.363–377.

Nesbitt, B.E. 1991. Phanerozoic gold deposits in tectonically active continental margins; *in* Foster, R.P., ed., Gold Metallogeny and Exploration, Blackie and Son Ltd., p.104– 132.

Nilsen, T.H. and McLaughlin, R.J. 1985. Comparison of tectonic framework and depositional patterns of the Hornelen strike–slip basin of Norway and the Ridge and Little Sulphur Creek strike–slip basins of California; *in* Biddle, K.T. and Christie–Blick, N., eds., Strike–Slip Deformation, Basin Formation, and Sedimentation, Society of Economic Paleontologists and Mineralogists, Special Publication No. 37, p.79–104.

Nilsen, T.H. and Sylvester, A.G. 1995. Strike–slip basins; *in* Busby, C.J. and Ingersoll, R.V., eds., Tectonics of Sedimentary Basins, Blackwell Science, p.425–457.

Ontario Geological Survey 1982. Airborne Electromagnetic and Total Intensity Magnetic Survey, Sioux Lookout Area, District of Kenora; by Aerodat Limited for Ontario Geological Survey, Geophysical/Geochemical Series, Maps 80553 to 80571, scale 1:20 000.

Ontario Geological Survey 1997. Sioux Lookout Area; Ontario Airborne Magnetic and Electromagnetic Surveys, ERLIS Data Set 1023, Ontario Geological Survey.

Ojakangas, R.W. 1985. Review of Archean clastic sedimentation, Canadian Shield: Major felsic volcanic contributions to turbidite and alluvial fan–fluvial facies associations; *in* Ayres, L.D., Thurston, P.C., Card, K.D. and Weber, W., eds., Evolution of Archean Supracrustal Sequences, Geological Association of Canada, Special Paper 28, p.23–47.

Page, R.O. 1978. Zarn Lake area, District of Kenora; *in* Summary of Field Work, 1978, Ontario Geological Survey, Miscellaneous Paper 82, p.45–48.

Page, R.O. 1984. Geology of the Lateral Lake Area, District of Kenora; Ontario Geological Survey, Open File Report 5518, 175p.

Page, R.O. and Christie, B.J. 1980a. Lateral Lake Area (West Half), District of Kenora; Ontario Geological Survey, Preliminary Map P.2371, Geological Series. Scale 1:15 840.

Page, R.O. and Christie, B.J. 1980b. Lateral Lake Area (East Half), District of Kenora; Ontario Geological Survey, Preliminary Map P.2372, Geological Series. Scale 1:15 840.

Page, R.O. and Clifford, P.M. 1977. Physical volcanology of an Archean vent complex, Minnitaki Lake area, northwestern Ontario; *in* Report of Activities, Part A, Geological Survey of Canada, Paper 77–1A, p.441–443.

Page, R.O. and Moller, E.B. 1979a. Zarn Lake Area (Northern Part), District of Kenora; Ontario Geological Survey, Preliminary Map P.2232, Geological Series. Scale 1:15 840.

Page, R.O. and Moller, E.B. 1979b. Zarn Lake Area (Southern Part), District of Kenora; Ontario Geological Survey, Preliminary Map P.2233, Geological Series. Scale 1:15 840.

Page, R.O., McNutt, R.H. and Clifford, P.M. 1978. Geochemistry of the Archean basalt–andesite suite of Minnitaki Lake, northwestern Ontario; abstract *in* Geological Association of Canada–Mineralogical Association of Canada–Geological Society of America 1978 Joint Annual Meeting, Abstracts with Programs, v.3, p. 467.

Paterson, S.R. and Tobisch, O.T. 1988. Using pluton ages to date regional deformations: problems with commonly used criteria; Geology, v.16, p.1108–1111.

Paterson, S.R., Vernon, R.H. and Tobisch, O.T. 1989. A review of criteria for the identification of magmatic and tectonic foliations in granitoids; Journal of Structural Geology, v.11, p.349–363.

Pearce, J.A. 1983. Role of sub–continental lithosphere in magma genesis at active continental margins; *in* Hawkesworth, C.J. and Norry, M.J., eds., Continental Basalts and Mantle Xenoliths, Shiva, p.230–249.

Pearce, J.A. 1996. A user's guide to basalt discrimination diagrams; *in* Wyman, D.A., ed., Trace Element Geochemistry of Volcanic Rocks: Applications for Massive Sulphide Exploration, Geological Association of Canada, Short Course Notes Vol. 12, p.79–113.

Pearce, J.A. and Cann, J.R. 1973. Tectonic setting of basic volcanic rocks determined using trace element analyses; Earth and Planetary Science Letters, v.19, p.290–300.

Pearce, J.A. and Peate, D.W. 1995. Tectonic implications of the composition of volcanic arc magmas; Annual Review of Earth and Planetary Sciences, v.23, p.251–285.

Pearce, J.A., Harris, N.B.W. and Tindle, A.G. 1984a. Trace element discrimination diagrams for the tectonic interpretation of granitic rocks; Journal of Petrology, v.25, p.956–983.

Pearce, J.A., Lippard, S.J. and Roberts, S. 1984b. Characteristics and tectonic significance of supra–subduction zone ophiolites; *in* Kokelaar, B.P. and Howells, M.F., eds., Marginal Basin Geology, Geological Society Special Publication No. 16 (Blackwell), p.77–94.

Perret, F.A. 1937. The eruption of Mt. Pelee 1929–1932; Carnegie Institution of Washington, Publication No. 458, 126p.

Peterson, D.M. 1997. GIS applications for Archean gold exploration: using Canadian mining camp GIS queries to target gold exploration in Minnesota; *in* Institute on Lake Superior Geology, Proceedings Volume 43, Part 1, p.49–50.

Petford, N. and Atherton, M.P. 1992. Granitoid emplacement and deformation along a major crustal lineament: the Cordillera Blanca, Peru; Tectonophysics, v.205, p.171–185.

Pettijohn, F.J. 1934. Conglomerate of Abram Lake, Ontario, and its extensions; Geological Society of America Bulletin, v.45, p.479–505 (incl. Plate 51 map, scale 1:126 720).

Pettijohn, F.J. 1935. Stratigraphy and structure of Vermilion Township, District of Kenora, Ontario; Geological Society of America Bulletin, v.46, p.1891–1908.

Pettijohn, F.J. 1936. Geology of East Bay, Minnitaki Lake, District of Kenora, Ontario; Journal of Geology, v.44, p.341–357.

Pettijohn, F.J. 1937. Early pre–Cambrian geology and correlational problems of the Northern Subprovince of the Lake Superior region; Geological Society of America Bulletin, v.48, p.153–202.

Pettijohn, F.J. 1939. “Coutchiching” of Thunder Lake, Ontario; Geological Society of America Bulletin, v.50, p.761–775.

Poulsen, K.H. and Franklin, J.M. 1981. Copper and gold mineralization in an Archean trondhjemitic intrusion, Sturgeon Lake, Ontario; *in* Current Research, Part A, Geological Survey of Canada, Paper 81–1A, p.9–14.

Ramsay, J.G. and Huber, M.I. 1987. The Techniques of Modern Structural Geology – Volume 2: Folds and Fractures; Academic Press (HBJ), 393 p.

Rast, N. and Horton, J.W., Jr. 1989. Melanges and olistostromes in the Appalachians of the United States and mainland Canada; An assessment; *in* Horton, J.W., Jr. and Rast, N., eds., Melanges and Olistostromes of the U.S. Appalachians, Geological Society of America, Special Paper 228, p.1–15.

Reid, J. 1978. Archean variolitic lavas; unpublished B. Sc. thesis, Queen’s University, Kingston, Ontario, 66p.

Robert, F. and Poulsen, K.H. 1997. World–class Archaean gold deposits in Canada: an overview; Australian Journal of Earth Sciences, v.44, p.329–351.

Rollinson, H.R. 1993. Using Geochemical Data: Evaluation, Presentation, Interpretation; Longman Scientific and Technical, 352 p.

Rowley, P.D., MacLeod, N.S., Kuntz, M.A. and Kaplan, A.M. 1985. Proximal bedded deposits related to pyroclastic flows of May 18, 1980, Mount St. Helens, Washington; Geological Society of America Bulletin, v.96, p.1373–1383.

Rust, B.R. 1978. Depositional models for braided alluvium; *in* Miall, A.D., ed., Fluvial Sedimentology, Canadian Society of Petroleum Geologists, Memoir 5, p.605–625.

Sage, R.P., Breaks, F.W., Stott, G.M., McWilliams, G.M. and Atkinson, S. 1974. Operation Ignace–Armstrong, Ignace–Graham Sheet, Districts of Thunder Bay, Kenora and Rainy River; Ontario Division of Mines, Preliminary Map P.964, Geol. Ser., scale 1:126 720.

Sajona, F.G., Maury, R.C., Bellon, H., Cotton, J., Defant, M.J. and Pubellier, M. 1993. Initiation of subduction and the generation of slab melts in western and eastern Mindinao, Philippines; Geology, v.21, p.1007–1010.

Sanborn–Barrie, M. 1988. Geology of the tectonic boundary zone between the English River and Winnipeg River Subprovinces, northwestern Ontario; *in* Summary of Field Work and Other Activities 1988, Ontario Geological Survey, Miscellaneous Paper 141, p.98–107.

Sanborn–Barrie, M. and Skulski, T. 1999. Tectonic assembly of continental margin and oceanic terranes at 2.7 Ga in the Savant Lake–Sturgeon Lake greenstone belt, Ontario; *in* Current Research 1999–C, Geological Survey of Canada, p.209–220.

Sasso, A.M. and Clark, A.H. 1998. The Farallon Negro Group, northwest Argentina: magmatic, hydrothermal and tectonic evolution and implications for Cu–Au metallogeny in the Andean back–arc; Society of Economic Geologists Newsletter, no.34, p.1, 8–18.

Satterly, J. 1943. Geology of the Dryden–Wabigoon Area; Ontario Department of Mines, Annual Report, vol. L, part II, 1941, p.1–67. Acc. by Map 50e, scale 1:63 360.

Saunders, A.D. and Tarney, J. 1984. Geochemical characteristics of basaltic volcanism within back–arc basins; *in* Kokelaar, B.P. and Howells, M.F., eds., Marginal Basin Geology, Geological Society Special Publication No. 16 (Blackwell), p.59–76.

Saunders, A. and Tarney, J. 1991. Back–arc basins; *in* Floyd, P.A., ed., Oceanic Basalts, Blackie, p.219–263.

Saunders, A.D., Storey, M., Kent, R.W. and Norry, M.J. 1992. Consequences of plume–lithosphere interactions; *in* Storey, B.C., Alabaster, T. and Pankhurst, R.J., eds., Magmatism and the Causes of Continental Break–up, Geological Society, London, Special Publication 68, p.41–60.

Schermer, E.R., Howell, D.G. and Jones, D.L. 1984. The origin of allochthonous terranes: perspectives on the growth and shaping of continents; Annual Review of Earth and Planetary Sciences, v.12, p.107–131.

Schreurs, G. and Colleta, B. 1998. Analogue modelling of faulting in zones of continental transpression and transtension; *in* Holdsworth, R.E., Strachan, R.A. and Dewey, J.F., eds., Continental Transpressional and Transtensional Tectonics, Geological Society, London, Special Publication 135, p.59–79.

Schumm, S.A. 1977. The Fluvial System; Wiley–Interscience, 338p.

Sengor, A.M.C., Gorur, N. and Saroglu, F. 1985. Strike–slip faulting and related basin formation in zones of tectonic escape: Turkey as a case study; *in* Biddle, K.T. and Christie–Blick, N., eds., Strike–Slip Deformation, Basin Formation, and Sedimentation, Society of Economic Paleontologists and Mineralogists, Special Publication 37, p.227–264.

Sibson, R.H., Robert, F. and Poulsen, K.H. 1988. High–angle reverse faults, fluid pressure cycling, and mesothermal gold–quartz deposits; Geology, v.19, p.551–555.

Skinner, R. 1969. Geology of the Sioux Lookout map–area, Ontario, a part of the Precambrian Shield (52 J); Geological Survey of Canada, Paper 68–45, 10p. Acc. by Map 14–1968, scale 1:250 000.

Smellie, J.L., ed. 1995. Volcanism Associated with Extension at Consuming Plate Margins; Geological Society Special Publication 81, 293p.

Smith, G.A. and Lowe, D.R. 1991. Lahars: volcano–hydrologic events and deposition in the debris flow–hyperconcentrated flow continuum; *in* Fisher, R.V. and Smith, G.A., eds., Sedimentation in Volcanic Settings, Society of Economic Paleontologists and Mineralogists, Special Publication 45, p.59–70.

Spang, J.H. and Evans, J.P. 1988. Geometrical and mechanical constraints on basement–involved thrusts in the Rocky Mountain foreland province; *in* Schmidt, C.J. and Perry, W.J., Jr., eds., Interaction of the Rocky Mountain Foreland and the Cordilleran Thrust Belt, Geological Society of America, Memoir 171, p.41–52.

Steidtmann, J.R. and Schmitt, J.G. 1988. Provenance and dispersal of tectogenic sediments in thin–skinned, thrusted terrains; *in* Kleinspehn, K.L. and Paola, C., eds., New Perspectives in Basin Analysis, Springer–Verlag, p.353–366.

Stern, R.A. and Hanson, G.N. 1991. Archean high–Mg granodiorite: a derivative of light rare earth element–enriched monzodiorite of mantle origin; Journal of Petrology, v.32, p.201–238.

Stott, G.M. and Corfu, F. 1991. Uchi Subprovince; *in* Thurston, P.C., Williams, H.R., Sutcliffe, R.H. and Stott, G.M., eds., Geology of Ontario, Ontario Geological Survey, Special Volume 4, Part 1, p.145–236.

Sun, S.–s. and McDonough, W.F. 1989. Chemical and isotopic systematics of oceanic basalts: implications for mantle composition and processes; *in* Saunders, A.D. and Norry, M.J., eds., Magmatism in the Ocean Basins, Geological Society, Special Publication No. 42, p.313–345.

Sutherland, I.G. and Colvine, A.C. 1979. The geology and mineralization of the Pickerel Arm, Canoe Lake, and High Lake bodies; *in* Summary of Field Work, 1979, Ontario Geological Survey, Miscellaneous Paper 90, p.233–243.

Sylvester, A.G. 1988. Strike–slip faults; Geological Society of America Bulletin, v.100, p.1666–1703.

Syme, E.C., Bailes, A.H., Stern, R.A. and Lucas, S.B. 1996. Geochemical characteristics of 1.9 Ga tectonostratigraphic assemblages and tectonic setting of massive sulphide deposits in the Paleoproterozoic Flin Flon Belt, Canada; *in* Wyman, D.A., ed., Trace Element Geochemistry of Volcanic Rocks: Applications for Massive Sulphide Exploration, Geological Association of Canada Short Course Notes Vol. 12, p.279–327.

Szewczyk, Z.J. and West, G.F. 1976. Gravity study of an Archean granitic area northwest of Ignace, Ontario; Canadian Journal of Earth Sciences, v.13, p.1119–1130.

Tamaki, K. 1985. Two modes of back–arc spreading; Geology, v.13, p.475–478.

Tamaki, K. 1988. Geological structure of the Japan Sea and its tectonic implications; Bulletin of the Geological Survey of Japan, v.39, p.269–365.

Tchalenko, J.S. 1970. Similarities between shear zones of different magnitudes; Geological Society of America Bulletin, v.81, p.1625–1640.

Tchalenko, J.S. and Ambraseys, N.N. 1970. Structural analysis of the Dasht–e Bayaz (Iran) earthquake fractures; Geological Society of America Bulletin, v.81, p.41–60.

Thompson, M.D. 1993. Late Proterozoic stratigraphy and structure in the Avalonian magmatic arc, southwest of Boston, Massachusetts; American Journal of Science, v.293, p.725–743.

Tikoff, B. and Greene, D. 1997. Stretching lineations in transpressional shear zones: an example from the Sierra Nevada Batholith, California; Journal of Structural Geology, v.19, p.29–39.

Tikoff, B. and Teyssier, C. 1992. Crustal–scale, en echelon "P–shear" tensional bridges: a possible solution to the batholithic room problem; Geology, v.20, p.927–930.

Tomlinson, K.Y., Bowins, R. and Hechler, J. 1999. Refinement of hafnium (Hf) and zirconium (Zr) ICP–MS analysis by improvement in the sample digestion procedure; *in* Summary of Field Work and Other Activities 1998, Ontario Geological Survey, Miscellaneous Paper 169, p.189–192.

Trowell, N.F. and Johns, G.W. 1986. Stratigraphic correlation of the western Wabigoon Subprovince, northwestern Ontario; *in* Wood, J. and Wallace, H., eds., Volcanology and Mineral Deposits, Ontario Geological Survey, Miscellaneous Paper 129, p.50–61.

Trowell, N.F., Bartlett, J.R. and Sutcliffe, R.H. 1982. Loggers Lake; Ontario Geological Survey, Map 2477, Precambrian Geology Series, scale 1:50 000.

Trowell, N.F., Bartlett, J.R. and Sutcliffe, R.H. 1983. Geology of the Flying Loon Lake area, District of Kenora; Ontario Geological Survey, Report 224, 109p. Acc. by Maps 2458, 2477, scale 1:50 000, and Chart A.

Trowell, N.F., Blackburn, C.E. and Edwards, G.R. 1980. Preliminary Geological Synthesis of the Savant Lake – Crow Lake Metavolcanic–Metasedimentary Belt, Northwestern Ontario, and Its Bearing upon Mineral Exploration; Ontario Geological Survey, Miscellaneous Paper 89, 30p. Acc. by Chart A.

Trowell, N.F., Blackburn, C.E., Edwards, G. and Sutcliffe, R.H. 1977. Savant Lake – Crow Lake Special Project, Districts of Thunder Bay and Kenora; *in* Summary of Field Work, 1977, Ontario Geological Survey, Miscellaneous Paper 75, p.25–49.

Trowell, N.F., Blackburn, C.E., Edwards, G.R. and Bartlett, J.R. 1978. Savant Lake – Crow lake Special Project, Districts of Thunder Bay and Kenora; *in* Summary of Field Work, 1978, Ontario Geological Survey, Miscellaneous Paper 82, p.28–44.

Turner, C.C. 1972. Archaean sedimentation: Alluvial fan and turbidite deposits, Little Vermilion Lake, northwestern Ontario; unpublished M. Sc. thesis, McMaster University,Hamilton, Ontario, 211p.

Turner, C.C. and Walker, R.G. 1973. Sedimentology, stratigraphy, and crustal evolution of the Archean greenstone belt near Sioux Lookout, Ontario; Canadian Journal of Earth Sciences, v.10, p.817–845.

van Wyk de Vries, B. and Merle, O. 1998. Extension induced by volcanic loading in regional strike–slip zones; Geology, v.26, p.983–986.

Vearncombe, J.R., Barley, M.E., Eisenlohr, B.N., Groves, D.I., Houstoun, S.M., Skwarnecki, M.S., Grigson, M.W. and Partington, G.A. 1989. Structural controls on mesothermal gold mineralization: examples from the Archean terranes of southern Africa and Western Australia; *in* Keays, R.R., Ramsay, W.R.H. and Groves, D.I., eds., The Geology of Gold Deposits: The Perspective in 1988, Economic Geology Monograph 6, p.124–134.

Walker, R.G. and James, N.P., eds. 1992. Facies Models: Response to Sea Level Change. Geological Association of Canada, 409 p.

Walker, R.G. and Pettijohn, F.J. 1971. Archaean sedimentation: Analysis of the Minnitaki basin, northwestern Ontario, Canada; Geological Society of America Bulletin, v.82, p.2099–2130.

Williams, H.R. 1989. Geological studies in the Wabigoon, Quetico and Abitibi–Wawa subprovinces, Superior Province of Ontario, with emphasis on the structural development of the Beardmore–Geraldton belt; Ontario Geological Survey, Open File Report 5724, 189 p.

Williams, H.R. 1991. Quetico Subprovince; *in* Thurston, P.C., Williams, H.R., Sutcliffe, R.H. and Stott, G.M., eds., Geology of Ontario, Ontario Geological Survey, Special Volume 4, Part 1, p.383–403.

Williams, H.R., Stott, G.M. and Thurston, P.C. 1992. Tectonic evolution of Ontario: Summary and Synthesis – Part 1: Revolution in the Superior Province; *in* Thurston, P.C., Williams, H.R., Sutcliffe, R.H. and Stott, G.M., eds., Geology of Ontario, Ontario Geological Survey, Special Volume 4, Part 2, p.1255–1294, 1323–1332.

Windley, B.F. 1995. The Evolving Continents, 3rd ed.; John Wiley and Sons, 526 p.

Wood, D.A. 1980. The application of a Th–Hf–Ta diagram to problems of tectonomagmatic classification and to establishing the nature of crustal contamination of basaltic lavas of the British Tertiary Volcanic Province; Earth and Planetary Science Letters, v.50, p.11–30.

Wyman, D. and Kerrich, R. 1988. Alkaline magmatism, major structures, and gold deposits: implications for greenstone belt gold metallogeny; Economic Geology, v.83, p.454–461.

Yogodzinski, G.M., Kay, R.W., Volynets, O.N., Koloskov, A.V. and Kay, S.M. 1995. Magnesian andesite in the western Aleutian Komandorsky region: implications for slab melting and processes in the mantle wedge; Geological Society of America Bulletin, v.107, p.505–519.

Location and General Geology of the Sioux Lookout Area

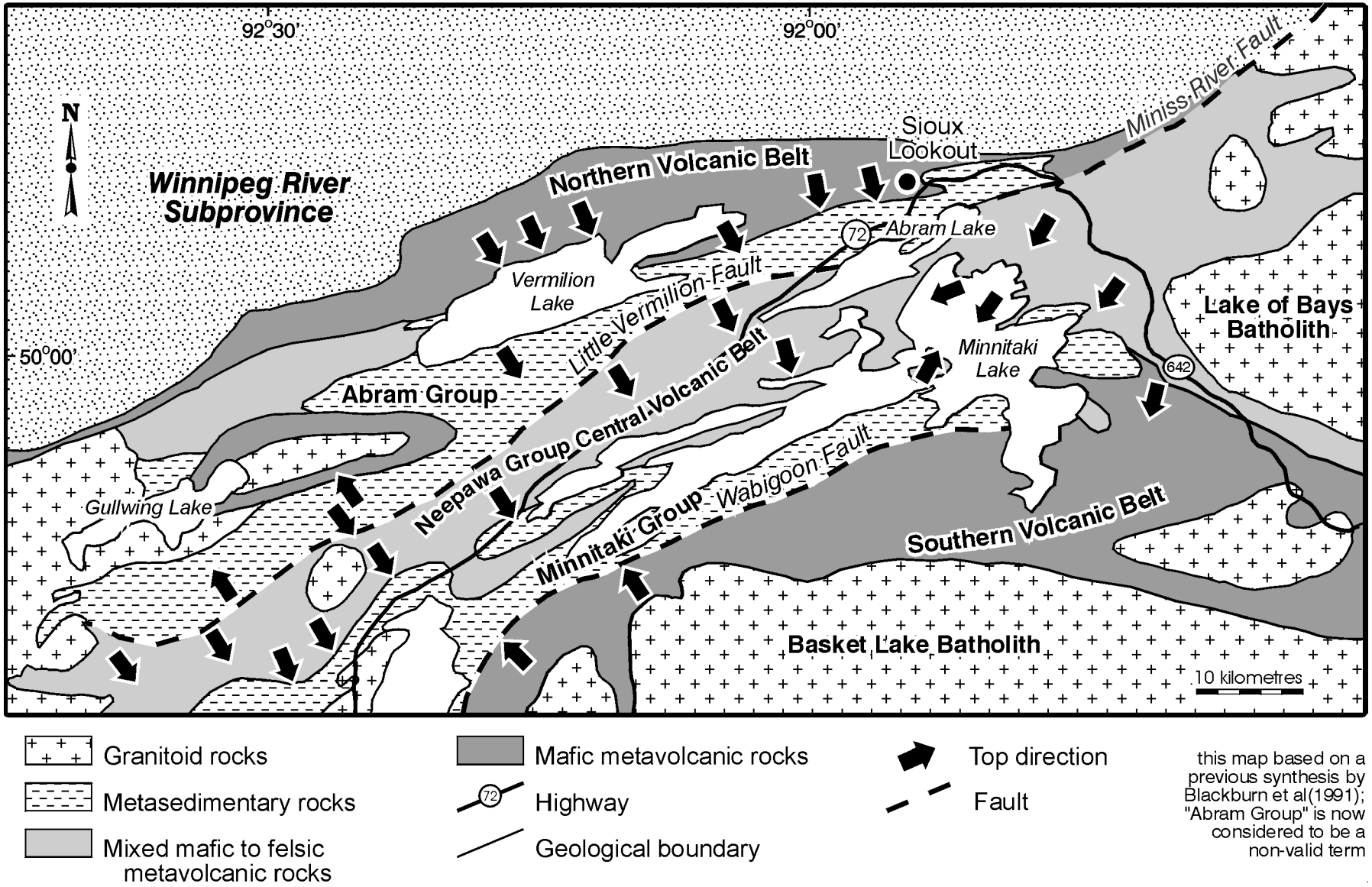

Figure 1a. Location and general geology of the Sioux Lookout area (1a: *after* Blackburn et al. 1991, Figure 9.12).

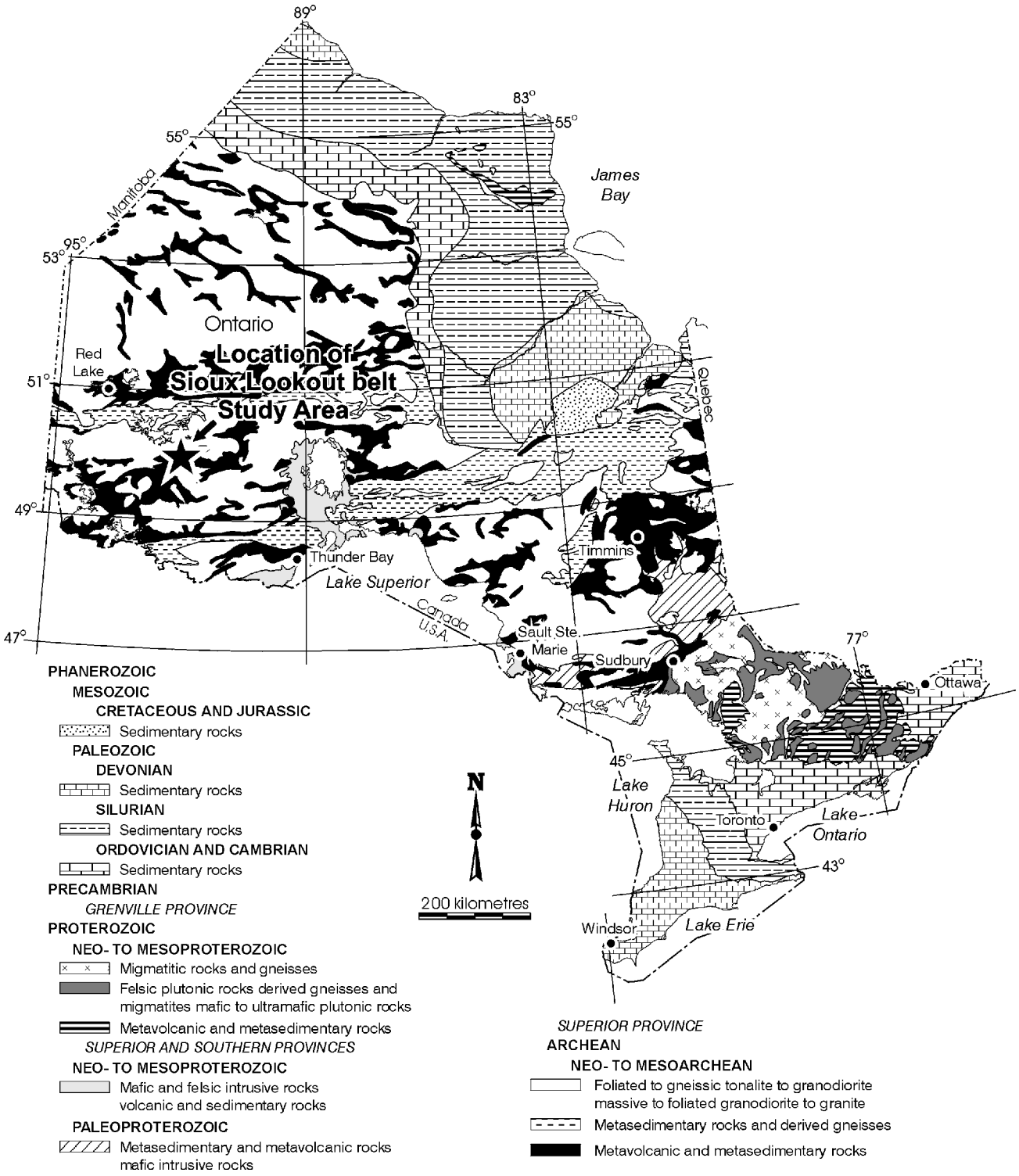

Figure 1b. Location of Sioux Lookout orogenic belt study area in northwest Ontario.

Tectonized Stratigraphic Cross-Section, Sioux Lookout Belt

30 km North-South Transect

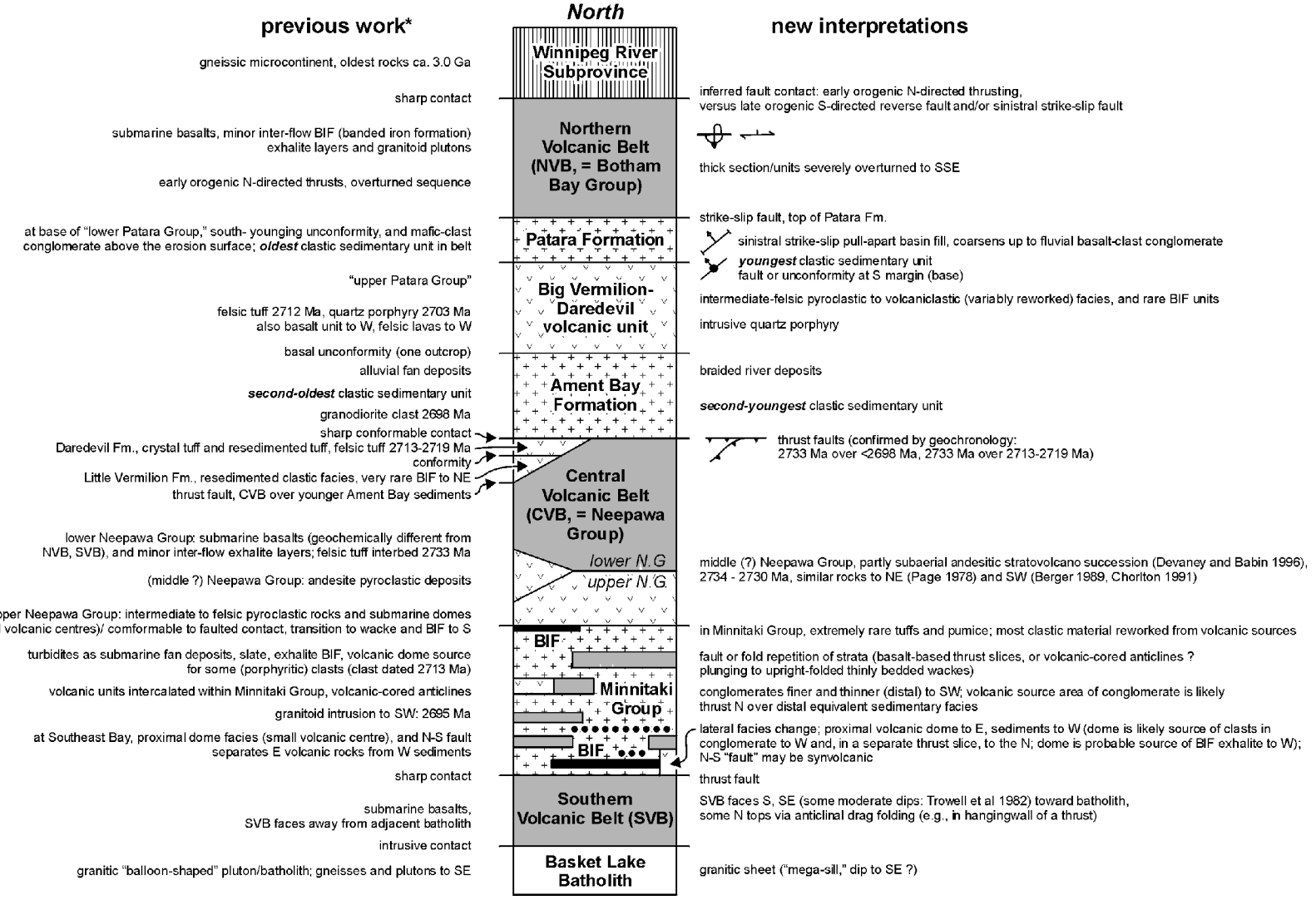

*previous work by: Ayer 1992; Beakhouse 1988, 1991; Berger 1989; Blackburn 1980; Blackburn et al 1985, 1991; Chorlton 1991; Davis 1990; Davis et al 1988; Johnston 1969, 1972; Page 1978, 1984; Page and Clifford 1977; Pettijohn 1934, 1935, 1937; Trowell et al 1978, 1980, 1982, 1983; Turner 1972; Turner and Walker 1973; Walker and Pettijohn 1971; U-Pb dates from: Davis and Trowell 1982, Davis et al 1988, Davis 1990, Blackburn et al 1991, and Devaney (1999a)..

Figure 2. Sioux Lookout orogenic belt north–south transect (annotated generalized cross–section) listing previous descriptions and interpretations (left side) versus new descriptions and interpretations of this study (right side).

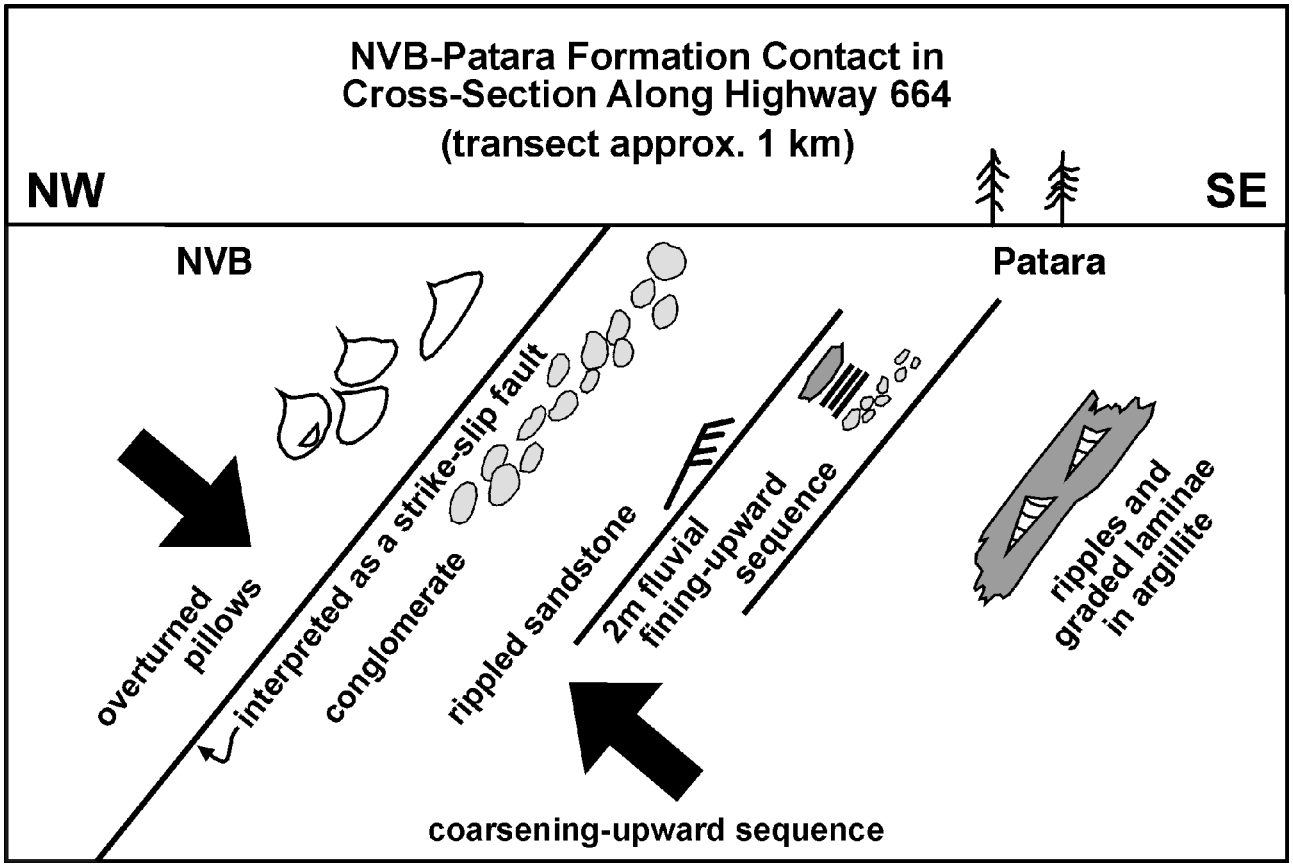

Figure 3. Roadside cross–section of the Patara Formation and adjacent Northern Volcanic belt (NVB).

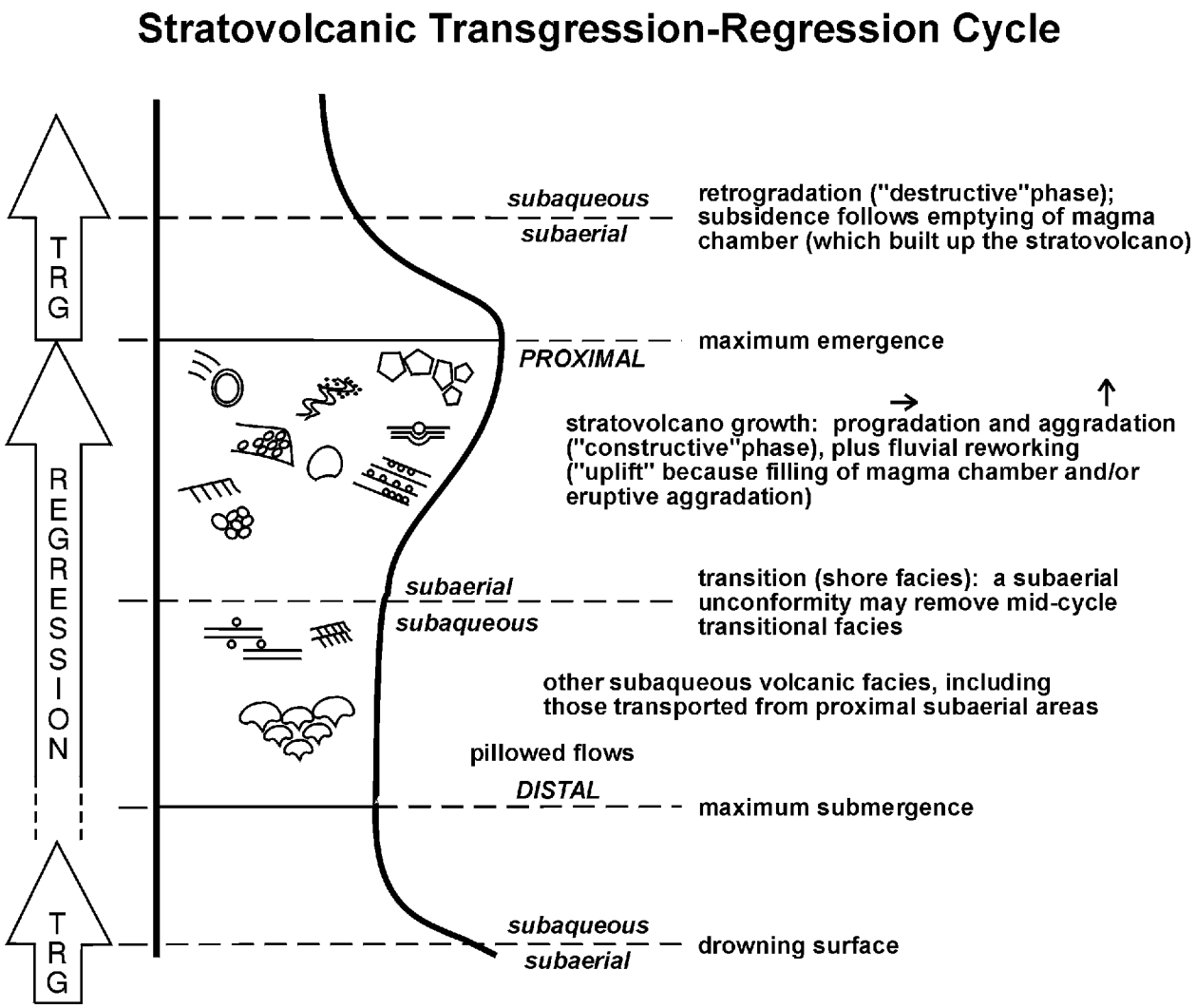

Figure 4. Stratovolcanic transgression–regression cycle model, an idealized composite based on the three cycles interpreted to be present at Northeast Bay of Minnitaki Lake (Devaney 1998). From bottom to top, graphic symbols represent features seen in the Northeast Bay outcrops: subaqueous pillowed lava, pebbly beds, climbing ripples, tightly packed clast–supported rounded–clast conglomerate, cross–bedding, low–angle bedding with normal or inverse grading, broken clast, talus at aa flow snout, bomb sag laminae, a "squiggly" synvolcanic dike (irregular and embayed margins, intruded into unlithified tuffs), airfall bomb clast, and coarse oligomict tuff–breccia with broken angular clasts (broken via ballistic impacts during block–and–ash flow transport, or former pyroclasts that broke along cooling cracks).

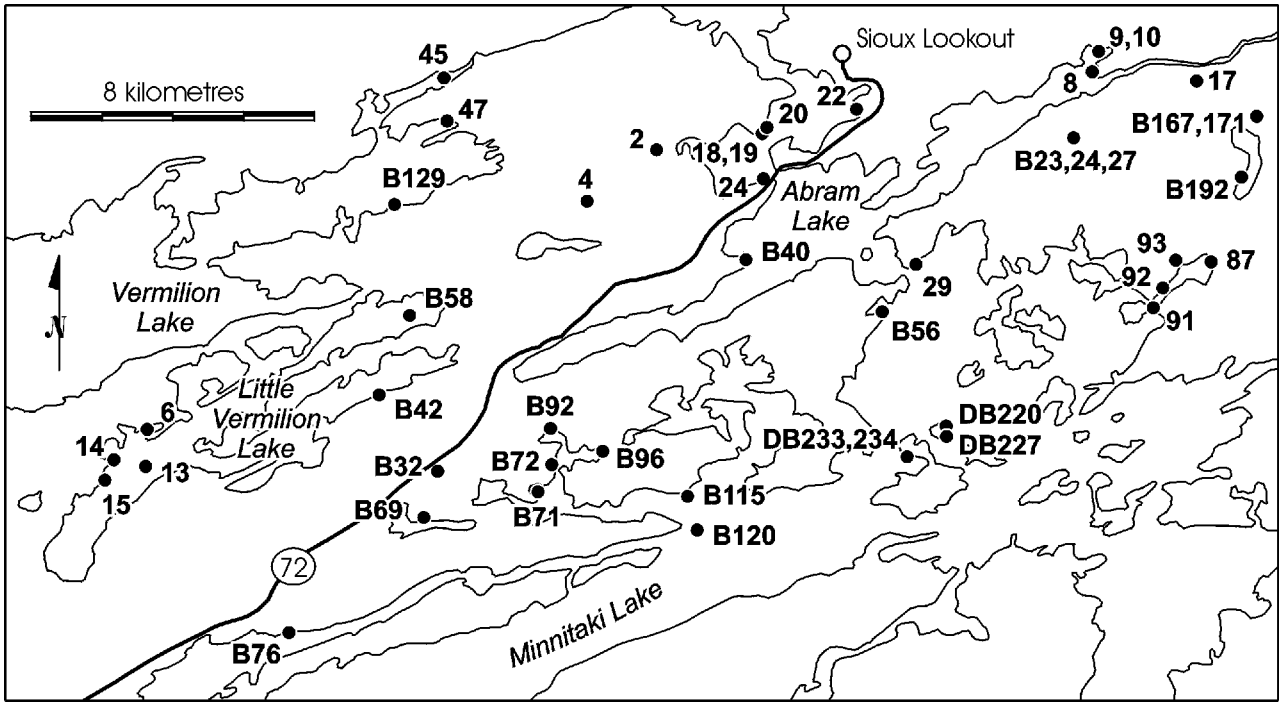

Figure 5a. Geochemical sample location map. (Samples 34, 35 and 36 are from north shore of Minnitaki Lake (Pickerel Arm) sites about 1.5 km south of the southwest corner of the figure.)

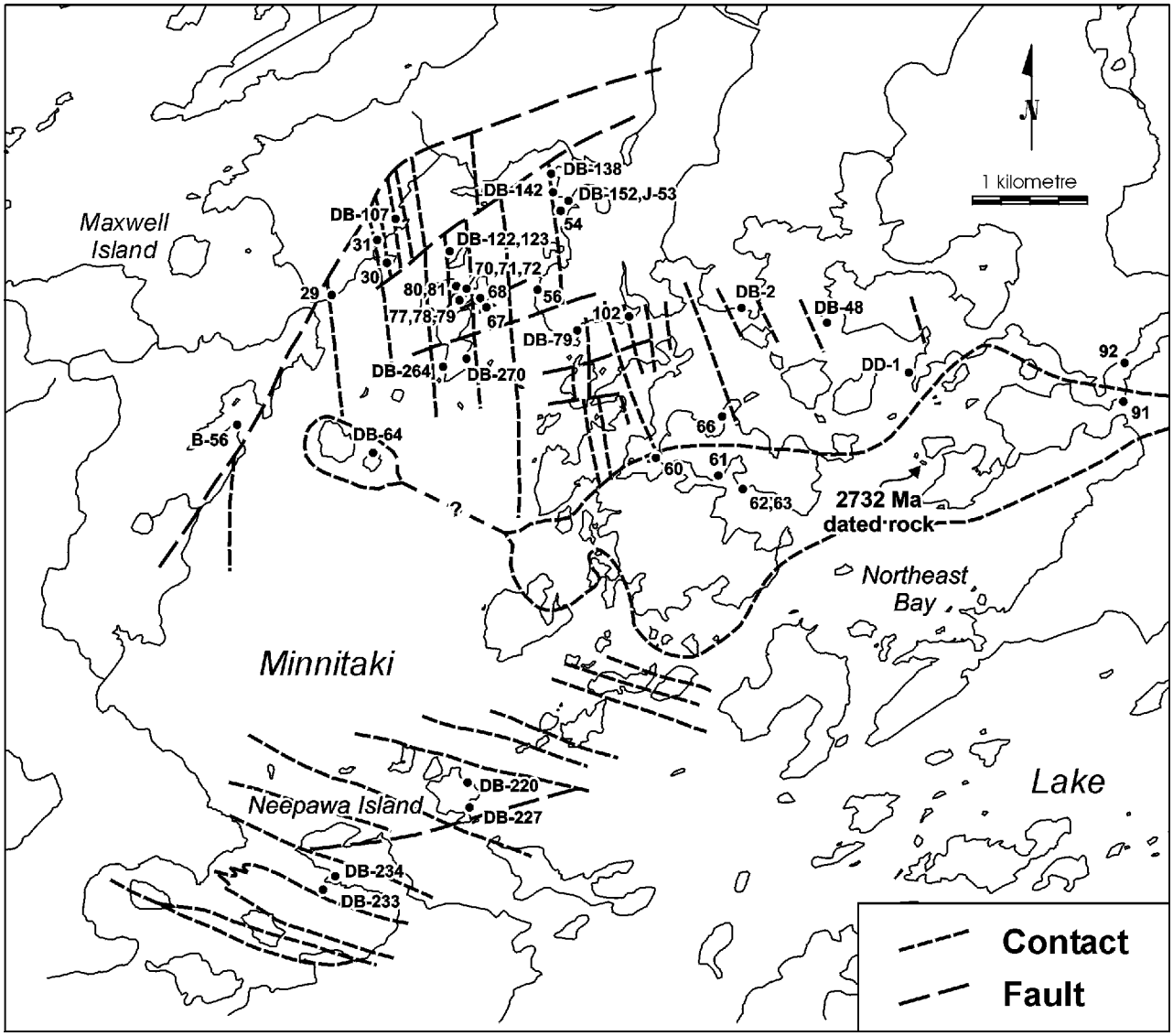

Figure 5b. Geochemical sample location map, Northeast Bay of Minnitaki Lake area.

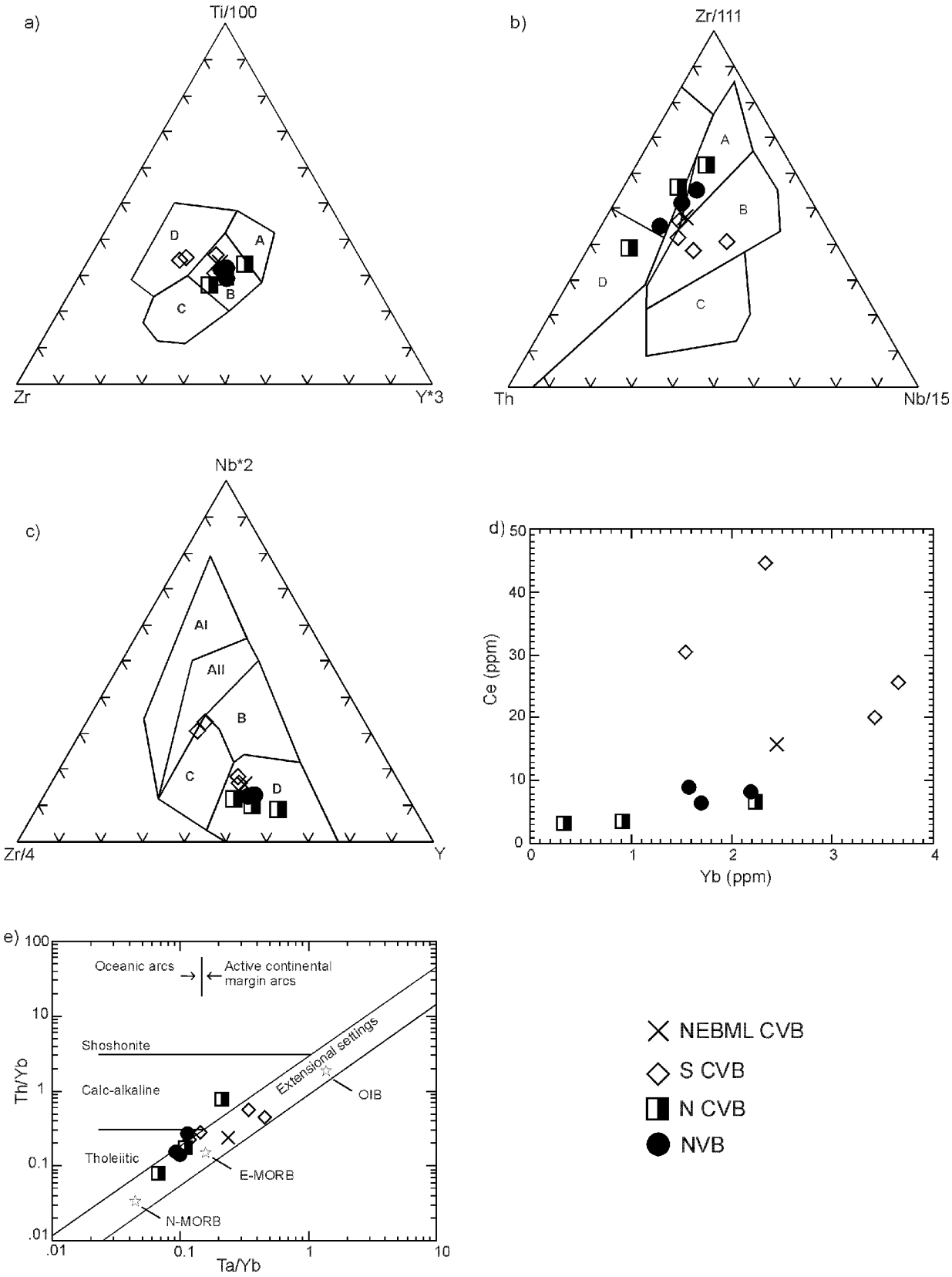

Figure 6. Discrimination plots showing inferred plate tectonic affinity of Sioux Lookout orogenic belt basalts: **a**) *after* Pearce and Cann (1973); A and C, volcanic arc basalt; B, mid–ocean ridge basalt + volcanic arc basalt; D, within plate basalt; **b**) *after* Wood (1980); A, mid–ocean ridge basalt; B, mid–ocean ridge basalt + within plate basalt; C, within plate basalt; D, volcanic arc basalt; **c**) *after* Meschede (1986); AI and AII, within plate alkali basalts; AII and C, within plate tholeiitic basalts; B, plume–influenced mid–ocean ridge basalt; C and D, volcanic arc basalt; D, normal mid–ocean ridge basalt; **d**) *after* Hawkesworth et al. (1993); most values are of "oceanic" or juvenile arc affinity (cf. Ayer and Davis 1997, Figure 8); *after* Pearce (1983; cf. Ayer and Davis 1997, Figure 7).

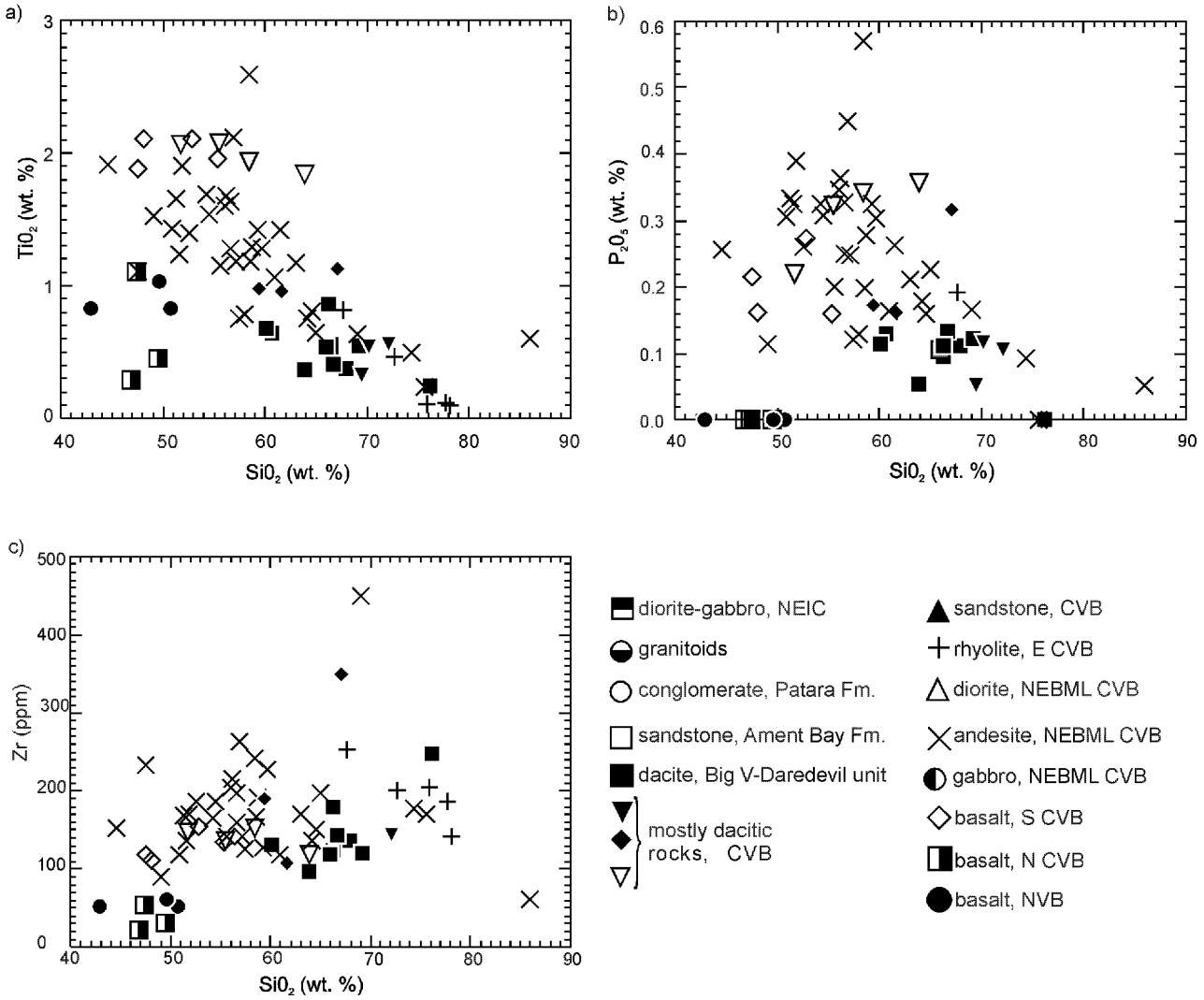

Figure 7. Plots of selected high field strength elements versus SiO_2 for all Sioux Lookout orogenic belt volcanic rock samples: **a**) TiO_2 versus SiO_2; **b**) P_2O_5 versus SiO_2; **c**) Zr versus SiO_2.

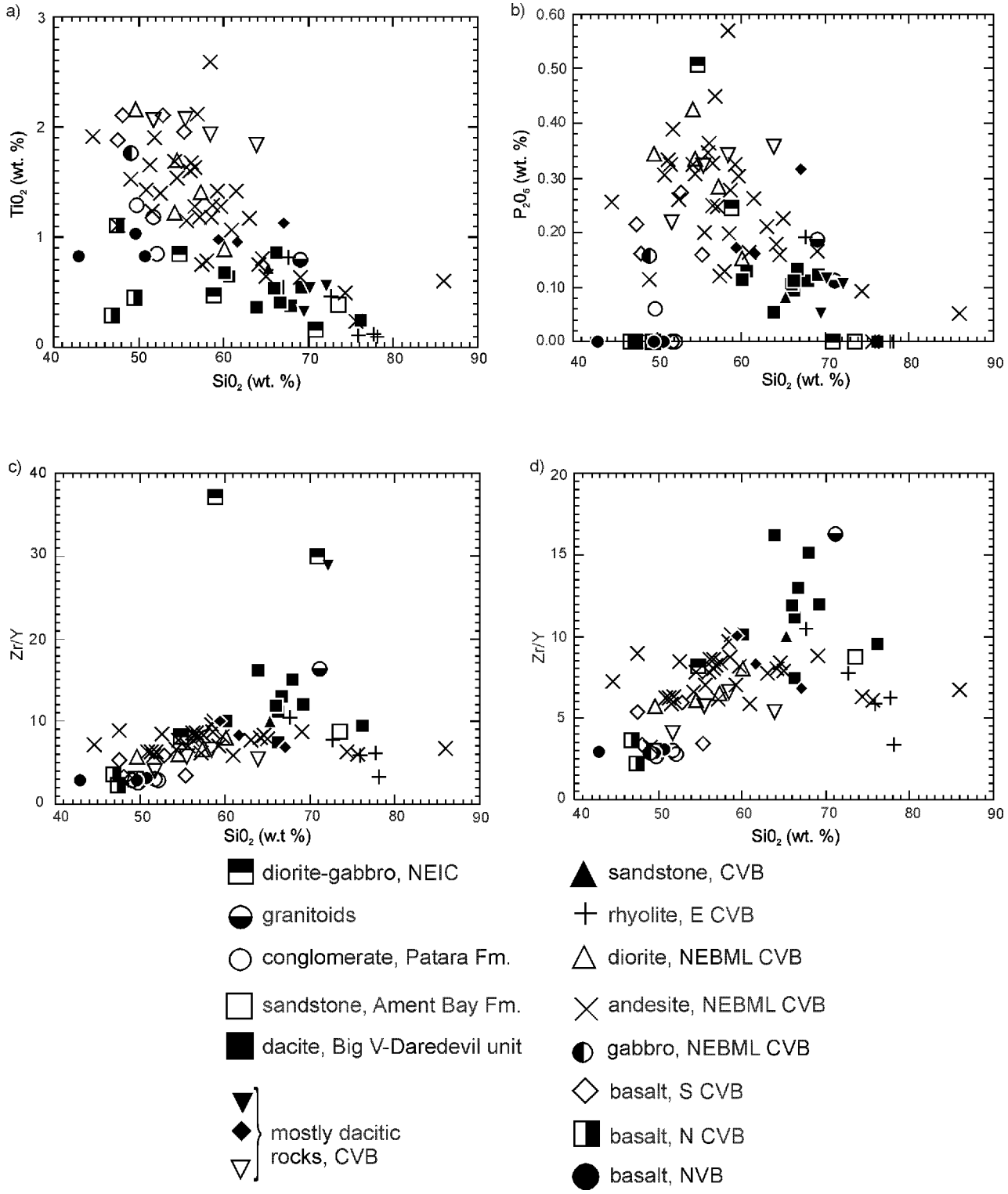

Figure 8. Plots of selected high field strength elements and a ratio (Zr/Y) versus SiO_2 (versus Y in e) for all Sioux Lookout orogenic belt samples: **a**) TiO_2 versus SiO_2; **b**) P_2O_5 versus SiO_2; **c**) Zr/Y versus SiO_2; **d**) Zr/Y versus SiO_2 (detail view of c); **e**) Zr versus Y; **f**) Nb versus SiO_2.

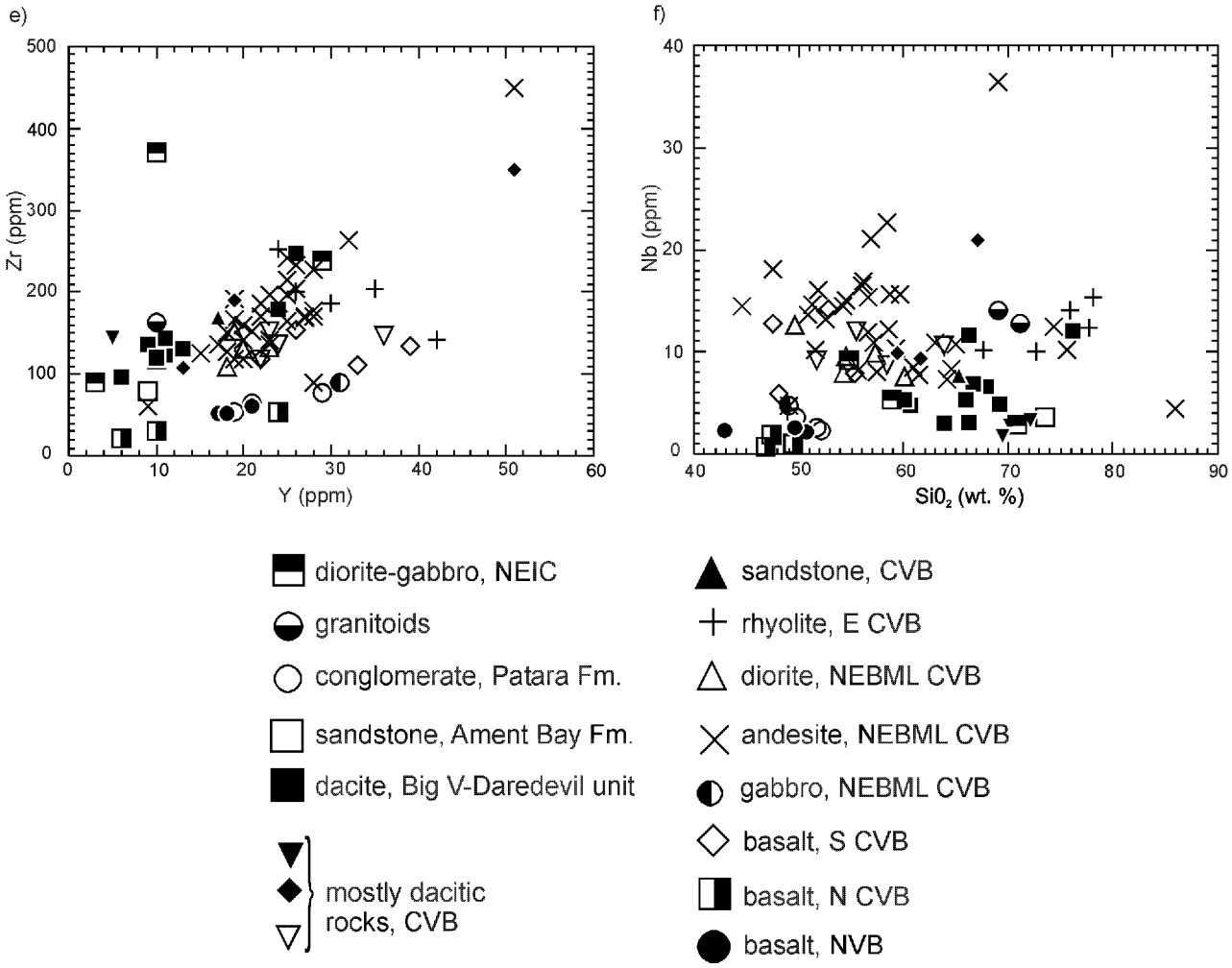

Figure 8. *Continued*

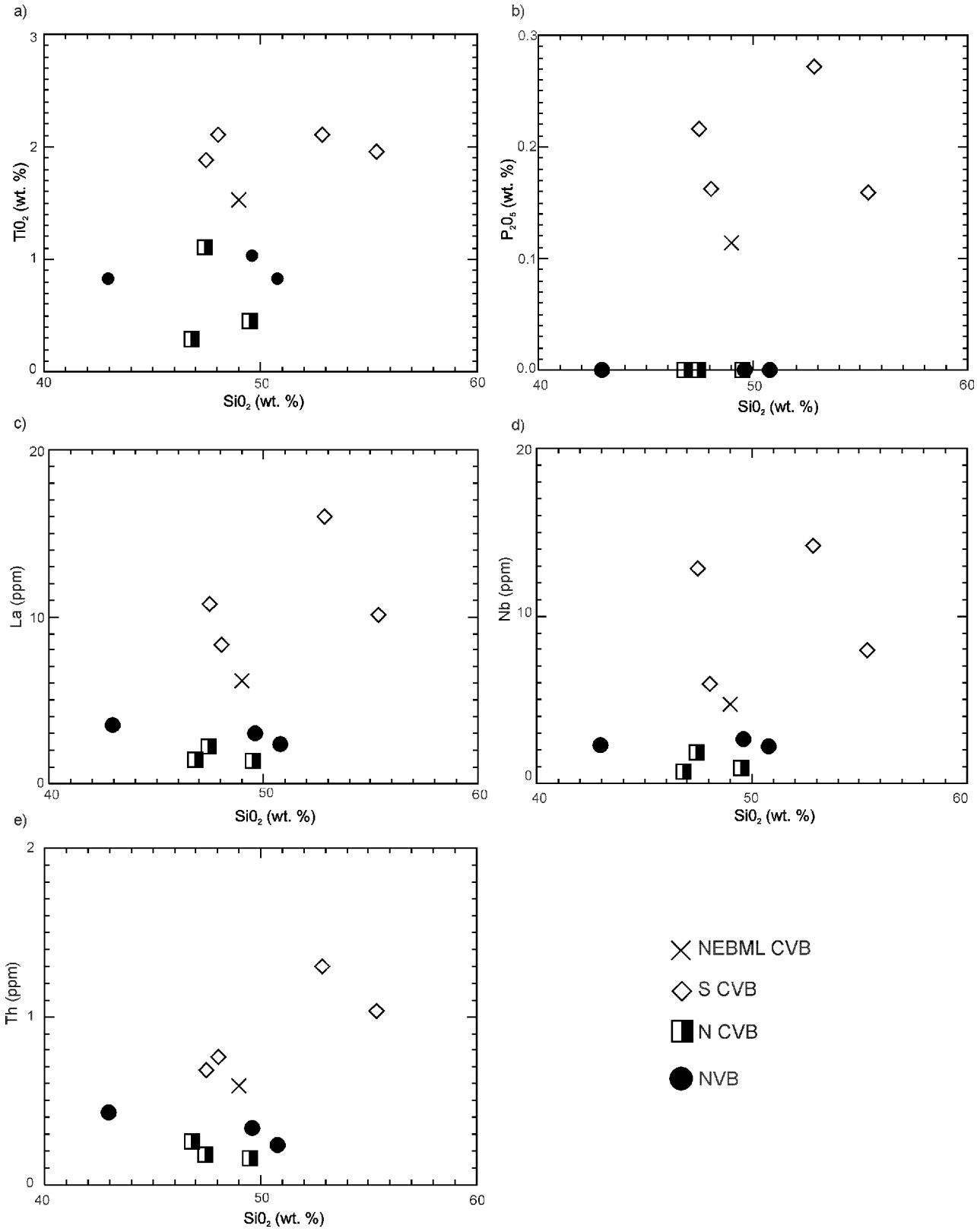

Figure 9. Plots of selected oxides and elements versus SiO_2 for Sioux Lookout orogenic belt basalts, showing subdivision into two sample groups (southern Central Volcanic belt basalts versus other basalts; see Table 5): **a**) TiO_2 versus SiO_2; **b**) P_2O_5 versus SiO_2; **c**) La versus SiO_2; **d**) Nb versus SiO_2; **e**) Th versus SiO_2; **f**) Zr versus SiO_2; **g**) Zn versus SiO_2.

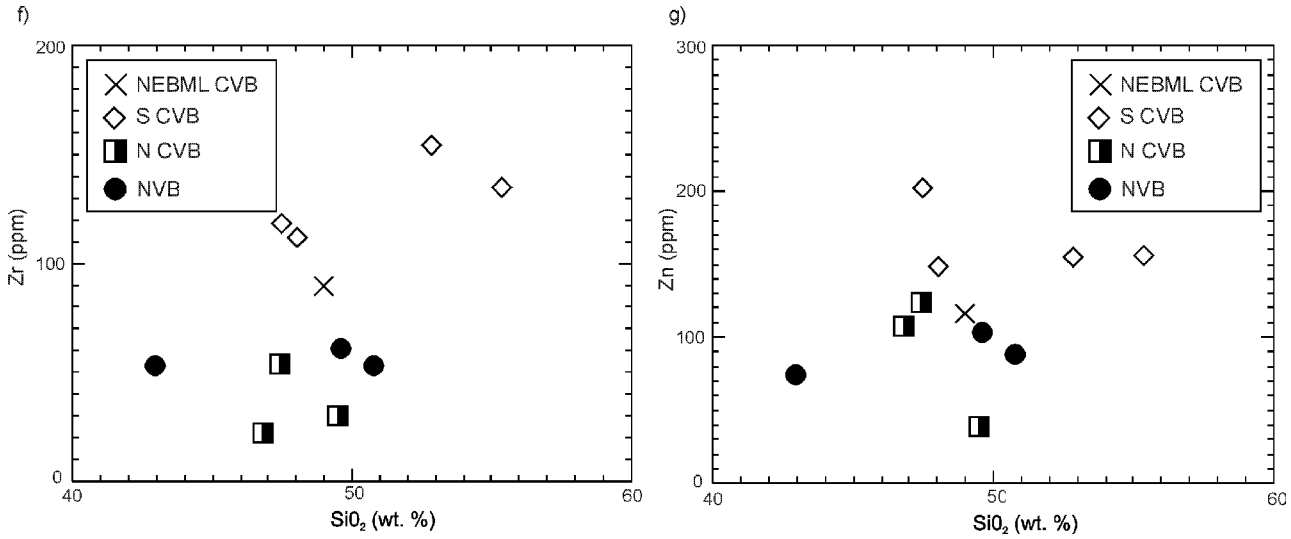

Figure 9. *Continued*

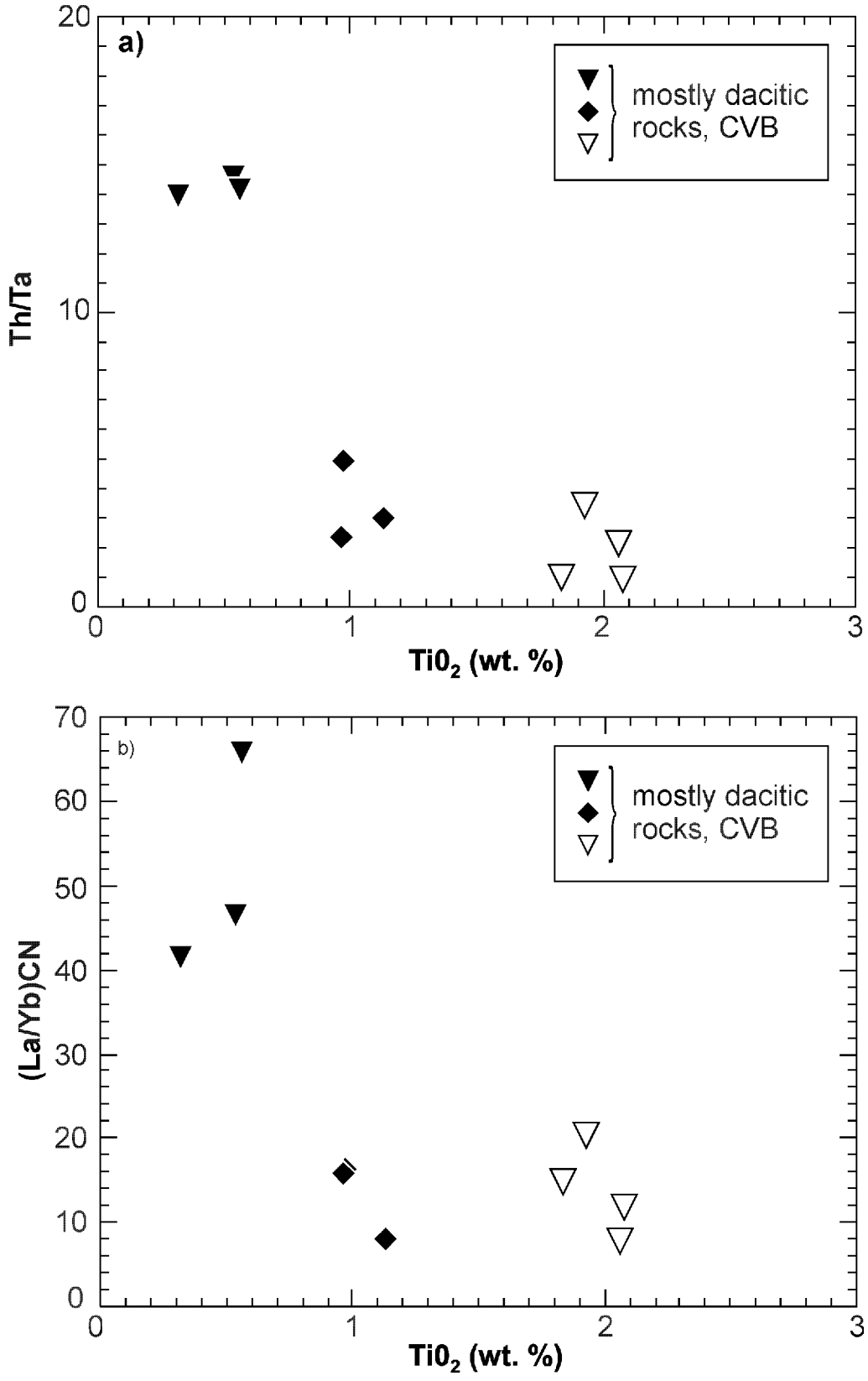

Figure 10. Plots of selected trace element ratios versus TiO_2 for selected Central Volcanic belt intermediate–felsic volcanic rocks, showing three distinct sample groups: **a**) Th/Ta versus TiO_2; **b)** chondrite–normalized La/Yb versus TiO_2.

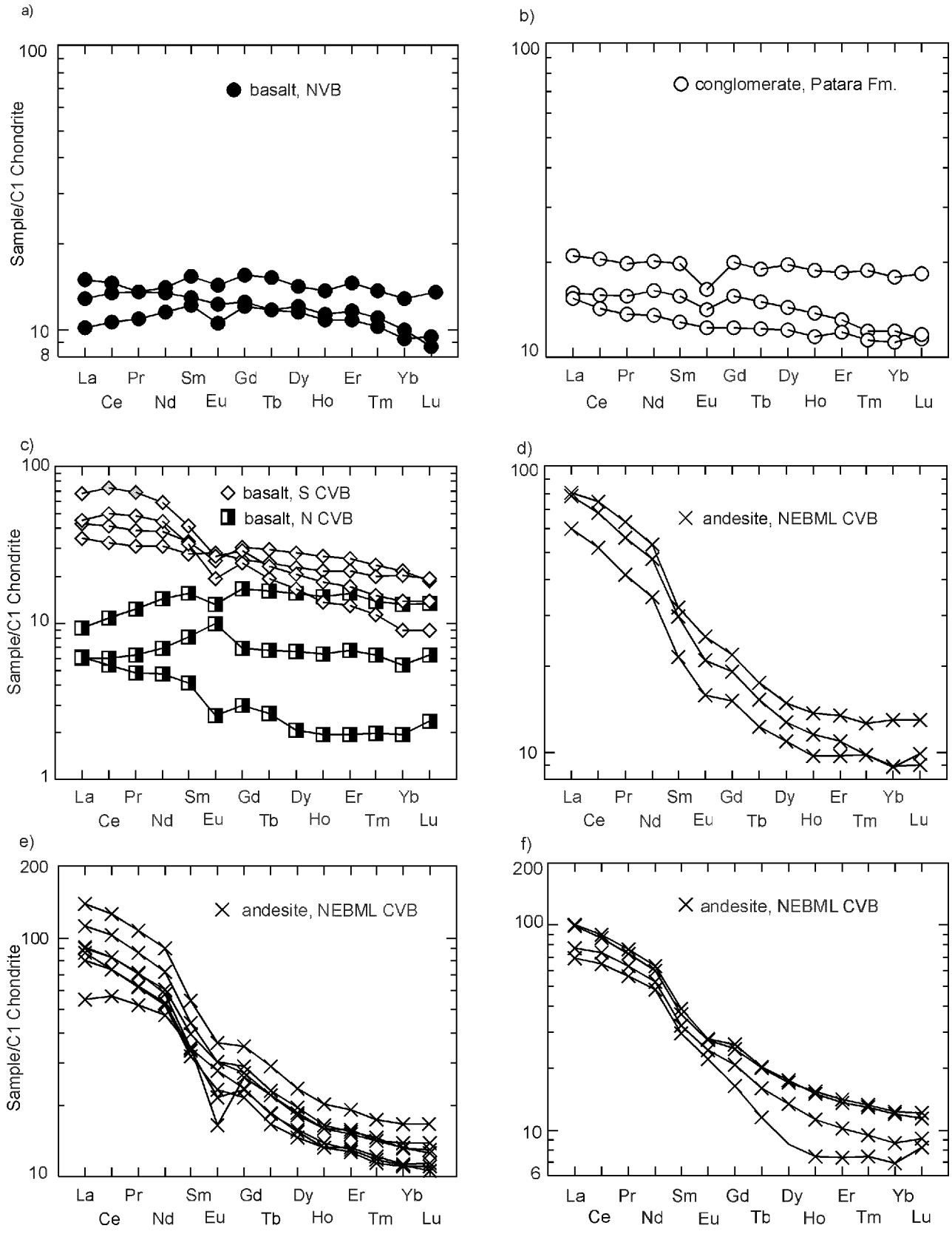

Figure 11. Chondrite–normalized rare earth element (REE) plots for samples of Sioux Lookout orogenic belt lithologies and stratigraphic units; d–h are for samples from the Northeast Bay of Minnitaki Lake (NEBML) area: **a**) Northern Volcanic belt basalt; **b**) Patara Formation basalt–clast conglomerate; **c**) north and south Central Volcanic belt basalt (note distinct north versus south sample groups); **d**) eastern (lower) andesitic strata (samples J–53, –54, –102); **e**) central (middle) andesitic strata (samples J–67, –68,

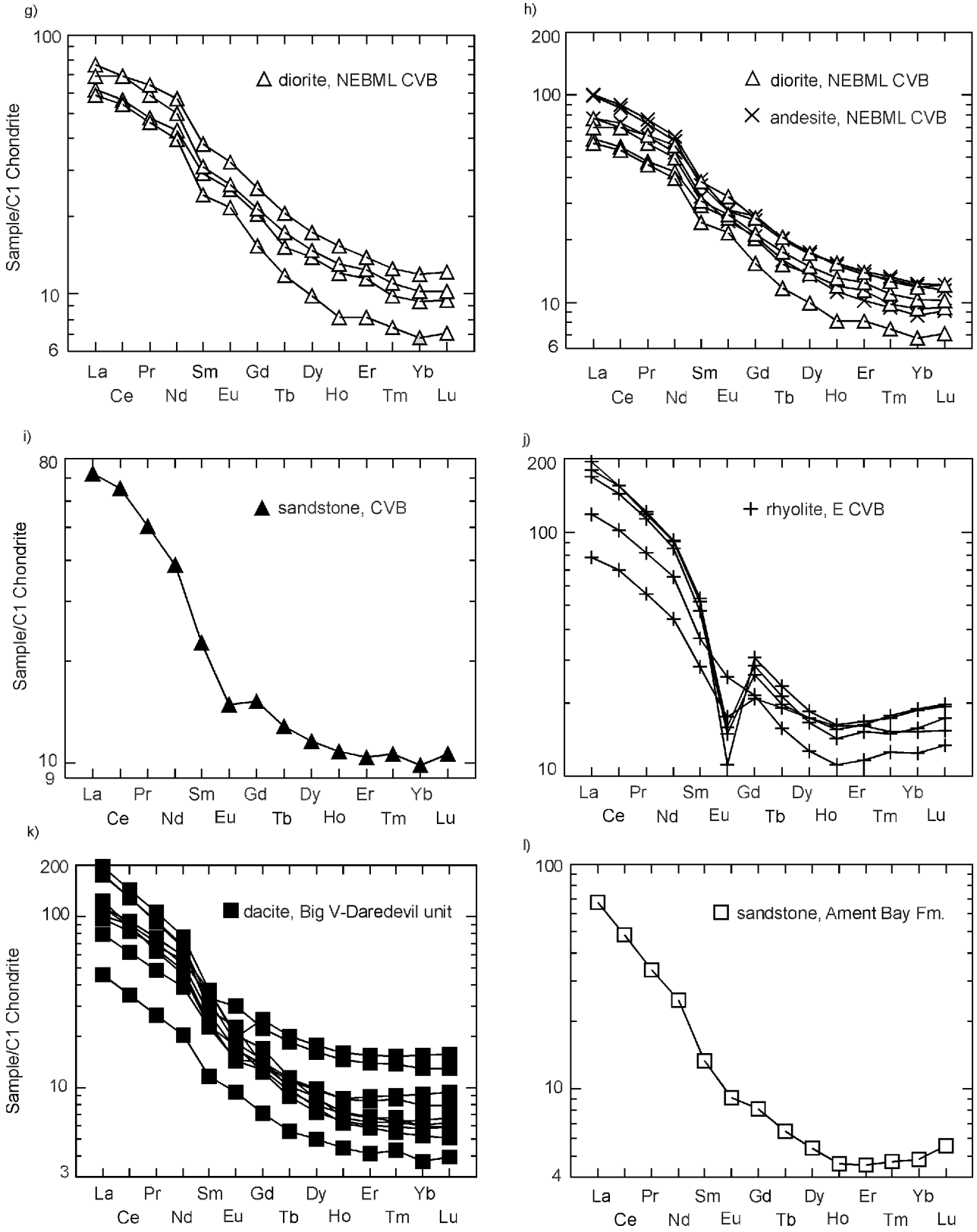

Figure 11. *Continued.* –77 to –81); **f**) western (upper) andestic strata (samples J–29, –30, –31, B–56); **g**) dioritic rocks; **h**) western (upper) andesitic strata (samples J–29 to –31) and dioritic rocks (samples J–60 to –63; shows overlap of the two sample groups within a narrow compositional range); **i**) a Central Volcanic belt sandstone (sample J–92); **j**) eastern Central Volcanic belt rhyolites (Superior Junction area samples); **k**) Big–Vermilion–Daredevil unit and Daredevil Formation intermediate–felsic volcaniclastic rocks; **l**) Ament Bay Formation sandstone (sample J–6);

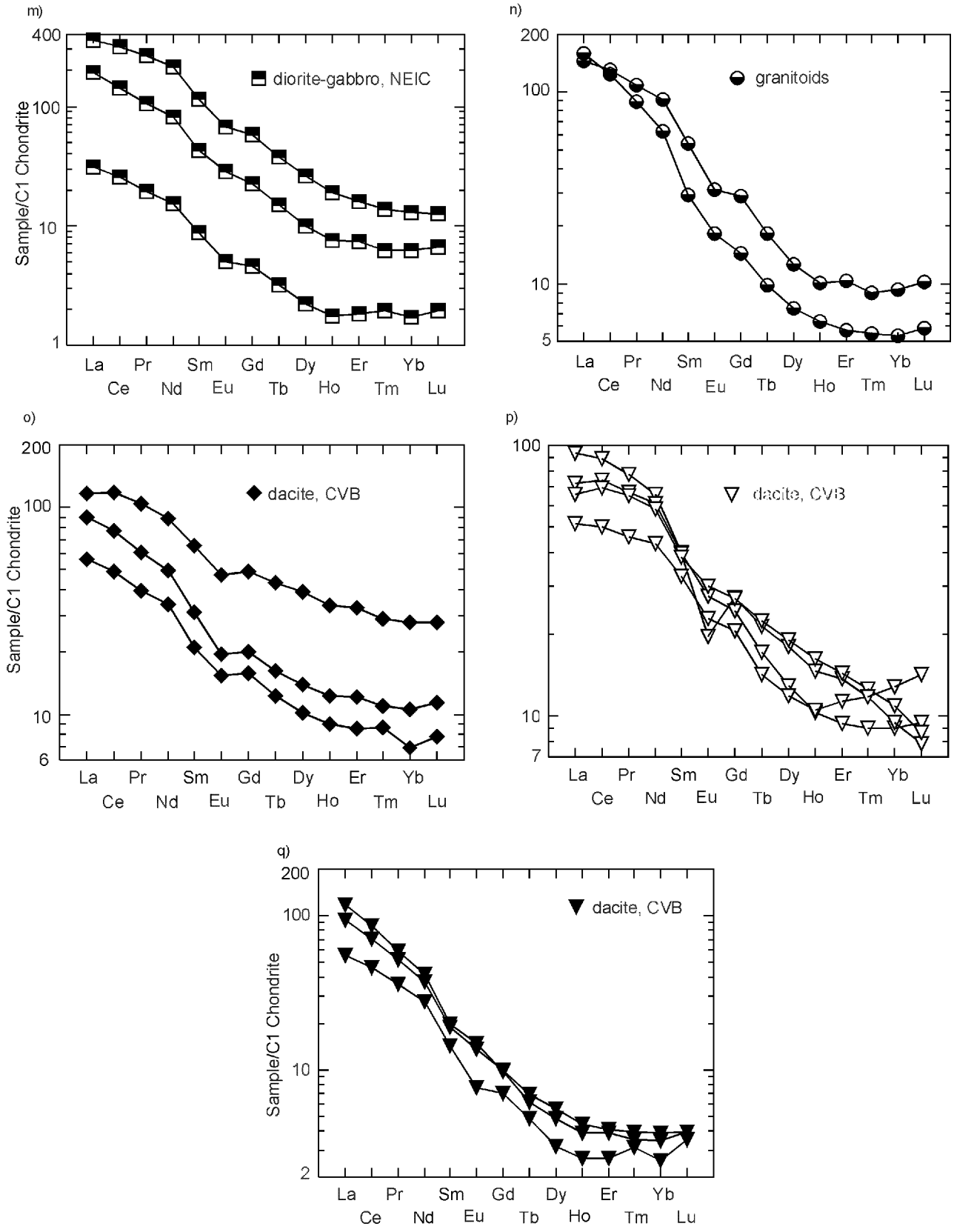

Figure 11. *Continued.* **m**) Northeast Intrusive Complex (NEIC) diorite–gabbro; **n**) granitoids; **o, p, q**) three Central Volcanic belt sample groups.

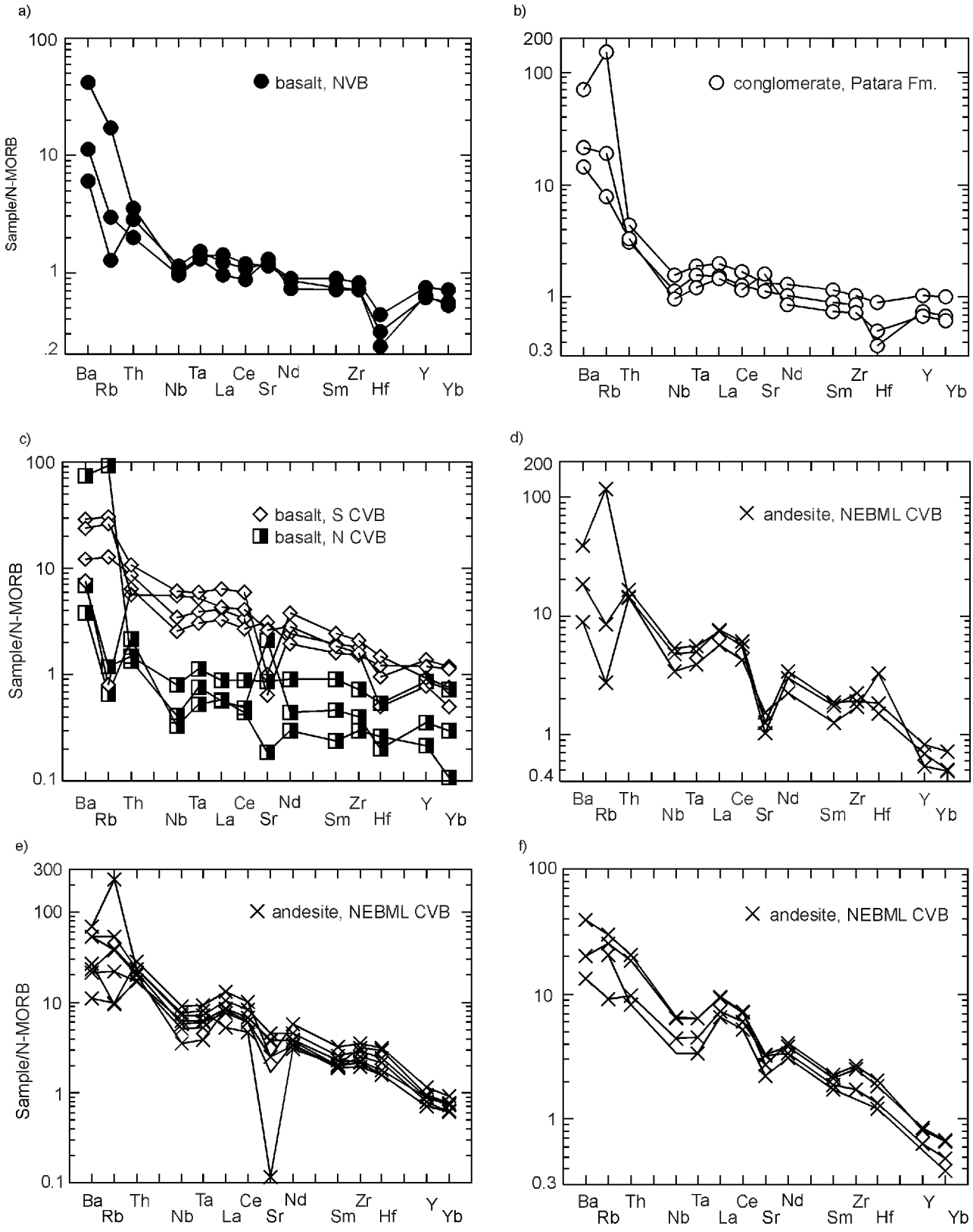

Figure 12. N–MORB normalized extended trace element plots ("spidergrams") for samples of Sioux Lookout orogenic belt lithologies and stratigraphic units; d–h are for samples from the Northeast Bay of Minnitaki Lake (NEBML) area: **a**) Northern Volcanic belt basalt; **b**) Patara Formation basalt–clast conglomerate; **c**) north and south Central Volcanic belt basalt (note distinct north versus south sample groups); **d**) eastern (lower) andesitic strata (samples J–53, –54, –102); **e**) central (middle) andesitic strata (samples J–67, –68, –77 to –81); **f**) western (upper) andestic strata (samples J–29, –30, –31, B–56);

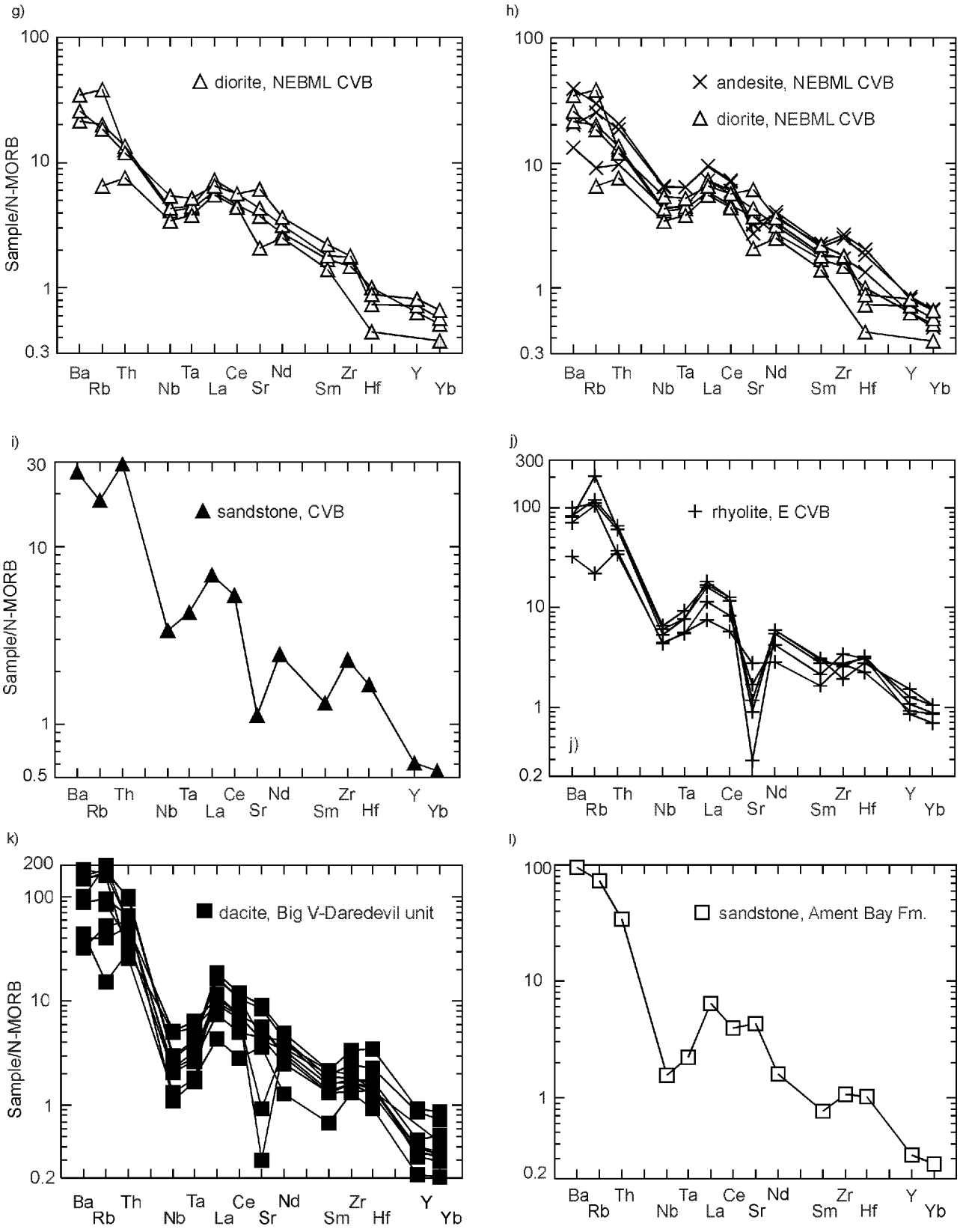

Figure 12. *Continued.* **g)** dioritic rocks; **h)** western (upper) andesitic strata (samples J–29 to –31) and dioritic rocks (samples J–60 to –63; shows overlap of the two sample groups within a narrow compositional range); **i)** a Central Volcanic belt sandstone (sample J–92); **j)** eastern Central Volcanic belt rhyolites (Superior Junction area samples); **k)** Big–Vermilion–Daredevil unit and Daredevil Formation intermediate– felsic volcaniclastic rocks; **l)** Ament Bay Formation sandstone (sample J–6);

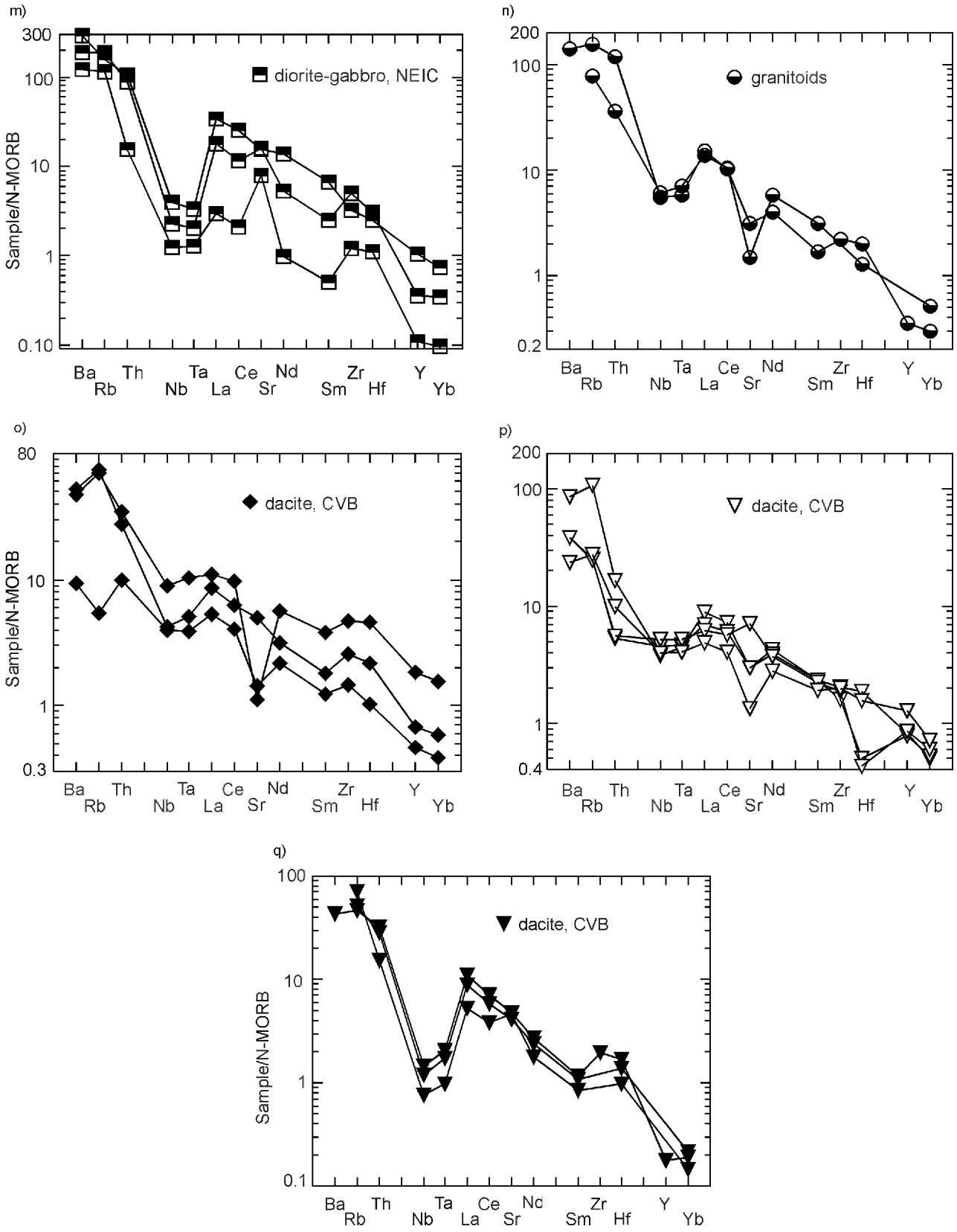

Figure 12. *Continued.* **m**) Northeast Intrusive Complex (NEIC) diorite–gabbro; **n**) granitoids; **o, p, q**) three Central Volcanic belt sample groups.

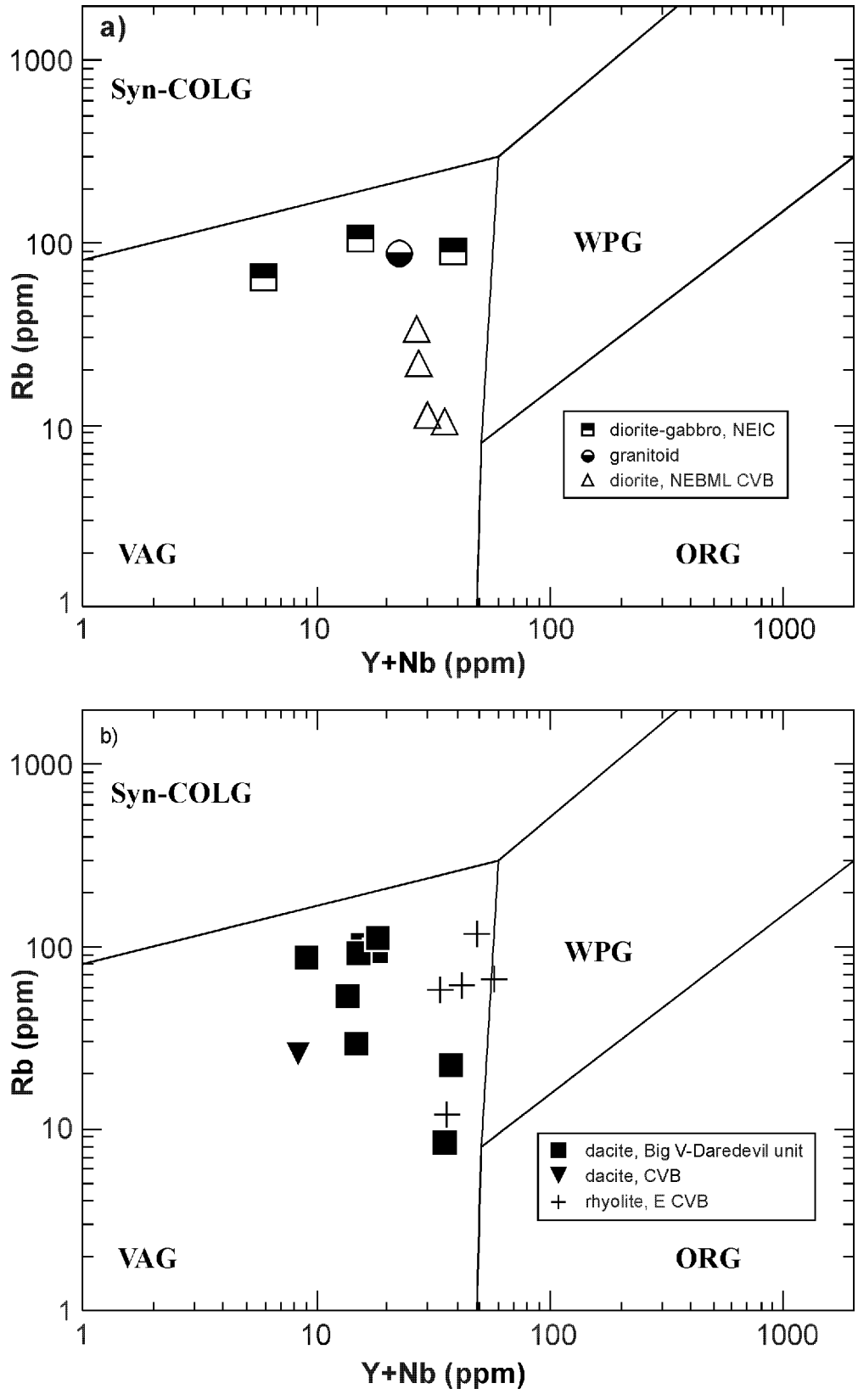

Figure 13. Rb versus Y+Nb discrimination diagram (*after* Pearce et al. 1984a) for: **a**) Sioux Lookout orogenic belt intrusive rocks; **b**) selected Sioux Lookout orogenic belt intermediate–felsic volcanic rocks. VAG, volcanic arc granite; syn–COLG, syn–collisional granite; WPG, within plate granite; ORG, ocean ridge granite. The VAG field is equivalent to the "I–type" granite field (Christiansen and Keith 1996, Figure 7A).

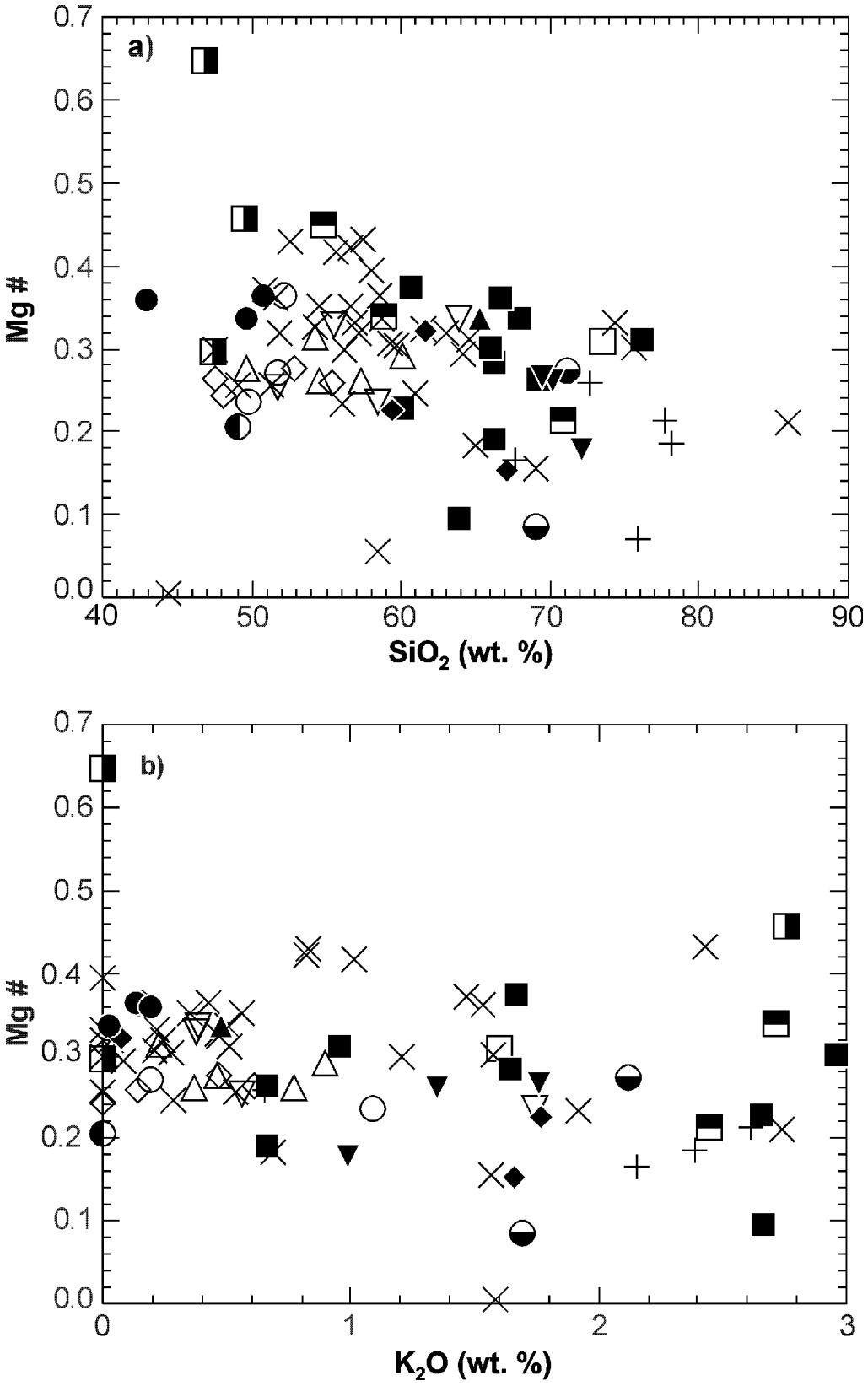

Figure 14. For all Sioux Lookout orogenic belt samples, plots of Mg# versus: **a**) SiO_2; **b**) K_2O; **c**) La/Sm. Interpreted Stages 1 to 4 (labelled) and NEIC rocks form distinct fields.

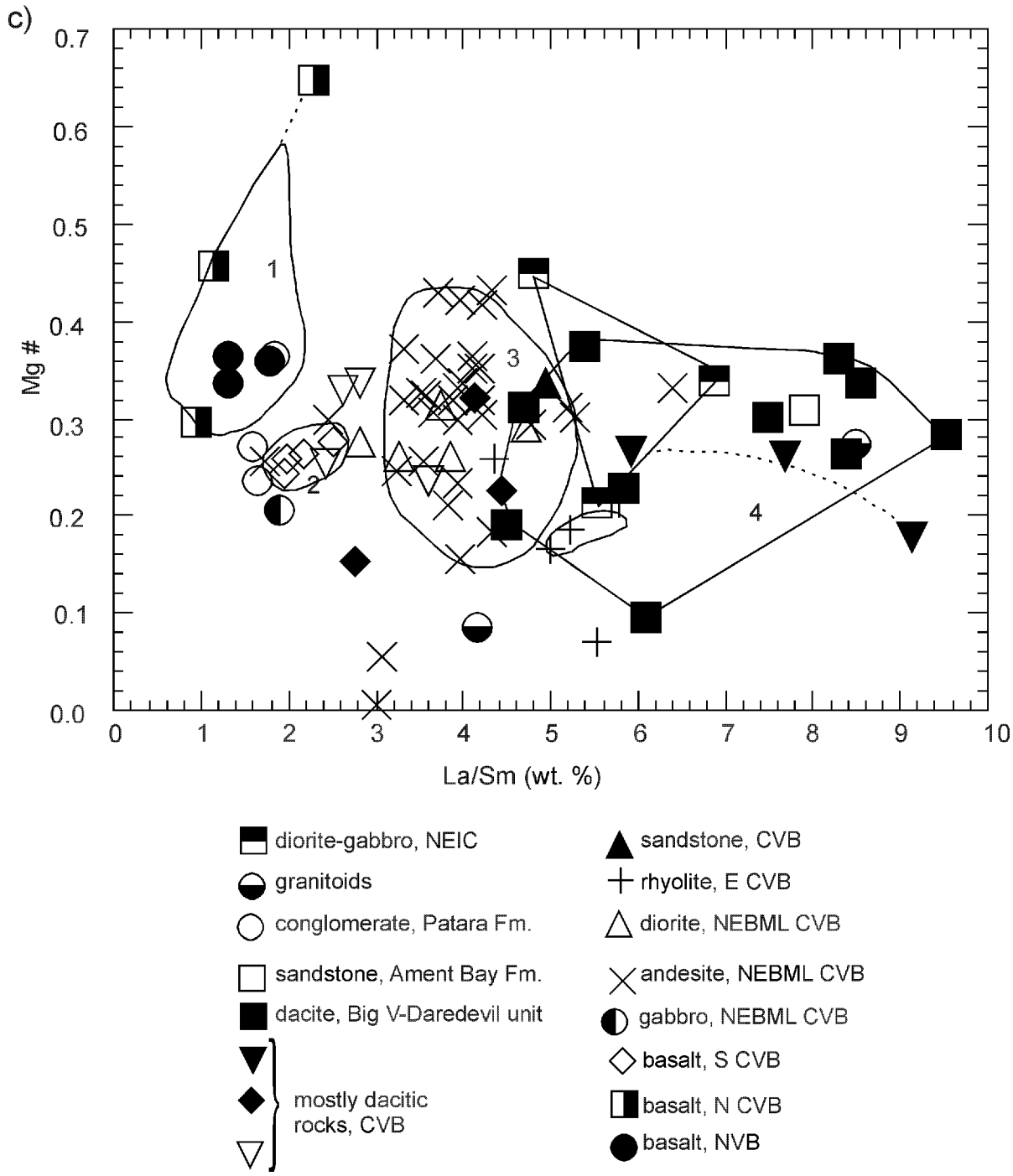

Figure 14. *Continued.*

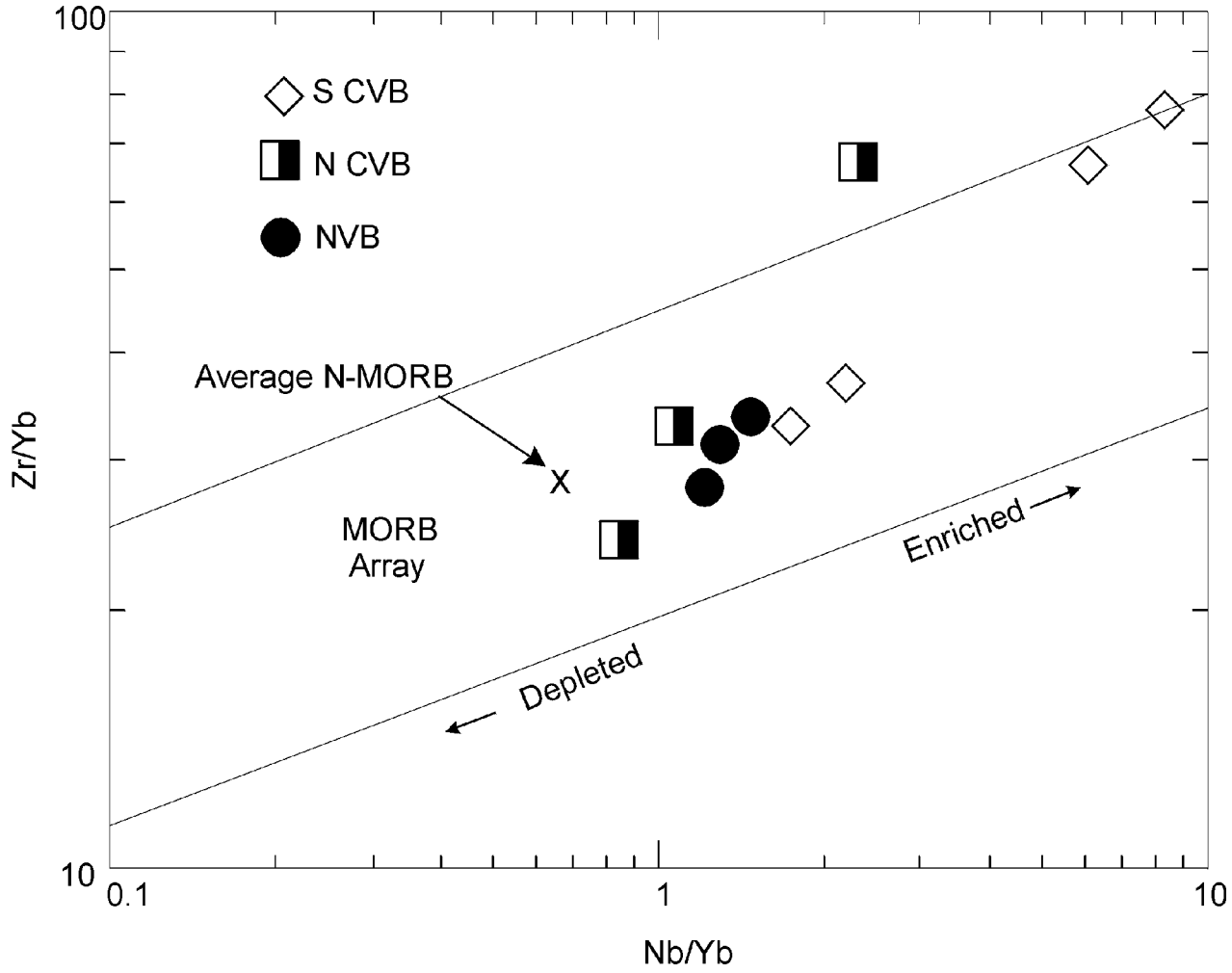

Figure 15. Zr/Yb versus Nb/Yb discrimination diagram (*after* Pearce and Peate 1995, Figure 2) for Sioux Lookout orogenic belt basalts.

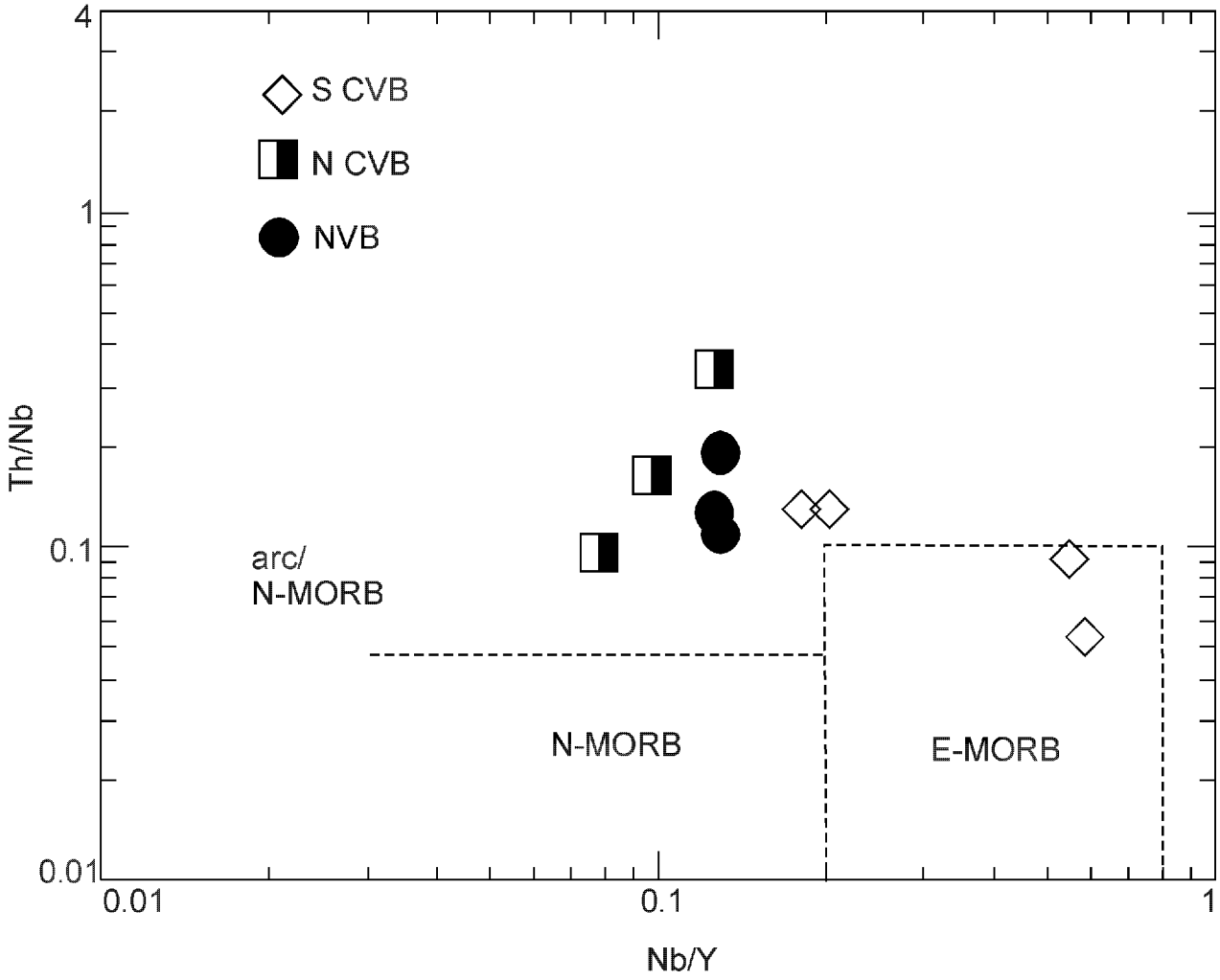

Figure 16. Th/Nb versus Nb/Y discrimination diagram (*after* Syme et al. 1996, Figure 16) for Sioux Lookout orogenic belt basalts. In some cases, samples plotting in the "arc/N–MORB" area may have been affected by crustal contamination (e.g., "attenuated continental settings" of Pearce 1996, p. 109).

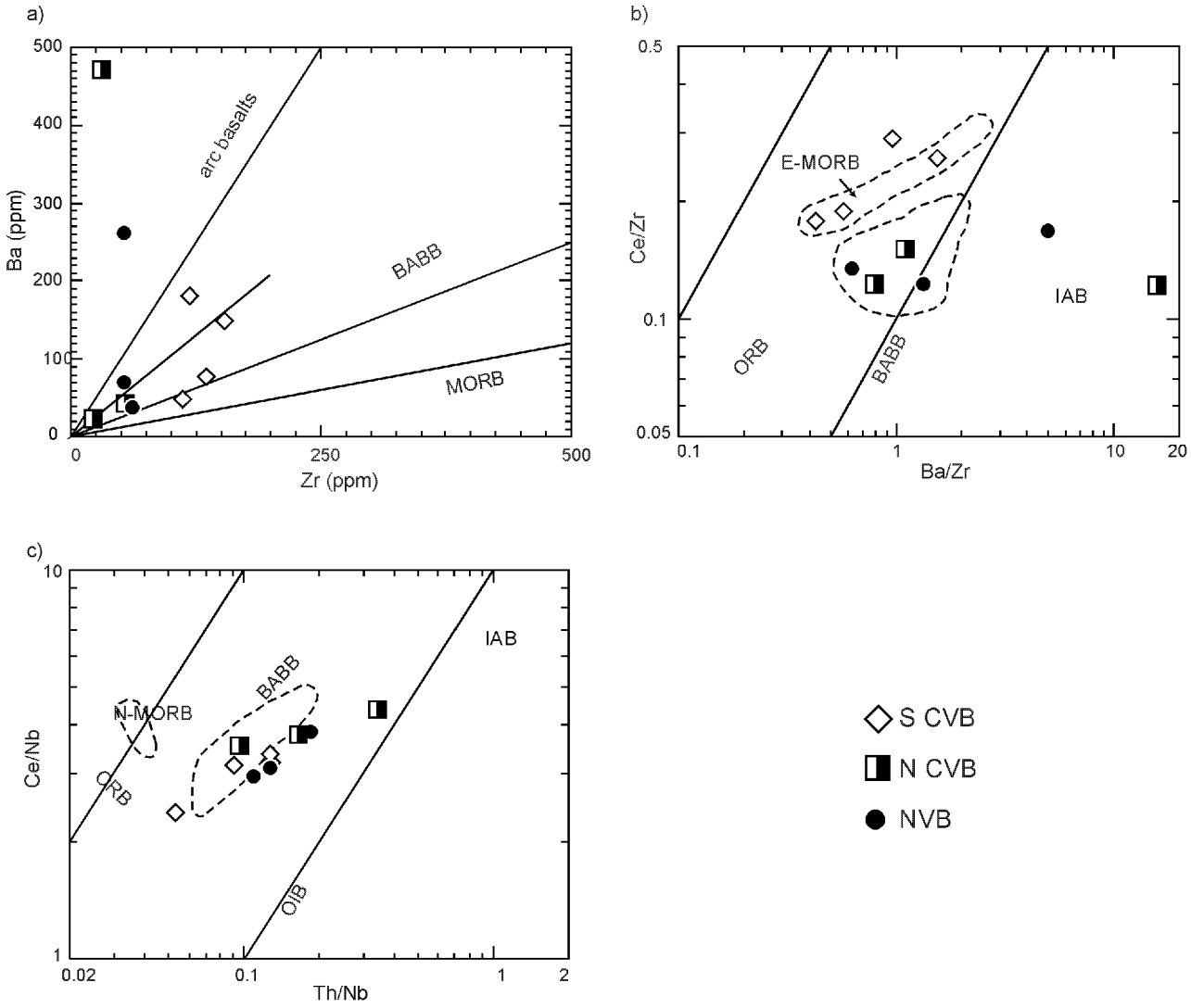

Figure 17. Discrimination diagrams (*after* Saunders and Tarney 1991, Figures 10.13, 10.15, 10.16) for Sioux Lookout orogenic belt basalts: **a**) Ba versus Zr; **b**) Ce/Zr versus Ba/Zr; **c**) Ce/Nb versus Th/Nb. BABB, back–arc basin basalts; ORB, ocean ridge basalt; IAB, island arc basalt; OIB, oceanic island basalt.

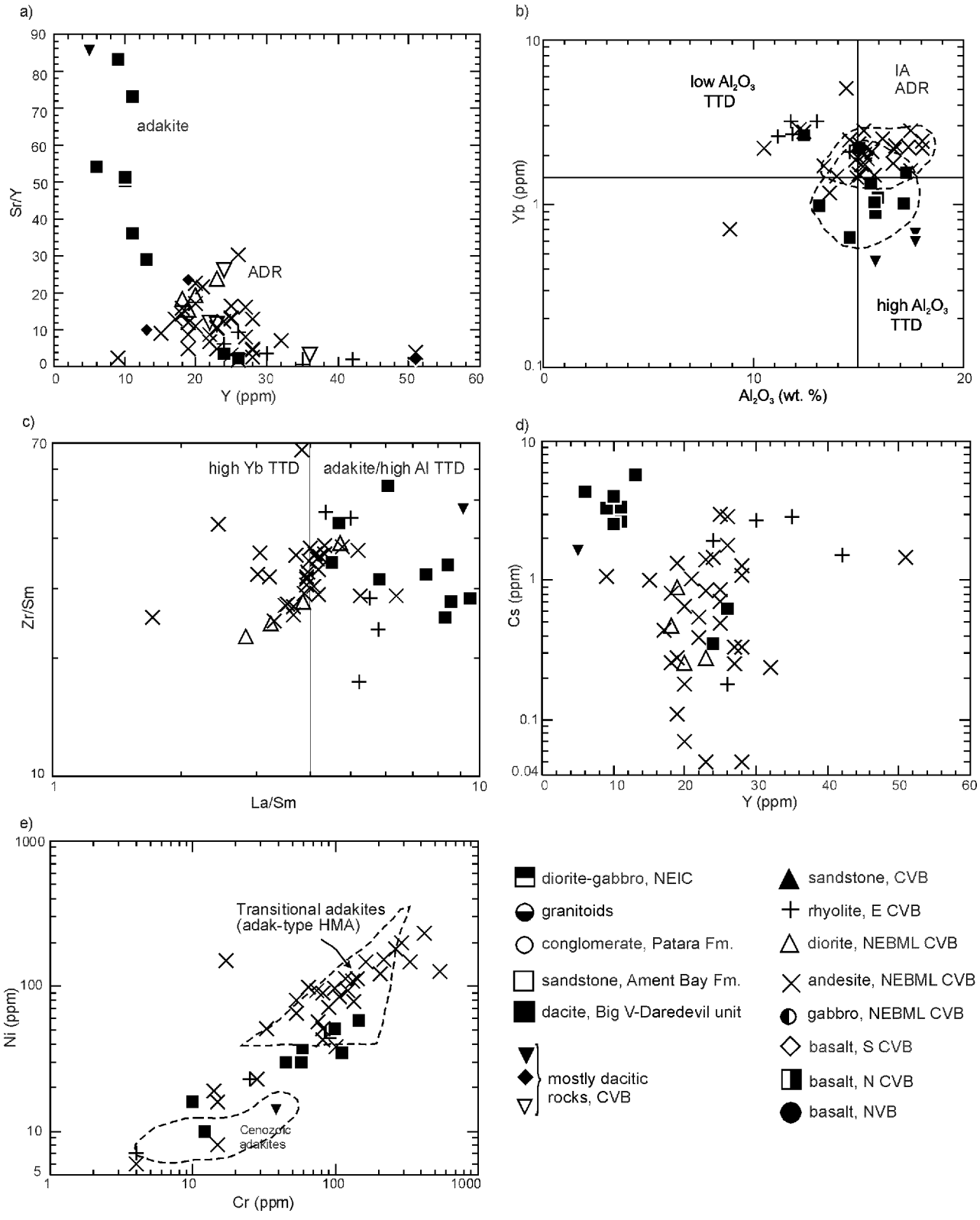

Figure 18. Adakite classification diagrams (*after* Drummond et al. 1996, Figures 2, 3, 5, 6, 8) for selected Sioux Lookout orogenic belt volcanic and volcaniclastic rocks: **a**) Sr/Y versus Y; **b**) Yb versus Al_2O_3; **c**) Zr/Sm versus La/Sm; **d**) Cs versus Y; **e**) Ni versus Cr. ADR = andesite–dacite–rhyolite, TTD = trondhjemite–tonalite–dacite, IA = island arc, HMA = high–magnesian andesite.

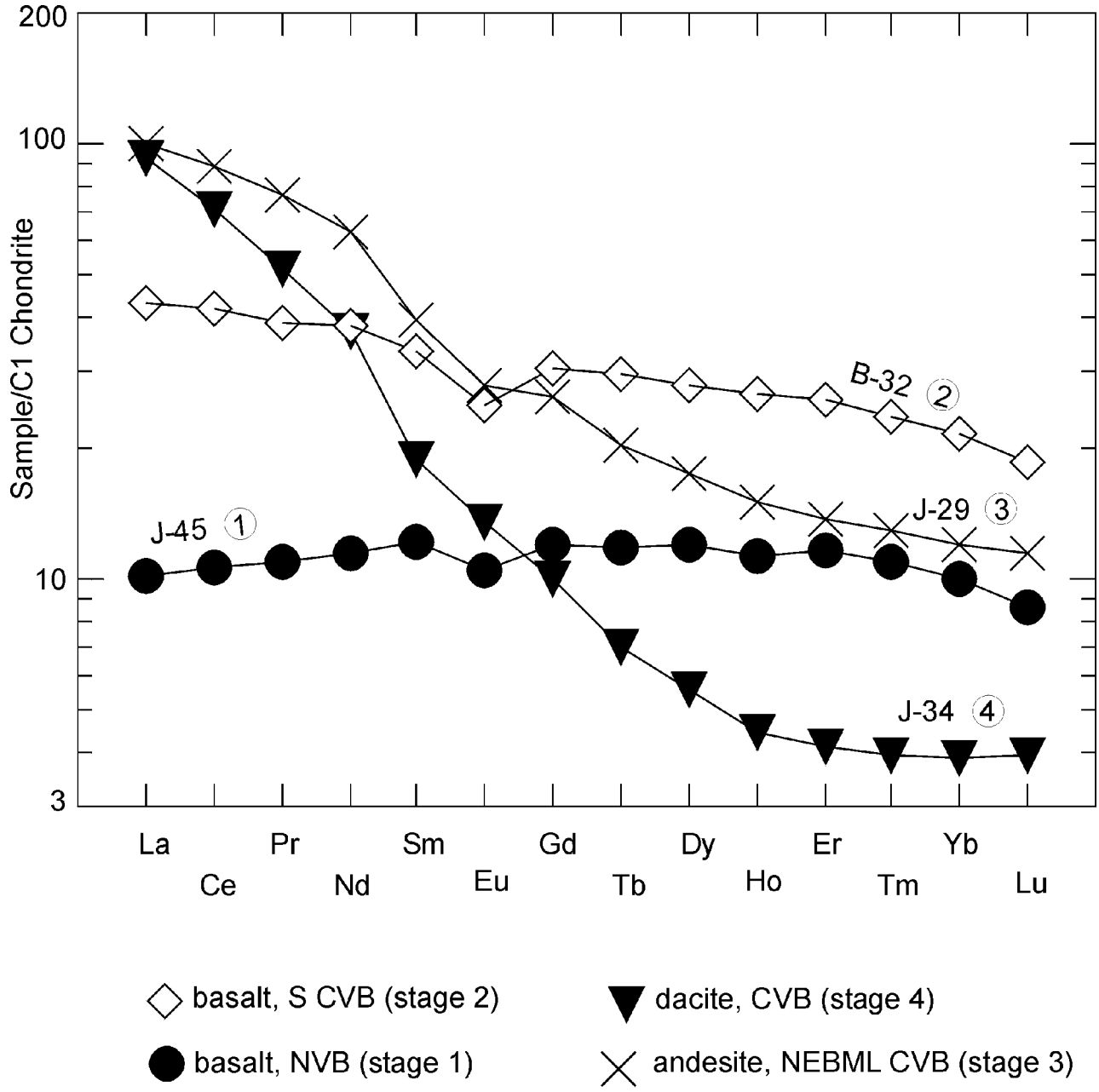

Figure 19. REE plots for representative samples of interpreted Stages 1 to 4 (stages circled). Note the increase in fractionation as expressed by the chondrite–normalized La/Yb ratio, over time, from Stage 1 to 4.

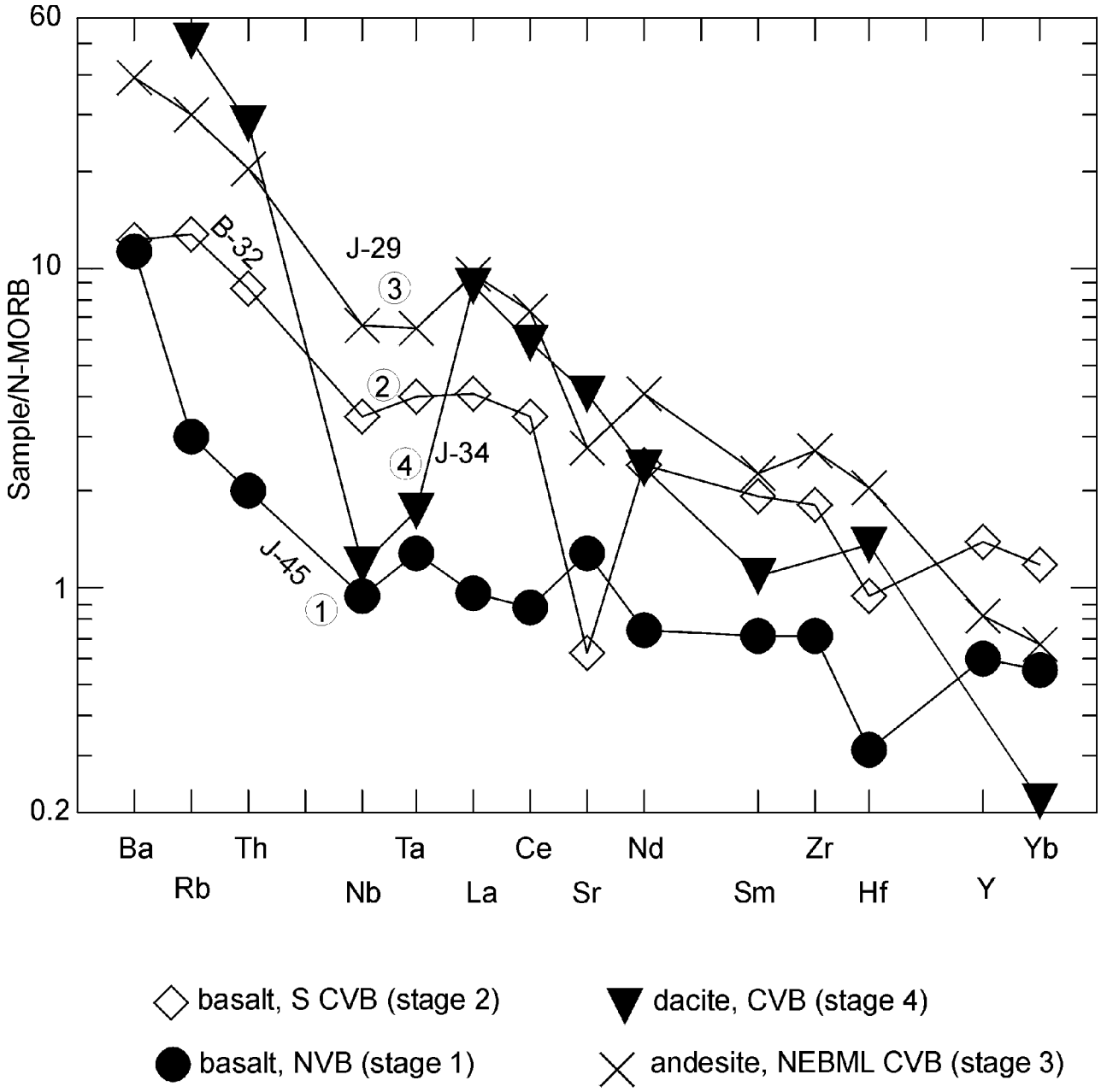

Figure 20. Extended trace element plots for representative samples of interpreted Stages 1 to 4 (stages circled). Note the increasingly large and well defined negative Nb anaomaly (a subduction signature) over time, from Stage 1 to 4.

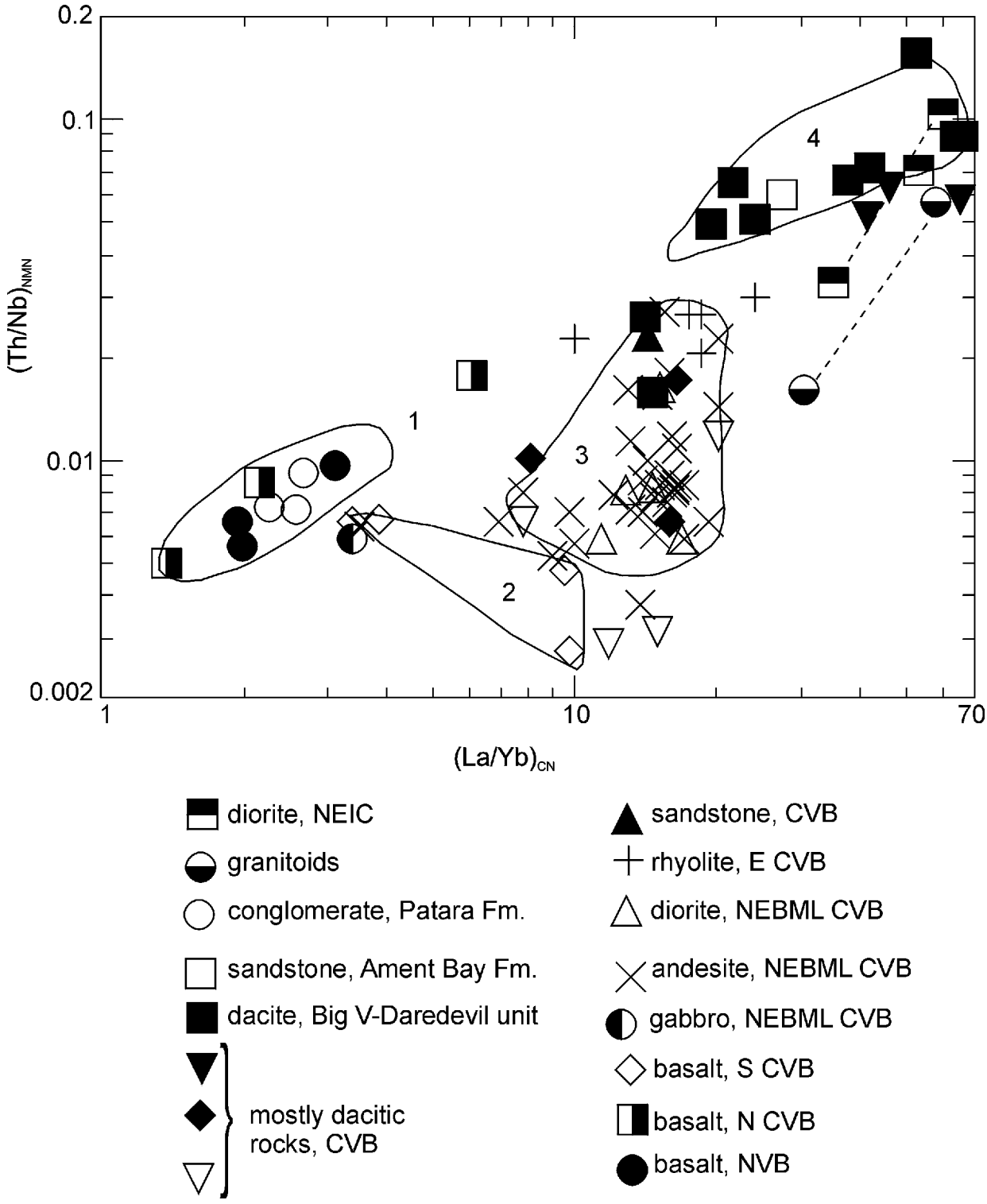

Figure 21. Plot of N–MORB normalized Th/Nb (a subduction signature) versus chondrite–normalized La/Yb (a fractionation measure) for all Sioux Lookout orogenic belt samples. Different lithologies and stratigraphic units define discrete sample groups, including the interpreted volcanic and tectonic Stages 1 to 4. The position of the fields for stages 2, 3 and 4 is interpreted to reflect progressive arc development (juvenile arc Stage 2, rifted arc Stage 3, mature arc Stage 4) during the ca. 2735–2712 (or –2704) Ma period.

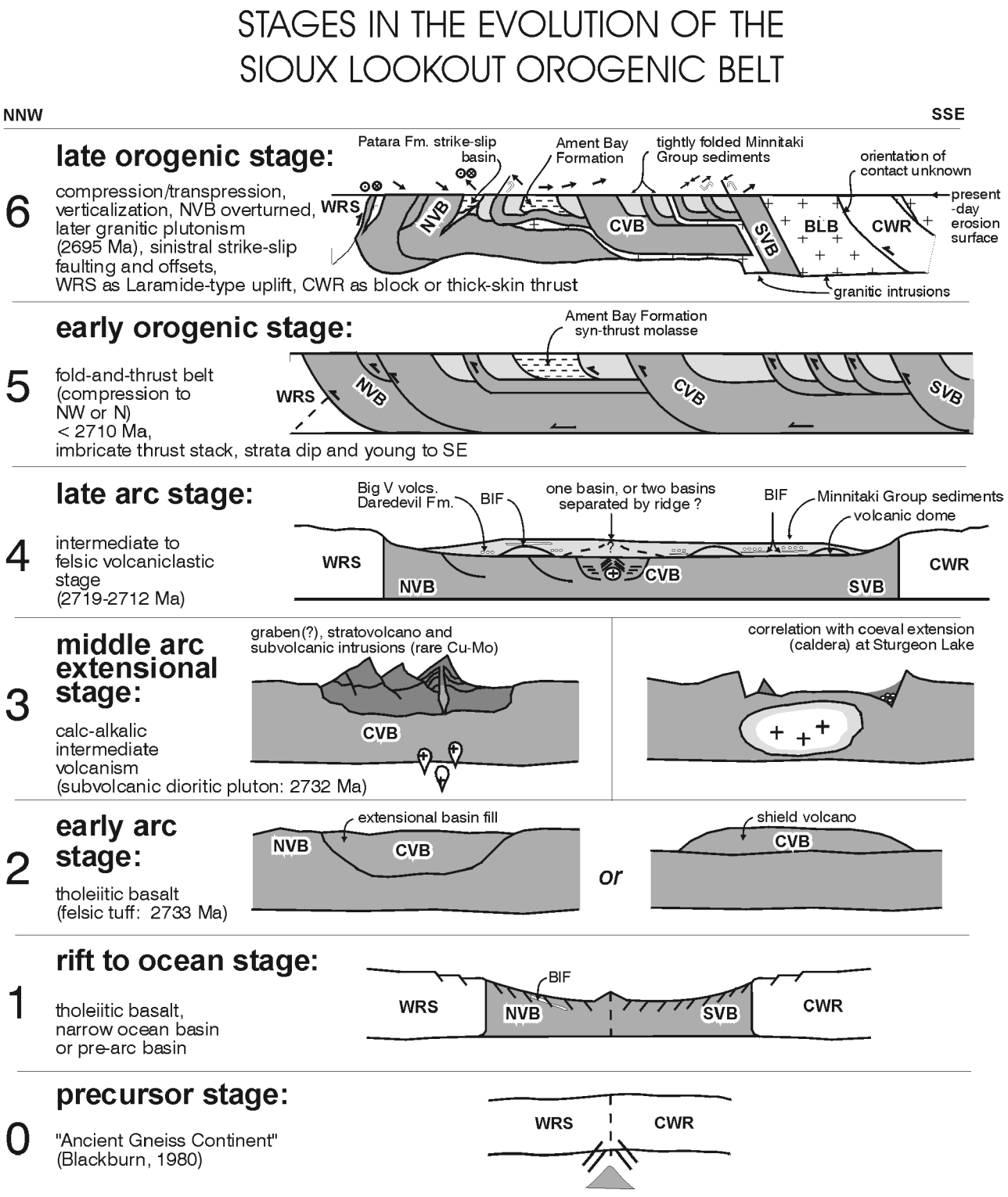

Figure 22a. Cross–sectional cartoon views of the interpreted evolutionary stages of the Sioux Lookout orogenic ("greenstone") belt. See text for qualifying statements and detailed explanations.

STAGES OF MINERALIZATION

6, late orogenic stage: late quartz or quartz-carbonate veins with erratic gold values; most Au occurrences are within the Neepawa (CVB) and Minnitaki groups and are distributed along two strike-parallel ENE-trending lineaments (this fact previously unrecognized); to the SW, the former Goldlund gold mine and the current Teck-Corona Thunder Lake gold prospect (in Zealand Twp.) are located along these two lineaments

5, early orogenic stage: quartz and/or carbonate veins

4, late arc stage: iron formation units within the sedimentary Minnitaki Group and the Big Vermilion-Daredevil volcanic unit (minor chemical sediments in volcaniclastic sediments): magnetite, pyrite and chert exhalites, and related synvolcanic hydrothermal alteration (sub-exhalite) in the underlying upper Minnitaki Group (including volcanic dome facies) and horizons of the Big Vermilion-Daredevil unit

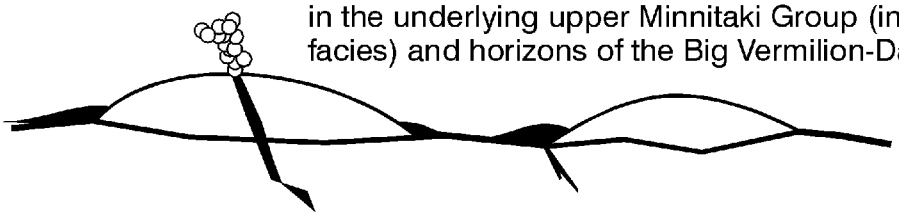

3, middle arc extensional stage: within the northeast CVB, merely incipient porphyry copper-type mineralization (rare Cu-Mo in and marginal to an intermediate subvolcanic intrusion) and no evidence of epithermal mineralization in a genetically linked andesitic stratovolcano succession

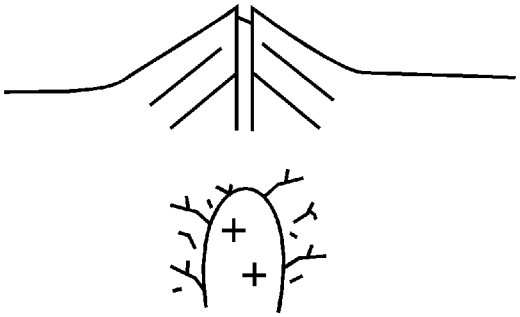

2, early arc stage: minor exhalite layers

1, rift to ocean stage: iron formation units within the basaltic NVB: magnetite, pyrite and chert exhalites from synvolcanic hydrothermal flow

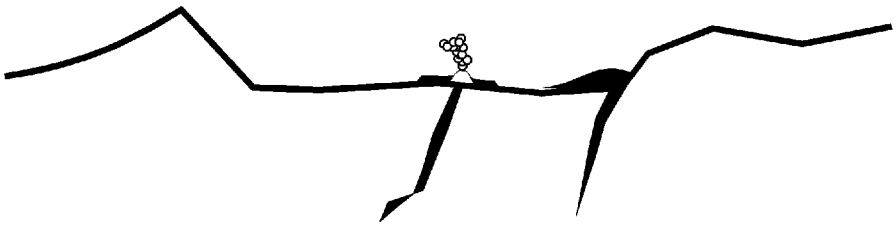

Figure 22b. Corresponding stages of mineralization.

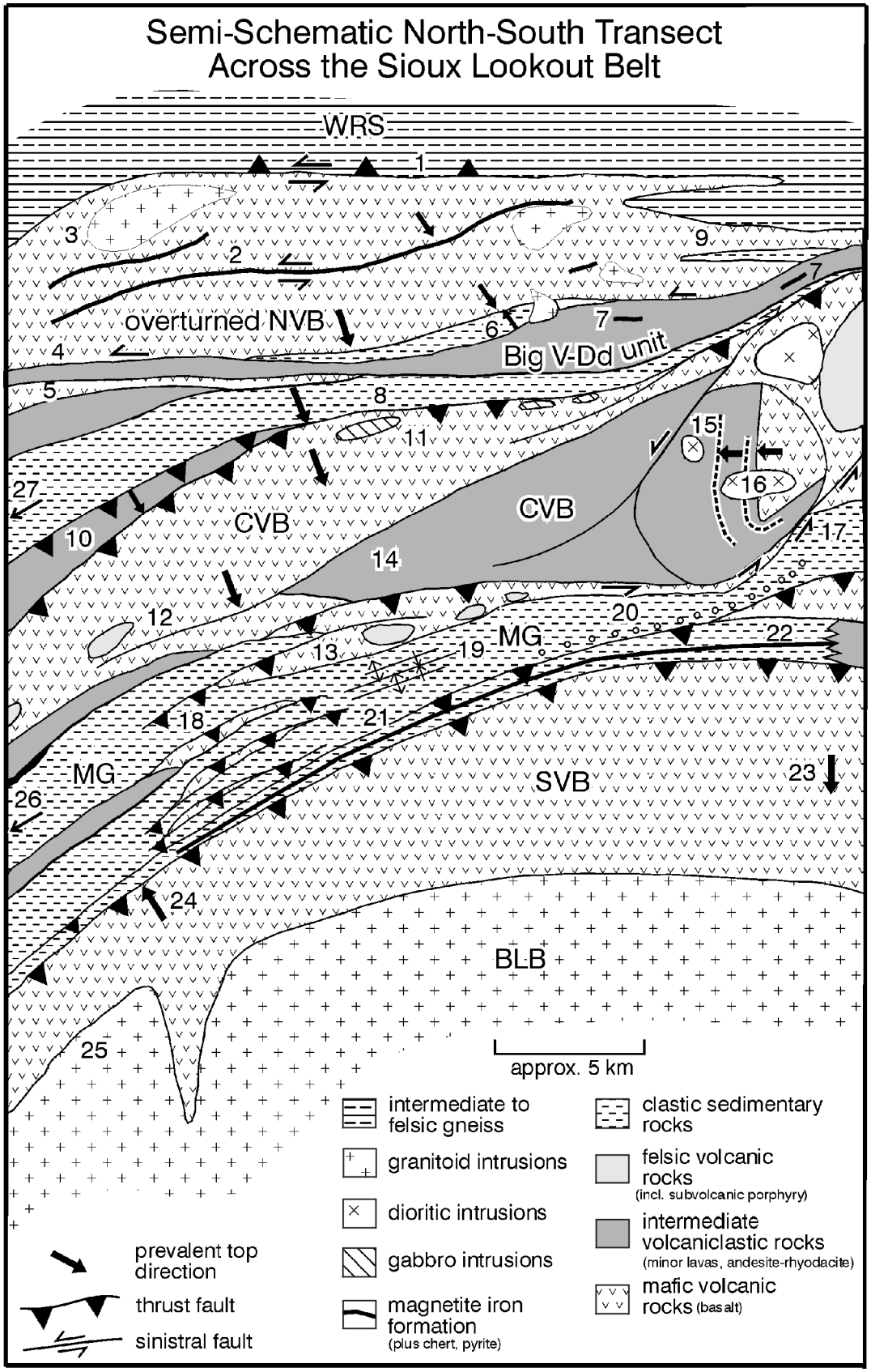

Figure 23. Semi–schematic map of the Sioux Lookout orogenic belt. Discussions of sites 1 to 27 are given in the text. Abbreviations: WRS, Winnipeg River subprovince; NVB, Northern Volcanic belt; Big V–Dd, Big Vermilion–Daredevil unit; CVB, Central Volcanic belt; MG, Minnitaki Group; SVB, Southern Volcanic belt, BLB, Basket Lake batholith.

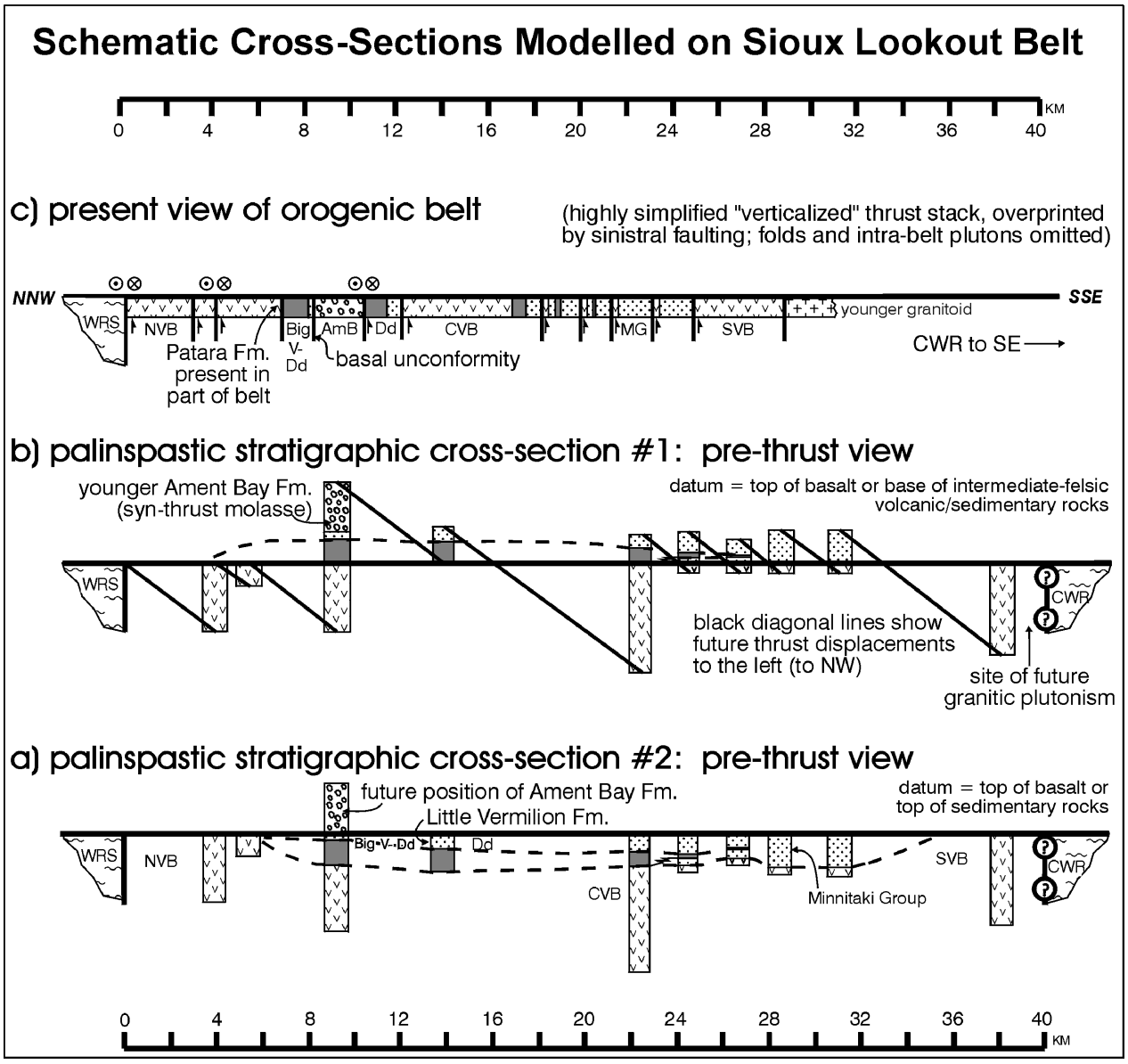

Figure 24. Schematic cross–sections of the Sioux Lookout orogenic belt, including modelled (hypothetical) palinspastic restoration of thrusts.

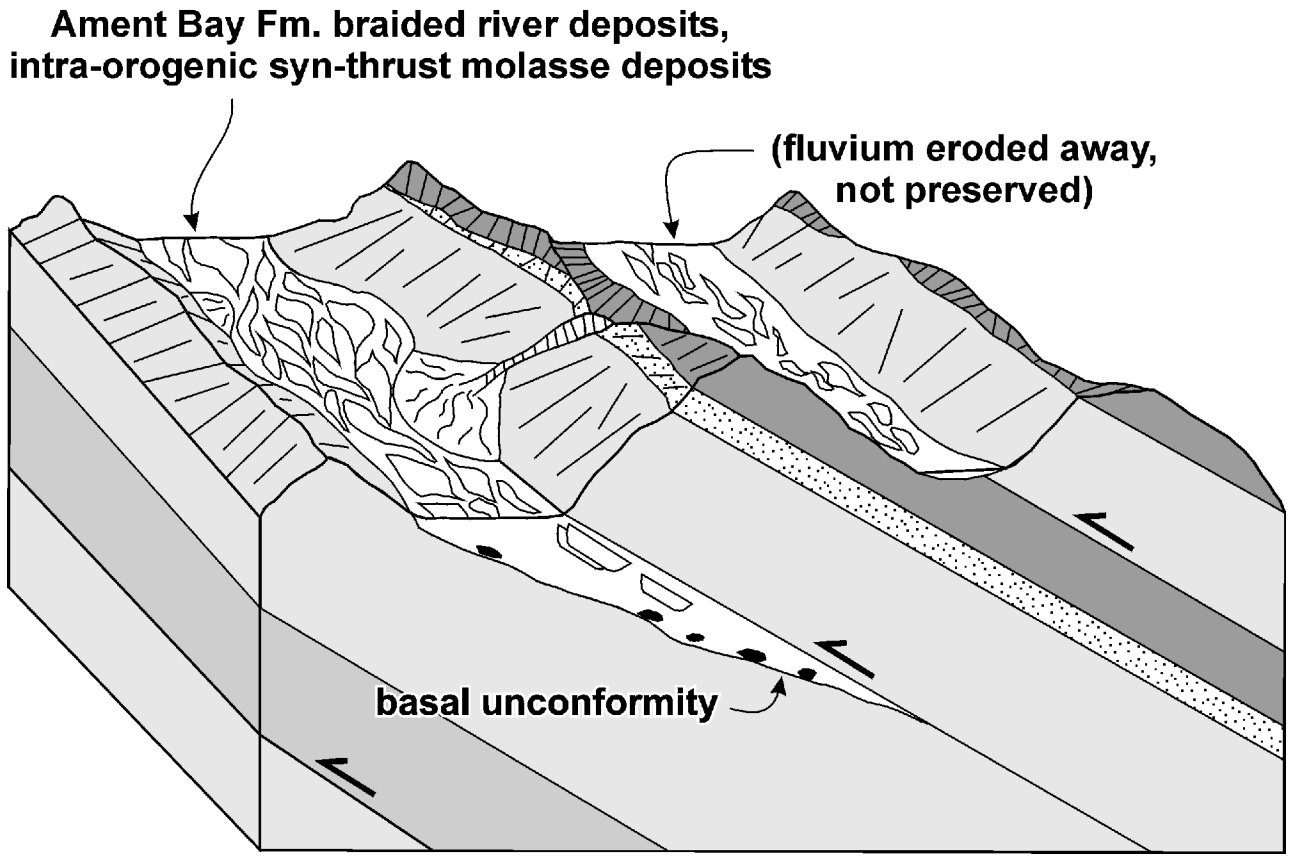

Figure 25. Stage 5 sedimentation and tectonics: syn–thrust molasse, piggyback basin paleogeographic scenario.

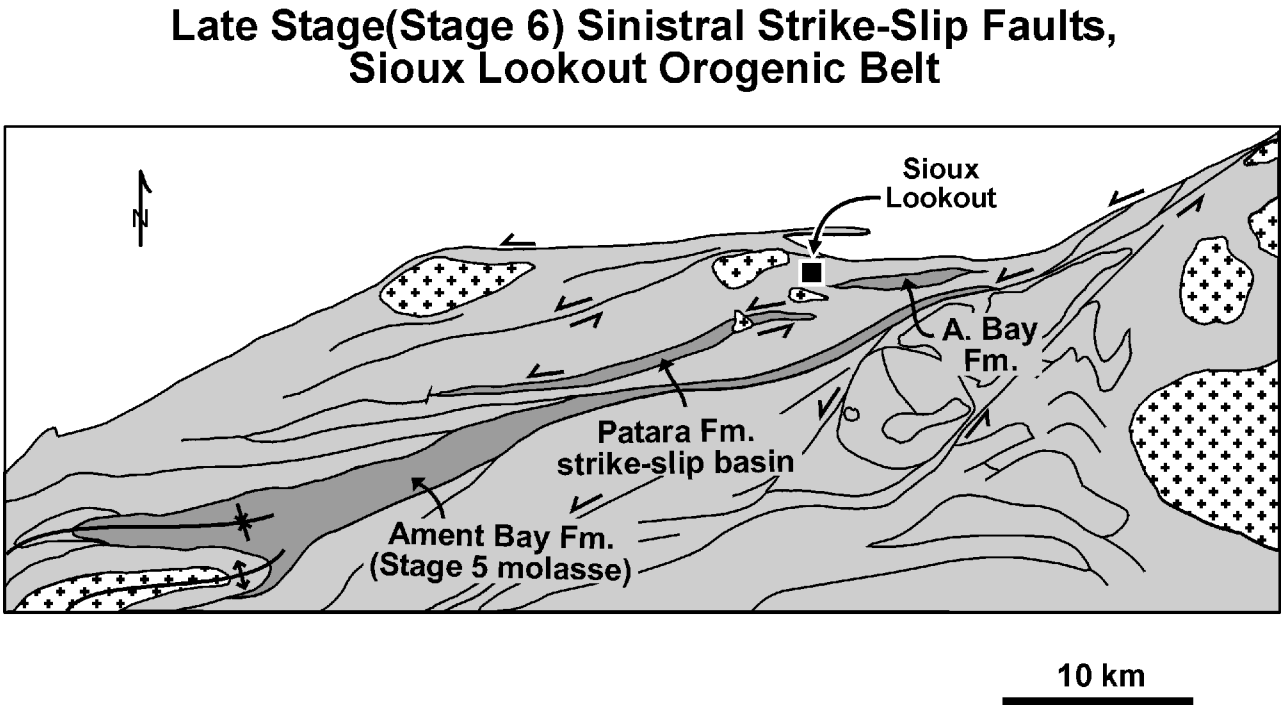

Figure 26. Stage 6 Sioux Lookout orogenic belt map: strike–slip duplexes, synorogenic and intra–orogenic sedimentary basins, and granitic intrusions.

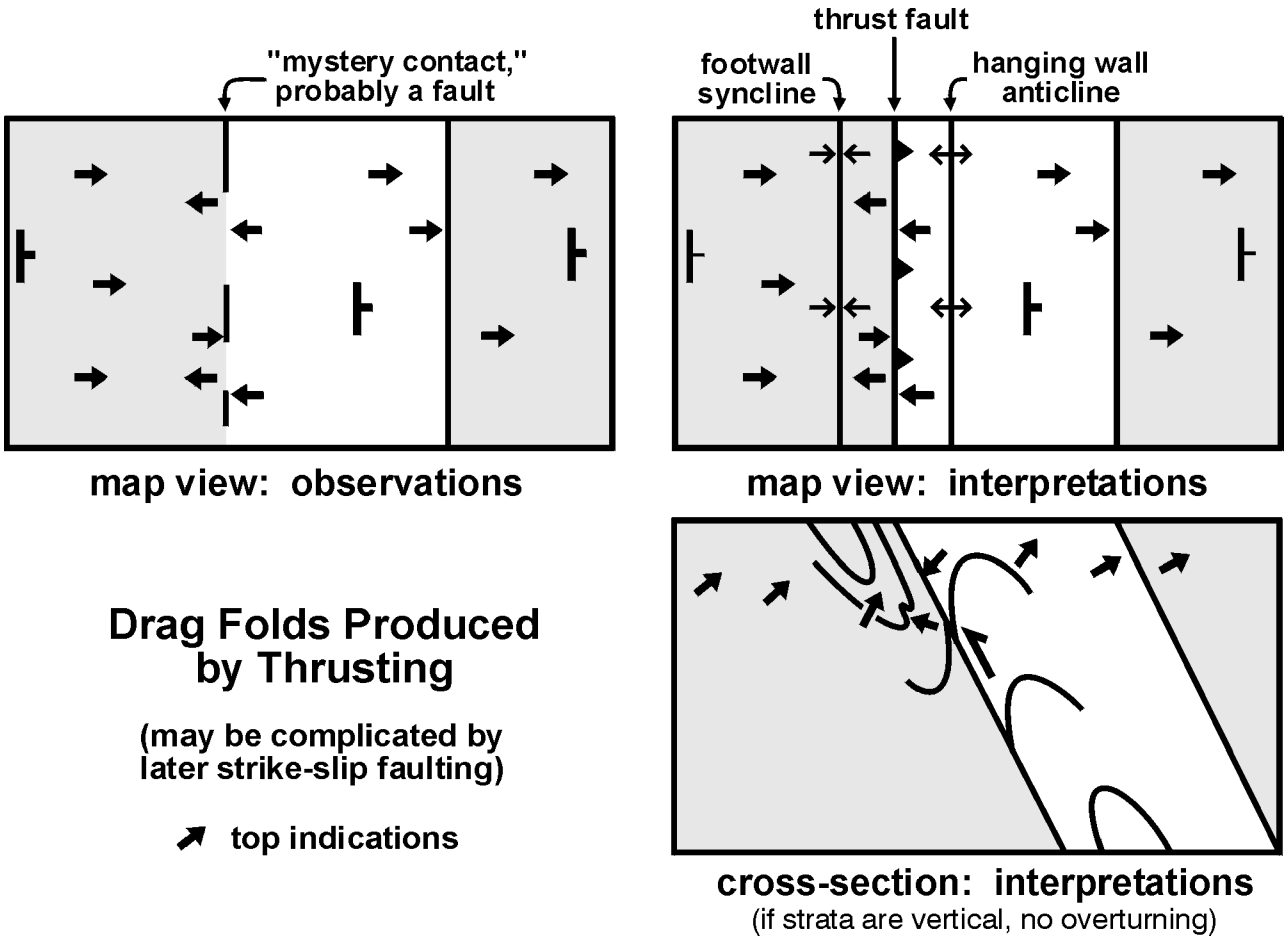

Figure 27. Cartoon scenario for drag folds produced by thrusting.

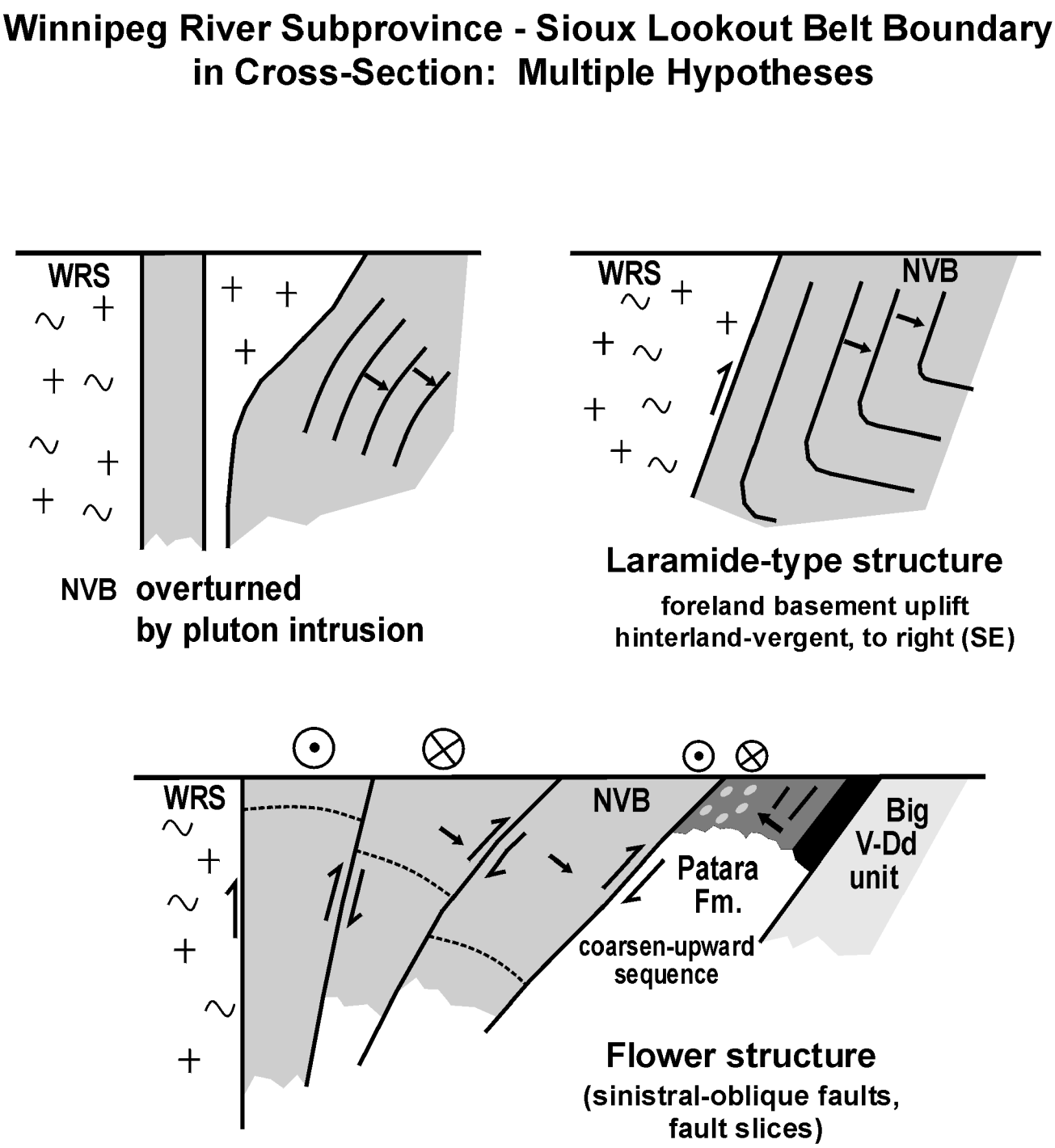

Figure 28. Cartoon views of potential Winnepeg River subprovince–Sioux Lookout orogenic belt boundary structures (multiple hypotheses).

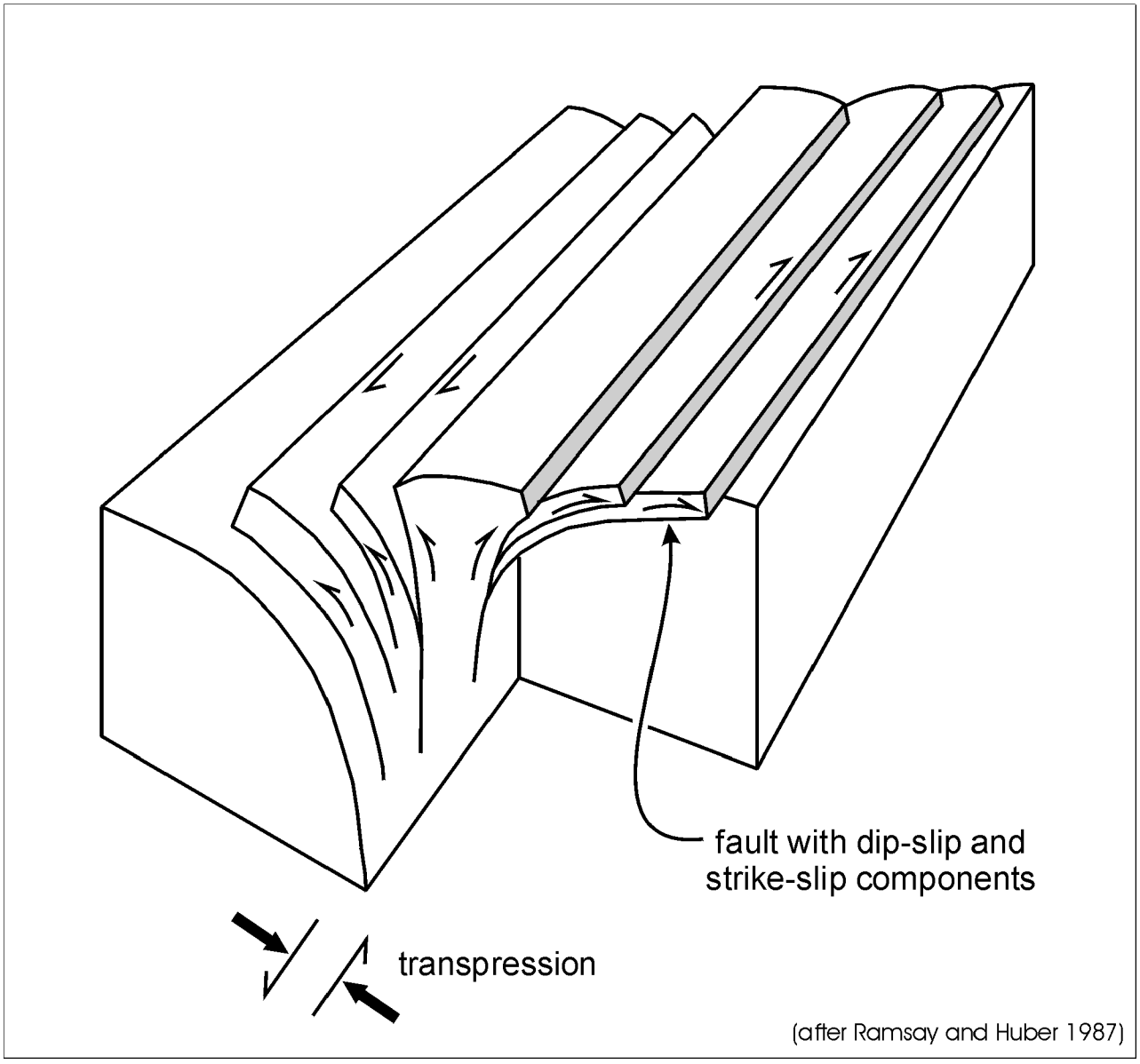

Figure 29. Sinistral–sense positive flower (palm tree) structure.

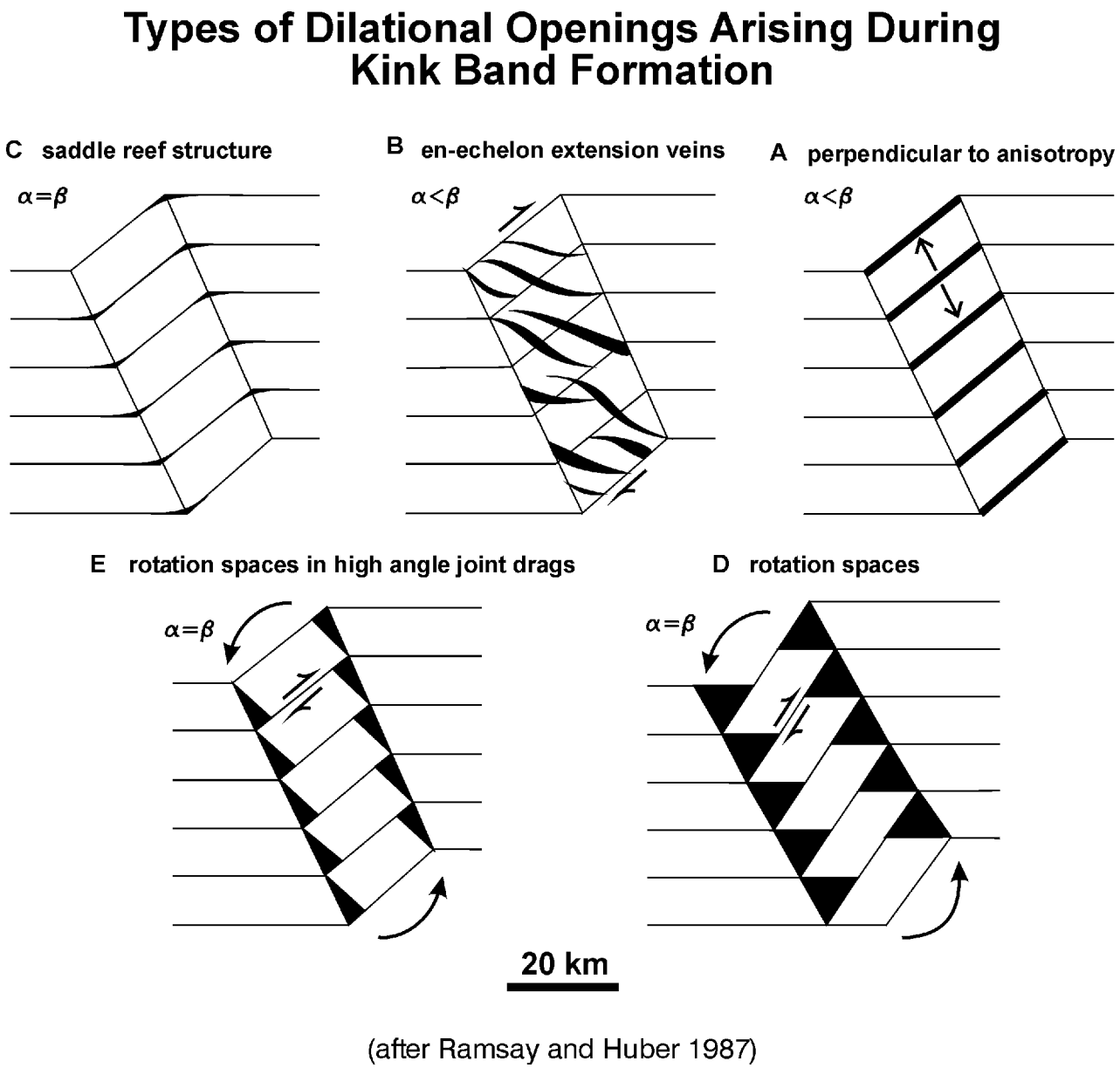

Figure 30. Theory of small–scale kink formation (*after* Ramsay and Huber 1987, Figure 20.36) applied to "mega–kinks" (note scale) with dilational openings as proposed sites for pluton intrusion.

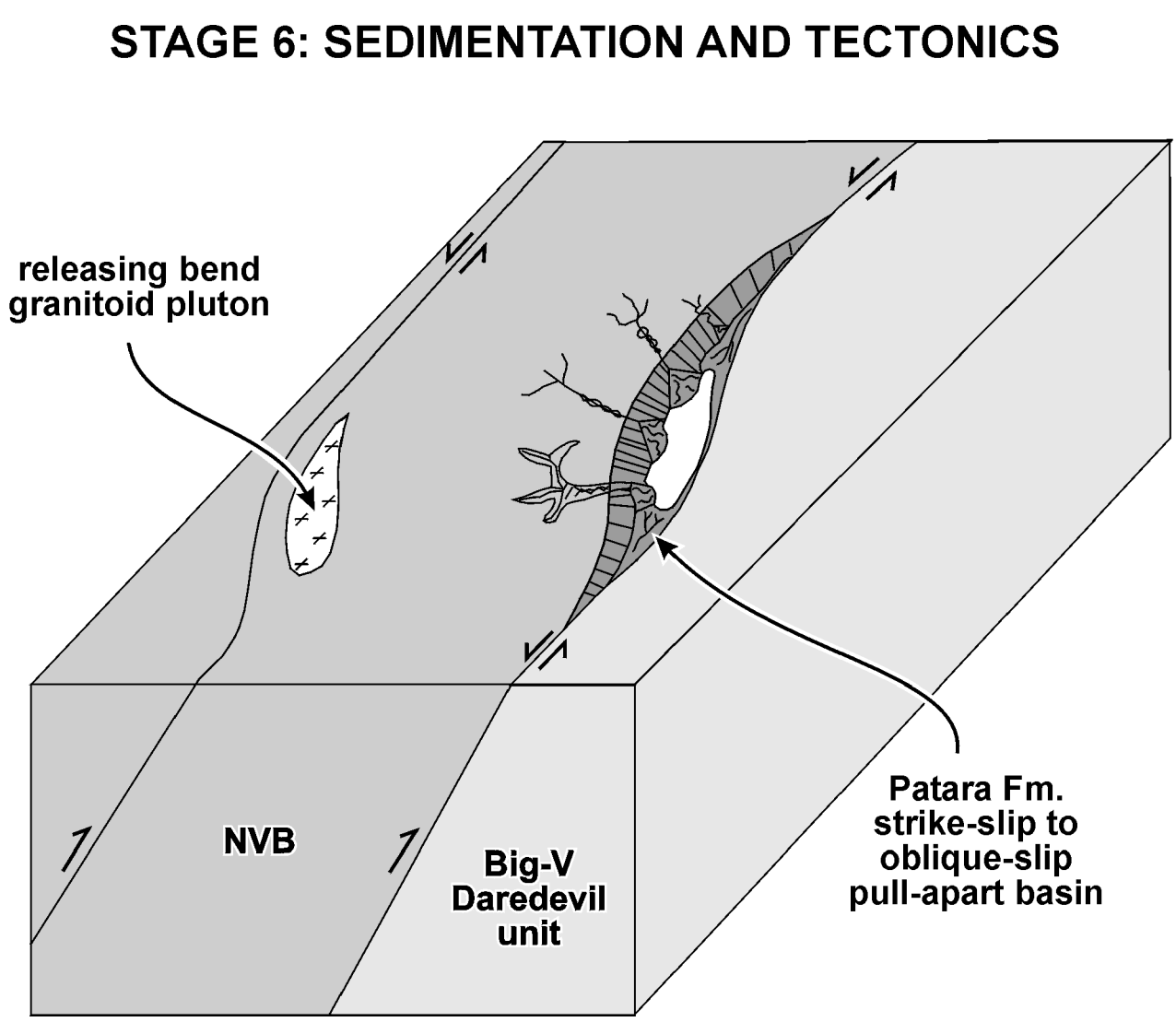

Figure 31. Stage 6 sedimentation and transtensional tectonics: pull–apart basin (Patara Formation) and releasing bend pluton.

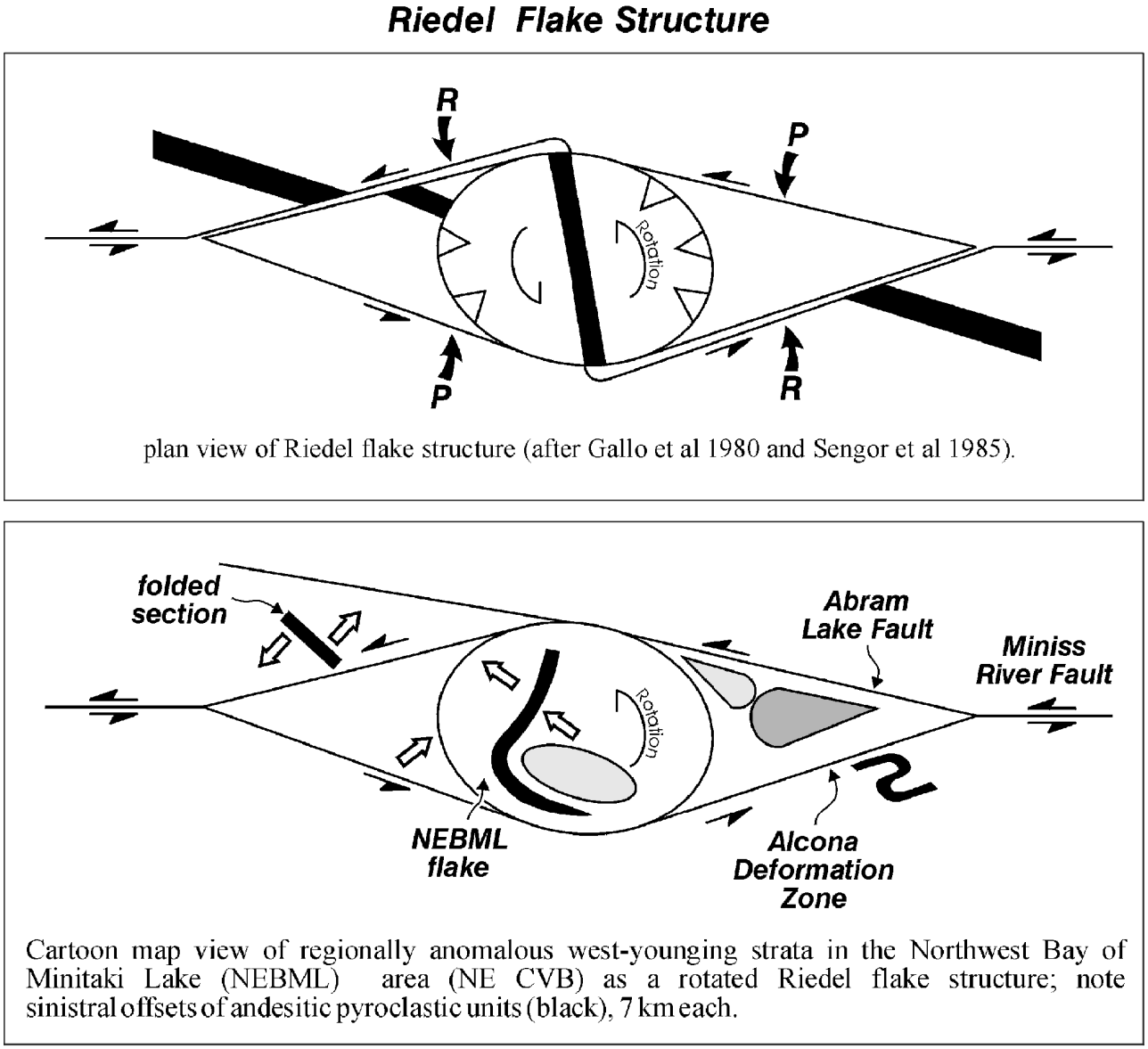

Figure 32. Riedel flake structure; theory in upper panel, application to Northeast Bay of Minnitaki Lake (NEBML) area in lower panel.

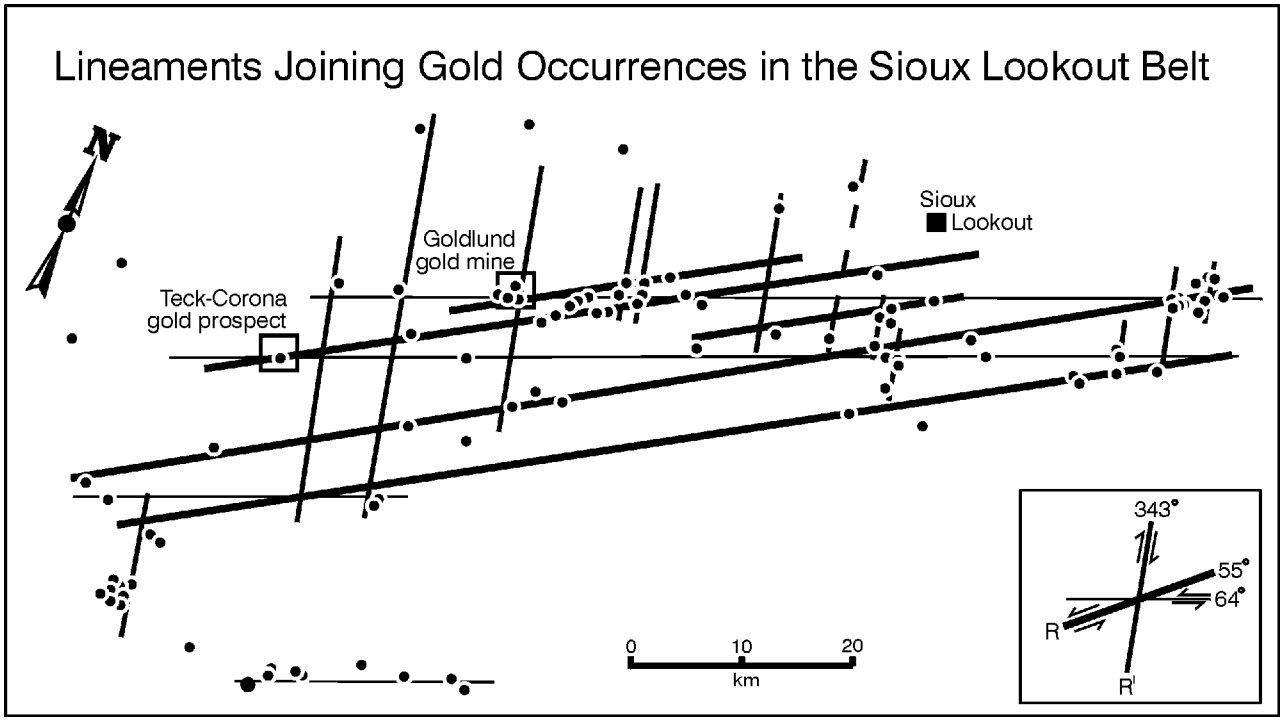

Figure 33. The proposed lineament pattern joining gold occurrences (black dots) in the Sioux Lookout orogenic belt (and equivalent rocks to the southwest) resembles a large–scale conjugate Riedel shear set (theory shown in inset; major stratigraphic and fault surfaces trend at about 64°).

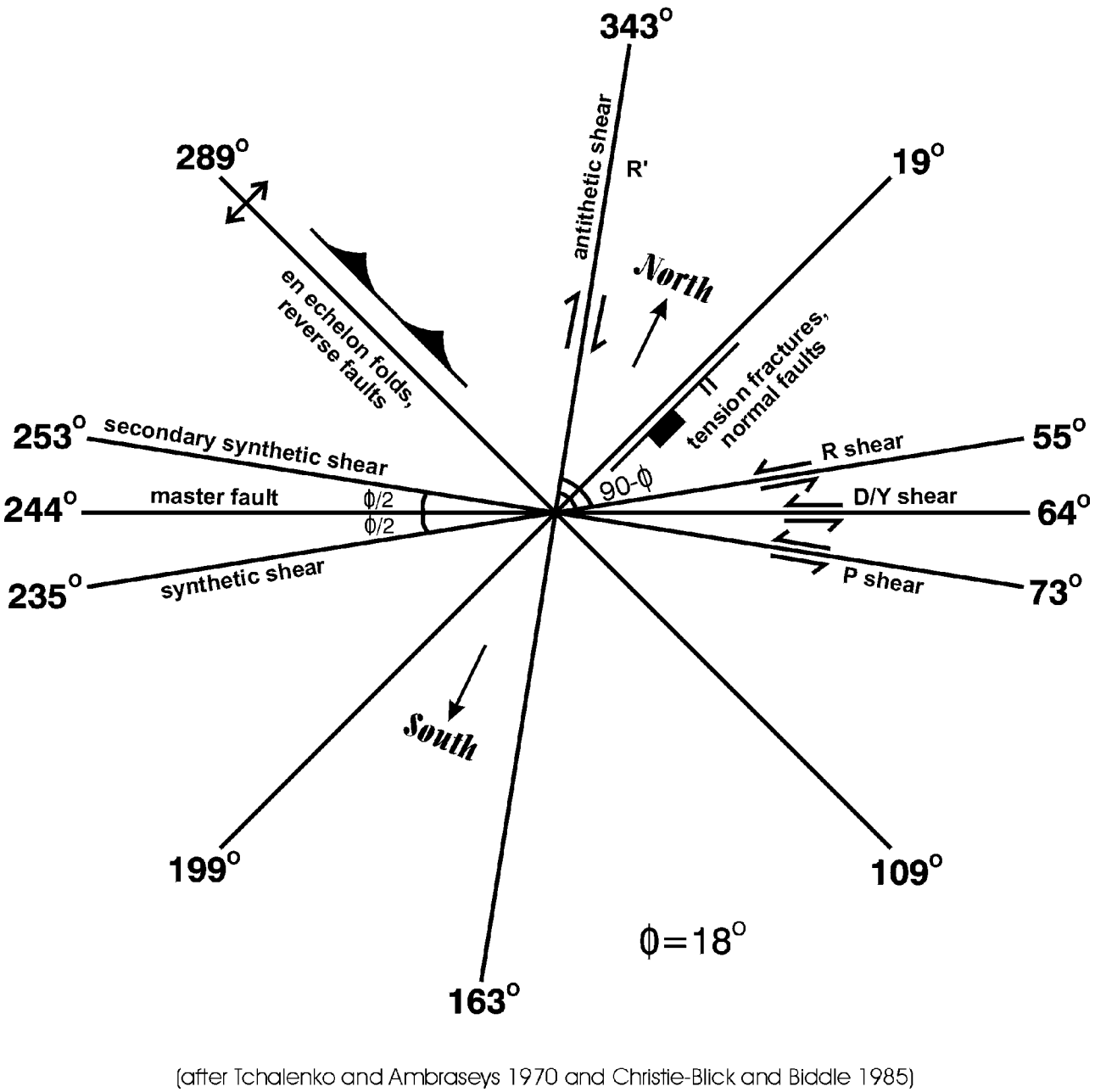

Figure 34. Theoretical shear fracture patterns, with azimuth orientations appropriate to the Sioux Lookout orogenic belt.

Table 1. Major and selected trace element data for Sioux Lookout orogenic belt samples.

Sample	**94JRD–0002**	**94JRD–0004**	**94JRD–0006**	**94JRD–0008**	**94JRD–0009**	**94JRD–0010**	**94JRD–0013**	**94JRD–0014A**
Rock Type	**Mafic cng**	**Mafic cng**	**Sandstone**	**Sandstone**	**Felsic tuff**	**Lapilli–tuff**	**Lapillistone**	**Tuff**
(field I.D.)								
SiO_2 %	48.47	46.14	70.68	62.84	66.34	65.40	62.84	64.44
Al_2O_3	15.02	13.84	11.95	15.13	15.46	15.43	16.35	14.64
MnO	0.41	0.28	0.06	0.10	0.05	0.06	0.08	0.14
MgO	4.77	4.71	1.92	2.41	1.69	2.14	2.38	1.62
CaO	8.88	8.15	2.17	2.52	3.14	3.51	1.85	1.99
Na_2O	2.11	2.19	3.25	3.67	3.98	4.12	2.86	5.93
K_2O	1.06	0.17	1.54	1.56	3.26	3.10	2.82	0.64
TiO_2	1.26	1.06	0.37	0.51	0.37	0.40	0.51	0.84
P_2O_5	0.06	<0.05	<0.05	0.09	0.11	0.13	0.10	0.11
Fe_2O_3*	15.48	12.71	4.28	6.05	3.34	3.78	5.50	6.91
LOI	0.82	9.27	3.42	4.37	1.10	1.23	3.28	2.41
TOTAL	98.34	98.52	99.64	99.26	98.84	99.29	98.57	99.67
S	0.30	0.01	0.01	0.04	0.01	0.02	0.04	0.02
CO_2	<0.10	5.65	1.57	1.96	<0.10	0.14	0.64	0.59
FeO	11.66	10.20	2.66	4.21	1.31	1.63	3.26	4.57
H_20^-	0.12	0.46	0.30	0.25	0.16	0.20	0.22	0.29
H_20^+	1.51	4.73	2.02	2.72	1.01	1.08	2.94	2.08
Ag ppm	3	2	1	2	2	3	2	2
Cd	2	2	2	2	2	2	2	2
Li	22	18	24	23	17	21	33	9
Hg	8	32	33	58	33	25	59	N.D.
Cl	250	N.D.	789	435	612	N.D.	1300	789
F	300	200	139	278	278	319	306	306
Co	69	50	16	18	11	12	16	11
Cu	109	107	31	37	14	14	61	18
Mo	N.D.	N.D.	N.D.	N.D.	9	9	9	N.D.
Ni	150	125	41	48	30	36	51	16
Sc	42	38	10	12	5	7	11	12
V	356	319	81	107	50	59	101	54
Zn	142	117	51	81	59	62	88	148
Au (ppb)	3	N.D.	5	4	N.D.	4	N.D.	N.D.
Y	29	21	9	11	9	11	10	24
Zr	77	64	79	123	136	143	119	179
Ba	442	135	604	553	996	1135	940	277
Cr	253	304	93	91	45	59	98	10
As	11	N.D.	11	6	N.D.	N.D.	13	N.D.
Pb	8	N.D.	11	16	28	32	14	N.D.
La	4.97	3.8	16.05	41.49	42.13	46.73	27.3	23.09
Ce	12.57	9.64	29.42	78.97	78.92	88.19	53.77	50.63
Pr	1.88	1.48	3.23	8.84	8.94	10.02	6.14	6.47
Nd	9.45	7.61	11.63	30.55	31.58	35.84	22.62	25.8
Sm	3.03	2.39	2.03	4.36	4.92	5.64	3.65	5.14
Eu	0.95	0.82	0.53	1.3	1.06	1.18	0.83	1.73
Tb	0.71	0.56	0.24	0.38	0.37	0.43	0.36	0.69
Gd	4.1	3.2	1.66	2.8	2.98	3.49	2.62	4.6
Dy	5	3.66	1.38	2.25	1.95	2.2	2	4.12
Ho	1.07	0.78	0.26	0.38	0.35	0.41	0.4	0.82
Er	3.07	2.17	0.75	1.04	0.96	1.13	1.1	2.3
Tm	0.48	0.31	0.12	0.16	0.14	0.16	0.17	0.35
Yb	3.05	2.06	0.82	1.1	0.89	1.02	1.01	2.2
Lu	0.47	0.29	0.14	0.17	0.13	0.16	0.15	0.33
Rb	85.42	10.74	40.84	53.74	101.35	93.69	93.06	8.50
Sr	119.57	103.07	385.99	396.18	749.63	805.79	503.75	83.33
Nb	3.66	2.66	3.59	2.59	6.62	6.97	5.26	11.66
Cs	11.61	0.42	2.06	3.35	3.28	2.68	4.01	0.35
Hf	1.83	0.77	2.11	3.08	3.29	2.93	2.62	4.67
Ta	0.25	0.21	0.29	0.22	0.53	0.55	0.43	0.73
Th	0.52	0.37	4.16	7.87	11.39	12.03	6.78	3.57
U	0.14	0.09	1.15	1.95	2.83	2.98	1.64	0.87

Table 1. *Continued.*

Sample	94JRD–0014B	94JRD–0015	94JRD–0015	94JRD–0017	94JRD–0018	94JRD–0019	94JRD–0020	94JRD–0022
Rock Type (field I.D.)	Tuff (alt.)	Tuff	(duplicate)	Lapilli–tuff	Sandstone	Volc cng	Mafic cng	Granitoid
SiO_2 %	74.27	56.31	55.96	73.30	58.17	68.03	50.67	69.76
Al_2O_3	12.06	14.50	14.39	12.57	16.72	12.92	15.23	15.29
MnO	0.04	0.13	0.13	0.02	0.12	0.12	0.21	0.05
MgO	1.22	4.13	4.13	0.17	2.91	2.01	6.58	1.05
CaO	1.15	5.34	5.30	0.61	2.63	3.51	10.49	1.72
Na_2O	4.84	3.12	3.12	0.20	3.20	4.88	1.64	4.80
K_2O	0.93	1.54	1.54	7.40	2.57	0.65	0.14	2.08
TiO_2	0.24	0.61	0.60	0.11	0.66	0.54	0.83	0.37
P_2O_5	<0.05	0.12	0.12	<0.05	0.11	0.12	<0.05	0.11
Fe_2O_3*	2.70	6.94	6.94	2.23	9.76	5.58	11.44	2.80
LOI	2.02	6.66	6.69	1.71	2.10	1.16	1.36	1.58
TOTAL	99.47	99.40	98.92	98.32	98.95	99.52	98.59	99.61
S	<0.01	0.04	0.04	0.11	0.15	0.26	0.09	0.02
CO_2	0.69	3.72	3.76	0.68	<0.10	0.11	<0.10	0.23
FeO	1.49	5.12	5.13	0.94	6.88	3.14	8.35	1.36
H_20^-	0.30	0.28	0.25	0.28	0.31	0.30	0.10	0.27
H_20^+	1.37	3.67	3.58	1.21	2.37	0.94	2.14	1.35
Ag ppm	2	3		2	3	2	4	2
Cd	2	2		2	2	2	2	2
Li	10	32		16	62	11	14	17
Hg	27	6		27	N.D.	11	21	N.D.
Cl	435	435		2375	1725	1500	N.D.	413
F	139	278		N.D.	306	278	190	139
Co	N.D.	22		N.D.	23	14	54	8
Cu	N.D.	40		14	81	32	112	9
Mo	N.D.	N.D.		10	N.D.	13	N.D.	9
Ni	10	96		N.D.	58	35	156	9
Sc	6	15		4	18	11	41	3
V	16	134		N.D.	165	108	282	45
Zn	30	84		135	92	63	100	59
Au (ppb)	N.D.	N.D.		4	N.D.	N.D.	N.D.	N.D.
Y	26	14		35	13	10	19	10
Zr	248	115		205	131	120	54	163
Ba	250	456		504	633	202	90	891
Cr	12	328		12	144	110	399	16
As	22	23		11	N.D.	N.D.	6	N.D.
Pb	N.D.	9		N.D.	16	25	N.D.	15
La	26.57	18.85	18.65	40.01	24.13	29.37	3.64	37.93
Ce	57.25	38.71	37.9	87.82	55.06	54.08	8.76	76.04
Pr	7.17	4.7	4.6	10.75	6.77	6	1.3	8.45
Nd	27.56	18.54	18.09	39.98	24.35	21.47	6.34	29.19
Sm	5.67	3.55	3.46	7.24	4.14	3.5	1.98	4.47
Eu	1.15	0.88	0.85	0.86	0.97	1.02	0.72	1.06
Tb	0.75	0.44	0.42	0.74	0.41	0.33	0.46	0.37
Gd	5.14	2.96	2.93	5.36	2.82	2.56	2.54	2.97
Dy	4.54	2.56	2.5	4.38	2.46	1.84	3.09	1.89
Ho	0.91	0.52	0.49	0.88	0.49	0.36	0.66	0.36
Er	2.58	1.45	1.38	2.7	1.46	1	1.99	0.95
Tm	0.39	0.21	0.22	0.45	0.23	0.15	0.29	0.14
Yb	2.63	1.38	1.34	3.21	1.56	0.97	1.9	0.91
Lu	0.4	0.22	0.2	0.5	0.24	0.15	0.3	0.15
Rb	22.31	46.39	46.88	116.61	111.60	29.14	4.44	86.20
Sr	26.88	408.93	400.77	26.17	375.92	513.15	146.34	278.51
Nb	12.02	4.81	4.81	14.08	5.31	4.94	2.26	12.79
Cs	0.63	1.14	1.14	2.89	5.69	2.57	0.79	4.13
Hf	7.00	2.95	2.85	6.30	3.52	3.00	1.02	4.10
Ta	0.84	0.39	0.36	1.02	0.37	0.35	0.16	0.76
Th	6.09	4.62	4.56	7.25	6.72	6.89	0.40	14.25
U	1.55	1.30	1.26	1.81	1.70	1.64	0.11	3.44

Table 1. *Continued*

Sample	94JRD–0024	94JRD–0029	94JRD–0030	94JRD–0031	94JRD–0034	94JRD–0034	94JRD–0035	94JRD–0036
Rock Type	Sandstone	Lapillistone	Tuff–breccia	Int pillow	Fel porphyry	(duplicate)	Tuff–breccia	Lapillistone
(field I.D.)								
SiO_2 %	59.15	53.78	51.55	54.84	66.77	66.76	68.59	52.94
Al_2O_3	13.48	14.54	14.79	12.93	16.58	16.85	16.84	14.92
MnO	0.04	0.13	0.15	0.15	0.04	0.03	0.05	0.12
MgO	1.17	6.48	5.92	3.67	0.67	0.68	0.29	2.62
CaO	2.05	5.16	5.96	7.14	3.29	3.26	2.81	4.90
Na_2O	2.65	3.46	2.96	3.77	3.61	3.66	3.58	3.01
K_2O	2.47	0.78	0.53	0.19	1.26	1.28	0.94	1.58
TiO_2	0.34	1.55	1.45	1.32	0.51	0.51	0.53	1.75
P_2O_5	0.05	0.31	0.29	0.30	0.11	0.11	0.10	0.31
Fe_2O_3*	11.20	8.88	10.94	8.30	1.94	1.93	1.34	8.47
LOI	5.87	4.13	4.22	7.08	4.27	4.50	4.43	7.74
TOTAL	98.47	99.19	98.76	99.69	99.05	99.57	99.51	98.36
S	4.31	0.01	0.01	0.01	0.02	0.02	0.01	0.04
CO_2	<0.10	0.82	0.56	4.44	2.41	2.44	2.18	5.57
FeO	1.21*	5.76	6.82	5.91	1.20	1.20	0.67	5.71
H_20^-	0.35	0.31	0.34	0.27	0.33	0.32	0.41	0.05
H_20^+	2.49	4.05	4.23	3.19	2.04	2.14	2.31	2.17
Ag ppm	3	3	3	3	2		2	3
Cd	2	2	2	2	2		2	2
Li	27	21	20	21	21		22	26
Hg	5	N.D.	19	N.D.	N.D.		N.D.	N.D.
Cl	N.D.	435	N.D.	250	2500		2500	750
F	300	208	310	278	540		433	417
Co	29	35	37	28	9		5	27
Cu	142	122	52	69	15		16	22
Mo	N.D.	N.D.	N.D.	N.D.	9		9	N.D.
Ni	30	198	122	65	21		14	73
Sc	7	19	20	14	6		7	17
V	72	162	172	125	64		55	168
Zn	47	119	134	101	54		19	105
Au (ppb)	N.D.	N.D.	N.D.	N.D.	N.D.		N.D.	N.D.
Y	6	23	24	18	7		5	23
Zr	97	198	187	127	121		144	152
Ba	969	245	128	83	395		271	541
Cr	58	293	205	53	22		38	91
As	18	N.D.	N.D.	N.D.	N.D.		N.D.	N.D.
Pb	30	N.D.	7	7	7		N.D.	N.D.
La	10.86	23.75	23.47	18.13	22.49	22.02	27.78	22.08
Ce	21.46	54.64	52.92	44.76	44.08	43.47	52.58	54.63
Pr	2.54	7.22	6.88	6.01	4.98	4.93	5.61	7.43
Nd	9.47	29.41	27.97	24.52	17.67	17.38	19.63	30.83
Sm	1.78	6.01	5.59	4.95	2.89	2.87	3.04	6.14
Eu	0.55	1.62	1.6	1.42	0.78	0.79	0.86	1.6
Tb	0.21	0.76	0.75	0.6	0.27	0.26	0.23	0.64
Gd	1.45	5.35	5.13	4.27	2.12	2.05	2	5.04
Dy	1.28	4.46	4.32	3.43	1.43	1.41	1.22	3.29
Ho	0.25	0.85	0.87	0.64	0.25	0.25	0.22	0.58
Er	0.68	2.26	2.33	1.69	0.69	0.68	0.64	1.55
Tm	0.11	0.33	0.34	0.24	0.1	0.1	0.09	0.23
Yb	0.63	2.03	2.08	1.48	0.63	0.66	0.59	1.52
Lu	0.1	0.29	0.31	0.23	0.1	0.1	0.1	0.24
Rb	88.37	16.86	14.04	5.07	28.45	28.36	25.79	59.39
Sr	324.78	248.35	293.79	287.82	366.11	367.28	427.50	269.33
Nb	3.09	15.39	15.05	10.34	2.77	2.75	3.39	8.81
Cs	4.31	0.84	1.46	0.26	1.27	1.27	1.61	1.89
Hf	1.90	4.22	3.76	2.74	2.74	2.81	3.47	3.86
Ta	0.24	0.85	0.85	0.59	0.25	0.23	0.27	0.58
Th	3.06	2.44	2.20	1.17	3.35	3.35	3.81	2.00
U	1.02	0.57	0.54	0.33	0.84	0.84	0.92	0.52

Table 1. *Continued*

Sample	94JRD–0045	94JRD–0047	94JRD–0053	94JRD–0054	94JRD–0056	94JRD–0060	94JRD–0061	94JRD–0062
Rock Type (field I.D.)	Mafic pillow	Lapilli–tuff	Int tuff	Felsic tuff	Porphyry	Diorite	Diorite	Diorite
SiO_2 %	49.82	37.57	52.28	55.86	53.49	52.18	54.30	51.17
Al_2O_3	15.30	11.66	14.33	14.35	17.23	17.66	15.94	15.41
MnO	0.19	0.47	0.12	0.12	0.11	0.14	0.13	0.10
MgO	6.60	5.55	5.67	4.77	2.88	3.56	3.26	5.52
CaO	10.91	20.04	6.65	6.23	5.90	5.39	5.93	3.56
Na_2O	2.76	1.38	1.42	4.04	2.69	3.98	4.11	4.75
K_2O	0.13	0.17	2.21	0.41	1.83	0.74	0.35	0.23
TiO_2	0.81	0.73	0.69	1.13	1.53	1.62	1.34	1.15
P_2O_5	<0.05	<0.05	0.11	0.19	0.33	0.32	0.27	0.41
Fe_2O_3*	11.56	9.93	7.50	8.32	9.46	10.02	9.21	12.08
LOI	0.93	11.67	7.89	2.23	3.20	3.40	3.86	5.17
TOTAL	99.01	99.17	98.87	97.65	98.64	99.01	98.69	99.55
S	0.09	0.01	<0.01	<0.01	0.04	<0.01	<0.01	0.21
CO_2	0.43	10.40	4.18	0.15	0.12	0.35	1.32	<0.10
FeO	9.00	6.58	5.57	5.47	4.92	6.02	6.04	5.63
H_20^-	0.06	0.30	0.31	0.24	0.29	0.41	0.23	1.35
H_20^+	1.32	2.59	4.48	2.71	3.55	3.51	3.24	4.59
Ag ppm	4	5	3	3	4	4	3	3
Cd	2	2	2	2	2	2	2	2
Li	10	17	34	14	16	17	14	16
Hg	N.D.	16	N.D.	N.D.	N.D.	N.D.	N.D.	1
Cl	N.D.	N.D.	N.D.	575	1313	346	1250	250
F	114	N.D.	333	400	500	455	417	398
Co	51	42	31	30	29	29	26	13
Cu	128	66	72	26	55	56	23	126
Mo	N.D.	N.D.	N.D.	N.D.	N.D.	N.D.	N.D.	N.D.
Ni	145	109	146	112	51	62	55	27
Sc	34	26	17	17	16	18	16	15
V	264	219	120	145	173	195	175	95
Zn	88	74	87	101	113	117	108	102
Au (ppb)	N.D.	N.D.	N.D.	N.D.	N.D.	N.D.	N.D.	N.D.
Y	17	18	15	19	26	18	20	14
Zr	53	53	126	166	204	110	131	79
Ba	71	262	249	117	507	216	135	106
Cr	290	240	332	143	33	41	35	149
As	N.D.	N.D.	N.D.	N.D.	N.D.	N.D.	N.D.	N.D.
Pb	N.D.	N.D.	N.D.	N.D.	N.D.	N.D.	N.D.	N.D.
La	2.41	3.54	14.25	18.63	26.36	14.6	18.25	14.5
Ce	6.5	8.9	31.52	41.78	62.08	34.48	42.39	34.17
Pr	1.04	1.29	3.96	5.32	8.18	4.53	5.56	4.48
Nd	5.38	6.28	16.19	21.95	33.58	20.01	23.28	19.3
Sm	1.86	1.98	3.29	4.54	6.69	4.49	4.73	3.73
Eu	0.61	0.71	0.92	1.21	1.85	1.47	1.53	1.28
Tb	0.44	0.44	0.46	0.57	0.87	0.57	0.65	0.44
Gd	2.47	2.56	3.11	3.94	6.07	4.2	4.41	3.2
Dy	3.06	2.91	2.77	3.22	5.16	3.52	3.75	2.57
Ho	0.64	0.61	0.55	0.65	1.02	0.68	0.74	0.49
Er	1.92	1.79	1.61	1.8	2.8	1.89	2.05	1.34
Tm	0.28	0.26	0.25	0.25	0.39	0.25	0.28	0.21
Yb	1.7	1.58	1.51	1.52	2.42	1.59	1.75	1.24
Lu	0.22	0.24	0.25	0.23	0.36	0.24	0.26	0.19
Rb	1.65	9.58	65.54	4.79	64.57	21.58	11.28	3.86
Sr	116.07	101.66	138.12	91.46	789.81	334.34	388.90	203.28
Nb	2.20	2.32	8.01	12.24	16.52	9.69	9.97	8.06
Cs	0.12	0.72	1.00	0.11	1.78	0.48	0.26	0.15
Hf	0.64	0.48	6.61	3.07	3.83	2.07	1.50	0.94
Ta	0.17	0.18	0.51	0.73	0.91	0.57	0.60	0.51
Th	0.24	0.43	1.75	2.00	2.68	1.53	1.61	0.94
U	0.06	0.11	0.43	0.53	0.65	0.31	0.34	0.24

Table 1. *Continued.*

Sample	94JRD–0062	94JRD–0063	94JRD–0066	94JRD–0067	94JRD–0068	94JRD–0070	94JRD–0071	94JRD–0072
Rock Type (field I.D.)	(duplicate)	Diorite	Porphyry	Lapilli–tuff	Lapilli–tuff	Int volcanic	Int volcanic	Int volcanic
SiO_2 %	50.96	47.62	57.25	54.22	52.63	46.59	36.57	53.29
Al_2O_3	15.40	16.00	16.20	14.79	14.15	16.02	8.61	15.94
MnO	0.10	0.15	0.10	0.13	0.15	0.15	0.04	0.02
MgO	5.48	4.78	3.74	5.12	7.21	6.13	0.18	0.63
CaO	3.56	9.44	5.83	6.93	5.35	6.86	5.26	2.34
Na_2O	4.73	2.54	4.93	3.48	2.84	2.52	0.01	0.09
K_2O	0.21	0.44	0.49	0.34	0.96	1.34	1.30	5.08
TiO_2	1.15	2.07	1.26	1.23	1.09	1.31	1.57	2.36
P_2O_5	0.40	0.33	0.27	0.24	0.19	0.28	0.21	0.52
Fe_2O_3*	12.05	12.54	7.37	9.40	10.07	10.33	28.38	10.94
LOI	5.13	2.65	2.25	3.34	4.23	7.18	13.59	5.26
TOTAL	99.18	98.56	99.70	99.22	98.87	98.70	95.72	96.48
S	0.21	0.15	0.01	0.01	<0.01	<0.01	13.40	0.89
CO_2	<0.10	0.15	0.18	0.56	0.71	3.91	<0.10	0.24
FeO	5.64	7.98	4.84	5.71	7.18	7.86	1.2*	0.63
H_20^-	1.51	2.27	0.25	0.26	0.31	0.55	1.46	1.33
H_20^+	4.59	3.37	2.48	3.33	4.06	5.10	3.06	4.15
Ag ppm		4	3	4	3	2	3	2
Cd		2	2	2	2	N.D.	N.D.	N.D.
Li		13	13	18	24	28	8	14
Hg		N.D.	N.D.	N.D.	N.D.	7	19	15
Cl		308	850	250	115	N.D.	N.D.	145
F		489	333	317	273	389	167	847
Co		42	23	33	40	39	67	11
Cu		102	N.D.	37	25	10	126	311
Mo		N.D.	N.D.	N.D.	N.D.	N.D.	N.D.	N.D.
Ni		98	93	109	152	146	149	19
Sc		22	15	19	20	22	13	24
V		260	137	173	169	192	158	228
Zn		126	70	107	116	148	90	27
Au (ppb)		N.D.	N.D.	N.D.	N.D.	N.D.	17	N.D.
Y		23	19	20	20	19	21	25
Zr		132	192	160	141	119	152	242
Ba		162	168	172	335	305	264	652
Cr		87	121	131	220	164	17	14
As		N.D.	N.D.	N.D.	N.D.	32	25	9
Pb		N.D.	N.D.	7	7	N.D.	12	N.D.
La	13.83	16.47	20.34	21.56	20.54	15.95	14.13	20.17
Ce	32.94	42.33	46.91	50.91	45.31	40.23	35.04	50.17
Pr	4.37	6.07	6.1	6.79	5.89	5.69	5.05	6.93
Nd	18.53	26.63	25.28	27.25	24.54	24.07	22.37	29.90
Sm	3.69	5.83	5.08	5.27	4.88	4.82	4.68	6.57
Eu	1.25	1.87	1.39	1.61	1.34	1.42	1.32	1.75
Tb	0.44	0.77	0.62	0.68	0.62	0.63	0.67	0.87
Gd	3.16	5.26	4.46	4.8	4.43	4.26	4.52	5.87
Dy	2.51	4.4	3.45	3.98	3.72	3.44	4.06	5.11
Ho	0.46	0.87	0.68	0.78	0.75	0.65	0.84	1.00
Er	1.34	2.3	1.94	2.14	2.19	1.85	2.41	2.97
Tm	0.19	0.32	0.28	0.3	0.31	0.26	0.33	0.43
Yb	1.15	2.02	1.77	1.89	1.91	1.61	2.20	2.80
Lu	0.18	0.31	0.28	0.27	0.29	0.25	0.31	0.43
Rb	3.69	10.35	12.89	5.30	21.34	39.80	42.01	137.28
Sr	187.93	548.55	226.95	341.27	221.46	167.87	454.61	80.66
Nb	7.96	12.69	15.61	11.94	8.16	13.65	14.49	22.64
Cs	0.12	0.28	0.28	0.18	0.65	1.34	1.02	2.98
Hf	0.91	1.81	4.76	3.27	3.24	2.73	3.08	5.81
Ta	0.50	0.69	0.89	0.69	0.50	0.72	0.84	1.28
Th	0.90	1.45	2.44	2.08	2.44	0.99	1.47	2.49
U	0.24	0.37	0.64	0.55	0.57	0.29	0.47	0.65

Table 1. *Continued.*

Sample	94JRD–0077	94JRD–0078	94JRD–0079	94JRD–0080	94JRD–0081	94JRD–0087	94JRD–0091	94JRD–0091
Rock Type	Porph dike	Int volcanic	Porph dike	Int dike	Lapilli–tuff	Pillow bxa	Granite	(duplicate)
(field I.D.)								
SiO_2 %	54.37	44.90	50.30	54.09	51.57	44.55	65.46	66.08
Al_2O_3	14.58	14.23	14.24	16.75	15.95	14.13	13.87	13.75
MnO	0.16	0.24	0.15	0.09	0.15	0.24	0.09	0.09
MgO	4.63	6.19	8.24	3.39	5.26	6.11	0.64	0.63
CaO	5.73	13.38	6.20	7.39	5.59	13.30	1.98	1.93
Na_2O	4.12	0.03	3.27	3.45	3.42	0.03	4.00	4.02
K_2O	0.21	<0.02	0.79	1.16	0.44	<0.02	1.58	1.62
TiO_2	2.02	1.05	1.34	1.61	1.61	1.04	0.79	0.76
P_2O_5	0.43	<0.05	0.25	0.35	0.31	<0.05	0.19	0.18
Fe_2O_3*	9.35	14.60	10.98	7.96	10.89	14.52	6.86	6.65
LOI	2.81	4.51	3.31	2.66	3.79	3.42	3.32	3.23
TOTAL	98.41	99.13	99.08	98.90	98.97	97.34	98.78	98.94
S	0.37	2.56	0.02	0.01	<0.01	0.03	0.01	0.01
CO_2	0.35	0.12	<0.10	0.14	0.21	0.19	1.39	1.34
FeO	6.06	1.23	8.18	4.44	7.23	8.83	3.56	3.54
H_20^-	0.46	0.63	0.32	0.26	0.47	0.43	0.40	0.32
H_20^+	3.39	2.83	4.24	2.97	4.35	4.27	2.24	2.16
Ag ppm	2	2	3	2	2	3	2	
Cd	N.D.	N.D.	N.D.	N.D.	N.D.	N.D.	N.D.	
Li	13	26	20	18	21	13	10	
Hg	18	21	10	8	5	9	6	
Cl	1484	132	171	1328	275	104	1563	
F	455	333	278	341	239	97	227	
Co	30	16	34	26	32	55	11	
Cu	64	35	9	83	9	199	12	
Mo	N.D.	N.D.	N.D.	8	N.D.	N.D.	N.D.	
Ni	97	43	233	89	80	110	8	
Sc	20	16	18	16	20	39	11	
V	182	155	156	150	182	349	30	
Zn	136	59	118	87	117	124	102	
Au (ppb)	271	1117	N.D.	N.D.	N.D.	N.D.	N.D.	
Y	32	26	22	25	25	24	38	
Zr	264	233	186	215	165	54	276	
Ba	69	432	147	333	136	43	328	
Cr	98	81	422	81	53	224	5	
As	60	>500	N.D.	N.D.	N.D.	43	N.D.	
Pb	N.D.	9	N.D.	8	N.D.	N.D.	N.D.	
La	32.95	13.09	19.06	26.41	21.30	2.20	32.72	34.49
Ce	77.19	34.70	45.29	62.84	50.55	6.65	76.23	79.75
Pr	10.24	4.99	5.96	8.25	6.73	1.17	9.98	10.38
Nd	42.01	22.19	25.00	33.61	28.36	6.64	40.92	42.73
Sm	8.38	5.34	5.13	6.72	6.07	2.36	8.26	8.31
Eu	2.10	0.95	1.25	1.76	1.76	0.76	1.73	1.81
Tb	1.08	0.82	0.69	0.86	0.82	0.60	0.66	0.68
Gd	7.23	5.35	4.73	5.98	5.59	3.39	5.61	5.86
Dy	5.94	4.60	3.90	4.93	4.68	3.94	3.43	3.22
Ho	1.14	0.90	0.75	0.93	0.90	0.84	0.58	0.57
Er	3.17	2.59	2.09	2.56	2.48	2.55	1.88	1.72
Tm	0.44	0.36	0.29	0.37	0.36	0.35	0.23	0.23
Yb	2.81	2.35	1.87	2.23	2.26	2.23	1.58	1.58
Lu	0.42	0.35	0.28	0.33	0.32	0.34	0.28	0.26
Rb	5.59	130.98	21.90	29.71	12.44	0.67	43.44	43.80
Sr	227.26	10.59	148.15	411.60	334.26	78.37	134.47	134.95
Nb	21.04	18.01	13.16	16.94	14.55	1.88	14.23	14.09
Cs	0.24	2.88	0.55	0.86	0.49	0.07	0.81	0.85
Hf	6.47	6.01	4.41	5.00	3.62	1.11	2.70	2.64
Ta	1.23	1.06	0.80	0.96	0.82	0.15	0.93	0.93
Th	3.40	2.81	2.54	2.78	2.02	0.18	4.27	4.35
U	0.89	0.74	0.65	0.69	0.53	0.08	1.02	1.03

Table 1. *Continued.*

Sample	94JRD–0092	94JRD–0093	94JRD–0102	94JRD–B023	94JRD–B024	94JRD–B027	94JRD–B032	94JRD–B040
Rock Type (field I.D.)	Tuff–sandst	Fel volcanic	Lapilli–tuff	Granite	Gabbro	Diorite	Lapill–tuff	Mafic volc
SiO_2 %	63.32	70.01	52.96	70.90	54.04	57.73	52.24	40.59
Al_2O_3	15.92	10.76	14.26	16.21	12.15	17.33	12.33	5.20
MnO	0.05	0.08	0.20	0.02	0.16	0.08	0.25	0.18
MgO	3.06	2.15	4.70	0.43	6.37	2.86	5.18	23.82
CaO	1.00	4.61	4.92	1.97	9.23	3.92	4.07	3.70
Na_2O	6.42	1.48	4.25	6.36	4.52	7.14	3.22	<0.01
K_2O	0.46	0.63	0.03	2.45	3.04	2.66	0.13	<0.02
TiO_2	0.70	0.45	1.10	0.16	0.84	0.47	1.85	0.25
P_2O_5	0.08	<0.05	0.23	<0.05	0.50	0.24	0.15	<0.05
Fe_2O_3*	6.06	6.14	10.04	1.59	7.81	5.58	14.94	13.02
LOI	2.34	2.38	5.99	0.79	1.01	1.18	3.88	11.41
TOTAL	99.41	98.69	98.68	100.88	99.67	99.20	98.24	98.17
S	<0.01	0.01	0.10	<0.01	0.01	0.01	<0.01	<0.01
CO_2	0.10	0.22	3.07	<0.10	<0.10	0.51	0.28	5.73
FeO	4.19	2.96	7.58	0.30	4.07	2.37	9.36	9.30
H_20^-	0.39	0.44	0.41	0.30	0.30	0.27	0.65	0.73
H_20^+	2.65	2.34	4.28	0.49	0.92	0.77	4.62	7.27
Ag ppm	1	1	2	1	3	2	2	2
Cd	N.D.	N.D.	N.D.	N.D.	N.D.	N.D.	N.D.	N.D.
Li	9	11	24	13	62	46	13	6
Hg	3	9	12	6	31	5	19	11
Cl	1563	1172	104	1953	1563	1563	104	243
F	341	113	239	227	938	1078	217	130
Co	14	13	30	N.D.	30	16	38	101
Cu	21	40	36	7	80	N.D.	43	6
Mo	8	N.D.	N.D.	9	N.D.	9	N.D.	N.D.
Ni	20	23	71	5	80	45	46	649
Sc	10	9	22	1	18	6	32	21
V	68	55	157	19	168	85	258	126
Zn	30	52	111	41	121	102	156	108
Au (ppb)	N.D.	N.D.	N.D.	N.D.	8	N.D.	N.D.	N.D.
Y	17	26	23	3	29	10	39	6
Zr	171	201	142	90	238	371	135	22
Ba	165	202	56	775	1830	1192	77	24
Cr	11	25	89	8	288	87	50	2111
As	N.D.	N.D.	N.D.	N.D.	N.D.	N.D.	N.D.	95
Pb	N.D.	N.D.	N.D.	13	19	25	N.D.	N.D.
La	17.18	18.68	19.03	7.36	84.33	45.32	10.14	1.44
Ce	40.04	42.59	45.72	15.54	191.21	87.67	25.56	3.32
Pr	4.78	5.28	6.02	1.86	25.13	10.06	3.70	0.46
Nd	18.00	20.46	24.83	7.16	100.43	38.20	17.80	2.19
Sm	3.48	4.29	4.90	1.33	17.57	6.60	5.10	0.63
Eu	0.86	1.02	1.47	0.29	3.87	1.66	1.46	0.15
Tb	0.48	0.71	0.65	0.12	1.42	0.56	1.10	0.10
Gd	3.13	4.29	4.49	0.94	11.92	4.65	6.28	0.61
Dy	2.93	4.40	3.77	0.56	6.60	2.55	7.11	0.53
Ho	0.61	0.91	0.77	0.10	1.08	0.43	1.50	0.11
Er	1.72	2.67	2.22	0.30	2.63	1.21	4.28	0.32
Tm	0.27	0.39	0.32	0.05	0.35	0.16	0.60	0.05
Yb	1.67	2.60	2.20	0.29	2.21	1.05	3.65	0.33
Lu	0.27	0.39	0.33	0.05	0.32	0.17	0.47	0.06
Rb	10.25	12.10	1.52	64.02	89.30	104.86	7.15	0.37
Sr	101.61	247.42	112.59	719.18	1391.12	1450.31	57.17	16.92
Nb	7.82	10.05	10.96	2.88	9.17	5.34	7.96	0.76
Cs	0.37	0.18	0.05	1.71	2.03	3.26	0.47	0.14
Hf	3.40	4.64	3.74	2.26	5.02	6.15	1.96	0.54
Ta	0.56	0.73	0.65	0.17	0.44	0.27	0.52	0.07
Th	3.50	4.39	1.68	1.86	12.66	10.70	1.03	0.26
U	0.75	1.16	0.45	0.50	2.08	2.01	0.28	0.08

Table 1. *Continued.*

Sample	94JRD–B042	94JRD–B056	94JRD–B056	94JRD–B058	94JRD–B69A	94JRD–B69B	94JRD–B071	94JRD–B072
Rock Type (field I.D.)	Mafic volc	Mafic volc	(duplicate)	Mafic volc	Tuff–breccia	Tuff–breccia	Tuff–breccia	Tuff–breccia
SiO_2 %	44.31	55.97	55.99	45.96	60.91	51.56	55.52	41.78
Al_2O_3	14.15	12.38	12.40	19.99	14.35	14.69	14.45	12.36
MnO	0.17	0.11	0.11	0.10	0.09	0.17	0.16	0.28
MgO	5.19	3.31	3.32	5.26	2.75	5.53	2.69	4.18
CaO	7.63	6.77	6.78	8.79	4.35	6.06	6.08	13.20
Na_2O	2.52	3.76	3.61	3.53	4.95	1.07	2.53	2.06
K_2O	<0.02	0.44	0.43	2.56	0.37	0.35	1.65	0.54
TiO_2	1.94	1.29	1.29	0.42	1.75	1.93	0.91	1.66
P_2O_5	0.15	0.24	0.24	<0.05	0.34	0.30	0.16	0.19
Fe_2O_3*	16.20	6.90	6.91	6.27	5.43	11.26	9.25	11.72
LOI	6.11	8.35	8.35	5.62	3.52	5.24	5.06	10.88
TOTAL	98.37	99.52	99.43	98.50	98.81	98.15	98.45	98.85
S	0.53	0.04	0.03	<0.01	0.10	0.01	<0.01	0.13
CO_2	2.64	6.18	6.17	4.99	1.40	1.01	2.29	8.28
FeO	10.36	5.01	5.01	4.00	3.13	7.70	5.72	8.36
H_20^-	0.66	0.44	0.40	0.47	0.41	0.48	0.33	0.30
H_20^+	5.10	2.84	2.84	3.99	2.51	5.16	3.33	4.28
Ag ppm	2	2		2	2	2	2	3
Cd	N.D.	N.D.		N.D.	N.D.	N.D.	N.D.	N.D.
Li	11	27		22	12	24	22	20
Hg	40	10		84	N.D.	6	4	6
Cl	N.D.	1172		250	1563	125	1750	N.D.
F	208	227		113	284	323	319	260
Co	54	28		24	39	49	25	34
Cu	139	152		N.D.	23	47	26	39
Mo	N.D.	N.D.		10	N.D.	N.D.	N.D.	N.D.
Ni	71	123		78	142	151	66	100
Sc	37	16		26	18	22	14	19
V	338	132		155	134	214	122	170
Zn	148	83		39	69	135	102	202
Au (ppb)	N.D.	N.D.		N.D.	N.D.	N.D.	N.D.	N.D.
Y	33	16		10	22	24	19	22
Zr	112	115		30	119	137	191	118
Ba	48	96		471	244	240	333	181
Cr	88	130		461	297	356	47	188
As	N.D.	N.D.		N.D.	N.D.	N.D.	N.D.	N.D.
Pb	N.D.	N.D.		N.D.	N.D.	N.D.	7	N.D.
La	8.29	15.56	16.20	1.41	17.17	15.56	21.26	10.72
Ce	20.03	38.34	39.37	3.66	45.71	42.71	47.00	30.42
Pr	2.92	5.16	5.36	0.59	6.37	6.19	5.75	4.57
Nd	14.41	21.42	22.52	3.24	28.34	27.22	23.08	20.62
Sm	4.23	4.38	4.54	1.24	6.07	5.92	4.78	4.92
Eu	1.62	1.27	1.29	0.58	1.14	1.75	1.14	1.12
Tb	0.90	0.41	0.43	0.25	0.80	0.84	0.61	0.72
Gd	5.24	3.49	3.37	1.42	5.61	5.57	4.14	4.99
Dy	5.74	2.13	2.16	1.66	4.58	4.83	3.53	4.21
Ho	1.22	0.39	0.42	0.36	0.83	0.92	0.70	0.77
Er	3.59	1.20	1.21	1.10	2.26	2.37	2.01	2.13
Tm	0.51	0.18	0.19	0.16	0.30	0.32	0.28	0.29
Yb	3.42	1.19	1.17	0.91	1.60	1.84	1.80	1.54
Lu	0.49	0.21	0.21	0.16	0.20	0.22	0.29	0.23
Rb	0.45	11.61	11.44	52.24	14.05	13.90	41.52	16.92
Sr	278.63	201.84	199.76	190.65	266.72	631.33	450.70	235.34
Nb	5.94	7.62	7.81	0.97	10.59	12.05	9.94	12.82
Cs	0.14	0.25	0.26	1.96	0.38	0.41	1.43	0.35
Hf	2.53	2.46	2.49	0.41	1.03	0.89	4.44	1.03
Ta	0.40	0.45	0.44	0.10	0.61	0.69	0.67	0.70
Th	0.76	0.93	0.99	0.16	0.64	0.67	3.31	0.68
U	0.22	0.30	0.32	0.07	0.18	0.20	0.77	0.19

Table 1. *Continued.*

Sample	94JRD–B076	94JRD–B092	94JRD–B096	94JRD–B115	94JRD–B120	94JRD–B120	94JRD–B129	94JRD–B167
Rock Type	Volc (alt.)	Tuff–breccia	Tuff–breccia	Int tuff	Q–f porph	(duplicate)	Mafic pillow	Rhyolite
(field I.D.)								
SiO_2 %	45.00	57.15	50.47	63.86	67.43	67.52	46.71	76.35
Al_2O_3	12.06	12.67	18.08	13.87	15.39	15.39	14.41	11.66
MnO	0.19	0.12	0.16	0.11	0.02	0.02	0.18	0.03
MgO	4.62	2.97	3.75	1.25	0.98	0.99	6.78	0.52
CaO	7.24	8.09	4.91	2.94	2.65	2.69	10.54	0.76
Na_2O	1.76	4.37	5.50	3.37	5.67	5.75	1.16	4.39
K_2O	0.49	0.07	0.45	1.58	1.76	1.71	0.02	2.57
TiO_2	1.79	0.89	2.01	1.08	0.30	0.31	0.97	0.12
P_2O_5	0.19	0.15	0.26	0.30	0.05	0.05	<0.05	<0.05
Fe_2O_3*	13.57	6.24	9.88	6.84	2.69	2.73	13.36	1.91
LOI	11.56	6.77	3.51	3.64	3.23	3.23	4.27	1.58
TOTAL	98.47	99.49	98.98	98.83	100.18	100.40	98.40	99.89
S	0.04	0.01	0.38	0.01	0.08	0.08	0.12	<0.01
CO_2	9.38	4.85	0.12	1.47	1.96	1.97	1.28	0.91
FeO	11.13	4.37	5.56	4.72	1.39	1.40	9.16	0.94
H_20^-	0.38	0.22	0.76	0.40	0.25	0.27	0.35	0.19
H_20^+	3.78	2.23	3.89	2.71	1.46	1.51	4.31	0.62
Ag ppm	2	2	2	1	1		3	N.D.
Cd	N.D.	N.D.	N.D.	N.D.	N.D.		N.D.	N.D.
Li	54	16	15	15	10		16	20
Hg	6	6	3	3	79		1	2
Cl	100	1250	657	2725	2075		125	1950
F	219	194	278	319	278		135	N.D.
Co	32	24	16	13	6		51	N.D.
Cu	69	40	38	12	N.D.		110	N.D.
Mo	N.D.	N.D.	N.D.	N.D.	9		N.D.	8
Ni	47	72	84	8	12		131	N.D.
Sc	30	14	24	14	4		37	4
V	315	146	215	29	41		290	N.D.
Zn	126	70	155	132	38		103	43
Au (ppb)	N.D.	N.D.	N.D.	N.D.	N.D.		N.D.	N.D.
Y	36	13	26	51	5		21	30
Zr	147	108	154	349	87		61	187
Ba	147	59	149	296	545		38	624
Cr	53	57	113	N.D.	17		316	12
As	N.D.	N.D.	N.D.	N.D.	N.D.		7	N.D.
Pb	N.D.	N.D.	N.D.	7	N.D.		N.D.	N.D.
La	12.21	13.37	15.99	27.61	13.18	13.04	3.05	45.72
Ce	30.53	30.11	44.54	72.36	28.21	28.37	8.21	94.59
Pr	4.33	3.76	6.47	9.84	3.33	3.39	1.29	11.24
Nd	20.10	15.85	27.70	41.22	12.85	12.87	6.55	42.46
Sm	5.03	3.24	6.35	9.97	2.24	2.20	2.35	7.90
Eu	1.32	0.90	1.54	2.72	0.46	0.44	0.83	0.92
Tb	0.53	0.46	0.86	1.62	0.19	0.18	0.57	0.79
Gd	4.24	3.24	6.00	10.01	1.38	1.45	3.18	5.84
Dy	3.00	2.58	5.19	9.98	0.78	0.81	3.61	4.23
Ho	0.59	0.51	1.04	1.90	0.14	0.15	0.77	0.81
Er	1.86	1.41	2.82	5.45	0.45	0.44	2.40	2.53
Tm	0.30	0.22	0.38	0.74	0.09	0.08	0.35	0.38
Yb	2.18	1.17	2.33	4.76	0.46	0.44	2.19	2.66
Lu	0.36	0.20	0.35	0.71	0.09	0.09	0.34	0.44
Rb	15.48	3.03	14.76	39.47	40.58	39.99	0.71	61.23
Sr	121.07	129.16	90.01	99.51	421.75	416.50	107.38	105.08
Nb	9.18	9.33	14.18	21.00	1.80	1.80	2.66	12.34
Cs	1.14	0.06	0.49	1.14	0.98	0.98	0.14	2.73
Hf	3.19	2.10	3.02	9.36	1.94	2.01	0.90	6.53
Ta	0.54	0.51	0.79	1.36	0.13	0.13	0.20	1.01
Th	1.18	1.20	1.30	4.13	1.89	1.81	0.34	7.20
U	0.28	0.32	0.39	1.17	0.55	0.58	0.12	1.64

Table 1. *Continued*

Sample	94JRD–B171	94JRD–B192	95JRD–B02	95JRD–B48	95JRD–B64	95JRD–B79	95JRD–B107	95JRD–B122
Rock Type (field I.D.)	Felsic tuff	Fel volcanic	Mafic volc	Int volcanic	Diorite	Int volcanic	Mafic tuff	Andesite
SiO_2 %	76.63	63.64	47.07	61.00	58.51	59.80	46.17	49.21
Al_2O_3	11.55	13.71	14.00	14.37	16.19	13.09	13.67	17.32
MnO	0.05	0.09	0.23	0.11	0.10	0.09	0.15	0.15
MgO	0.42	1.29	5.62	2.89	2.93	1.88	5.72	3.95
CaO	1.33	2.56	8.99	4.40	6.20	16.04	9.12	8.38
Na_2O	3.80	3.37	2.25	4.49	4.47	<0.01	1.76	3.10
K_2O	2.34	2.03	<0.02	0.08	0.87	0.28	1.37	0.51
TiO_2	0.10	0.77	1.47	0.72	0.87	1.05	1.11	1.59
P_2O_5	<0.05	0.18	0.11	0.17	0.15	0.16	0.29	0.32
Fe_2O_3*	1.85	6.50	16.29	6.92	7.14	5.78	10.07	11.51
LOI	2.06	4.69	3.13	4.38	1.82	3.37	10.13	3.03
TOTAL	100.13	98.82	99.16	99.52	99.25	101.54	99.56	99.08
S	<0.01	0.28	0.07	0.01	0.04	<0.01	0.15	0.01
CO_2	1.11	3.36	0.44	2.11	0.45	2.21	6.35	0.45
FeO	0.85	3.12	10.69	5.08	3.47	1.56	7.37	7.63
H_20^-	0.21	0.33	0.18	0.16	0.14	0.07	0.08	0.14
H_20^+	0.94	1.99	3.87	2.76	1.87	1.30	4.53	3.40
Ag ppm	N.D.	1	4	2	3	3	3	3
Cd	N.D.	N.D.	N.D.	N.D.	N.D.	N.D.	N.D.	N.D.
Li	19	13	15	12	20	8	25	14
Hg	16	5						
Cl	652	1825						
F	417	347						
Co	N.D.	8						
Cu	24	12	142	32	56	N.D.	56	68
Mo	8	N.D.	N.D.	10	12	10	8	10
Ni	N.D.	7	79	51	48	127	180	98
Sc	3	12	29	12	13	19	16	19
V	6	20						
Zn	73	80	116	84	95	28	115	124
Au (ppb)	N.D.	N.D.						
Y	42	24	28	17	19	20	23	27
Zr	141	252	90	137	152	118	136	169
Ba	517	449	83	119	343	119	257	423
Cr	10	4	135	81	36	541	266	65
As	N.D.	N.D.	N.D.	N.D.	N.D.	N.D.	N.D.	7
Pb	28	N.D.	N.D.	N.D.	9	N.D.	N.D.	N.D.
La	42.42	27.99	6.14	17.05	18.38	11.91	18.51	22.04
Ce	94.66	62.13	15.72	38.72	39.13	27.86	43.32	52.47
Pr	11.46	7.79	2.42	4.99	5.02	3.88	5.81	7.32
Nd	43.29	30.47	11.46	18.81	19.3	16.33	23.16	30.14
Sm	8.13	5.60	3.57	3.58	3.9	3.69	5.04	6.2
Eu	0.65	1.48	1.24	1.03	1.11	1.08	1.58	1.75
Tb	0.87	0.59	0.77	0.51	0.58	0.58	0.76	0.85
Gd	6.27	4.42	4.58	3.44	3.8	3.85	5.03	5.83
Dy	4.67	3.24	5	2.97	3.42	3.56	4.52	4.82
Ho	0.92	0.63	0.99	0.58	0.64	0.69	0.81	0.9
Er	2.78	1.92	2.8	1.64	1.84	1.93	2.09	2.48
Tm	0.44	0.32	0.38	0.22	0.26	0.26	0.27	0.34
Yb	3.19	2.10	2.45	1.5	1.69	1.71	1.74	2.2
Lu	0.49	0.34	0.35	0.22	0.26	0.26	0.25	0.32
Rb	67.13	58.66	2.96	13.8	33.31	2.31	31.66	7.95
Sr	79.45	148.99	139.76	220.44	296.97	451.83	241.27	437.16
Nb	15.31	10.24	4.77	7.34	7.69	8.48	10.24	14.6
Cs	1.54	1.94	1.08	0.44	0.9	0.07	1.42	0.25
Hf	5.66	6.32	2.12	3.27	2.68	1.97	3.1	3.6
Ta	1.20	0.72	0.58	0.83	1.86	0.53	0.57	0.88
Th	7.91	4.05	0.59	2.56	2.43	1.16	1.55	1.98
U	1.75	1.06	0.16	0.59	0.75	0.29	0.38	0.49

Table 1. *Continued.*

Sample	95JRD–B123	95JRD–B138	95JRD–B142	95JRD–B152	95JRD–B152	95JRD–B220	95JRD–B227	95JRD–B233
Rock Type (field I.D.)	Lapilli–tuff	Gabbro	Cherty tuff	Int tuff	(duplicate)	Int tuff	Int tuff	Altered tuff
SiO_2 %	47.89	46.86	72.71	53.63	53.90	56.95	66.93	61.00
Al_2O_3	15.41	17.07	12.14	14.25	14.25	14.26	13.95	14.06
MnO	0.15	0.22	0.02	0.13	0.13	0.13	0.10	0.07
MgO	5.43	3.85	1.50	5.05	5.07	4.07	1.00	2.53
CaO	6.41	7.48	1.74	6.61	6.65	5.39	2.14	5.38
Na_2O	3.21	3.41	6.05	4.23	4.23	3.52	5.04	4.41
K_2O	0.22	<0.02	<0.02	<0.02	<0.02	0.26	1.52	0.48
TiO_2	1.76	1.69	0.48	0.72	0.73	1.22	0.62	0.76
P_2O_5	0.36	0.15	0.09	0.12	0.12	0.29	0.16	0.15
Fe_2O_3*	11.54	14.86	3.02	7.78	7.83	9.36	5.39	5.58
LOI	6.47	3.35	1.18	6.29	6.31	3.39	2.72	3.95
TOTAL	98.86	98.94	98.93	98.81	99.22	98.84	99.57	98.37
S	0.01	0.01	0.02	0.01	0.01	0.03	0.01	0.11
CO_2	2.81	0.30	0.12	3.28	3.28	0.76	1.36	2.14
FeO	9.04	8.95	1.99	5.61	5.95	5.17	2.99	3.63
H_20^-	0.22	0.24	0.06	0.16	0.19	0.18	0.08	0.20
H_20^+	4.57	3.92	1.17	3.44	3.60	3.23	1.57	2.28
Ag ppm	3	3	2	3		3	2	2
Cd	N.D.	N.D.	N.D.	N.D.		N.D.	N.D.	N.D.
Li	22	20	7	26		18	12	11
Hg								
Cl								
F								
Co								
Cu	65	76	17	67		50	7	26
Mo	N.D.	N.D.	13	10		N.D.	8	11
Ni	112	43	23	137		84	6	57
Sc	18	28	8	16		14	10	12
V								
Zn	115	105	48	77		100	135	83
Au (ppb)								
Y	27	31	28	15		28	51	18
Zr	171	89	177	116		228	449	151
Ba	182	126	22	35		480	515	163
Cr	118	50	28	232		107	4	76
As	N.D.	N.D.	N.D.	N.D.		N.D.	N.D.	18
Pb	N.D.	N.D.	N.D.	8		10	N.D.	N.D.
La	22.78	6.67	39.56	10.93		26.63	50.82	21
Ce	56.04	16.49	75.77	24.5		59.7	121.29	45.12
Pr	8.06	2.51	9.18	3.2		7.98	16.66	5.71
Nd	32.94	11.67	33.54	12.61		31.6	65.3	21.62
Sm	6.88	3.51	6.19	2.74		6.3	12.78	4.04
Eu	1.82	1.28	1.16	0.79		1.58	2.74	1.29
Tb	0.89	0.76	0.87	0.39		0.88	1.72	0.54
Gd	6.19	4.5	5.74	2.66		6.05	11.33	3.68
Dy	4.95	5.12	4.95	2.42		5.09	9.71	3.06
Ho	0.89	1.07	0.97	0.48		0.96	1.86	0.56
Er	2.52	3.02	2.84	1.36		2.65	5.21	1.56
Tm	0.34	0.42	0.41	0.18		0.35	0.75	0.21
Yb	2.16	2.74	2.75	1.28		2.26	5.1	1.45
Lu	0.32	0.39	0.42	0.19		0.33	0.76	0.2
Rb	9.67	3.63	0.33	0.99		10.05	50.08	19.78
Sr	219.92	286.19	72.12	117.27		366.97	199.03	259.13
Nb	16.07	4.8	12.51	6.47		15.65	36.34	8.35
Cs	0.33	0.87	0.05	0.04		0.33	1.46	0.81
Hf	3.87	1.44	5.27	2.39		4.52	10.91	3.47
Ta	0.91	0.45	0.89	0.45		0.99	2.07	0.57
Th	1.89	0.55	5.49	1.6		3.29	6.11	2.32
U	0.47	0.12	1.33	0.4		0.8	1.46	0.58

Table 1. *Continued.*

Sample	95JRD–B234	95JRD–B264	95JRD–B270	95JRD–DD1
Rock Type (field I.D.)	Altered tuff	Volc (alt.)	Volc (alt.)	Felsic tuff
SiO_2 %	59.94	83.56	63.22	71.94
Al_2O_3	14.36	8.61	15.70	11.57
MnO	0.10	<0.01	0.04	0.03
MgO	3.13	0.29	1.39	0.94
CaO	4.11	0.26	4.45	2.47
Na_2O	5.38	0.15	4.64	4.20
K_2O	<0.02	2.67	0.67	1.50
TiO_2	1.11	0.59	0.63	0.23
P_2O_5	0.20	0.05	0.22	<0.05
Fe_2O_3*	6.67	1.09	6.20	2.18
LOI	3.98	1.67	1.36	2.53
TOTAL	98.99	98.94	98.53	97.59
S	0.04	0.15	0.42	0.14
CO_2	1.84	<0.10	0.26	1.51
FeO	4.99	0.23	3.59	1.10
H_20^-	0.16	0.16	0.14	0.06
H_20^+	2.64	1.32	1.73	1.23
Ag ppm	2	1	2	2
Cd	N.D.	N.D.	N.D.	N.D.
Li	12	5	11	6
Hg				
Cl				
F				
Co				
Cu	49	41	107	N.D.
Mo	8	9	10	10
Ni	94	38	16	8
Sc	13	5	7	5
V				
Zn	92	61	30	26
Au (ppb)				
Y	22	9	25	28
Zr	171	61	198	171
Ba	160	348	287	651
Cr	74	101	15	15
As	56	67	N.D.	N.D.
Pb	N.D.	N.D.	N.D.	N.D.
La	20.15	3.48	23.43	31.51
Ce	46.28	7.82	51.72	67.75
Pr	6.15	1.05	6.85	8.64
Nd	24.27	4.24	26.76	31.74
Sm	4.82	0.91	5.41	5.98
Eu	1.25	0.29	1.53	1.11
Tb	0.68	0.16	0.78	0.84
Gd	4.63	0.93	5.16	5.52
Dy	3.97	1.12	4.59	5.01
Ho	0.72	0.22	0.9	0.98
Er	2.05	0.68	2.57	2.9
Tm	0.27	0.09	0.36	0.42
Yb	1.74	0.7	2.51	2.83
Lu	0.26	0.11	0.38	0.43
Rb	13.77	52.68	27.52	60.69
Sr	190.53	10.29	321.76	128.08
Nb	10.96	4.45	10.73	10.18
Cs	0.39	1.07	0.7	1.27
Hf	3.57	1.42	5.29	4.55
Ta	0.71	0.3	0.76	0.79
Th	2.51	0.57	3.34	5.34
U	0.59	0.23	0.82	1.21

Table 2. Classification of unaltered versus altered Sioux Lookout orogenic belt samples (Northeast Bay of Minnitaki Lake is abbreviated as "NEBML").

Stratigraphic/lithological Unit	Sample #	Alteration (U, unaltered; C, carbonate altered; O, other alteration)
Northern Volcanic belt: basalt	45	U
	47	C
	B129	C
Patara Fm.: basalt–clast conglomerate	2	U
	4	C
	20	U
Central Volcanic belt: northern basalt subunit	87	O
	B40	C
	B58	C
Central Volcanic belt: southern basalt subunit	B32	U
	B42	C
	B72	C
	B96	U
Central Volcanic belt: NEBML area, mostly basaltic andesite	B56	C
	29	U (C?)
	30	U (C?)
	31	C
	DB107	C
	DB122	U
	DB123	C
	67	U
	68	O
	70	C
	71	O
	72	O
	77	U
	78	O
	79	U
	80	U
	81	U
	DB270	U
	DB264	O
	56	U
	DB79	C(+O?)
	102	C
	53	C
	54	U
	DB138 (gabbro)	U
	DB142	U
	DB152	C
	66	U
	DB02 (basalt)	U
	DD1 (felsic tuff–sandstone)	(C?)
	DB48	C
	DB220	U
	DB227	(C?)
	DB233	C
	DB234	C

Table 2. *Continued.*

Northeast Bay Pluton: diorite–tonalite (subvolcanic equivalent to basaltic andesite)	60	U
	61	C
	62	O
	63	O
	DB64	U
Central Volcanic Belt: mostly dacitic pyroclastic rocks	34	C(?)
	35	C(?)
	36	C
	B69A	C(?)
	B69B (mafic)	C
	B71	C
	B76 (mafic)	C
	B92	C
	B115	C
	B120	C
	92 (sandstone)	U
Central Volcanic Belt: rhyolite	17	O
	93	U
	B167	O
	B171	(C?)
	B192	(C?)
Big Vermilion–Daredevil unit and Daredevil Fm.	8	C
	9	
	10	U
	13	U
	14A	
	14B	
	15	C
	18	U
	19	U
	24	O
Ament Bay Fm.	6 (sandstone)	C(?)
Northeast Intrusive Complex (NEIC)	B23	
	B24	U
	B27	U
Granitoids	22	
	91	(C?)

Table 3. Average major oxide compositions (re–calculated volatile–free; listed as elements for brevity) of Sioux Lookout orogenic belt stratigraphic or lithological units.

St.	Unit	Si	Al	**Ti**	**Fe***	**Mn**	**Mg**	**Ca**	**Na**	**K**	**P**
6	Pat	51.2	15.5	1.11	14.0	0.32	5.6	9.7	2.1	0.47	0.02
5	AB	73.5	12.4	0.38	4.4	0.06	2.0	2.3	3.4	1.60	0.10
4	BVD	66.3	15.3	0.52	6.5	0.09	2.3	2.9	4.1	2.04	0.04
4c	Cifv	70.6	17.1	0.47	2.1	0.03	0.7	3.0	4.5	1.4	0.09
4b	Cifv	57.4	15.3	1.98	10.7	0.16	4.3	6.2	2.9	0.8	0.31
4a	Cifv	62.7	14.6	1.02	7.9	0.14	2.5	6.1	3.6	1.2	0.22
4t	Cifv	63.2	15.7	1.19	7.2	0.11	2.7	4.8	3.9	1.01	0.31
4	SJ	74.4	12.5	0.32	3.9	0.06	1.0	2.0	2.7	3.09	0.24
3	NEpl	55.1	17.0	1.48	10.7	0.13	4.2	6.4	4.2	0.54	0.16
3	NEan	58.9	15.1	1.23	9.1	0.13	4.4	6.6	3.5	0.66	0.20
2	S Cb	50.9	15.4	2.01	14.3	0.23	5.0	8.2	3.6	–	–
1	N Cb	47.9	14.2	0.62	12.4	0.19	13.2	9.3	1.3	0.92	0.15
1	NVB	47.8	14.7	0.90	12.4	0.31	6.8	15.1	1.9	0.12	0.25

Abbreviations: St., Stage; 4t; total of 4a+4b+4c (which are three subgroups of the "mostly dacitic rocks"); Pat, Patara Formation; AB, Ament Bay Formation; BVD, Big Vermilion–Daredevil unit and Daredevil Formation; Cifv, Central Volcanic belt (CVB) intermediate–felsic volcanic rocks; SJ, Superior Junction area rhyolitic rocks; Nepl, Northeast Bay pluton, Nean, NEBML andesite; S Cb, south Central Volcanic belt subunit, N Cb, north Central Volcanic belt subunit; NVB, Northern Volcanic Belt, Fe, total iron*

Table 4. Altered Sioux Lookout orogenic belt samples classified via high/low major oxide abundances (listed as elements for brevity).

Unit	Altered sample#	Highs	Lows
NVB	47	CO_2, LOI, Ca	Si
	B129	CO_2, LOI (Ca?)	
Patara Formation	4	CO_2, LOI	
CVB: N basalt subunit	87		Si, Na
	B40	CO_2, LOI, Mg, Fe*	Si, Al, Na
	B58	CO_2, LOI, Ca	
CVB: S basalt subunit	B42	CO_2, LOI, Fe* (Ca?)	
	B72	CO_2, LOI, Ca	Si
CVB: NEBML andesite	B56	CO_2, LOI (Ca?)	
	29(?)	LOI	
	30(?)	LOI	
	31	CO_2, LOI, Ca	
	DB107	CO_2, LOI, Ca	
	DB123	CO_2, LOI (Ca)	
	68	LOI	
	70	CO_2, LOI, Ca	
	71	LOI, Fe*, S	Si, Al, Na
	72	LOI, K	Na
	78	LOI, Fe*, S (Ca?)	Si, Na
	DB264	Si	Al, Mn, Ca, Na
	DB79	CO_2, Ca (Si?)	Na
	102	CO_2, LOI	
	53	CO_2, LOI, Ca	
	DB152	CO_2, LOI, Ca	
	DD–1(?)	CO_2	
	DB48	CO_2, LOI, Si	
	DB227(?)	CO_2	
	DB233	CO_2, LOI (Ca?)	
	DB234	CO_2 (LOI)	
Northeast Bay Pluton	61	CO_2 (LOI)	
	62	CO_2, Fe*	
	63	Ca, Fe	
CVB: mostly dacitic, pyroclastic rocks	34	CO_2, LOI	
	35	CO_2, LOI	
	36	CO_2, LOI	
	B69A	CO_2 (LOI)	
	B69B	CO_2, LOI, Ca	
	B71	CO_2, LOI, (Ca?)	
	B76	CO_2, LOI, Fe* (Ca?)	Si
	B92	CO_2, LOI, Ca	
	B115	CO_2 (LOI)	
	B120	CO_2 (LOI)	
CVB: rhyolite	17	K	Ca, Na
	B167	(Si?)	(Ca?)
	B171	CO_2 (Si?)	
	B192	CO_2, LOI	
Big Vermilion–Daredevil unit and Daredevil Fm.	8	CO_2, LOI (Mg?)	
	15	CO_2, LOI, Mg	
	24	LOI, S	
Ament Bay Fm.	6	CO_2	
Granitoid	91	CO_2 (LOI)	

Fe, total iron; LOI, loss on ignition (volatiles)*

Table 5. Subdivision of Sioux Lookout orogenic belt basaltic units and subunits.

Unit	TiO_2	P_2O_5	La	Nb	Th	Zr	Zn
DB–02 sample	M 1.5%	M 0.11%	M 6 ppm	M 5 ppm	M 0.6 ppm	M 90 ppm	M 120 ppm
CVB S basalt	H 2	H 0.2	H 10	H 10 (var.)	H 1.0 (var.)	H 130	H 170
CVB N basalt	L =<1%	L 0.0	L =<2	L 1	L 0.2	L 30	L 100
NVB basalt	L 1%	L 0.0	L 2–3	L 2	L 0.3	L 50	L 80

Abbreviations: L, low; M, moderate; H, high; var., variable. Values listed are generalized approximations.

Table 6. Average values of selected trace element ratios for Sioux Lookout orogenic belt stratigraphic and lithological units.

Stage	Unit	Zr/Y	Th/Ta	Ce/Yb	La/Yb_{CN}	La/Nb_{NMN}
–	Granitoids	16	11.7	67.0	44.3	2.9
–	NEIC	25	26.4	75.5	49.6	7.2
6	Pat	3	2.1	4.5	2.5	1.6
5	AB	9	14.3	35.9	27.3	4.8
4	BVD	12	17.0	49.8	35.6	6.0
4c	Cifv	29	14.2	73.2	51.2	8.4
4b	Cifv	5	1.9	25.4	13.7	1.8
4a	Cifv	8	3.4	22.4	13.5	1.7
4t	Cifv	10	6.1	37.5	23.9	3.6
4	SJ	7	6.5	27.7	17.7	3.0
3	NEpl	7	2.1	23.7	14.1	1.9
3	NEan	7	3.0	23.6	14.2	1.8
2	S Cb	5	1.6	12.9	6.6	1.2
1	N Cb	3	2.2	5.7	3.2	1.6
1	NVB	3	1.8	4.4	2.4	1.3

(abbreviations as in Table 3; NEIC, Northeast Intrusive Complex)

Table 7. Summary of discrimination plot fields per Sioux Lookout orogenic belt unit.

Stratigraphic **Unit**	**Pearce and Cann (1973) diagram**	**Wood (1980) diagram**	**Meschede (1986) diagram**	**Interpreted Stage (this study)**
Big Vermilion–Daredevil unit	–	volcanic arc (calc–alkalic)	–	4
CVB (mostly dacitic rocks: “ifv”)	–	MORB and within plate, volcanic arc (calc–alkalic)	–	4
Superior Junction rhyolites	–	volcanic arc (calc–alkalic)	–	4
NEBML basaltic andesite	volcanic arc, within plate	MORB and within plate, volcanic arc (calc–alkalic)	within plate (alkali and tholeiitic fields)	3
CVB S basaltic subunit	MORB, within plate	MORB and within plate (and near MORB and volcanic arc tholeiite)	volcanic arc	2
CVB N basaltic subunit	MORB	MORB, volcanic arc (tholeiiticand calc alkalic fields)	normal MORB	1
NVB	MORB	MORB, volcanic arc (tholeiite)	normal MORB	1

(MORB, mid–ocean ridge type basalt)

Table 8. Summary of interpretations from geochemically based tectonic setting discrimination diagrams.

Lithology	Geochemical classifica–tion	Arc, tectonic style	Interpreted Stage #	Interpreted Arc Stage
dacite, rhyolite; mostly pyroclastic	calc–alkalic	island/con–tinental arc	4	mature arc
basaltic andesite; flows and pyroclastic	fairly calc–alkalic (near tholeiitic; transitional to within plate and E–MORB)	island arc (variable; minor cont. arc, minor extensional)	3	locally rifted arc (a middle stage)
basalt; flows (+rhyolite? Bimodal?)	tholeiitic to variable (within plate, volcanic arc, E–MORB)	island arc (island arc > oceanic arc)	2	juvenile/ incipient arc
basalt; flows	tholeiitic, N–MORB	oceanic arc	1	pre–arc rift basin (or “back–arc basin”)

Metric Conversion Table

Conversion from SI to Imperial			Conversion from Imperial to SI		
SI Unit	*Multiplied by*	*Gives*	*Imperial Unit*	*Multiplied by*	*Gives*
		LENGTH			
1 mm	0.039 37	inches	1 inch	**25.4**	mm
1 cm	0.393 70	inches	1 inch	**2.54**	cm
1 m	3.280 84	feet	1 foot	**0.304 8**	m
1 m	0.049 709	chains	1 chain	20.116 8	m
1 km	0.621 371	miles (statute)	1 mile (statute)	**1.609 344**	km
		AREA			
1 cm^2	0.155 0	square inches	1 square inch	**6.451 6**	cm^2
1 m^2	10.763 9	square feet	1 square foot	**0.092 903 04**	m^2
1 km^2	0.386 10	square miles	1 square mile	2.589 988	km^2
1 ha	2.471 054	acres	1 acre	0.404 685 6	ha
		VOLUME			
1 cm^3	0.061 023	cubic inches	1 cubic inch	**16.387 064**	cm^3
1 m^3	35.314 7	cubic feet	1 cubic foot	0.028 316 85	m^3
1 m^3	1.307 951	cubic yards	1 cubic yard	0.764 554 86	m^3
		CAPACITY			
1 L	1.759 755	pints	1 pint	0.568 261	L
1 L	0.879 877	quarts	1 quart	1.136 522	L
1 L	0.219 969	gallons	1 gallon	**4.546 090**	L
		MASS			
1 g	0.035 273 962	ounces (avdp)	1 ounce (avdp)	28.349 523	g
1 g	0.032 150 747	ounces (troy)	1 ounce (troy)	**31.103 476 8**	g
1 kg	2.204 622 6	pounds (avdp)	1 pound (avdp)	**0.453 592 37**	kg
1 kg	0.001 102 3	tons (short)	1 ton (short)	**907.184 74**	kg
1 t	1.102 311 3	tons (short)	1 ton (short)	**0.907 184 74**	t
1 kg	0.000 984 21	tons (long)	1 ton (long)	**1016.046 908 8**	kg
1 t	0.984 206 5	tons (long)	1 ton (long)	**1.016 046 90**	t
		CONCENTRATION			
1 g/t	0.029 166 6	ounce (troy)/ ton (short)	1 ounce (troy)/ ton (short)	34.285 714 2	g/t
1 g/t	0.583 333 33	pennyweights/ ton (short)	1 pennyweight/ ton (short)	1.714 285 7	g/t

OTHER USEFUL CONVERSION FACTORS

	Multiplied by	
1 ounce (troy) per ton (short)	31.103 477	grams per ton (short)
1 gram per ton (short)	0.032 151	ounces (troy) per ton (short)
1 ounce (troy) per ton (short)	20.0	pennyweights per ton (short)
1 pennyweight per ton (short)	0.05	ounces (troy) per ton (short)

Note: Conversion factors which are in bold type are exact. The conversion factors have been taken from or have been derived from factors given in the Metric Practice Guide for the Canadian Mining and Metallurgical Industries, published by the Mining Association of Canada in co-operation with the Coal Association of Canada.

ISSN 0826–9580
ISBN 0–7778–9540–4

Master Code For All Lithologies

i .... laminated (<1 cm thick)	F ... boulders, cobbles, blocks, bombs (>64 mm)
j .... thinly bedded (1-10 cm thick)	G .. pebbles (2-64 mm)
k ... medium bedded (10-30 cm thick)	H ... coarse-, very coarse-grained (0.5-2 mm)
l .... thickly bedded (>30 cm thick)	I ... medium-grained (0,25-0.5 mm)
m .. garnet porphyroblasts	J ... very fine-, fine-grained (0.06-0.25 mm)
n ... (other) porphyroblasts	K ... clast-supported framework
o ... gneissic	L ... matrix-supported
q ... mineral clots	M .. monolithic (oligomictic)
r ... chloritic schist	N ... heterolithic (polymictic)
w ... epidote	O .. pillow breccia
z ... quartz-sericite schist	P ... hyaloclastic
A ... aphanitic	Q .. pumiceous clasts
B ... fine-grained (<1 mm)	R ... porphyritic clasts
C ... medium-grained (1-5 mm)	S ... mixed composition: mafic matrix, felsic/intermediate clasts
D ... coarse-grained (>5 mm)	U ... (other) volcanic breccias
E ... pegmatoid (>1 cm)	V ... tectonic breccias
	W .. vein
	X ... dike
	Y ... sill
	Z ... xenoliths

SYMBOLS

- Bedrock outcrop/locality
- Bedding, top unknown (inclined, vertical)
- Bedding, top (arrow) from grading (inclined, vertical, overturned)
- Cross-bedding (inclined, vertical, overturned)
- Lineation, with plunge
- Schistosity (first generation; strike only, inclined, vertical)
- Schistosity (second generation)
- Fold, with plunge
- Pillow lava; top (arrow) from shape and packing (inclined, overturned)
- Clast elongation
- Shear zone
- Geological boundary/contact
- Fault

ABBREVIATIONS

Ag ... silver	magn ... magnetite
Au ... gold	py ... pyrite
bx ... breccia	s ... sulphides (mainly pyrite)
c ... carbonate	sil ... silica
chl ... chlorite	tour ... tourmaline
cp ... chalcopyrite	

SOURCES OF INFORMATION

Johnston, F.J. 1969. Western Minnitaki Lake Area; Ontario Dept. of Mines, Map 2155, scale 1:31 680.

Johnston, F.J. 1972a. Vermilion Lake Sheet; Ontario Division of Mines, Map 2242, scale 1:31 680.

Johnston, F.J. 1972b. Abram Lake Sheet; Ontario Division of Mines, Map 2243, scale 1:31 680.

Page, R.O. and Christie, B.J. 1980. Lateral Lake Area (East Half), District of Kenora; Ontario Geological Survey, Preliminary Map P.2372, Geological Series, scale 1:15 840.

Trowell, N.F., Bartlett, J.R. and Sutcliffe, R.H. 1982. Loggers Lake; Ontario Geological Survey, Map 2477, Precambrian Geology Series, scale 1:50 000.

Metric conversion factor: 1 foot = 0.3048 m.

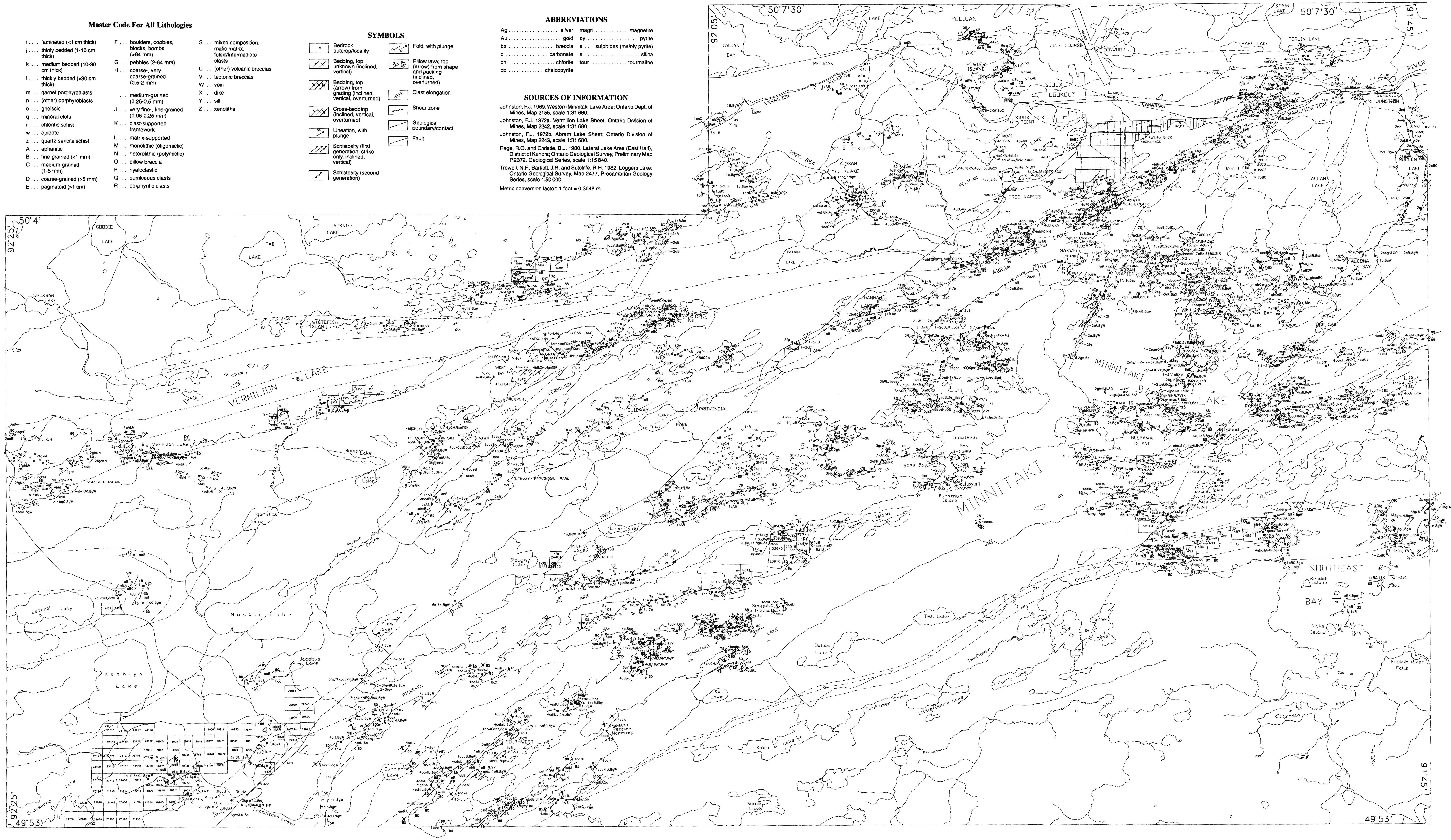

Ontario

Ontario Geological Survey

MAP P.3342

PRECAMBRIAN GEOLOGY
SIOUX LOOKOUT AREA

Scale 1:50 000

1000 m 0 1 2 km

NTS Reference: 52 J/4

LEGEND

ARCHEAN

8 Felsic to Intermediate Intrusive Rocks ("9" if late, post-tectonic)
- 8a Granite
- 8b Granodiorite
- 8c Tonalite
- 8d Diorite
- 8e Pegmatite
- 8f Aplite
- 8g Quartz
- 8h Porphyritic

INTRUSIVE CONTACT

7 Mafic Rocks
- 7a Diabase
- 7b Gabbro
- 7c Amphibolite

6 Felsic to Intermediate (Meta-)Intrusive/ Subvolcanic Rocks
- 6a Quartz porphyry
- 6b Feldspar porphyry
- 6c Quartz-feldspar porphyry

5 Chemical Metasedimentary Rocks
- 5a Chert
- 5b Chert and magnetite
- 5c Magnetite
- 5d Hematite
- 5e Pyrite

4 Clastic Metasedimentary Rocks
- 4a Conglomerate
- 4b Arenite
- 4c Wacke
- 4d Argillite/siltstone
- 4e Slate
- 4g Schist

3 Felsic Metavolcanic Rocks

2 Intermediate Metavolcanic Rocks

1 Mafic Metavolcanic Rocks
- 1a Massive
- 1b Pillowed
- 1c Amygdaloidal/vesicular
- 1d Variolitic/spherulitic
- 1e Porphyritic
- 1f Tuff
- 1g Lapilli-tuff, lapillistone
- 1h Tuff-breccia

CREDITS

Geology by: J.R. Devaney and A. Borowik, 1994; J.R. Devaney, D. King and D. Babin, 1995.

Assisted in the field by M. Mackenzie, B. MacFarlane, M. Mitchell, M. Smethurst, P. Smoter, D. Leng, J. Brownbill and W. Chisel.

Computer drafting by J.R. Devaney, A. Borowik, K. Mahoney and B. Leonard.

To enable the rapid dissemination of information, this map has not received a technical edit. Discrepancies may occur for which the Ontario Geological Survey does not assume liability. Users should verify critical information.

Issued 1995.

Information from this publication may be quoted if credit is given. It is recommended that reference to this map be made in the following form:

Devaney, J.R., Borowik, A., King, D. and Babin, D. 1995. Precambrian geology, Sioux Lookout area; Ontario Geological Survey, Preliminary Map P.3342, scale 1:50 000.